Connections of Pipe Piles to Bridge Bent Caps: Full-Scale Tests

by

Maria Emilia Clavijo Calderon

A thesis submitted to the Graduate Faculty of
Auburn University
in partial fulfillment of the
requirements for the Degree of
Master of Science

Auburn, Alabama
May 10, 2025

Keywords: composite construction, headed bar, load testing, reinforced concrete, shear stud, substructure, steel pipe

Approved by

Robert W. Barnes, Chair, PhD., PE, Professor, Department of Civil and Environmental Engineering
Kadir C. Sener, Co-chair, PhD., PE, Assistant Professor, Department of Civil and Environmental Engineering
Matthew Yarnold, PhD., PE, Associate Professor, Department of Civil and Environmental Engineering

ABSTRACT

Due to their durability, strength, and adaptability to challenging conditions, large-diameter steel pipe piles are a promising solution for multi-span bridges. However, guidance on practical and effective connections between steel pipe piles and concrete members is limited. An ongoing study is focused on steel pipe pile to concrete bent cap connections in substructures, including full-scale tests of five connection types: (1) headed-bars, (2) hooked-bars, (3) straight-bars, (4) welded shear studs, and (4) an annular ring welded at the pile end, which are documented in this thesis.

Connection subassemblages, each consisting of a 36 in. diameter pile and a 54 in. deep bent cap, were fabricated. A 3 ft diameter steel pile was used in all cases. Specimens were subjected to lateral load cycles of increasing intensity, inducing internal forces to simulate service conditions and ultimate strength. Different types of sensors were used to measure the displacement of the specimens, the strains of the steel pile and reinforcing bars, and the rotation of the pile. Constructability of the connections was discussed, comparing the ease of construction of each type of connection.

Results and observed behavior of all five specimens were favorable under service- and strength-level loads. The three reinforcing steel connections vastly exceeded the capacities estimated using conservative design assumptions and principles. This demonstrates the significant contribution of the steel pipe pile to the capacity of the system. The welded mechanical anchorage connections showed a behavior closer to the estimated capacities that include the contribution of the pile. The different types of connections presented in this study demonstrated to provide an alternative to current practices. The annular ring and headed-bar connections represent a great alternative to reduce the construction time of the connections.

ACKNOWLEDGEMENTS

I want to express my deepest gratitude to my advisor, Dr. Robert Barnes, for believing in this young engineer from day one. Thank you for your guidance, support, and encouragement, but most importantly, for your patience and humanity, which have shaped me and helped me grow both as an engineer and as a person.

I would also like to thank Dr. Kadir Sener and Dr. Levent Isbiliroglu for their contributions to this project.

I want to thank Dr. Matthew Yarnold for his insightful comments that were used to improve this thesis.

To my Auburn friends, thank you for always taking a moment to encourage and support me. You have made this experience truly unforgettable.

I am deeply grateful for the love and support of my family (Clavijo Calderón), who have been with me from afar. Thank you for always believing in me and for making me feel accompanied and supported. I couldn’t have done this without you.

Thank you to my Auburn family (The Barnes) for caring for me and supporting me as my own family.

And above all, I want to thank God for His providence and love.

TABLE OF CONTENTS

LIST OF TABLES

LIST OF FIGURES

CHAPTER 1 INTRODUCTION

1.1 BACKGROUND

Bridges are vital structures that have been constructed for centuries to enable efficient transportation of people and goods across obstacles. The evolution of bridge construction and design has been evident over the years.

Modern bridges are designed to withstand different types of loads to meet demands for durability, load-carrying capacity, and resilience when subjected to various conditions. Material selection and the construction techniques used to erect a bridge are essential to obtain efficient and cost-effective structures.

The types of bridges available in the U.S. range from simple beam and girder designs to more complex suspension or movable structures, depending on the conditions and needs of each project. The Federal Highway Administration (FHWA) National Bridge Inventory (2021) identified 618,456 bridges and about 10,000 projects to build, rehabilitate, and replace bridges annually in the U.S. This large number of bridge structures has increased the need for accelerated, innovative, and more efficient design and construction processes.

The primary components of a bridge are superstructure, substructure, and foundations. The superstructure is the part of a bridge that directly carries the moving loads and transfers them to the substructure elements. The main superstructure components are the deck, haunch, barrier and sidewalk, girders, stiffeners, and diaphragms. The substructure is formed by a group of structural elements supporting the superstructure and transferring loads to the foundation. The substructure typically comprises piers, abutments, and bent caps. Similarly, the foundation is the component that anchors the bridge to the ground and transfers the loads from the substructure to the soil. It includes piles, drilled shafts, or footings. Figure 1-1 shows the main components of a conventional bridge.

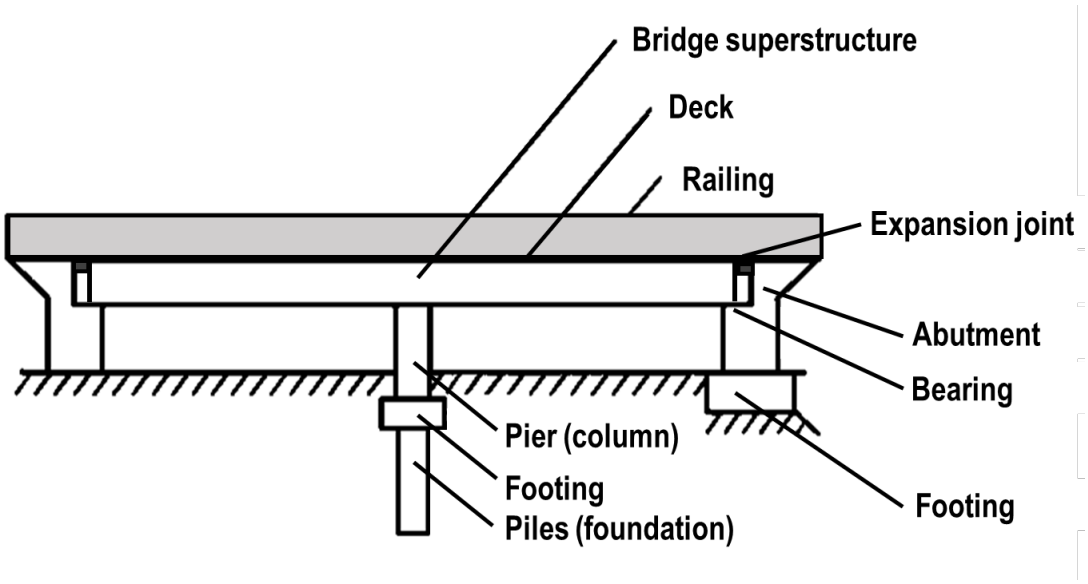

Figure 1-1: Primary bridge components
(Adapted from Barker and Puckett, 2021)

Multi-span configurations are required when bridges cross long distances, and multiple piers are necessary to support the structure. For this configuration, several types of piers are used, such as reinforced concrete solid piers, concrete-filled tubes, hollow piers, walls, arched piers, or steel piers. Some of these alternatives have certain limitations. Steel pipe piles have become a good option for bridge foundations and piers for multi-span bridge substructures due to their exceptional load-carrying capacity, durability, and adaptability to challenging conditions. Figure 1-2 depicts the use of steel pipe piles for bridge substructures.

Figure 1-2: Steel pipe piles for bridge substructures (Kappes et al. 2016)

Despite the advantages steel pipe piles offer, their use is relatively new. A critical aspect of this system is the design of the connection between the pile and the bent cap, as shown in Figure 1-3. This design must consider numerous factors to ensure proper structural performance, ease of construction time and effort, and cost-effectiveness relative to other available methods.

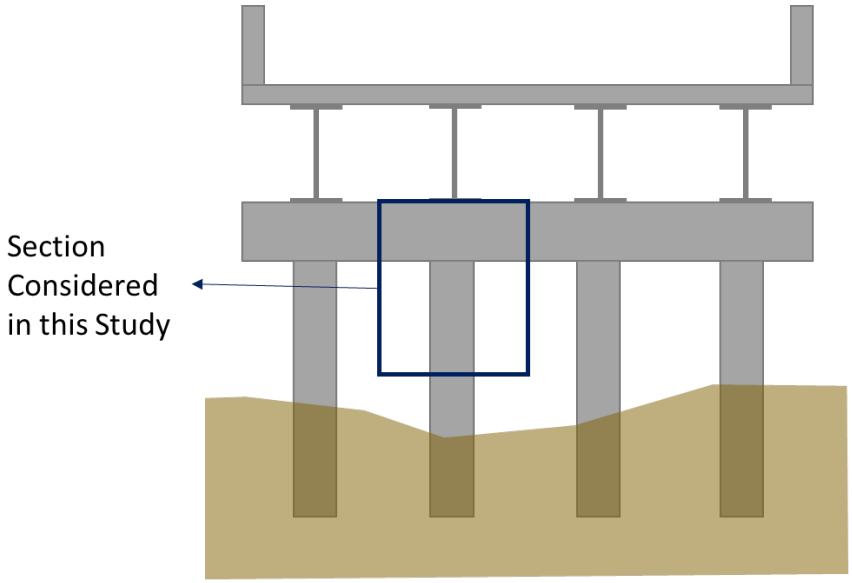

Figure 1-3: Element connection of pile to bent cap (Adapted from Kappes et al., 2016)

1.2 PROJECT OBJECTIVES

The Alabama Department of Transportation (ALDOT) has sponsored the research project "Development of Pipe Pile to Bent Cap Connection for ALDOT Bridges" conducted by the Auburn University Highway Research Center.

The main objective of the overall project is:

Establishing a robust connection detail and design methodology for steel pipe pile to bent cap connection for ALDOT bridges.

Other objectives of this project include:

- Developing a testing plan to evaluate several alternative approaches for connecting pipe piles to bent caps.
- Load testing of several candidate pipe piles to bent cap connection types conducted at the Auburn University Advanced Structural Engineering Laboratory.

- Using advanced finite element models validated by load testing to conduct parametric analyses to refine and optimize the design and detailing methodology.
- Develop and deliver a comprehensive technical report that includes recommendations for adding an ALDOT standard drawing and detailing of a pipe pile to bent cap connection.

1.3 THESIS OBJECTIVES

This thesis describes the information collected from developing a portion of the aforementioned research project.

The objectives of the research described in this thesis are:

- Evaluate the structural behavior of five different connection types under cycles at service- and extreme-load levels of lateral force, and
- Evaluate the constructability of five different connection types between steel piles and concrete bent caps.

The five different connection types evaluated are: (1) headed bars, (2) hooked bars, (3) straight bars, (4) welded shear studs, and (5) an annular ring.

1.4 SCOPE

This study focused on full-scale testing of five steel pipe pile to concrete bent cap connection types. Each specimen consisted of a 36 in. diameter steel pipe pile and a 54 in. deep concrete bent cap. The specimens include identical bent cap reinforcement details and different connection details for each. The connection types include three configurations with reinforcing bars and two with mechanical anchorage welded to the pile without reinforcing bars. All specimens were fabricated at the Auburn University Advanced Structural Engineering Laboratory (ASEL). All bent caps were constructed with a standard ALDOT Class B concrete mixture for bridge substructures and reinforced to correspond with a standard configuration for ALDOT bridges.

Specimens were subjected to a pseudo-static lateral load to simulate service and ultimate strength conditions after reaching a concrete compressive strength of 4000 psi.

The specimens were monitored with a variety of sensors to measure strains, rotations, and displacements during laboratory testing.

All five specimens were fully built in the laboratory. The constructability of each connection was compared, considering the difficulty of assembling them.

1.5 ORGANIZATION OF THE THESIS

Chapter 2 provides a review of the body of knowledge relevant to this study. This chapter provides a discussion of the current design and construction process of the most common pier types used in Alabama. It describes the different embedment depths for the pile types and the current connection design approaches. This chapter elaborates on the current state of practice of several state transportation agencies (DOTs) that have implemented steel pipe piles for bridge piers. The need for further exploration and research on steel pipe pile-to-cap connections is established in this chapter.

Chapter 3 provides a discussion of the design and fabrication of the experimental specimens. This chapter describes the previous work that was performed to develop the design of the specimens used in this study. The properties of the materials, concrete mixture, mixture proportions, and fresh and hardened concrete properties of each specimen are described in this chapter. Also, the fabrication process and details of each specimen configuration can be found in this chapter.

Chapter 4 provides details of the methodology used to investigate the performance of the experimental specimens, including instrumentation, test setup, loading, and cycling procedures. This chapter includes a description of all types of sensors and the location of the instrumentation used in this study.

Chapter 5 presents the outcomes of the experimental testing. This chapter includes numerical and visual data. The results of the behavior of the five connection types and cracking patterns are presented in this chapter.

Chapter 6 summarizes the research, provides discussions, conclusions, and offers recommendations based on the information presented in this thesis. Limitations of this study and suggestions for the continuation of the project were made based on the findings.

CHAPTER 2 REVIEW OF RELEVANT RESEARCH

Relevant information about bridge substructure elements, construction methods, and the performance of different connection subassemblages are described in this chapter. A comparison of the most common types of piles for bridges used in the state of Alabama is made based on previous research.

2.1 PREVIOUS STUDIES

Significant research has been conducted on bridge design. Pile foundations and bridge substructures have been the main focus areas when it comes to accelerated bridge construction (ABC). Substructure bridge components must perform adequately under different loads and circumstances. Considerable loads must be transferred from the superstructure to the substructure through the pile caps into the piles.

Due to the performance or construction challenges that the most prevalent multi-span bridge configurations present, other alternatives have been investigated. Bridge substructure elements like H-shaped steel piles and reinforced concrete drilled shafts have been found to have several disadvantages.

Steel pipe piles provide a design and construction alternative for multi-span bridges for spans of more than 50 ft. Many previous studies have evaluated the performance of different pile-to-pile cap (PTPC) connections.

2.1.1 Steel H-piles

H-piles, also known as driven piles, are extensively employed for bridge substructures and deep foundations. These piles are common for small to mid-size bridges where the outermost H-piles resist the overturning moments induced by lateral loads, typically inclined at a slope of 1.5:12. These are connected to small or medium-size bent caps with an embedment depth of approximately 12 in. Due to the small size of the H-piles, these typically carry only one girder line on top of each pile. A nonstructural concrete can encase the steel H-piles to prevent section loss, or these steel sections can be galvanized to protect them from corrosion. The concrete encasements provide

additional stiffness even when they are not considered to be structural elements (Marshall et al. 2017).

H-shaped steel pile-to-pile cap connections represent a very typical type of substructure configuration. However, research has shown several problems with this practice (Xiao et al. 2006) like unintentional failure modes due to the presence of substantial moments despite the pin connection design or the inability to fully develop ultimate design tensile capacity. Cracking and damage of the bent cap, as shown in Figure 2-1, especially in the case of exterior piles, have been found, resulting in several issues with their long-term performance (Marshall et al. 2017).

Figure 2-1: Flexural cracking of the bent cap (Marshall et al. 2017).

Steel H-pile-to-concrete cap connections are a popular type of bridge construction in many states of the U.S. This may signify a vulnerable system, especially when subjected to lateral loads where the substructure and subsequent superstructure may expect damage (Shama, Mander, and Aref 2002). Many factors can affect the performance of the pile-to-pile cap connection, including the fixity of the pile head and the pile embedment length.

Castilla et al. (1984), recommended for a condition close to full fixity, an embedment depth into the cap equal to or greater than twice the pile diameter.

Gonçalves (2022) stated that the embedment length greatly influenced the structural behavior of the pile caps. Similarly, Arockiasamy and Arvan (2022) expressed that embedment length alone can contribute to adequate connection moment capacities without a detailed connection.

Shama, Mander, and Aref (2002) developed some equations to determine the required embedment length and the tension reinforcement in the cap to ensure the failure of the connection to occur in the pile instead of the cap. This was based on assuming the compression stress distribution is linear with a maximum stress of $0.85 f'_c$. The required tension reinforcement was calculated considering the cracked concrete could not carry any tension.

2.1.2 Reinforced Concrete Piles

Reinforced concrete piles or concrete drilled shafts are extensively implemented for bridge substructures. These are often used when high load capacity is required in large spans or wide bridges subjected to axial and lateral loads. These consist of cast-in-place elements where an extensive cylindrical excavation is necessary to accommodate the reinforcing cages. These are filled with concrete, and finally, the formwork is removed to obtain the pile. Oppositely to driven piles, one drilled shaft can carry multiple girders, which means a reduction in the number of piles but an increase in the size of each pile. As a result, the size of the bent cap also increases. However, despite their excellent performance, it is known that constructing these elements requires a costly and time-consuming process. Large and heavy reinforcement cages are needed, and the time for concrete to gain enough strength delays the construction process (Sharma 2023).

Reinforced concrete piles are widely used for deep foundations where a system of piles is required to withstand a large force demand when spread footings cannot be used due to the characteristics of the soil. This methodology is preferred for many structures like bridges, high-rise structures, and others. The capacity of the piles depends on several factors, such as the fixity of the head of the pile, the embedment into the soil and the cap, pile-to-cap connection, and the properties of the soil (Arockiasamy and Arvan 2022; Eastman 2011; Arvan and Arockiasamy 2023).

The pile-to-pile cap (PTPC) connections can be affected by several factors, including the fixity of the pile. These can be generally considered rigid or pinned, as shown in Figure 2-2, depending on the type of loads that they will carry and the connection detailing (Eastman 2011). Pinned connections can be assumed when the reinforcement between the pile and the cap is limited or nonexistent, and the main purpose of the elements is to resist vertical loads (Eastman 2011). A rigid connection can be accomplished by a detailed connection between the pile and the cap or sufficient pile embedment to resist lateral loads (Richards, Rollins, and Stenlund 2011; Hannigan et al. 2016). A rigid pile-to-pile cap connection is desired for bridges under seismic loading to help control deflections. This could be achieved by extending steel reinforcement into the pile cap (Richards, Rollins, and Stenlund 2011). The pile head fixity can be associated with large ductility demands when subjected to lateral loads requiring special connection details (Arockiasamy and Arvan 2022) The presence of a detailed connection can provide adequate lateral resistance. However, plain embedment length can provide enough moment capacity of the piles (Arvan and Arockiasamy 2023; Richards, Rollins, and Stenlund 2011).

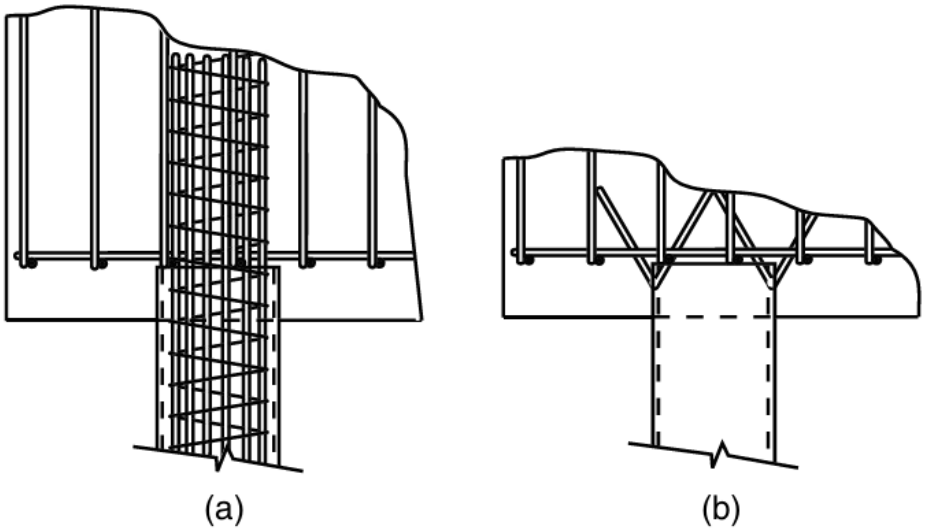

Figure 2-2: Pile-to-cap fixity examples: (a) rigid; (b) pinned (Silva and Seible, 2001)

Pile embedment length is an essential factor that can contribute to the moment capacity and ductility of the system (Arockiasamy and Arvan 2022). Plain embedment length can provide, in some cases, enough capacity for the system. This represents a cost-effective alternative that significantly reduces construction time (Richards, Rollins,

and Stenlund 2011). Stephens and McKittrick (2005) studied the performance of pile-to-pile cap connections subjected to high transverse loads and reported that the embedment length of the pile is of primary interest as it affects the connections' capacity.

A thorough review of published literature has been made about plain embedment, with conclusions like the ones presented above. However, several authors recommended further investigations to understand the behavior of the steel-concrete juncture (Arvan and Arockiasamy 2023; Richards, Rollins, and Stenlund 2011).

2.1.3 Concrete Filled Tubes

Concrete-filled tubes (CFTs) are structural elements that provide excellent performance with significant strength, stiffness, and ductility compared to other typically reinforced concrete elements. This is one of the most preferred options for accelerated bridge construction (ABC). This option provides cost savings due to the accelerated and efficient construction and the lack of steel reinforcement inside the pile. Also, the steel pipe piles used for these elements serve as a ductile permanent casing for the concrete fill, providing enough capacity and reducing construction time instead of just being used as a shell or form element.

While significant research has been conducted on the structural performance of CFTs demonstrating great behavior, little investigation has been made on the details of their connection to reinforced concrete caps. Stephens, Lehman, and Roeder (2015) studied different connections between CFTs and concrete bent caps, obtaining great results on stiffness, strength, ductility, and deformation capacity. An initial design methodology of concrete-filled steel tube to concrete pile-cap connections was developed (Kappes et al. 2016) and the necessary U-bar configuration and size as an alternative accelerated bridge construction for seismic zones.

Other research studies on CFTs (Arockiasamy and Arvan 2022; Arvan and Arockiasamy 2023; Kappes et al. 2016) describe similar results as those described in Sections 2.1.1 and 2.1.2, where the embedment length was found to be one of the most important parameters that greatly influence the performance even when no additional reinforcement is present in the connection.

Lehman and Roeder (2012), studied a connection consisting of an annular ring welded at the base of the steel tube and embedded directly into the footing, as described in Figure 2-3. This study demonstrated that longer embedment depth achieved far in excess of enough drift capacity for seismic zones and extreme load conditions with minimal system degradation. Similarly, a study of the punching shear behavior of a CFT determined that the use of shear studs significantly contributed to the punching shear resistance of the system (Tan et al. 2022).

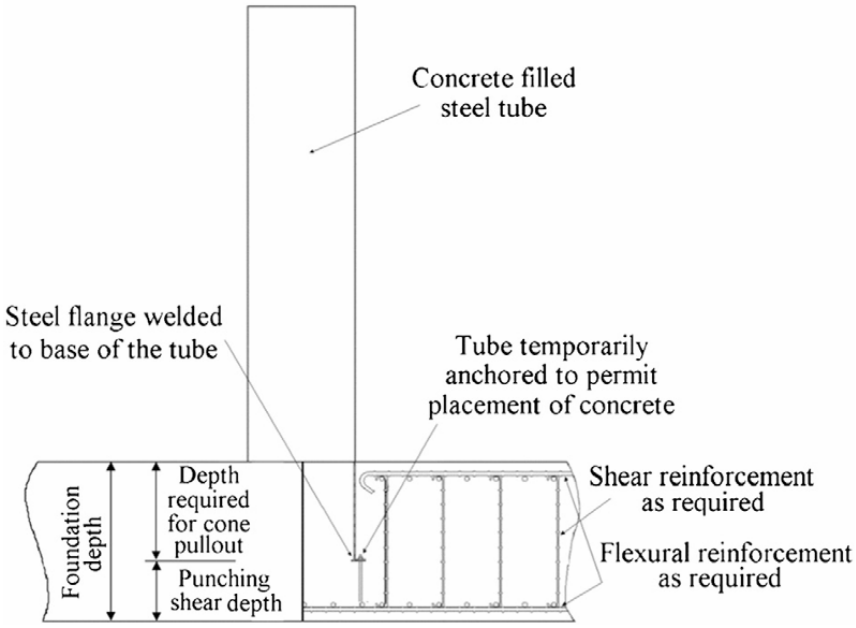

Figure 2-3: CFT experimental configuration (Lehman and Roeder 2012)

Based on all the information presented herein, a standardized design methodology for connections has not been developed yet. However, various authors highlight the benefits of using this type of construction system (Lehman and Roeder 2012; Kappes et al. 2016; M. T. Stephens, Lehman, and Roeder 2015). Further investigation is needed to obtain insights into the ideal type of connection to join the piles to the caps, taking advantage of the excellent performance that steel piles can offer.

2.1.4 Hollow Steel Pipe Piles

Bridge construction has been dominated by the use of reinforced concrete; however, the use of steel piles as a bridge pier material has gained relevance. This system's

advantages include using a very ductile material and an easier and faster construction process. However, these advantages can be limited by the inadequate system to connecting the piles with the caps (Steunenberg, Sexsmith, and Stiemer 1998). Connections between piles and bent caps are essential components of accelerated bridge construction (ABC).

Steunenberg, Sexsmith, and Stiemer (1998) investigated the behavior of the connection between hollow steel pipe piles and precast concrete caps. The connection involved welding the pile top to a steel plate embedded at the concrete cap's face. The testing involved cycling lateral loads. The results include the formation of a plastic hinge in the pile with a desirable seismic performance and full hysteresis loops. Little evidence of distress was found in the pile cap.

As shown in Figure 2-4, single steel pipe pile to concrete cap connections without reinforcement were investigated by Eastman (2011). The investigation showed that minimal pile embedment could provide significant moment capacity and stiffness. A large bearing area to embedment depth ratio proved to greatly affect strength, while a small ratio showed little contribution of the bearing mechanism to the strength of the connection.

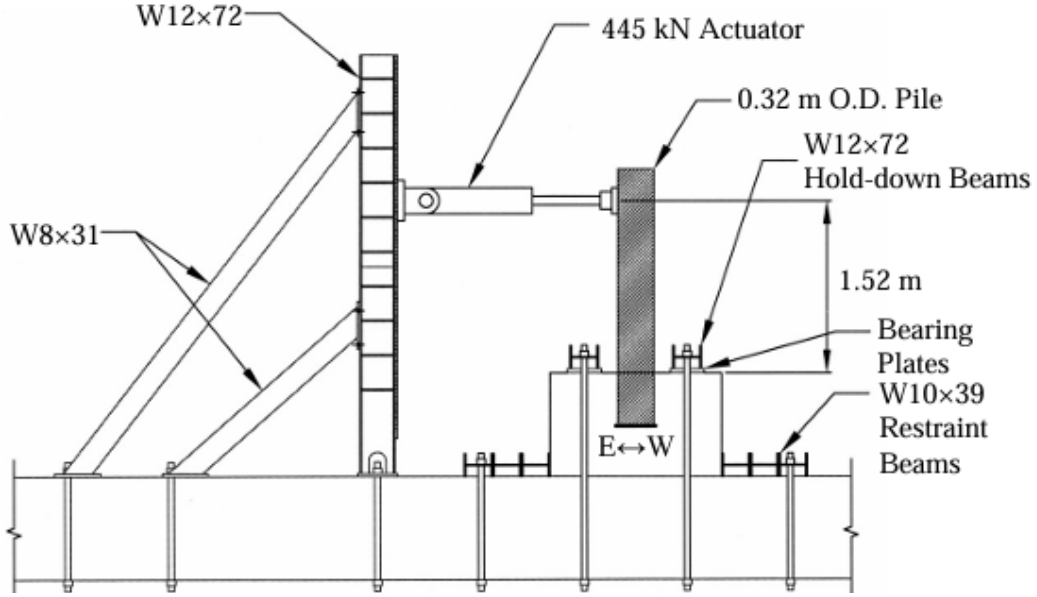

Figure 2-4: Hollow steel pile test setup (Eastman 2011)

Limited information exists on the performance of hollow steel piles as an alternative to other methods described earlier in this section. CFTs were discussed, and

the lack of a methodology to design their connection to caps occurs similarly to hollow steel piles. Steel pipe piles provide great capacity and ductility and excellent performance under challenging environmental conditions such as marine environments and soft soils. Implementing the use of hollow steel pipe piles for bridge substructures could provide a more efficient design as the capacity of the pile is taken into consideration instead of just using this element as a shell. Additionally, a significant reduction in the construction time can be obtained with this erection method, as there is no need for concrete inside the pile to gain strength or complicated reinforcing configurations.

2.2 PREVIOUS STATE AGENCIES RESEARCH

Several state transportation agencies have implemented steel pipe piles in the U.S. for bridges requiring high resistance to forces and challenging environmental factors. However, a design methodology does not exist. The lack of reference provokes a high uncertainty about how to detail connections and the necessary embedment length for the pile, all while improving the construction process and cost-efficiency.

The use of steel pipe piles connected to concrete pile caps for bridge substructures has been widely used in some states of the U.S. A clear example of the success of this type of construction is the Montana Department of Transportation (MDOT), which has found it very effective due to its speed in construction, low maintenance, and low cost. However, MDOT found a lack of a validated methodology to design pipe pile-to-pile cap connections, especially for systems subjected to lateral loads (J. Stephens and McKittrick 2005).

From a survey conducted by Sharma (2023), twenty-eight states in the U.S. acknowledged the use of steel pipe piles for bridge structures. However, twenty-one states design their connections based on specific applications.

For design purposes, it is very important to predict the failure mechanism of the pile-to-pile cap connection. Crushing and splitting of the concrete surrounding the pile, forming a plastic hinge in the pile, or a combination of mechanisms can be expected. Failure of the cap and over-reinforced concrete drill shafts are common issues found in existing bridges.

The lack of a standard design methodology resulted in several DOTs developing their design considerations and researching connections.

2.2.1 California DOT

2.2.1.1 Concrete-Filled Tube Bridge Pier Connections for ABC

Stephens et al., (2015) used experimental methods to develop design procedures for concrete-filled tube columns to cap beam connections. Three connections were studied: a connection with an annular ring welded to the steel tube, a welded dowel connection where the ring of the head dowels was welded to the tube, and a reinforced concrete connection with a traditional reinforcing cage of ring-headed dowels and transverse reinforcement. All specimens used precast cap beams, which are shown in Figure 2-5.

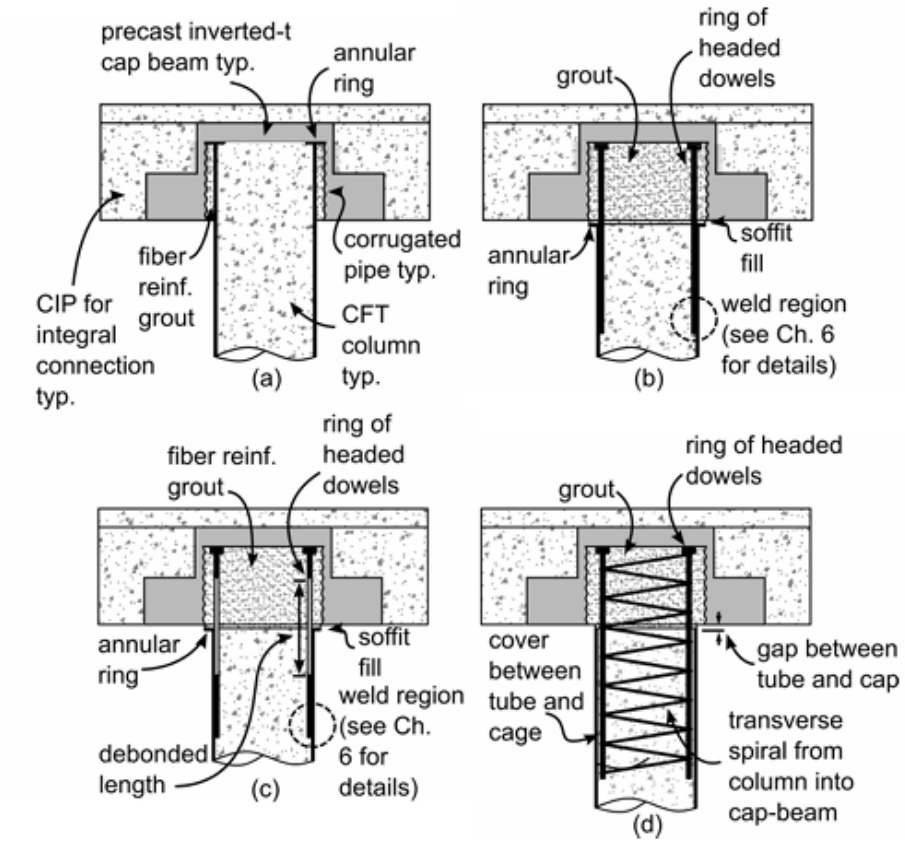

Figure 2-5: (a) Embedded ring connection, (b) and (c) Welded dowel connections, and (d) Reinforced concrete connections (Stephens et al., 2015)

According to Stephens et al. (2015), the embedded ring connection (ER) provides large strength, stiffness, and deformation capacity with a ductile failure. This

connection provides advantages such as accelerated construction and post-event inspection and repair, in addition to its great performance.

The results from the Welded Dowel Connection (WD) demonstrated a significant strength, stiffness, and deformation capacity (M. T. Stephens, Lehman, and Roeder 2015). However, the WD connection is prone to large over-strength. Two distinct failure modes were observed: cap beam failure, where the dowels were pulled out of the cap, and yielding and fracture of the dowels. Different from the ER connection, this connection did not provide much advantage in rapid construction with additional disadvantages on post-event inspection and repair.

Finally, the Reinforced Concrete Connection (RC) presented stiffness and strength significantly lower than a CFT component as the longitudinal reinforcing ratio controlled the strength of the RC (M. T. Stephens, Lehman, and Roeder 2015). In addition to the capacity reduction, this connection encountered similar challenges to a traditional RC column, where the assemblage process is inefficient and the post-event inspection is difficult.

2.2.2 Alaska DOT

2.2.2.1 Concrete-Filled Steel Pile to Concrete Bent Cap Connections

Silva et al. (1999) aimed to validate the design recommendations for the seismic design of reinforced concrete bridge bents with cast-in-place steel shells. This study consisted of a full-scale proof test of a bridge bent with three cast-in-place steel shell columns, as shown in Figure 2-6. Some important considerations were column longitudinal reinforcement, anchorage of column longitudinal reinforcement, steel shell embedment, confinement of plastic hinges, cap beam, and joint design.

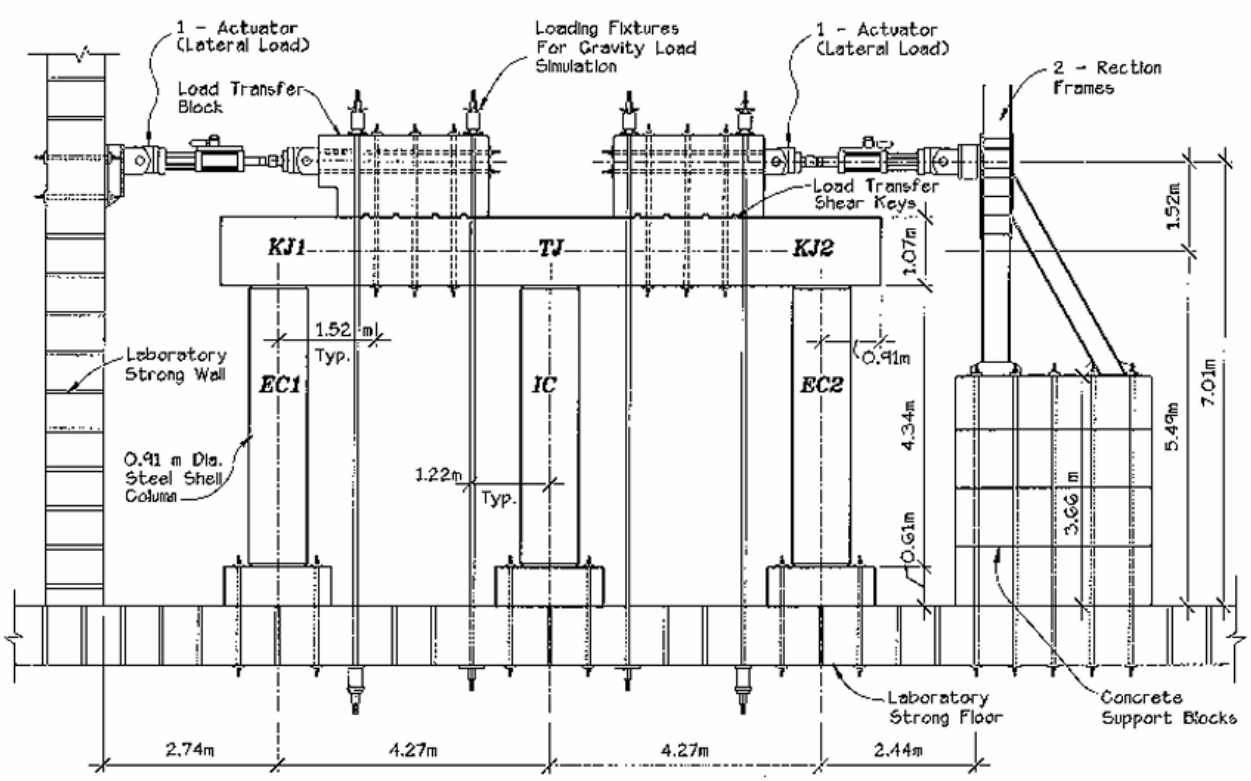

Figure 2-6: Test configuration (Silva et al., 1999)

The specimen consisted of three steel shell columns with an inner reinforced concrete core. The cap beam was constructed with a reinforcing steel cage and concrete. The three joint designs consisted of vertical stirrups outside and inside of the joint, horizontal hoops, and additional top and bottom longitudinal reinforcement in the cap, as described in section 4.3 of the document.

For a fully reinforced concrete configuration as described above, the joint design with a reduced amount of reinforcement was sufficient to ensure a desirable response for a multi-column bent under seismic loads (Silva et al. 1999).

2.2.2.2 Steel Pile to Steel Beam Cap Connections

The seismic performance of hollow steel pipe pile to cap beam moment resisting connection was evaluated for the Alaska DOT. This occurred as an alternative to the undesirable failure modes of hollow piles directly welded to a steel cap beam (Fulmer, Kowalsky, and Nau 2013). The authors described two alternatives that performed well and provided the desired behavior from all the connections tested under lateral loads.

A modified weld-protected connection was presented as an alternative. In this connection, the circular steel pipe section had a thicker upper region, with the intention of obtaining a buckling region away from the welded regions, as shown in Figure 2-7.

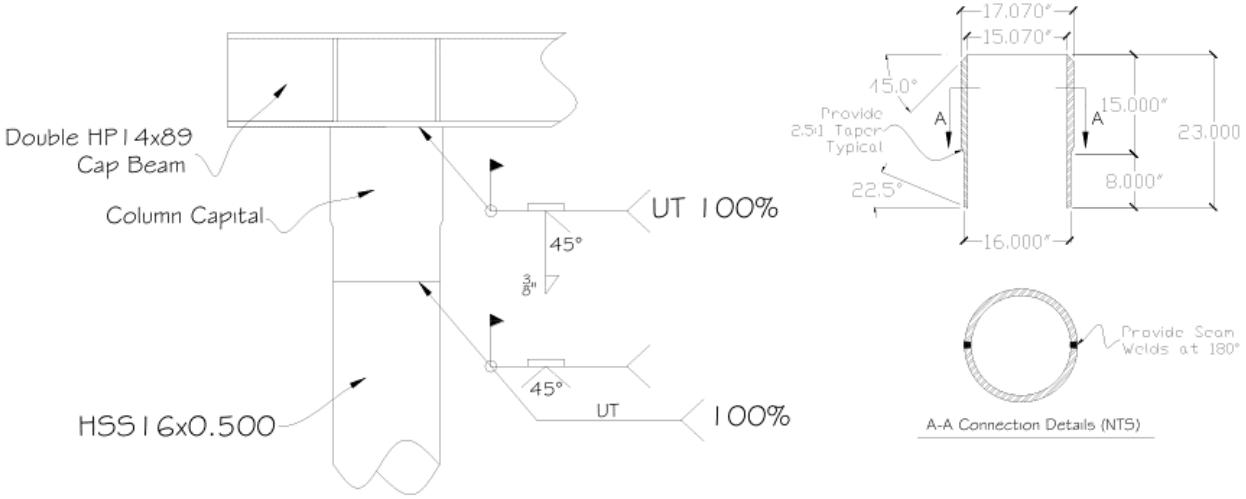

Figure 2-7: Column capital connection detail (Fulmer et al., 2013)

Another connection recommended by Fulmer et al. (2013) is a grouted shear stud connection, as described in Figure 2-8. This consisted of a pocket-style configuration where 12 lines of welded shear studs were located at 30-degree intervals around the outer face of the pile and inside the bigger pipe section. This pocket was grouted after the pile had been inserted into the stub pile.

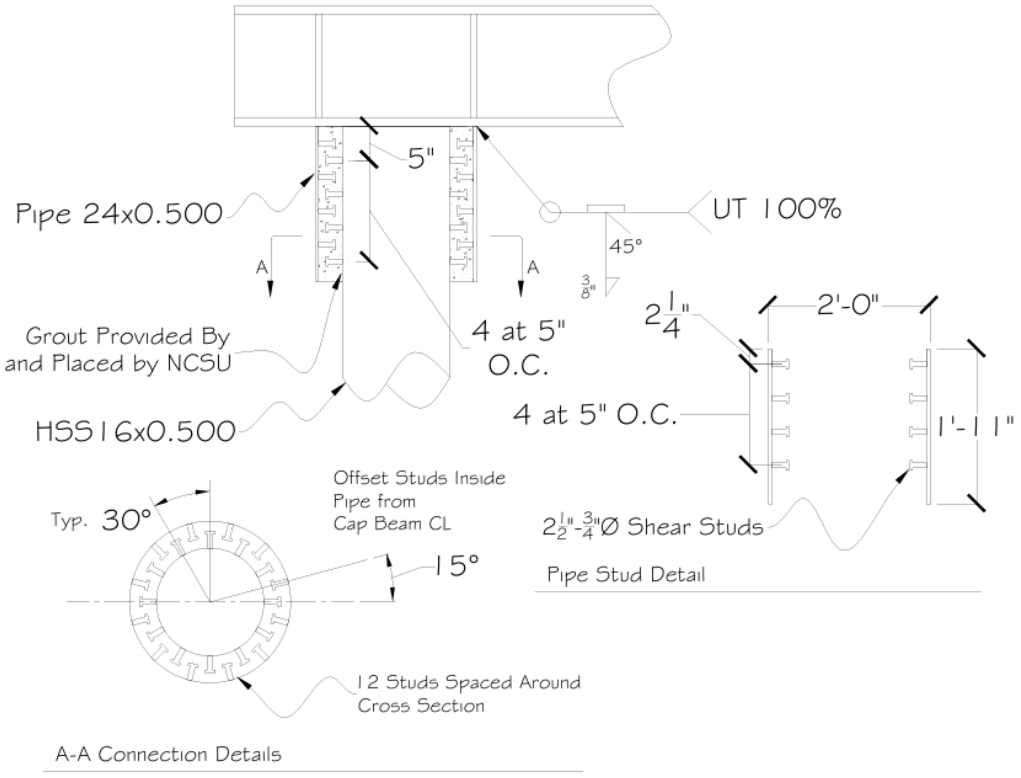

Figure 2-8: Grouted shear stud connection detail (Fulmer et al., 2013)

The physical results of the tests demonstrated the effective composite connection with a desirable failure mode with the hinging of the pile wall. Additionally, critical welded regions were protected by the configuration of the system. This ensured these regions remained elastic.

2.2.3 Montana DOT

2.2.3.1 Performance of Steel Pipe Pile to Concrete Cap Connections: Phase I

Concrete-filled steel pipe columns joined to concrete caps are commonly used in Montana to support multi-span bridges. McKittrick et al., (1998) investigated the behavior of the connections under extreme seismic and ice loads based on a 3D finite element (FE) model and compared it to a half-scale experimental test.

The model had no longitudinal reinforcing steel in the 8 in. pile, which had a 1 ft embedment depth into the 1 ft 6 in. square cap. It was tested by applying a gradually increasing lateral load to the free edge of the pile, as shown in Figure 2-9.

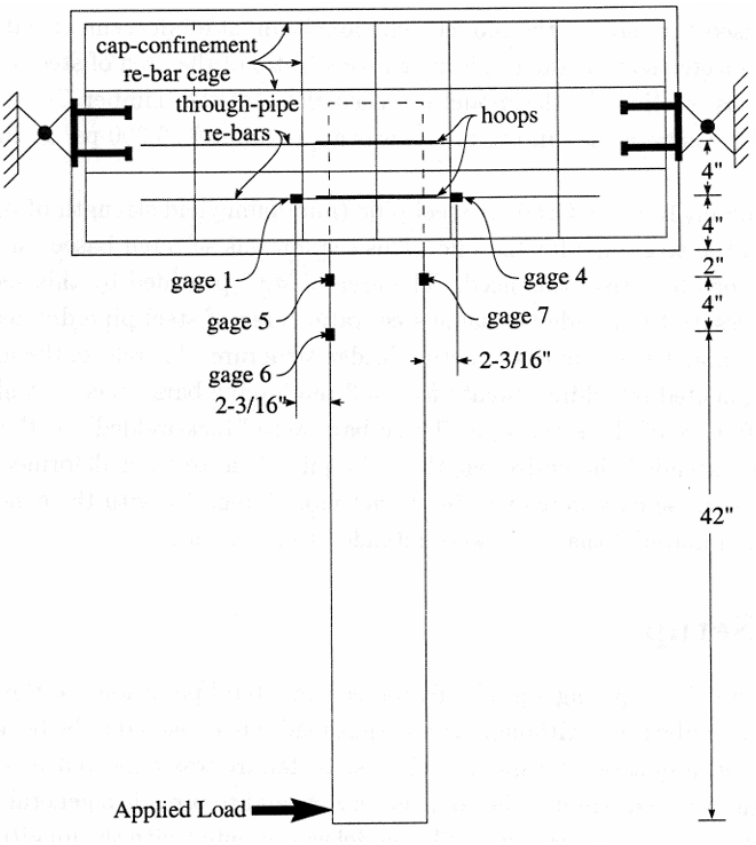

Figure 2-9: Overview of the experimental specimen (McKittrick et al., 1998)

The study demonstrated that the effect of seismic loads in the connection depends on varied factors like the horizontal fixity of the deck, which affects how the load is transmitted to the pile (McKittrick et al. 1998). Additionally, the pile height and soil type significantly affect the spectral response of the structure. On the other hand, the pile/cap embedment depth of 12 in. (1.5 times the diameter of the pile) appeared to be sufficient to bond the concrete and steel surfaces (McKittrick et al. 1998).

2.2.3.2 Performance of Steel Pipe Pile to Concrete Cap Connections: Phase II

Concrete-filled tubes connected at the top by a concrete pile cap were commonly implemented by MDOT due to their speed in construction, low maintenance, and low cost. Their capacity to carry in-service gravity loads could be predicted confidently (J. Stephens and McKittrick 2005). However, the capacity of a connection under extreme lateral loads was very uncertain. This study investigated five models in the laboratory, in which the amount of reinforcement in the beam cap varied for all specimens, as depicted in Figure 2-10.

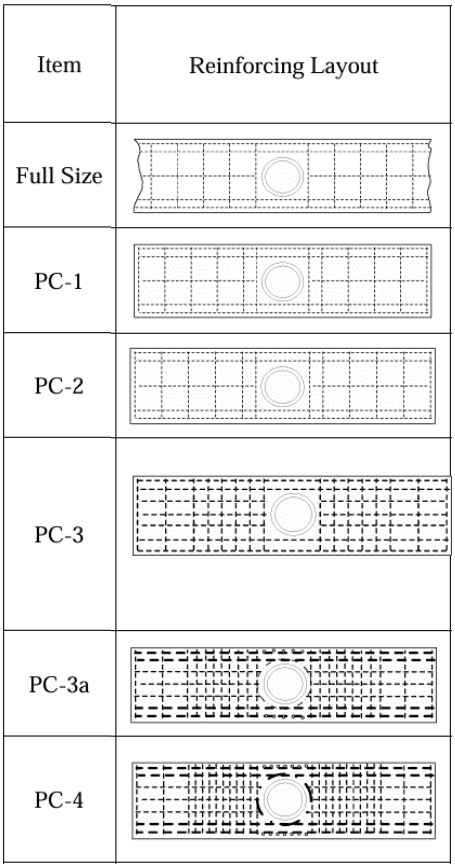

Figure 2-10: Reinforcement in caps (Stephens and McKittrick 2005) Adapted

The project progressed by increasing the amount of longitudinal and transverse reinforcement in the pile cap, varying the longitudinal steel ratio from 0.40 to 2.83 and the transverse steel ratio from 0.09 to 0.70. PC-3, PC-3a, and PC-4 included a spiral reinforcing cage inside the tube in the portion embedded in the concrete cap.

Stephens & McKittrick (2005) stated that the first two specimens failed with tension cracking of the concrete cap with a capacity of 75 percent of the calculated plastic moment. The third specimen (PC-3) slightly increased the moment capacity with a similar failure as the first two specimens. The PC-3a connection failed similarly due to tension cracking of the concrete cap; however, a substantial increase in the moment capacity was observed, with a loss of ductility. The final connection had a significant increase in reinforcing ratio, and the failure occurred through the formation of a plastic hinge in the pipe pile. The moment capacity exceeded the calculated plastic moment by 26 percent.

2.2.3.3 Performance of Steel Pipe Pile to Concrete Cap Connections: Phase III

Concrete-filled tubes are widely used in bridge substructures and foundations due to their high load-carrying capacity and speed in construction. Kappes, Berry, and Stephens (2013) investigated the performance of four U-bar connections for concrete-filled tubes (CFTs) to concrete caps, as shown in Figure 2-11. The CFT's embedment length, U-bar configuration, and the concrete pile strength were primary variables in this investigation.

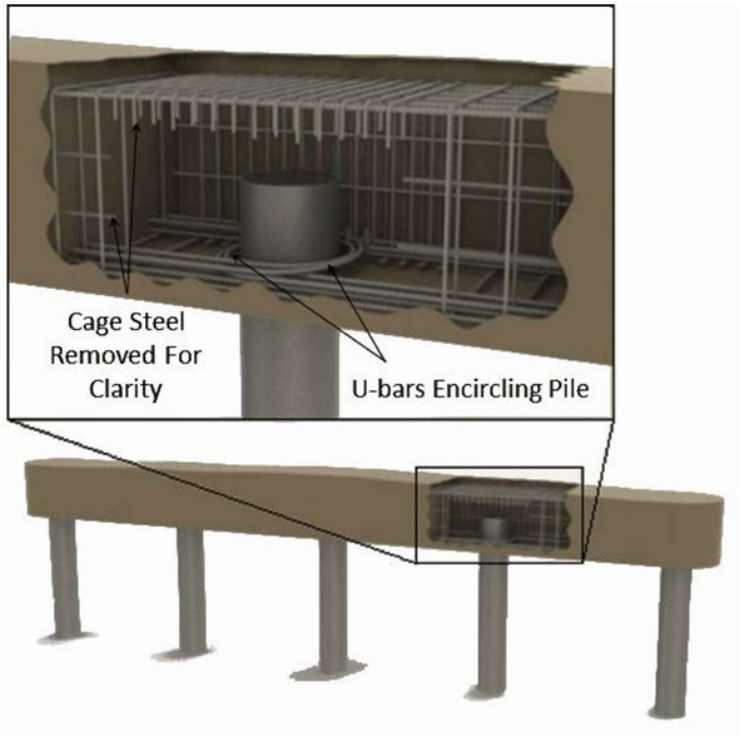

Figure 2-11: MDOT U-bar connection (Kappes et al., 2013)

Kappes et al., (2013) conducted four monotonic tests and two cyclic tests on six specimens. A summary of the test results is described in Figure 2-12. Specimen VT1 failed with the formation of a plastic hinge in the pile, while all the other specimens failed by a fracture in the concrete cap. In the cyclic tests, substantial cyclic degradation of the cap was reached at approximately 3 percent drift in all cases. The stacked U-bars will provide the same behavior in both directions.

	Test	U-bar Configuration	U-bar Location	Pile Embedment Length	Concrete Strength	Failure Mechanism	Maximum Moment at Failure
Monotonic	VT1	Single #7 U-bar in each direction	Exterior Only	9.0 in	6250 psi	Plastic hinge in steel pipe pile	119.2 ft·kip
	VT2	Single #4 and #5 U-bar in each direction	Exterior Only	11.75 in	3800 psi	Fracture of the concrete pile cap	173.8 ft·kip
	VT2.5	Single #7 U-bar in each direction	Exterior Only	9.0 in	6250 psi	Fracture of the concrete pile cap	138.5 ft·kip
	VT3	Single #7 U-bar in each direction	Exterior Only	10.375 in	4100 psi	Fracture of the concrete pile cap	151.7 ft·kip
Cyclic	CT1	Single #4 and #5 U-bar in each direction	Exterior Only	11.75 in	4200 psi	Fracture of the concrete pile cap	172.4 ft·kip
	CT2	Single #4 and #5 U-bar in each direction	Interior and Exterior	11.75 in	4200 psi	Fracture of the concrete pile cap	181.8 ft·kip

Figure 2-12: Summary of test results (Kappes et al., 2013)

Kappes et al., (2013) found that the current design provisions produce conservative designs across the limit states with respect to ultimate capacity. However, despite the great insights of this study, a series of aspects still need to be addressed to obtain a complete design methodology.

2.3 SUMMARY

A significant amount of work has been done to explore the behavior of pile-to-cap connections. Over the years, a variety of configurations have been evaluated with FE models and experimental testing of steel H-piles, reinforced concrete piles, hollow steel piles, and concrete-filled tubes. The effort to obtain information on this area demonstrates the relevance of investigating this topic.

Several factors seem to contribute to the behavior of the connections and the different failure modes, with the embedment depth of the pile into the cap being the most recurrent. Similarly, the level of detail in the connection contributed to the level of fixity of the pile, influencing the moment capacity of the systems. Other factors like the amount of reinforcement of the concrete bent cap and different anchoring systems, influenced the overall performance of the connection.

Despite the significant investigation conducted to obtain alternative ways to connect pile-to-pile caps, there is no specific guide in the design methodology of the different alternatives. Many results show the substantial capacity of steel pipe piles and the advantages they provide for efficient structural configurations.

Despite the valuable insights obtained, most research studies addressed specific scenarios, leaving other conditions and configurations unaddressed. Current design practices follow specific needs with the limitations in the existing guidelines. The study described in this thesis addresses these gaps by systematically evaluating five connection types under gradually increasing lateral pseudo-static loading under the same laboratory conditions. The different connections investigated in this research reflected the analysis of variables such as the embedment length, bearing area, type of reinforcement, and anchorage type.

CHAPTER 3 DESIGN AND FABRICATION OF SPECIMENS

3.1 INTRODUCTION

The experimental specimens used in this research study consisted of five cast-in-place concrete bent caps connected to steel pipe piles by five connection subassemblages. A standard ALDOT Class B concrete mixture design was used for fabricating all specimens. The design and fabrication of these specimens are described in this chapter.

3.2 PROJECT SPECIFICATIONS

The design and material specifications of the specimens considered for this study are presented in this section.

3.2.1 Connections Design

Previous to this project, a study on the feasibility of using steel pipe piles for ALDOT bridges was conducted by Rosy Sharma (2023). All five connections designed by Sharma were done according to the ALDOT design specifications, the design provisions of the American Concrete Institute (2019), and the AASHTO LRFD Bridge Design Specification (2020).

This section summarizes the connection details proposed by Sharma, which were used as the basis for this project. Additional details can be found in Sharma's thesis in chapters 4 and 6.

3.2.1.1 Demands

The demands on top of the pile obtained by Sharma (2023) for a layout of two large-diameter piles and six girders are presented herein. The analysis was made in accordance with AASHTO (2020) with the governing load case coming from the Strength-III limit state.

Axial load demand P_u=*530 kips*

Flexural Demand M_u=*292 kip-ft*

Shear demand perpendicular to bent cap V_{uz}=*9 kips*

Shear demand parallel to bent cap V_{ux}=*21 kips*

Figure 3-1 describes the configuration used in Sharma's analysis.

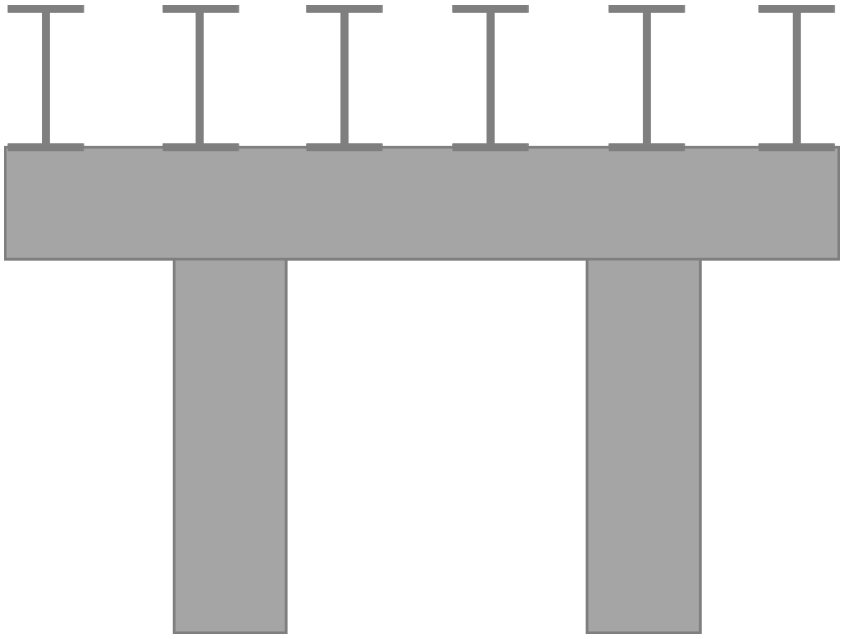

Figure 3-1: Configuration of two piles and six girders.

3.2.1.2 Design Considerations

Sharma (2023) proposed robust connections between the steel pipe pile and the reinforced concrete bent cap. The summary of the proposed considerations is presented below:

1. The steel pipe pile has a 3 ft diameter with a wall thickness of ½ in.
2. The pile extends to the bent cap with through holes to allow the reinforcement to pass through without conflict.
3. Concrete plugs are included at the top of the pile and then transition to a hollow steel pipe pile.
4. The cross-section dimensions of the concrete bent cap are 4 ft x 4 ½ ft.

3.2.1.3 Proposed Connections

Sharma (2023) proposed three types of reinforcing steel connections consisting of reinforcing bars extending from the concrete bent cap to the steel pipe pile filled with a concrete plug. Additionally, two other types of connections consisting of mechanical

connections welded on the top of the piles were also proposed. A summary of the five types of connections developed by Sharma (2023) are presented as follows:

1. Headed reinforcing bars with mechanical anchors with transverse confining reinforcement
2. Hooked reinforcing bars with 180° bend hooks with transverse confining reinforcement
3. Straight reinforcing bars with transverse confining reinforcement
4. Shear studs welded to the exterior face of the pile
5. Annular ring welded on top of the pile

Sharma's thesis provides additional details about the capacity of each type of connection in Chapter 4 and Appendices F, G, and H. Figure 3-2 summarizes the connections proposed by Sharma (2023).

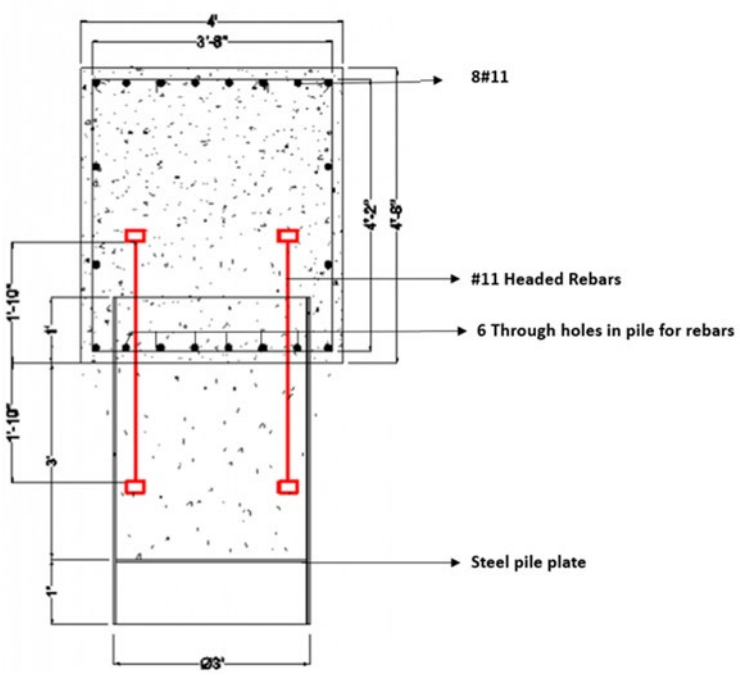

1. Headed-bar connection

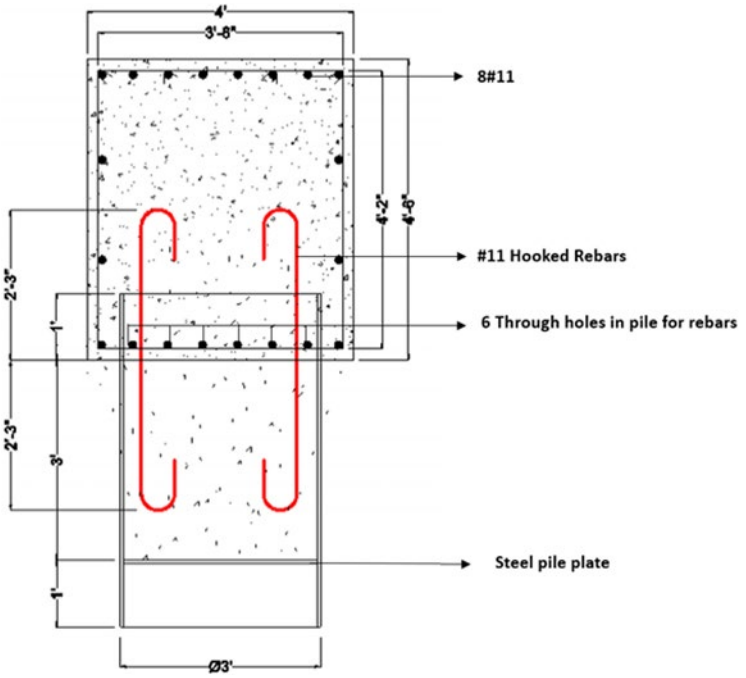

2. Hooked-bar connection

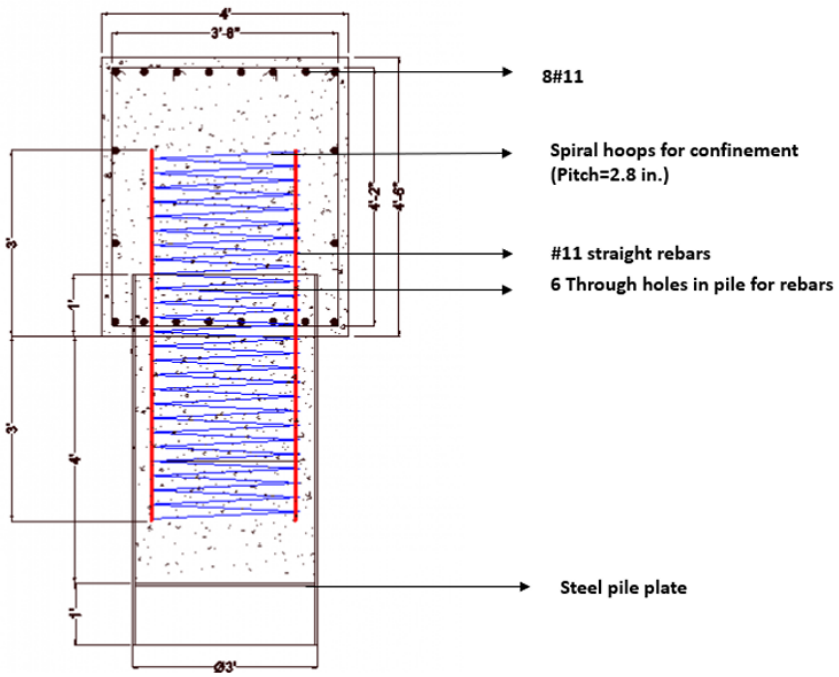

3. Straight-bar connection

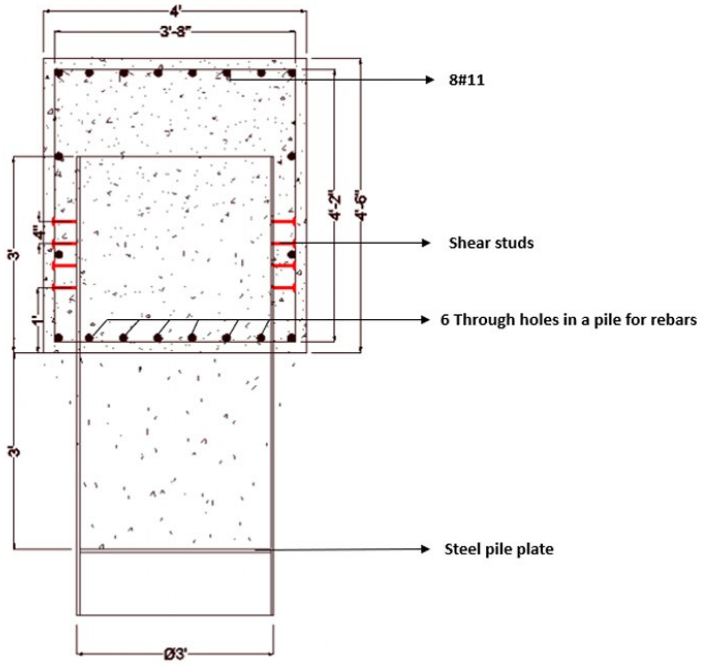

4. Shear stud connection

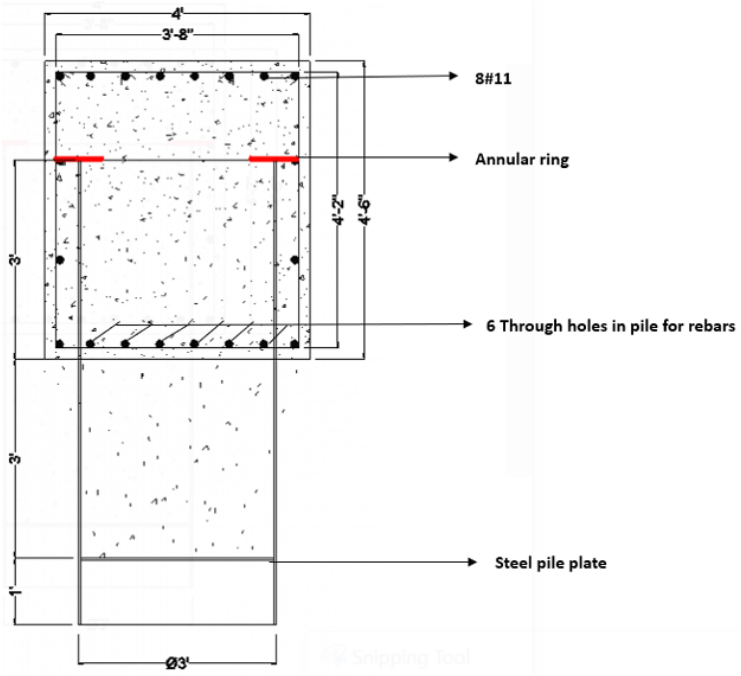

4. Annular ring connection

Figure 3-2: Connections proposed by Sharma (2023)

3.2.2 ESTIMATED CAPACITY OF THE SPECIMENS

The capacity of the specimens was estimated. The predicted capacity of the reinforcing-bar connections was based on the flexural strength of the reinforced concrete plug cross section neglecting the contribution of the pipe pile. This capacity was obtained by using *Response2000*, developed at the University of Toronto by Evan C. Bentz (2000). Eight No. 11 bars evenly distributed in the circular cross section were considered, resulting in a nominal moment capacity (M_n) of 937.5 kip-ft. Several assumptions were made to obtain the predicted strength:

1. No contribution of the steel pipe pile to the strength of the cross-section
2. Zero axial force on this section
3. Plane sections remain plane
4. Strain compatibility between concrete and steel reinforcing bars
5. Linear-elastic/perfectly plastic behavior of steel reinforcing bars
6. Concrete compressive strength equal to the 28-day compressive strength of the first (headed-bar) test specimen
7. Reinforcing steel yield strength equal to the test value reported by the manufacturer

For the shear stud specimen, which had no reinforcing bars, a nominal moment capacity (M_n) of 769.6 kip-ft was obtained based on the predicted contribution of the 36 shear studs to the pile anchorage capacity. To accommodate all 36 shear studs, an increased embedment was necessary (3 ft).

The annular ring specimen has a calculated flexural capacity of 2225 kip-ft based on an iterative design approach using the embedment depth formula from the Washington DOT Design Manual (2024). The concrete failure is expected to occur before the ring yields or reaches full capacity.

The nominal (plastic) moment capacity (M_n) of hollow steel pile alone is 2370 kip-ft, based on the manufacturer-supplied yield stress.

3.2.3 Material Properties Requirements

The material properties used for the design of the specimens, such as concrete, spiral welded steel, and mild steel, are described in this chapter.

3.2.3.1 Steel Pipe Pile Properties

The specifications for the fabrication of spiral-weld steel pipes involve several ASTM standards. A1011 and A1018 are used for the coil to meet physical and chemical requirements. Others, like A139, A252, A500, and A1085, are used for manufacturing pipes.

A hollow pipe with 3 ft (36 in.) diameter with ½ in. thickness requires an available yield strength of 70 ksi.

3.2.3.2 Reinforcing Steel Properties

The design requirements for mild reinforcing steel follow ASTM A615 Grade 60. The yield strength of steel (f_y) corresponds to 60 ksi. The longitudinal tension and compression reinforcement consist of No. 11 bars. The transverse shear stirrups consist of No. 5 reinforcing bars. This configuration is true for bent caps and all the connections with reinforcing bars.

3.2.3.3 Concrete Properties

The Alabama Department of Transportation Standard Specifications for Highway Construction (2022) sections 501 and 512 specify the type of concrete used for different structures. For this project, Class B Concrete Mixture Design is specified for cast-in-place bridge substructures and bridge superstructures.

Figure 3-3 describes the requirements for Class B concrete according to ALDOT specifications. The target properties for a Class B concrete mixture include a concrete compressive strength (f'_c) of 4000 psi at 28 days, the strength required for the specimens to be tested in the laboratory.

PREQUALIFICATION REQUIREMENTS FOR CONCRETE MIXTURE DESIGN				
Concrete Class	Class A	Class B	Class C	Class D
Minimum 28-Day Compressive Strength (psi) {Mpa}	3,000 {21}	4,000 {28}	3,000 {21}	3,000 {21}
Maximum Water/Cementitious Materials Ratio	0.50	0.45	0.55	0.45
Range of Total Air Content (%)	2.5 - 6.0	2.5 - 6.0	2.5 - 6.0	2.5 - 6.0
Slump (in) {mm}	3.0 {75}	3.5 {90}	3.0 {75}	7.0 {180}
Maximum 28-Day Drying Shrinkage (%)	--	0.04	--	--
Largest Nominal Maximum Aggregate Size (in) {mm}	1.0 {25}	1.0 {25}	1.0 {25}	1.0 {25}

Figure 3-3: ALDOT section 501 requirements for concrete mixtures

As shown in Figure 3-2, the air content range was specified to be 2.5%-6.0%. Similarly, a w/c of 0.5 and 3.5 in. target slump were specified for the concrete mixture.

3.3 EXPERIMENTAL PROGRAM DESIGN

Based on the proposed connections mentioned before, the experimental program was designed accordingly.

All figures presented in this section represent the specimens built in the laboratory. In this case, upside down, opposite to the position they would have in a bridge, as described in Figure 3-4. This allows for a more straightforward construction process and laboratory testing. The following sub-sections refer to the reinforcement, with the top corresponding to the tension reinforcing bars and the bottom to the compression reinforcing bars.

Figure 3-4: Test specimen adapted to laboratory conditions

The five connections proposed for this experimental study are shown in Figure 3-5. The reinforcement of the bent cap and the details of each connection are found in the subsequent sections of this chapter.

Figure 3-5: Proposed connections

The proposed test configuration is shown in Figure 3-6. All five specimens were built full-scale and tested in this position, allowing consistency and simplifying the necessary processes. Due to the size and weight of each, transportation was also simpler in this position.

The loading protocol consisted of pseudo-static loads applied laterally in the direction of the load represented by a green arrow in Figure 3-5. The applied load cycles at different load levels are described in detail in section 4.2 of this thesis. In this portion of the research project, only lateral loads were applied as they are expected to represent the worst-case scenario. The combined effects of axial compression will be evaluated in the next portion of the project.

Figure 3-6: Proposed test configuration

It is important to monitor the response of the specimens throughout the test. Different types of instrumentation were used to measure strain, displacement, and rotation of the specimens during testing. The details of all the instrumentation used for this experimental study can be found in section 4.3 of this thesis.

3.3.1 SPECIMEN DETAILS AND CONFIGURATION

Five full-scale specimens were fabricated for this experimental study. The configuration of each specimen, the procedure to fabricate them, and the post-fabrication characteristics are detailed in this section.

Five substructure connection types used for this study are described below. The specimen types are named as follows:

1) Head, 2) Hook, 3) Straight, 4) Stud, and 5) Ring.

3.3.1.1 Concrete Bent Cap

The design considerations of the reinforced concrete bent cap follow standard ALDOT specifications.

The concrete bent cap design configuration was consistent for all five experimental specimens. It consisted of a 4 ft x 4.5 ft x 12 ft rectangular concrete cap reinforced by 20 No. 11 reinforcing bars and 16 No. 5 stirrups.

Figure 3-7 shows the longitudinal reinforcement layout. Sixteen longitudinal reinforcing bars with 180° bend hooks and four headed bars that pass through the steel pipe pile on the top of the bent cap represent the flexural reinforcement. The minimum inside diameter bend for a No. 11, 180-degree hooked bar is $8d_b$, with a straight extension greater than $8d_b$ or 2.5 in.

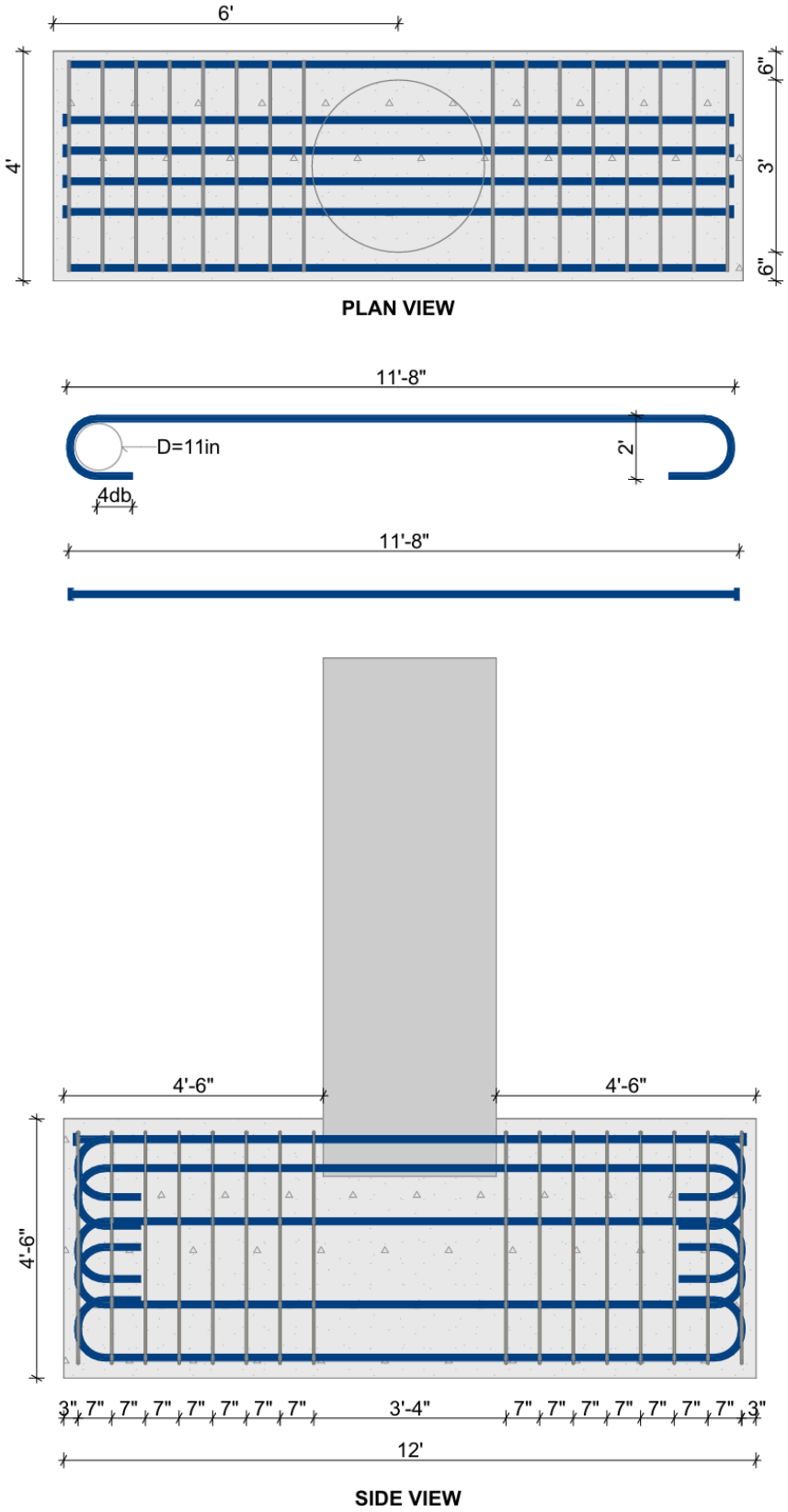

Figure 3-7: Bent cap longitudinal reinforcement

The transverse reinforcement consisted of sixteen 4-legged No. 5 bars every 7 in. formed using 32 U bars and 16 C bars. The details of the stirrups are shown in Figure 3-8. For 135-degree hook stirrups, a minimum inside bend of $4d_b$ is required for No. 5 bars. A straight extension of the maximum between $6d_b$ and 3 in. is also necessary.

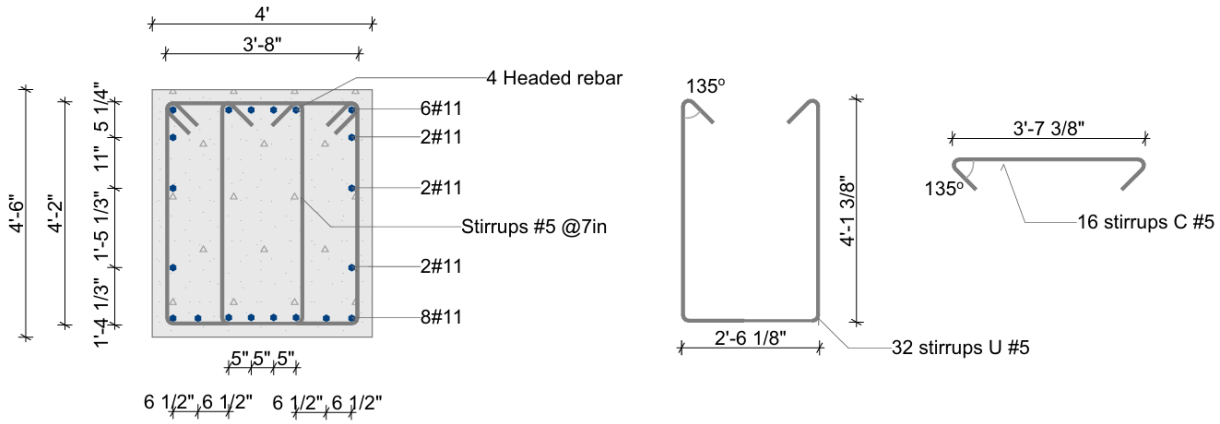

Figure 3-8: Bent cap transverse reinforcement

A spiral welded hollow steel pipe pile was placed on top of each specimen at the center of the bent cap. A 3 ft diameter, ½ in. thickness, and 9 ft long steel pipe pile was used for each of the three reinforcing steel connection specimens with reinforcing steel connections. On the other hand, the two specimens with welded mechanical anchorages used a 3 ft diameter, ½ in. thickness, and 11 ft long steel pipe pile. The embedment depth of each pile can be found in the corresponding subsections. A representation of the pile sizes used in this study is shown in Figure 3-9.

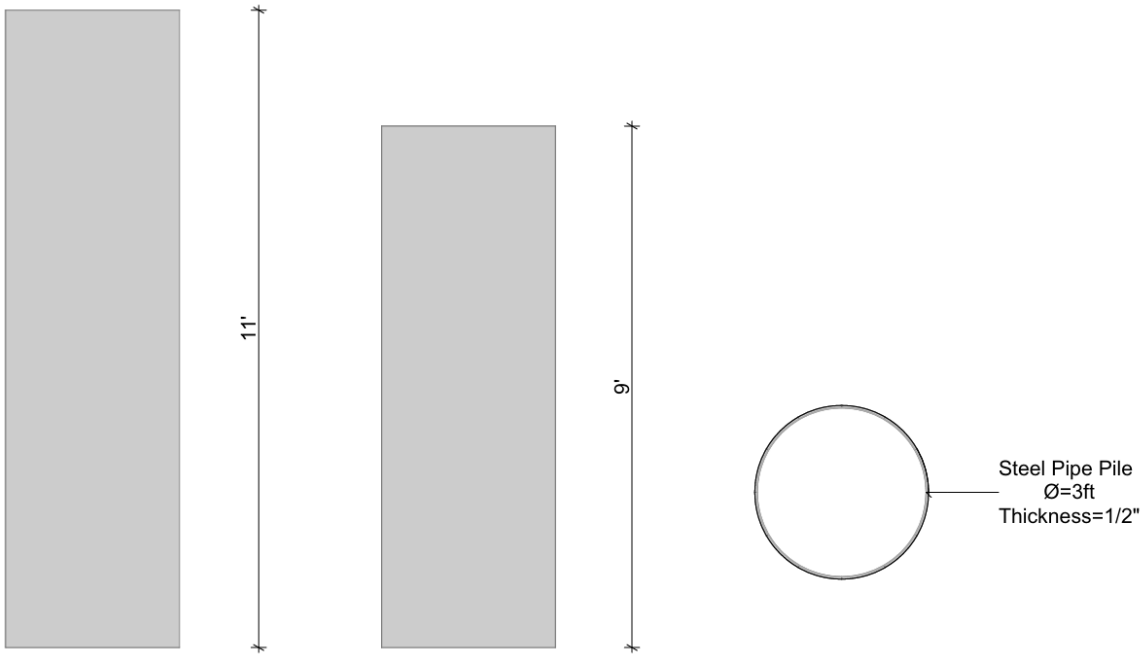

Figure 3-9: Steel pipe pile sizes

3.3.1.2 Specimen 1: Headed-Bar Connection (Head)

The headed-bar connection (Head) consists of eight No. 11 mild steel bars with mechanical steel terminators at the ends. The total length of the headed bars is 44 in. The development length for the headed bar connection was determined by following ACI 318 (2019). Due to the anchorage resistance provided by the terminators at the ends, the development length of these bars is expected to decrease compared to straight bars. This type of reinforcement offers a compact solution and avoids steel congestion during construction.

Five No. 5 hoops were evenly spaced along the length used for transverse confinement and shear resistance. The circular hoops have a total length of 126.53 in., including a 26 in. lap for a 32 in. diameter circumference. Figure 3-10 shows the layout for this connection subassemblage.

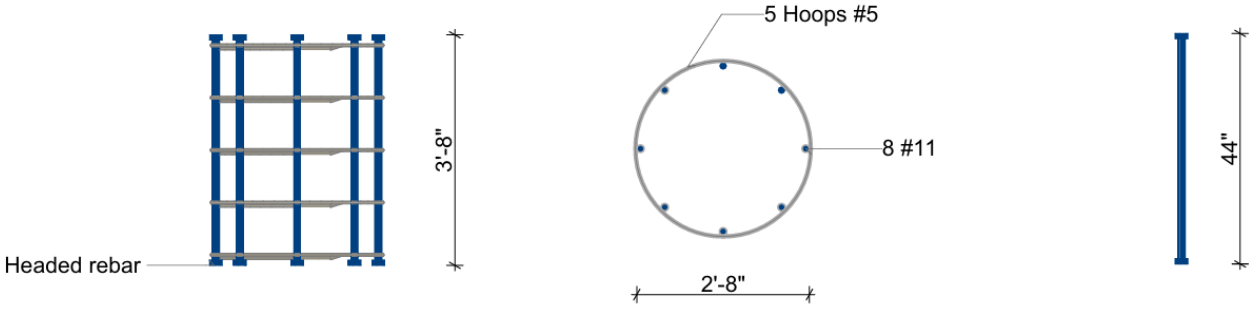

Figure 3-10: Headed-bar connection layout

The concrete bent cap configuration follows the description of section 3.3.1.1. The steel pipe pile used for this specimen is 9 ft long. The headed bars connection was placed inside the steel pile, with the middle of the connection reinforcing cage coinciding with the top of the concrete bent cap. This resulted in the headed-bar connection extending 1 ft and 10 in. into the concrete bent cap, as illustrated in Figure 3-11.

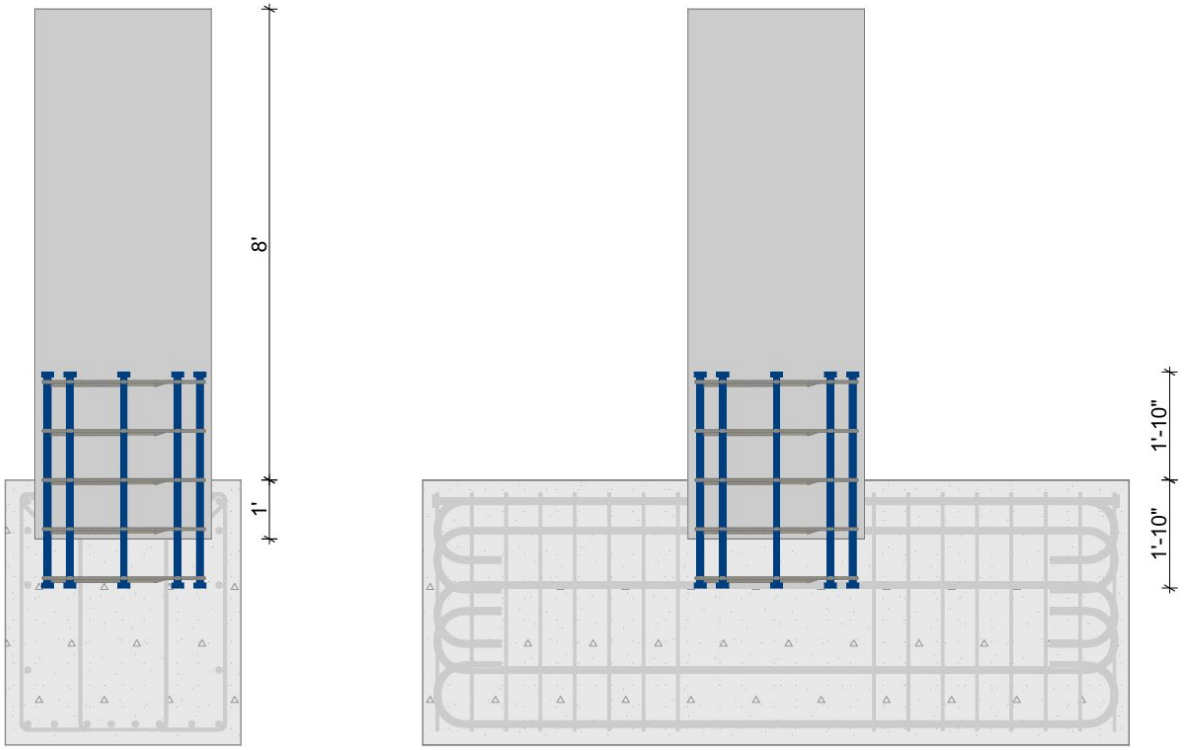

Figure 3-11: Headed-bar connection location

The steel pipe pile was embedded 1 ft below the maximum moment point for this specimen. A 3 ft. concrete plug was placed to facilitate force transfer between the pile and the bent cap and confine the reinforcement in the connection region. The concrete

plug also anchors the reinforcing bars that extend into the hollow pile, which prevents connection movement and provides environmental protection to the steel reinforcement. This configuration is shown in Figure 3-12.

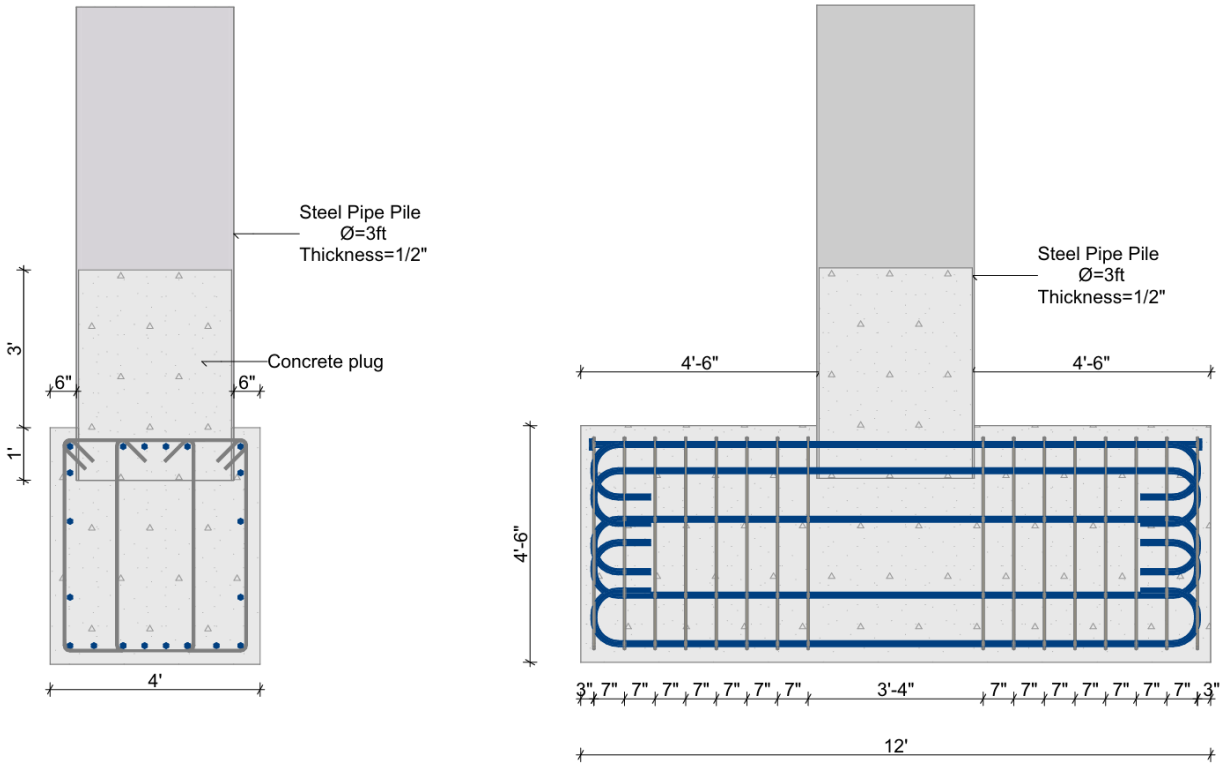

Figure 3-12: Concrete plug size and pile embedment depth

3.3.1.3 Specimen 2: Hooked-Bar Connection (Hook)

The hooked-bar connection (Hook) comprises eight No. 11 steel bars with a length of 4.5 ft. The development length of the hooked bars was calculated by following the AASHTO (2020), section 5. These 180° hooks decrease the development length of the steel into the concrete compared to straight bars. A minimum inside bend diameter of $8d_b$ and a straight extension greater than $4d_b$ or 2.5 in. is necessary. This type of element is commonly employed in reinforced concrete structures. However, constructability issues should be considered when selecting hooked anchorages, especially for 180-degree hooks.

Five No. 5 hoops were evenly distributed along the length to provide confinement and shear resistance of the connection. The circular hoops have a total length of

126.53 in., including a 26 in. lap for a 32 in. diameter circumference. Figure 3-13 shows the layout for this connection subassemblage.

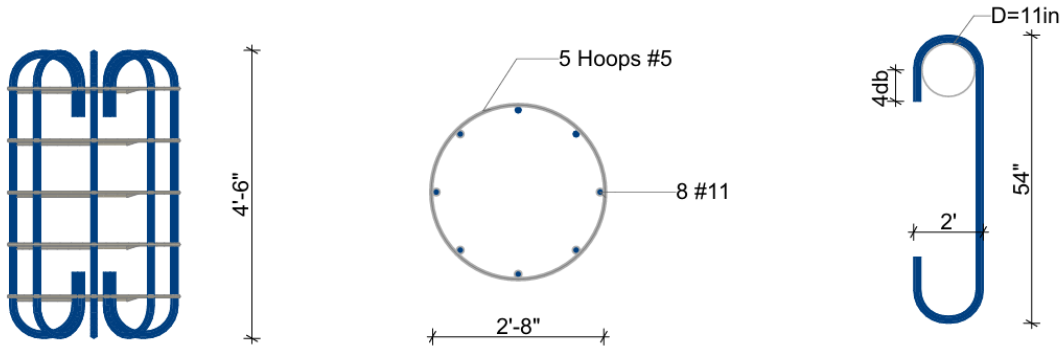

Figure 3-13: Hooked-bar connection layout

The concrete bent cap configuration used in this specimen follows the description of section 3.3.1.1. The steel pipe pile used for this specimen is 9 ft long. This resulted in the hooked-bar connection extending 2 ft and 3 in. into the concrete bent cap, as shown in Figure 3-14.

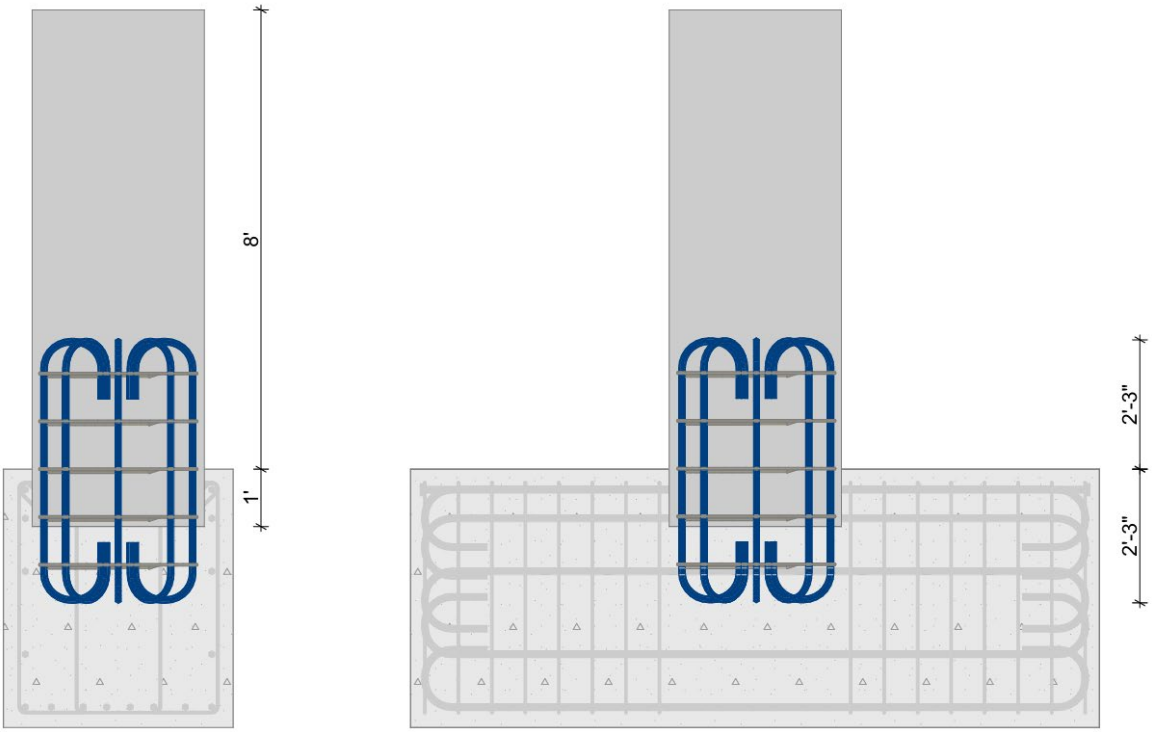

Figure 3-14: Hooked-bar connection location

Similar to section 3.3.1.2, the steel pipe pile was embedded 1 ft below the top of the bent cap for this second specimen. A 3 ft. concrete plug was placed to facilitate

force transfer between the pile and the bent cap and confine the reinforcement in the connection region. Additionally, the concrete plug provides anchorage to the reinforcing bars that extend into the hollow pile, which prevents connection movement and provides environmental protection to the steel reinforcement. This design configuration is shown in Figure 3-15.

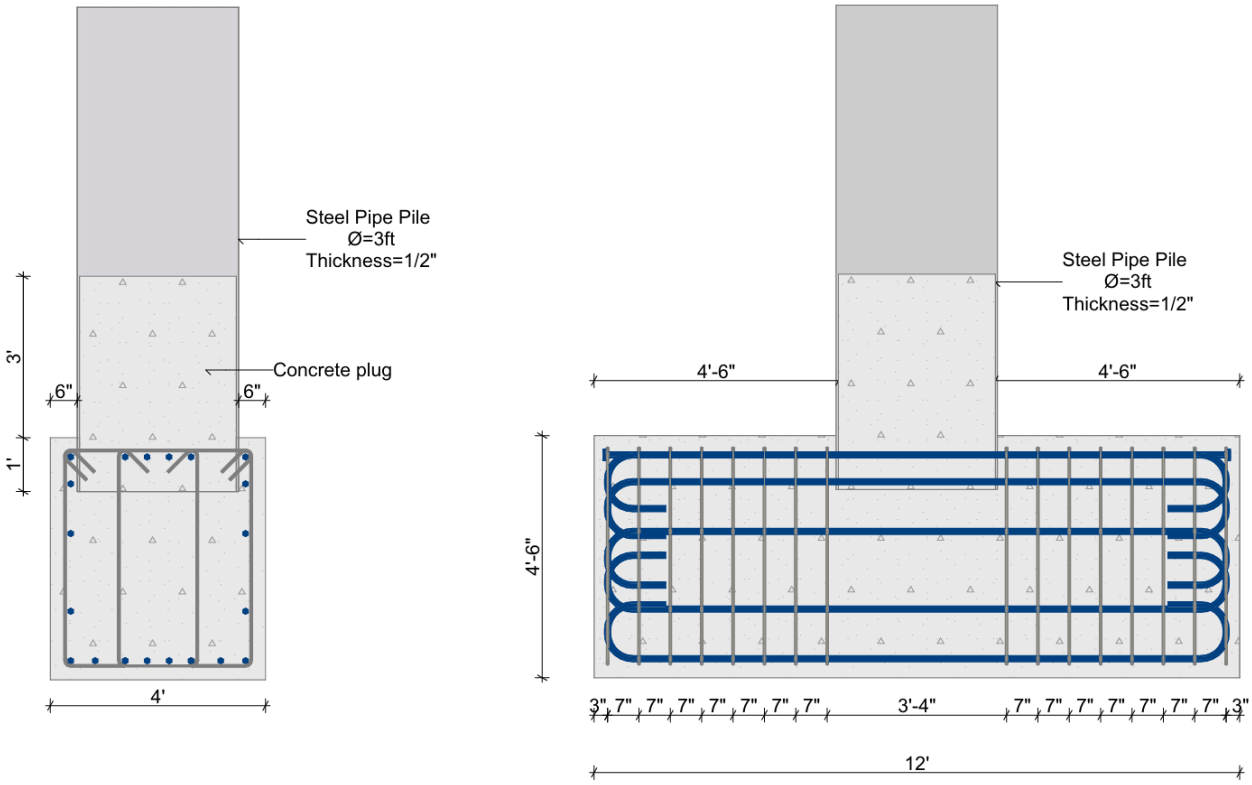

Figure 3-15: Concrete plug size and pile embedment depth

3.3.1.4 Specimen 3: Straight-Bar Connection (Straight)

The straight-bar connection (Straight) specimen comprises eight No. 11 steel bars with a full length of 7 ft each. This reinforcement layout represents the connection with a full development length, which can be significantly longer than the other alternatives with steel terminators or hooks presented in this section. The development length of the straight bars was calculated using the AASHTO (2020) specifications in section 5. This option is sometimes not feasible in locations with limited space. However, it is a simple and very economical option when its use is possible.

Due to the length of the connection, nine No. 5 hoops were evenly distributed along the length to provide confinement and shear resistance to the connection. The

circular hoops have a total length of 126.53 in., including a 26 in. lap for a 32 in. diameter circumference. The number of hoops on this connection provides stability to the reinforcing cage during construction. Figure 3-16 shows the layout for this connection subassemblage.

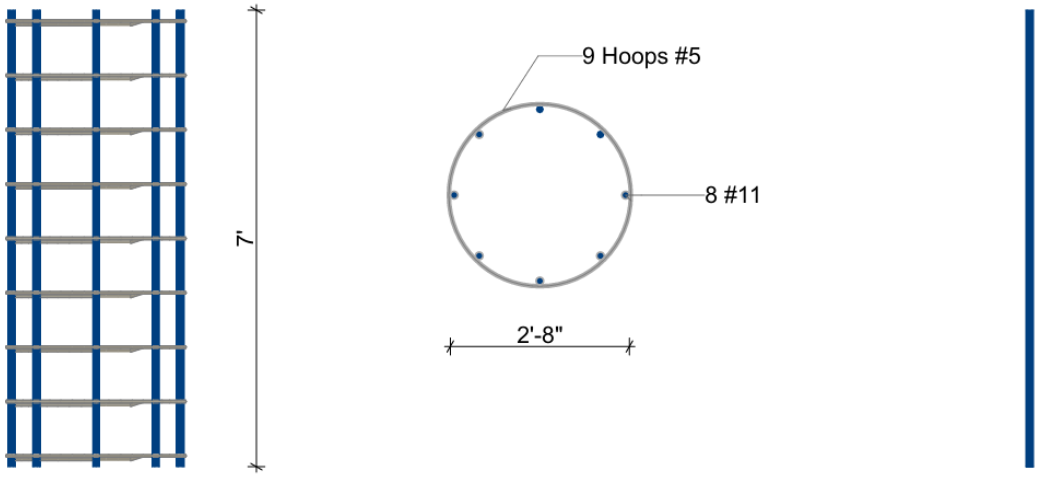

Figure 3-16: Straight-bar connection layout

The concrete bent cap configuration used in this specimen follows the description of section 3.3.1.1. The length of the steel pipe pile used for this specimen is 9 ft. This resulted in the straight-bar connection extending 3 ft and 6 in. into the concrete bent cap, as shown in Figure 3-17.

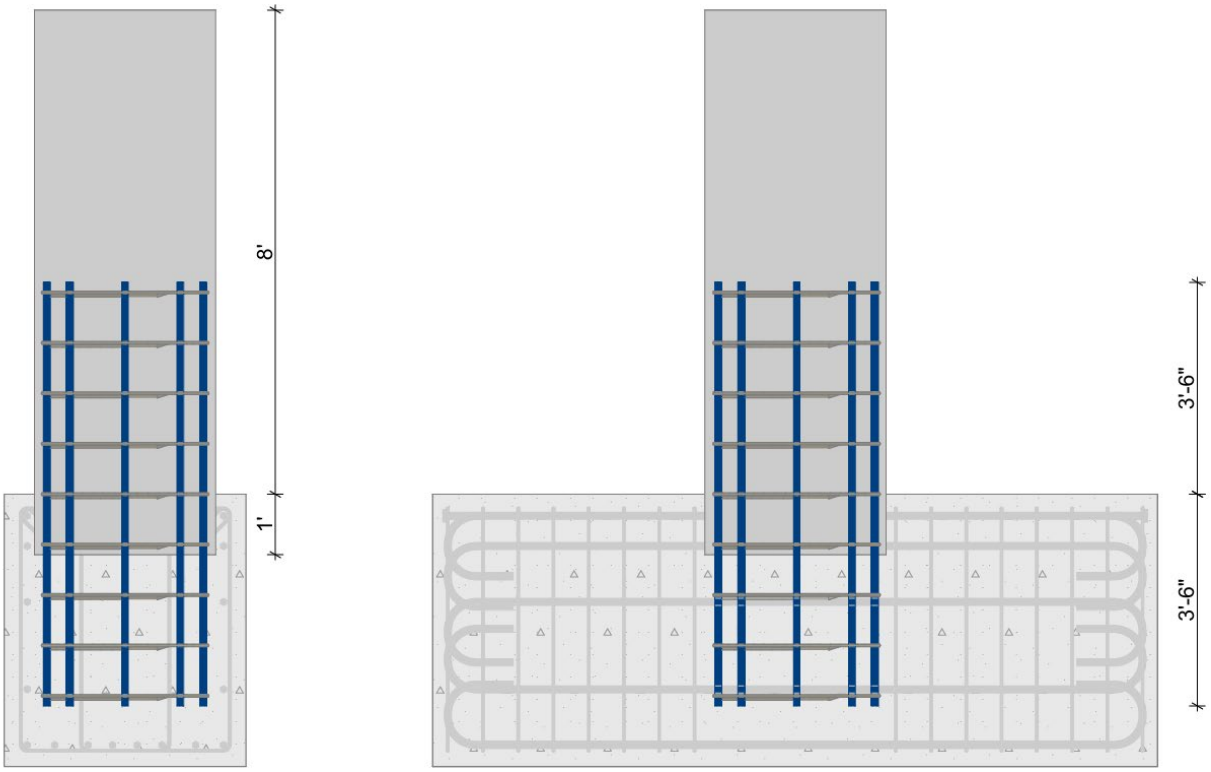

Figure 3-17: Straight-bar connection location

For this third specimen, the steel pipe pile was embedded 1 ft below the top of the bent cap. A 4 ft concrete plug was placed to facilitate force transfer between the pile and the bent cap and confine the reinforcement in the connection region. Additionally, the concrete plug provides anchorage to the reinforcing bars that extend into the hollow pile, which prevents connection movement and provides environmental protection to the steel reinforcement. This configuration is shown in Figure 3-18.

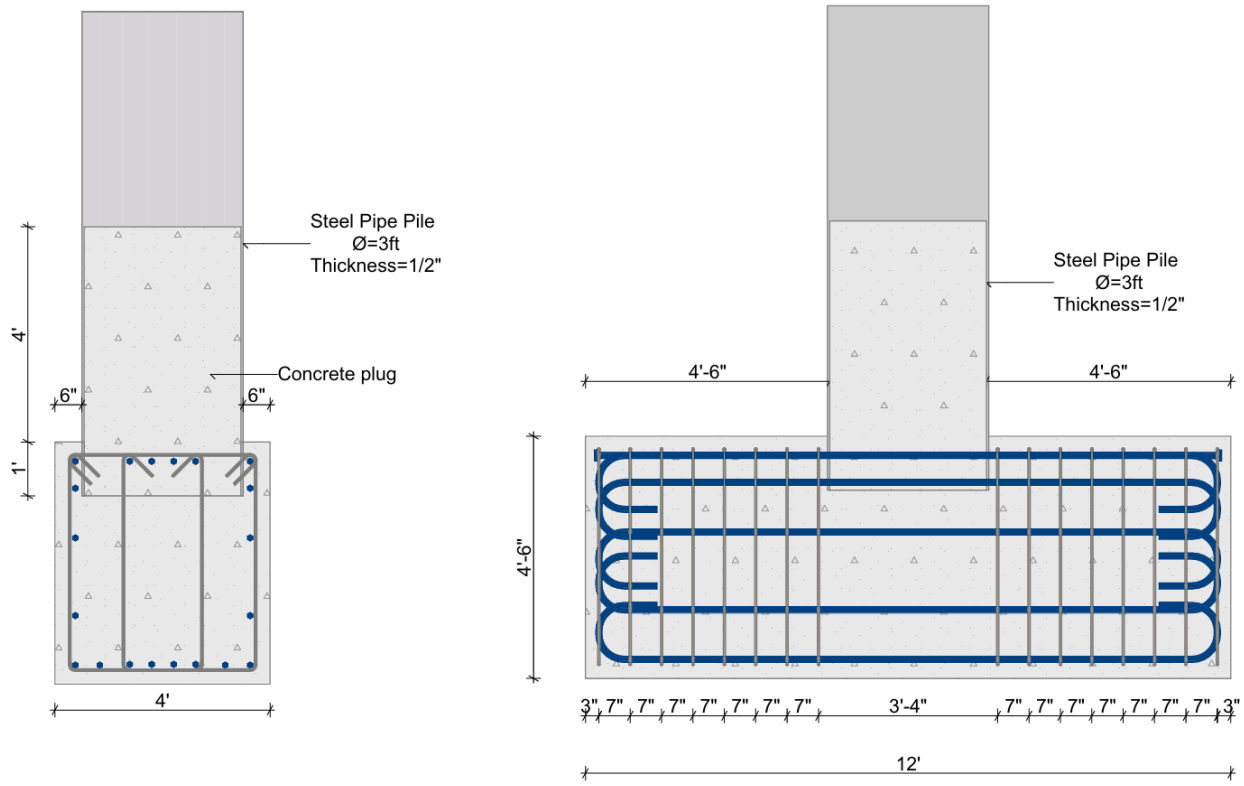

Figure 3-18: Concrete plug size and pile embedment depth

3.3.1.5 Specimen 4: Shear Stud Connection (Stud)

The shear stud connection (Stud) is one of the two in this study, anchored to the concrete bent cap by mechanical connectors welded to the outer face of the steel pile. This type of connection eliminates the requirement of reinforcing bars that join the steel pipe pile and the concrete bent cap together. Shear studs simplify the shear transfer with a strong punching shear and pullout capacity. The installation process of these connectors can be made off-site, reducing the erection time.

For this specimen, 36 shear studs were welded at the bottom of the pile, distributed in three layers of 12 each. Each shear stud consists of a 6 in. long by ¾ in. thick steel element with a ½ in. thick head. This configuration is shown in Figure 3-19 below. The design of the shear resistance follows the requirements of AASHTO (2020), section 6.

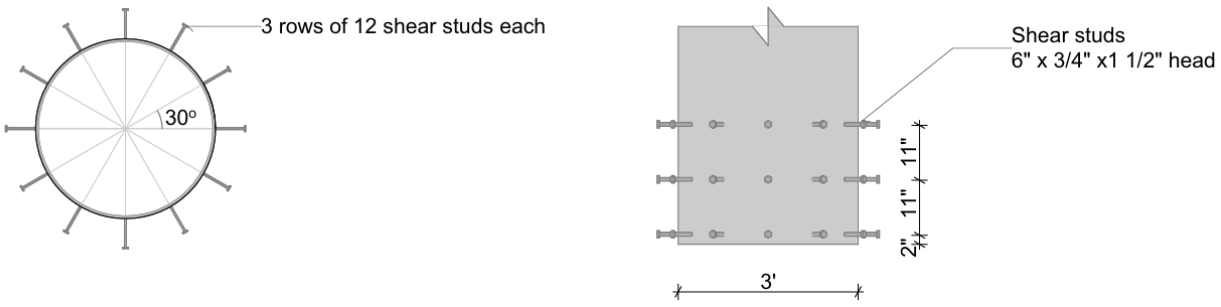

Figure 3-19: Shear stud connection layout

The concrete bent cap configuration used in this specimen follows the description of section 3.3.1.1. However, minor modifications were made to the side reinforcement locations to avoid conflict with the shear studs. The length of the steel pipe pile used for this specimen is 11 ft. The bottom of the pile was located 3 ft. below the top of the bent cap, as shown in Figure 3-20.

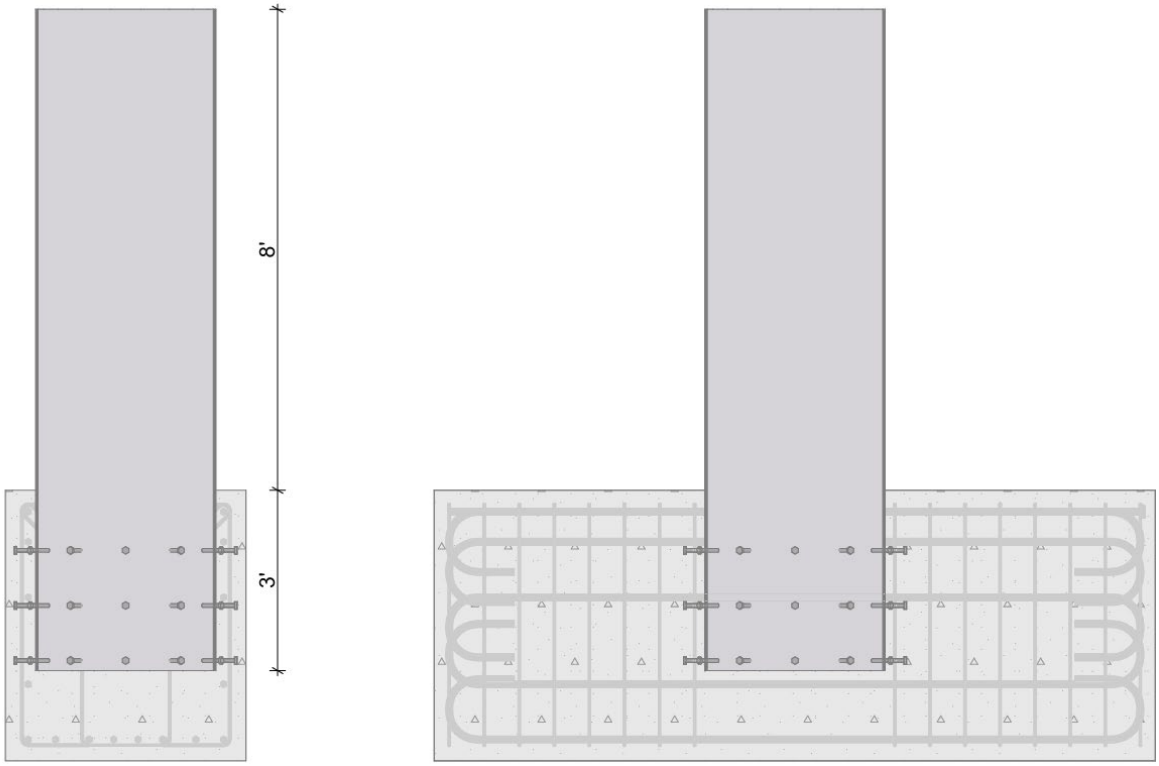

Figure 3-20: Shear stud connection location

For this shear stud specimen, the steel pipe pile was embedded 3 ft below the top of the bent cap. A 3 ft. concrete plug was placed to facilitate force transfer between the pile and the bent cap. Unlike previous specimens, the hollow pile is simply filled with

concrete and lacks additional internal reinforcement. This configuration is shown in Figure 3-21.

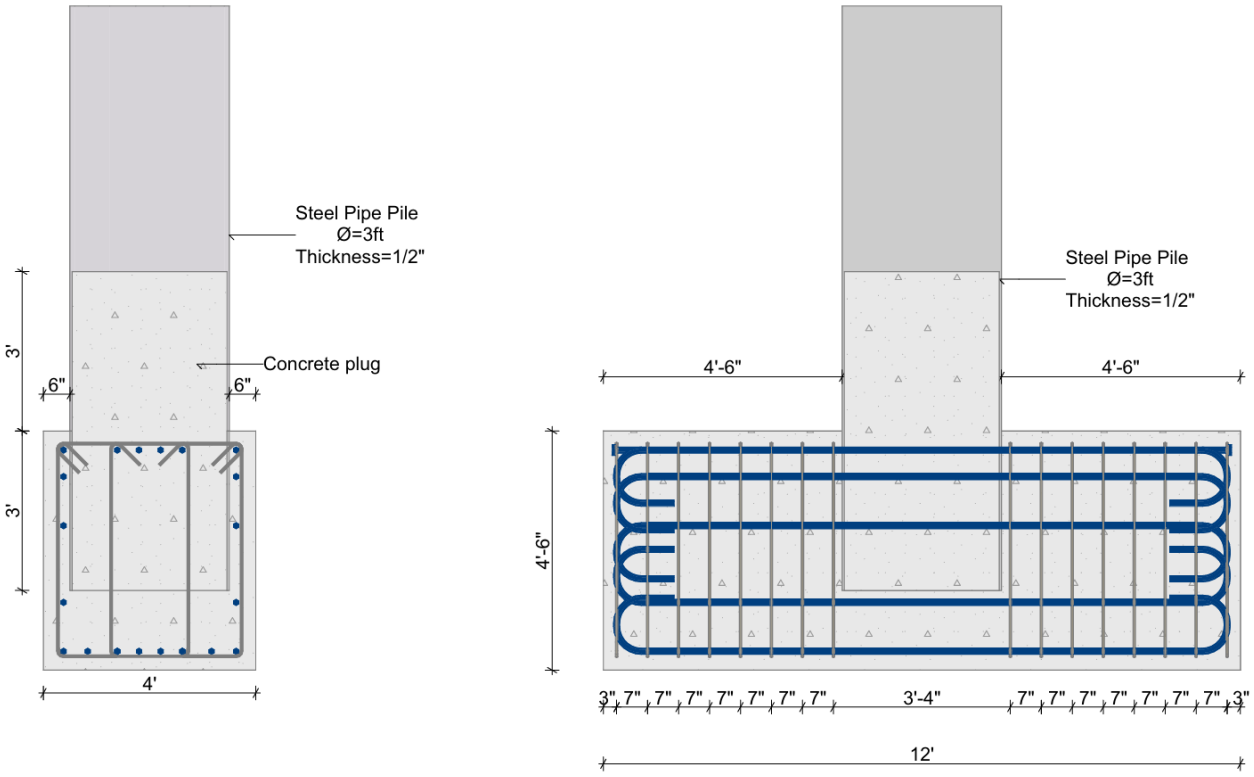

Figure 3-21: Concrete plug size and pile embedment depth

3.3.1.6 Specimen 5: Annular Ring Connection (Ring)

The last specimen studied is the annular ring connection (Ring). As its name indicates, a steel annular ring is welded to the bottom of the pile to help anchor the steel pipe pile to the concrete bent cap. This element eliminates the need for reinforcing cages that serve as a connection. This type of mechanical connection minimizes on-site efforts since the weld is made off-site, reducing the erection time and completely avoiding reinforcement congestion.

The annular ring implemented for this study has the same thickness as the steel pile, ½ in. An exterior diameter of 3 ft 8 in. and an interior diameter of 2 ft 4 in. was necessary to achieve the required anchorage. The configuration of this type of anchorage is shown in Figure 3-22. The design of the ring connections follows section 7 of the WSDOT Design Manual (2024).

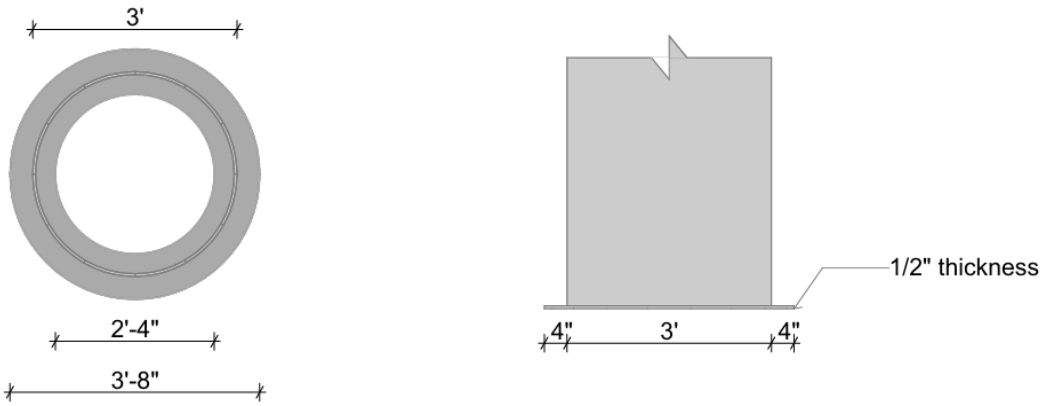

Figure 3-22: Annular ring connection layout

The concrete bent cap configuration used in this specimen follows the description of section 3.3.1.1 without any modifications. The steel pipe pile used for this specimen is 11 ft long. The bottom of the pile was located 2 ft below the top of the bent cap, as shown in Figure 3-23.

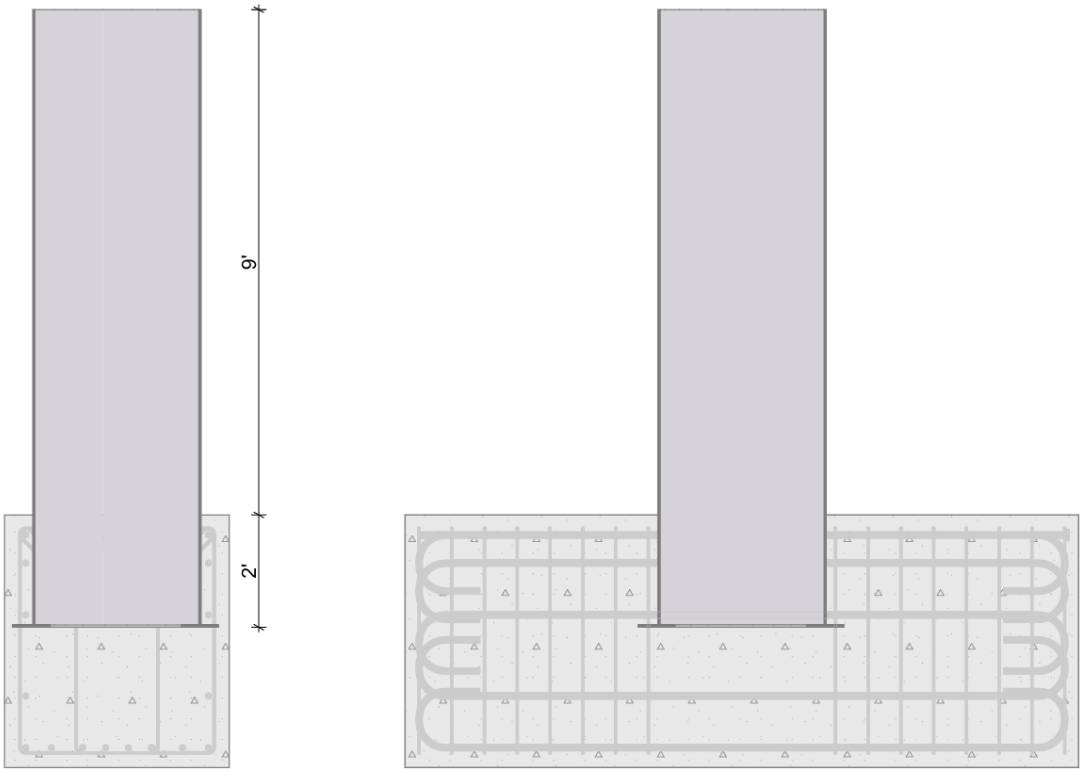

Figure 3-23: Annular ring connection location

For this fifth specimen, the steel pipe pile was embedded 2 ft below the top of the bent cap. A 3 ft concrete plug was placed to facilitate force transfer between the pile and the bent cap. Unlike the reinforcing steel connection specimens, the hollow pile is

only filled with concrete and lacks additional internal reinforcement. This configuration for the Annular Ring specimen is shown in Figure 3-24.

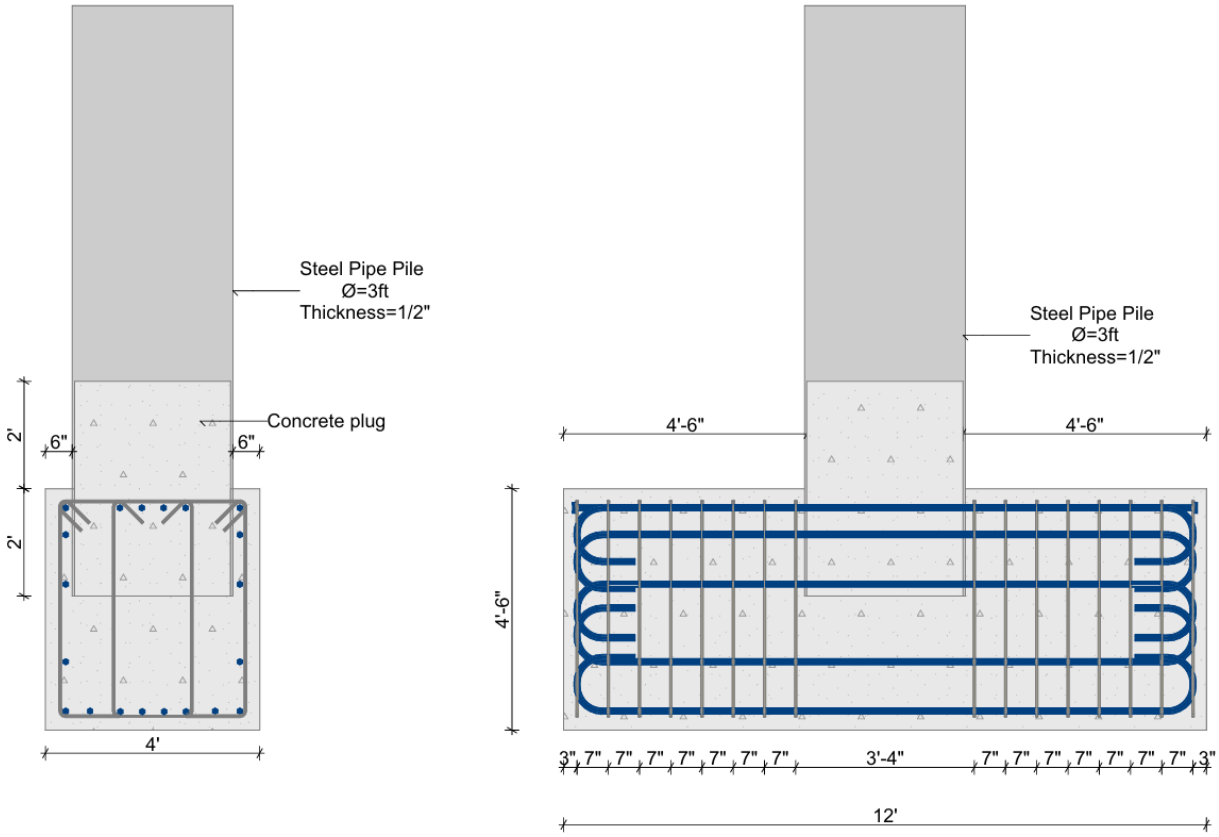

Figure 3-24: Concrete plug size and pile embedment depth

3.4 MATERIAL PROPERTIES

The materials used in the fabrication of the experimental specimens used in this study are described in this section. Concrete, steel reinforcement, and steel pipe pile properties are described based on the provider's tests, delivery certifications and post-fabrication testing.

The certifications of the materials delivered at the laboratory can be found in the Appendix section of this thesis.

3.4.1 Steel Pipe Piles

Five spiral weld pipes were received, as shown in Figure 3-25, with the corresponding certificate of conformance found in Appendix G. The steel pipes follow ASTM A252 Gr.

3 standards. The outside diameter of 36 in. and ½ in. thickness comply with the specifications of section 3.2.2.1 of this thesis. From the material certification, physical tests showed a yield strength of 65.8 ksi for the 9 ft and the 11 ft long piles, except for the 11 ft pile for the Stud specimen, which has a yield strength of 73.6 ksi.

Figure 3-25: Steel pipe piles used for fabrication of specimens

3.4.2 Reinforcing Steel

As shown in Figure 3-26, a total of 9,493 lbs of ASTM 615 (AASHTO M31), Grade 60 reinforcing bars were delivered at ASEL. This corresponds to 395 elements, which correspond to the reinforcement of five bent caps and three connections.

Physical testing showed that the yield strength of the reinforcing bars corresponds to 67.5 ksi for the No. 11 bars and 74.4 ksi for the No. 5 bars.

Figure 3-26: Reinforcing bars used for specimen fabrication

A description of all the reinforcing bars received for constructing the five specimens described in section 3.3 is presented in Table 3-1 below.

Table 3-1: Delivered reinforcement characteristics

	Bar No.	Type	#	Total length	Comments
Bent Caps	11	Headed bars	20	11 ft 6 in.	Threaded head terminators at ends. ASTM A970
		Hooked bars	80	14 ft 10 in.	180-degree hooks at the ends
	5	U stirrups	160	11 ft 7 in.	135-degree standard hooks at ends
		C stirrups	120	4 ft 6 in.	135-degree standard hooks at ends
Reinforcing steel connections	11	Headed bars	8	5 ft 6 in.	Threaded head terminators at ends. ASTM A970
	11	Hooked bars	8	7 ft 8 in.	180-degree hooks at the ends
	11	Straight bars	8	7 ft 6 in.	-
	5	Circular stirrups	19	10 ft 2 in.	32 in. diameter and 22 in. lap

3.4.3 Head Terminators

The threaded head terminators used for the Head specimen connection and the top tension steel reinforcing bars in the concrete bent caps follow ASTM A970. Figure 3-27 shows the heads used in this study.

Figure 3-27: Threaded head terminators used for specimen fabrication

3.4.4 Shear Studs

The shear studs used for this study follow ASTM A379. Nelson Nelweld 6000 Welder was used with ceramic ferrules FB 3/4 F152. The studs have an ultimate tensile stress (F_u) of 73.6 ksi based on the material certificate data. Figure 3-28 shows the shear studs used.

Figure 3-28: Shear studs used for the specimen fabrication

3.4.5 Annular Ring

The annular ring welded at the bottom of the pile for the Ring connection follows ASTM A572 Grade 50 with a yield strength (F_y) of 59 ksi based on the corresponding material certification. Figure 3-29 depicts the annular ring used on this project.

Figure 3-29: Annular ring used for specimen fabrication

3.4.6 Concrete

ALDOT Class B concrete mixture was used for all five specimens in this study. The characteristics of each mixture delivered on-site, fresh property testing, and hardened property testing are described for each specimen in this section.

3.4.6.1 Concrete Mixtures

The information presented in Table 3-2 summarizes the information received by the concrete provider related to the concrete mixture of each specimen.

Table 3-2: Concrete mixtures

Specimen	Total Yards	Cement (lbs)	Sand (lbs)	Stone (lbs)	Water (lbs)	HRWR (oz)
Head	7.50	5000	9885	12762	244.6	1877
Hook	10.13	6988	13523	17488	341.2	2572
Straight	10.69	6630	14278	18312	349.4	2222
Stud	9.67	6077	12746	16477	288.2	2423
Ring	10.19	6394	13383	17337	289.9	2563

The materials used in the concrete mixtures come from the following sources:

Concrete sand from Foley Materials in Montgomery, AL.

Coarse aggregate size 57 from Vulcan Materials in Notasulga, AL.

Water reducer is Darnlok 785.

Cement Type 1L from Argos.

3.4.6.2 Fresh Concrete Property Testing

The specimens were cast in the high bay of the Advanced Structural Engineering Laboratory using a ready-mix truck from JDL Concrete to provide 9.0 - 11.0 cubic yards needed for each specimen cast.

To ensure good conditions of the delivered concrete for every specimen, tests were performed on fresh concrete before concrete placement to ensure values within the permissible ranges.

The slump test, was performed in accordance with AASHTO T 119. It is used to determine how workable and flowable the consistency of fresh concrete is. Figure 3-30 depicts how the test is performed.

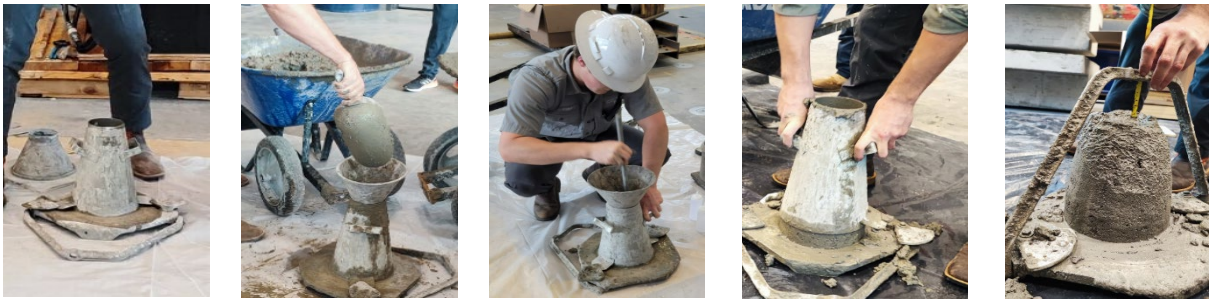

Figure 3-30: Slump test process

Another test used to measure fresh concrete properties is the air content test, which is used to quantify the percentage of air entrained in the concrete sample. This test was performed using the pressure method per the requirements of AASHTO T 160. This process can be seen in Figure 3-31.

Figure 3-31: Air content test

In addition to the tests mentioned previously, the temperature of the concrete and its weight are data that were also registered for each specimen. A summary of the fresh concrete properties is described in Table 3-3 below.

Table 3-3: Fresh concrete properties

Specimen	Placement Date	Slump (in)	Air Content (%)	Temperature (°F)
Head	4/11/2024	4.25	5.5	70
Hook	6/6/2024	6.0	4.5	80
Straight	8/13/2024	5.5	5.6	90
Stud	11/19/2024	3.5	4.5	70
Ring	10/23/2024	4.0	5.5	72

The data above shows that the air content complies with ALDOT specifications described in section 3.2.2.3 of this thesis for all specimens. According to the ALDOT specifications, there is a +1 in. tolerance for slump. However, the target slump of 3.5 in.

+1 in. tolerance was not achieved for some of the concrete mixtures. It is important to mention that the last didn't adversely affect the concrete 28-day compressive strength (f'_c) or at the moment of concrete placement for any of the specimens.

3.4.6.3 Hardened Concrete Property Testing

On the day of concrete placement, 4 x 8 in. cylinders were made in accordance with ASTM C31. For this size of cylinders, two layers of concrete, each rodded 25 times, and 12 taps were necessary. Figure 3-32 illustrates the making process of the cylinders.

Figure 3-32: Cylinders making process

Two types of curing methods were used. For each specimen, half of the cylinders were transferred to a curing room the day after concrete placement. This process followed ASTM C192 (AASHTO R39) for moist-cured cylinders. The other half remained next to the cast-in-place specimen to be air-cured in the same environment as their respective specimen. All cylinders were used to perform compressive strength tests at 7 days, 28 days, and on the day of specimen testing. A summary of the compressive strength results obtained for all five specimens is presented in Table 3-4.

Table 3-4: Compressive strength results

Specimen Name	Specimen Number	Age (days)	Compressive Strength (psi) Air Dry	Compressive Strength (psi) Moist Cured
Head	1	7	3,820	-
		28	4,450	4,950
		176*	4,960	6,820
Hook	2	7	3,930	4,050
		28	4,530	4,520
		131*	5,280	5,400
Straight	3	7	3,640	3,720
		28	4,170	3,930
		78*	4,100	4,600
Stud	4	7	4,120	4,350
		28	5,110	5,380
		22*	5,230	5,360
Ring	5	7	4,150	4,310
		28	5,330	5,070
		35*	5,120	5,380

* Age of specimen on the day of testing

A standard ASTM C39 (AASHTO T22) test method for the compressive strength of the cylindrical concrete specimens was followed. All specimens exceeded the compressive strength (f'_c) of 4000 psi for air dry conditions at 28 days. Additionally, a compressive strength significantly greater than 4 ksi is achieved on the testing day for all specimens, which are represented by an asterisk on the third row of each specimen on the table above.

3.5 SPECIMEN FABRICATION

Five full-scale connection assemblages were fabricated for this study. The steps prior to and during the casting of these specimens are presented in this section.

3.5.1 Reinforcement Cages

The configuration of the five bent cap reinforcing cages is described in section 3.3.1.1. Since all specimens have an identical steel reinforcement configuration, all followed the same fabrication process.

Prior to starting to build the first reinforcing cage, all steel bars that required a strain gauge were put aside. All the strain gauge locations were marked and ground, then taped to avoid oxidation. This process is shown in Figure 3-33.

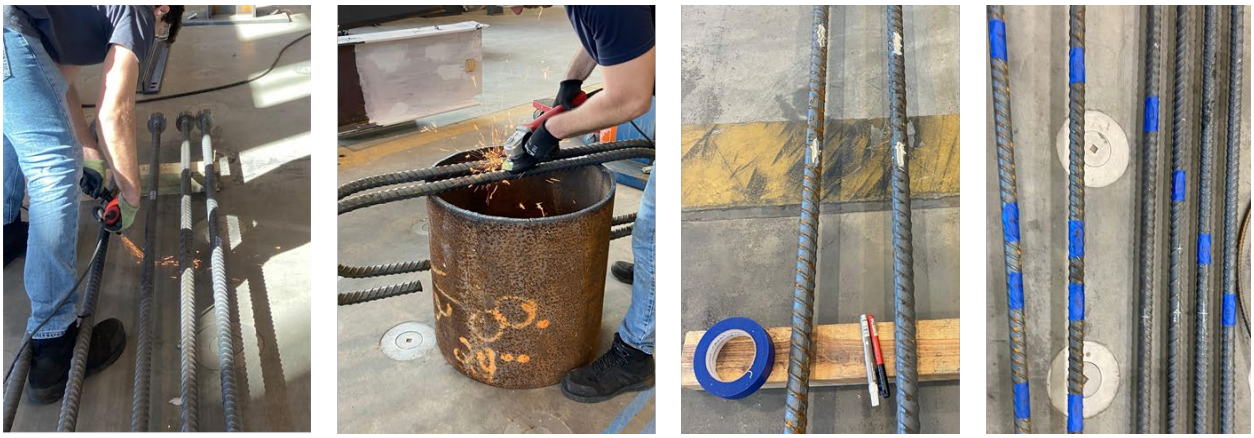

Figure 3-33: Preparation of steel reinforcement

The next step was to prepare the stands that were used to build the cages. Six stands and wood pieces were placed to support the heavy reinforcing cage, as shown in Figure 3-34. This structure supported all bars hanging 5 in. above the floor level.

Figure 3-34: Structure to support the reinforcing cage

Once the supporting structure was ready, the top corner No. 11 hooked bars were placed. Then, all U-shaped bars were placed on top and tied with C-shaped bars to form the shear-reinforcing stirrup configuration illustrated in Figure 3-4. Finally, all the remaining No. 11 bars were placed in their position and tied with an X-shaped tie where two or more bars were encountered. The U-shaped bars were not perfectly bent by the fabricator, which made it challenging to keep the spacing as needed. It was necessary to check the spacing multiple times during the construction process to get a final product that was close to the original design. The remaining four top No. 11 headed bars were placed at the end of the construction process once the bent cap reinforcement, the connection reinforcement, and the steel pile were in place.

The bent cap reinforcing cage is shown in Figure 3-35. Each of these had an approximate weight of 1.04 U.S. tons.

Figure 3-35: Side views of bent cap reinforcing steel cage

For the three reinforcing steel connection specimens, the reinforcing cages were fabricated following a process similar to the one stated earlier in this section. The circular shape of the hoops complicated the fabrication of these elements, creating instability in the subassemblage.

Figure 3-36 shows the fabrication of the connection utilizing headed bars. The configuration of this element followed the specifications and details depicted in Figure 3-9. To ensure the hoops had the same diameter, each was measured and tied before being placed along the No. 11 headed bars.

Figure 3-36: Headed-bar connection

The second connection that was fabricated is the hooked bar connection. This one not only had instability issues due to the circular hoops but also had congestion problems with the 180-degree hooked ends of the No. 11 bars, as seen in Figure 3-37. The process of building this connection was difficult and time-consuming. It took longer than the straight-bar connection assemblage, considering it had less hoops on its configuration.

Figure 3-37: Hooked-bar connection

The third fabricated connection is the straight bar connection. The number of hoops increased for this connection, providing more stability. Also, similar to the headed bar connection, this one did not have congestion of the reinforcement. Figure 3-38 illustrates this connection.

Figure 3-38: Straight-bar connection

After all the reinforcing cages described in this section were fabricated, all the strain gauges were attached to the corresponding locations. Section 4.1.3 of this thesis describes the process of attaching, securing, and coating steel strain gauges. The wires of the instruments were secured to avoid any damage during the move and assemblage process.

3.5.2 Steel Pipe Pile

The preparation process for the steel pipe piles was similar for the 9 ft and 11 ft long piles. Due to the rusty conditions of the surface of the piles, the first step in the process was to pressure wash them to remove residues. Then, marking the vertical axis and determining the location of strain gauges and holes was essential.

Prior to attaching the strain gauges, it was necessary to torch the holes for the long, headed reinforcing bars to pass through and the holes for them to be lifted with the crane. The next step was to move the 0.85 U.S. tons of steel pile inside the laboratory with a forklift and grind the surface to remove any oxidation prior to attaching steel strain gauges. This process is shown in Figure 3-39.

Figure 3-39: Steel pipe pile preparation

After the pile surface was ready, all the strain gauges were attached to their designated locations. Section 4.1.3 of this thesis describes the process of attaching, securing, and coating steel strain gauges. The wires were secured to avoid damage during the move and assemblage process.

3.5.3 Structure Assemblage

The assemblage of the structure was similar for all specimens. Using a 30-ton crane, the steel reinforcing cage was moved to the concrete placement location. Following this step, the corresponding steel pipe pile was placed inside the reinforcing cage, and the connection was moved inside the pipe pile, as shown in Figure 3-40. This process was simplified for the two specimens with mechanical anchorage welded to the pile due to the lack of reinforcement inside the pile.

Figure 3-40: Final connection assemblage

Once both elements were in place, they were lifted by a 30-ton crane and secured into the header beam of the frame to keep it in place. The remaining four long, headed bars were then placed through the holes at the bottom of the pile and secured with ties.

Additionally, PVC pipes were placed in the locations where the post-tensioning bars were necessary in a vertical position. Similarly, horizontal PVC pipes were necessary to insert the lifting straps to transport the specimen into the testing location. All the elements mentioned above are shown in Figure 3-41.

Figure 3-41: Assemblage of structure

3.5.4 Additional Operations Prior to Casting

Several steps must be taken before casting a specimen. One important step is to secure all the sensor cables to avoid damage during concrete placement and vibration. For this process, strong tape was used to hide the cables under the reinforcement and guide them to a common exit point. This step is essential to ensure that the data can be collected and the strain gauge information is not lost.

Another very important step is the fabrication and placement of formwork. This consisted of plywood surfaces joined by 2x6 wood lumber. The interior surfaces were coated with polyurethane to ease the stripping process. These forms were reused for all five specimens.

Finally, after the formwork was in place, a total of 32 pencil rods were used to tighten the forms in both directions. The final product of the structure prior to casting is shown in Figure 3-42.

Figure 3-42: Specimen prior to casting

3.5.5 Concrete Placement

On the day of concrete placement, a 9 yd^3 ready-mix truck arrived at the Advanced Structural Engineering Laboratory high bay. Several fresh concrete properties were measured as described in section 3.4.6.2. The concrete mixture followed the ALDOT Class B specifications and was described for each specimen in section 3.4.6.1.

After corroborating that all the fresh properties were as necessary, the forms were filled using a concrete-placing bucket lifted by a crane. Concrete vibration was necessary to compact the freshly poured concrete and remove air bubbles. This process took between 4 and 5 hours per specimen, as depicted in Figure 3-43.

Figure 3-43: Concrete placement process

The process described above occurred in three stages. The first two stages were carried out until the bent cap was full of concrete and properly vibrated. The third stage happened to fill out the steel pipe pile to the desired concrete plug height. It is recommended to have a low slump to ease this process and avoid concrete dripping out of the forms or overfloat. Figure 3-44 describes the three stages required to place the concrete with green arrows.

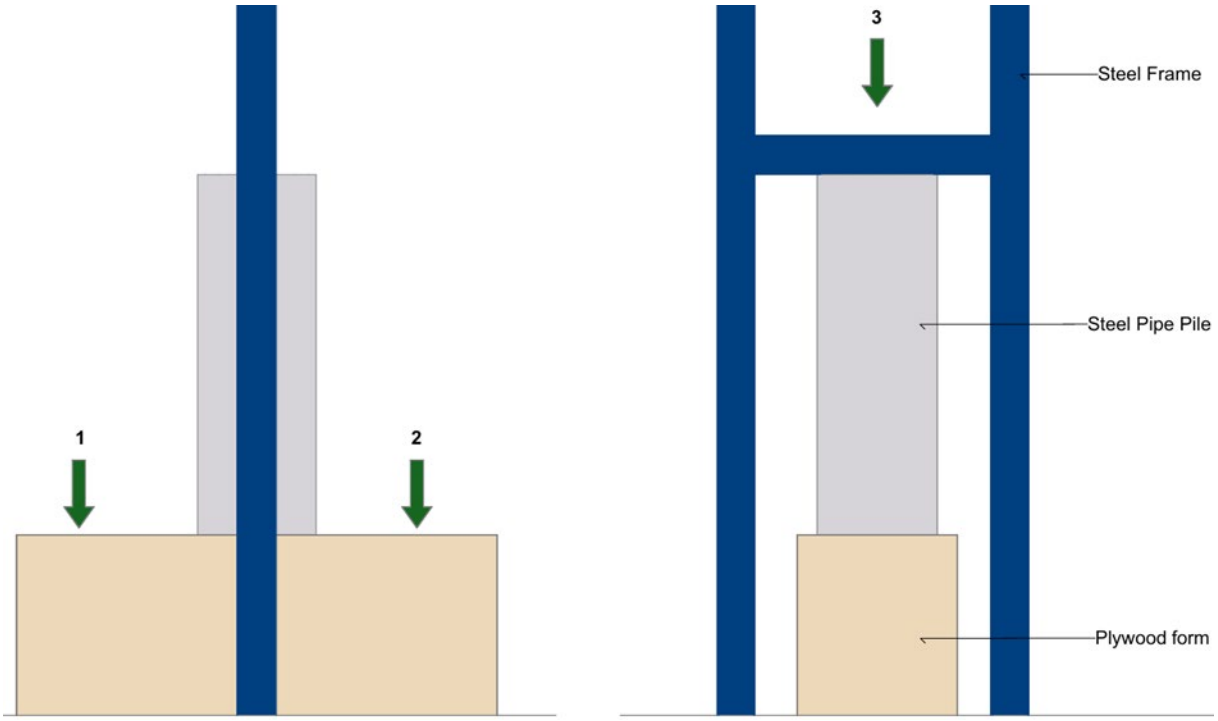

Figure 3-44: Stages of concrete placement

After the concrete was placed, 2x6 wood was used to screed off the excess concrete from the top of the bent cap. This step was made to ensure a smooth surface, as shown in Figure 3-45, which was later used to attach concrete strain gauges.

Figure 3-45: Smoothened bent cap surface

Along with the concrete bent cap, 4x8 in. concrete cylinders were made according to ASTM specifications, as described in section 3.4.6.3.

After the concrete achieved the initial set, the specimens were covered with wet burlap according to AASHTO M182 Class 3. Polyethylene plastic was placed on top of the burlap to avoid drying and rewetted as needed to ensure moisture conditions. The specimens were cured until the day of form removal which was typically after 7 days. Figure 3-46 shows the final specimen after the forms are removed from the bent cap.

Figure 3-46: Specimen after form removal

CHAPTER 4 TESTING OF THE EXPERIMENTAL SPECIMENS

This chapter describes the load testing performed on all five experimental specimens described in Chapter 3. A description of the applied loading can be found in conjunction with the details of the instrumentation and data acquisition system (DAQ) used to monitor specimen response during these laboratory tests.

4.1 TEST SETUP

All five tests were conducted at the Auburn University Advanced Structural Engineering Laboratory (ASEL). The equipment used for this purpose is described in this section. All specimens were tested next to a strong wall, as shown in Figure 4-1.

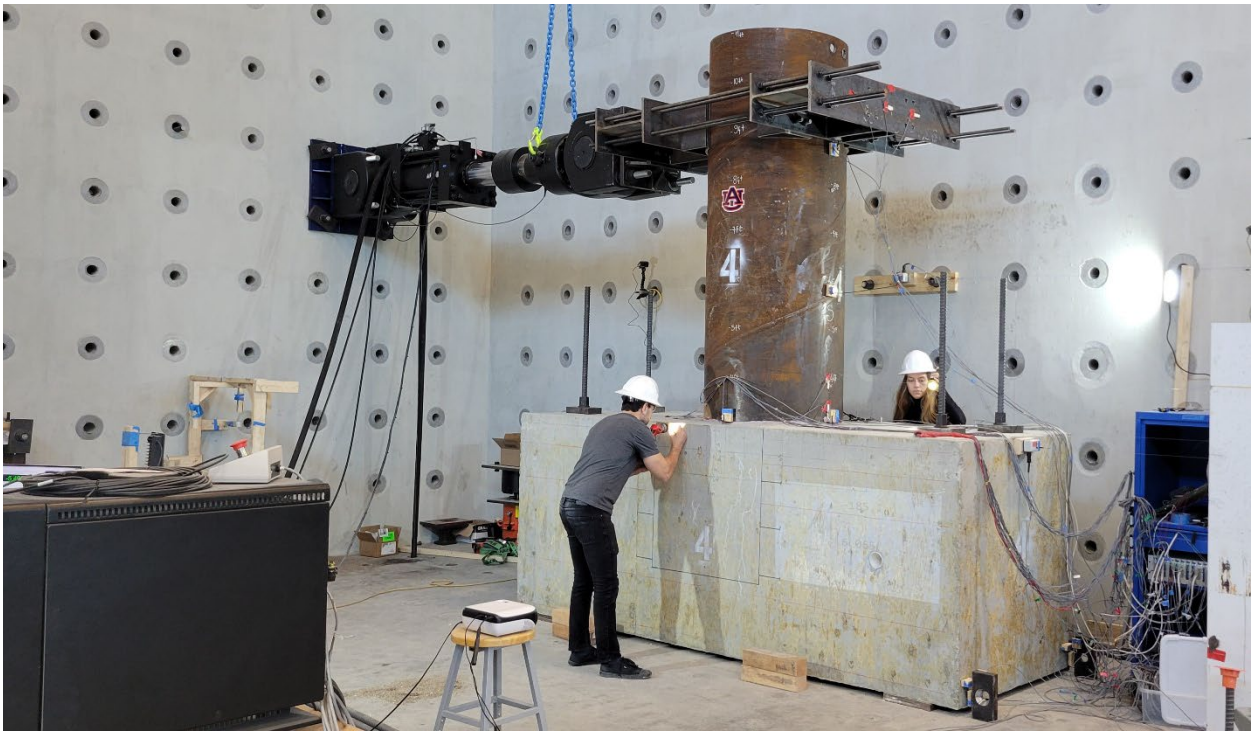

Figure 4-1: Testing location

Figures 4-2 and 4-3 describe all the elements of the test setup incorporated into the experimental tests.

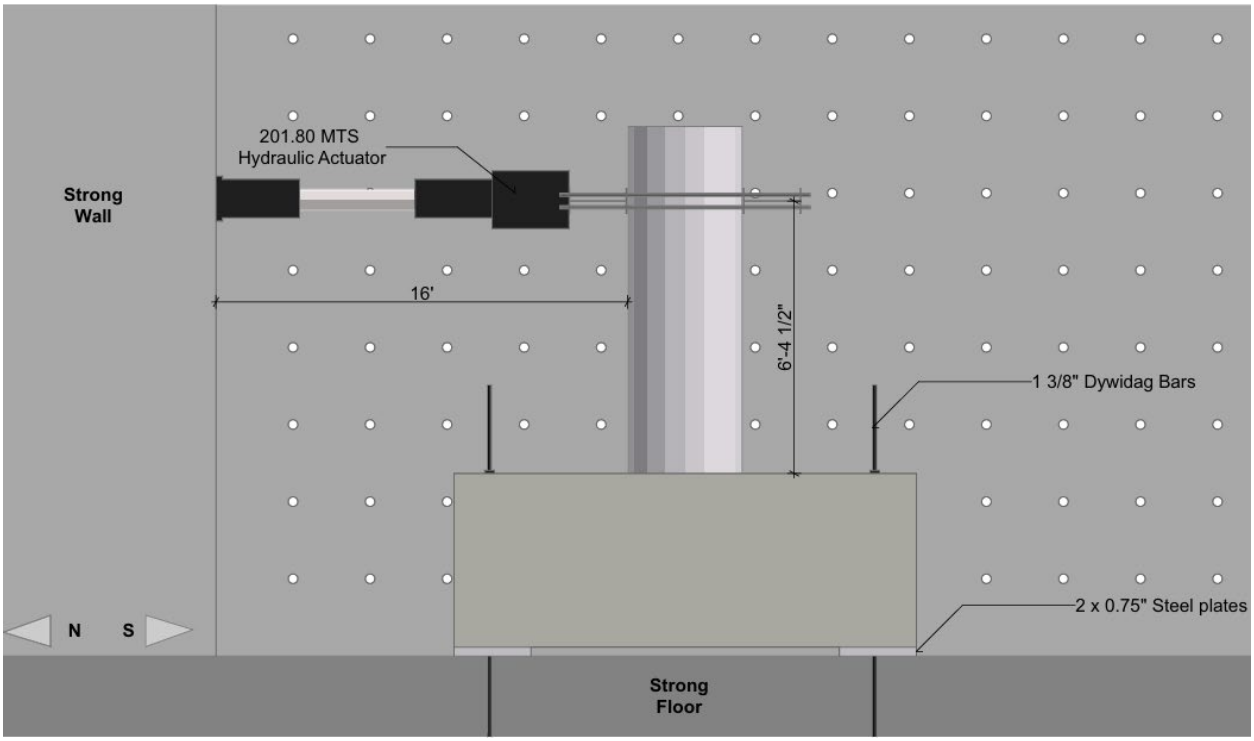

Figure 4-2: Test setup side view

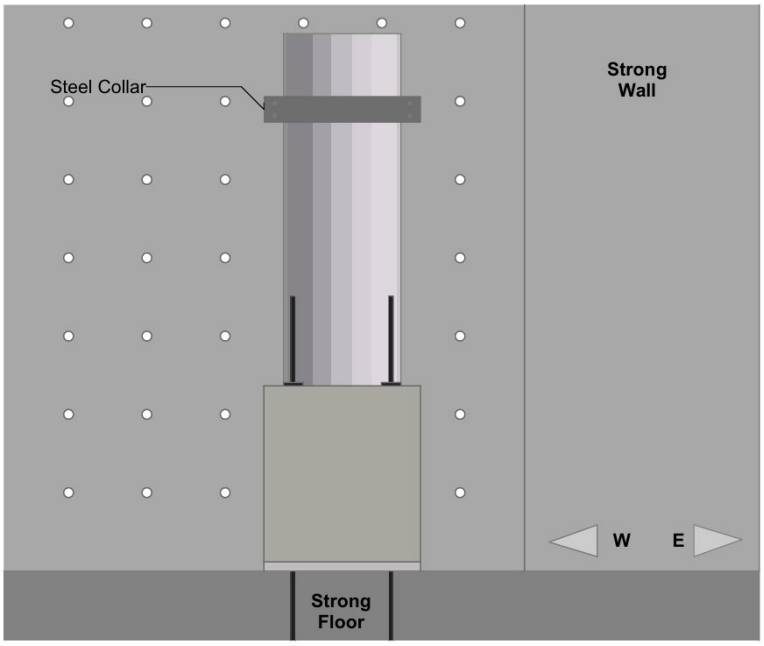

Figure 4-3: Test setup rare view

Every specimen had an approximate weight of 37.2 kips (18.6 tons). As shown in Figure 4-4, a 30-ton crane was necessary to move the specimens from the casting position to the testing position.

Figure 4-4: Transportation of specimens

4.1.1 Support Conditions

Two steel plates on both ends supported the specimens, providing a two-point support, as shown in Figure 4-2. Four dywidag bars with a diameter of 1 3/8 in. were placed vertically on the corners of the bent cap and post-tensioned to provide support. As shown in Figure 4-5, round HSS sleeves with an interior diameter of 1.69 in. were used to keep the dywidag bars in place.

Figure 4-5: Dywidag bar and sleeve

4.1.2 Actuator

An MTS 201.80 hydraulic actuator was used to apply the loading displacement on all five tests. It has a 301-kip capacity in tension and 446 kips in compression. The tension direction was used in this test. As shown in Figure 4-6, the actuator was attached to the steel pipe pile through a loading collar, which was used to pull the pile towards the strong wall in the north direction at a height of 6 ft and 4.5 in.

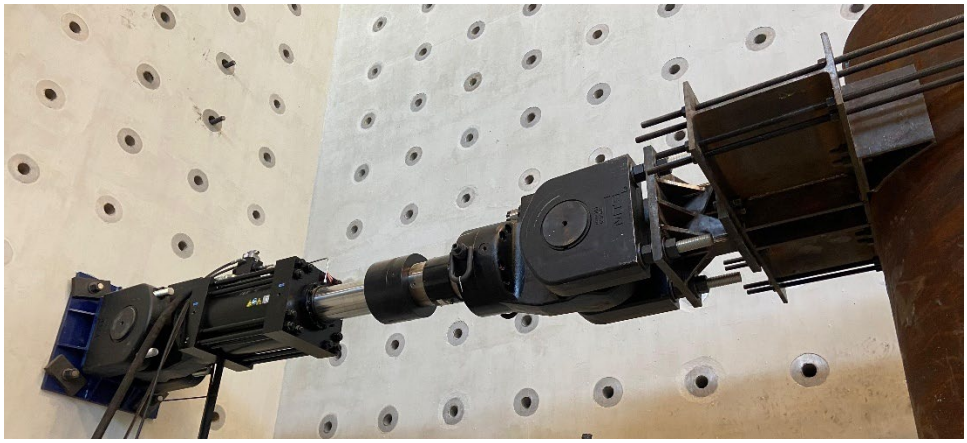

Figure 4-6: MTS 201.80 actuator

4.2 LOAD PROTOCOL

The lateral load was applied, which was planned to increase progressively in cycles until one of three things occurred: the specimen failure, the actuator capacity was reached, or the support limits were reached. In this study, failure was not reached for any of the specimens. The maximum lateral load for the three reinforcing steel

connections (reinforcing bars) was 276 kips. The actuator's full tension capacity (301 kips) was used for the two specimens with mechanical anchorage welded at the bottom of the pile.

4.2.1 Cycles and Loads

The reinforcing-bar connection capacity of 938 kip-ft was estimated based on cross-sectional analysis described in section 3.2.2, not including the potential contribution of the steel pipe pile. This capacity corresponds to an applied load of 147 kips. Load levels corresponding to 20%, 40%, 60%, and 80% of the RC capacity and maximum load were applied with different cycles. An initial load of 10 kips was applied to ensure all sensors functioned adequately. For load levels from 20% to 80%, three cycles were performed on each load level. This information is summarized in Figure 4-7.

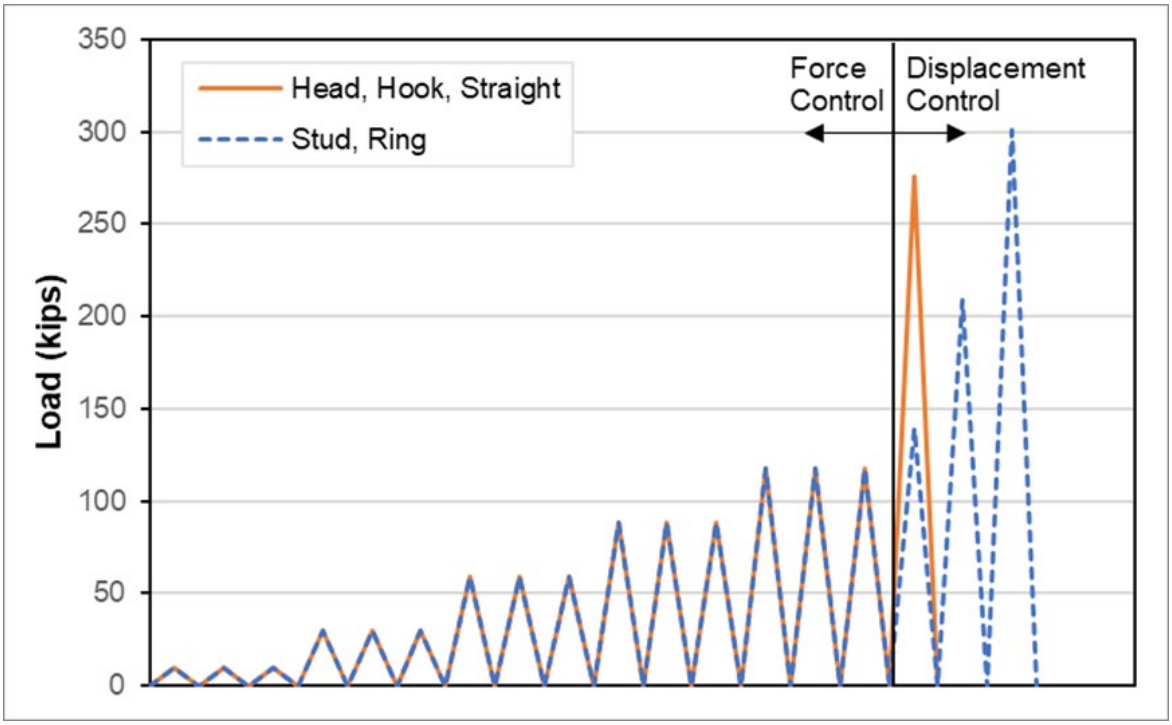

Figure 4-7: Load protocol

Force control of the actuator was used during the test until 88.2 kips (60%) was reached. Displacement control of the actuator was used for 117.6 kips (80%) and maximum load.

Tables 4-1 and 4-2 summarize the applied lateral loads for all the specimens.

Table 4-1: Load application for reinforcing steel connections

	Load Level	Load (kip)	No. Cycles	Notes
Force Control	0	10	3	Check sensor data and test setup
	1	29.4	3	20% of RC cross-section capacity
	2	58.8	3	40% of RC cross-section capacity
	3	88.2	3	60% of RC cross-section capacity
	4	117.6	3	80% of RC cross-section capacity
Displacement Control	5	276	1	Maximum test setup limit

Table 4-2: Load application for welded mechanical anchorage connections

	Load Level	Load (kip)	No. Cycles	Notes
Force Control	0	10	3	Check sensor data and test setup
	1	29.4	3	Consistency with previous tests with RC connections
	2	58.8	3	Consistency with previous tests with RC connections
	3	88.2	3	Consistency with previous tests with RC connections
	4	117.6	3	Consistency with previous tests with RC connections
Displacement Control	5	139.7	1	New load level
	6	209.3	1	New load level
	7	301	1	Maximum load, actuator tensile capacity

As described in Tables 4-1 and 4-2, the maximum load is different for the reinforcing bar connections and the welded mechanical anchorage connections. The test was terminated at 276 kips for the Head, Hook, and Straight specimens due to excessive deformation observed in the loading fixtures. This issue was corrected for the last two specimens, Stud and Ring, and the tests could be conducted until the tensile capacity of the actuator was reached (301 kips).

In all five tests, none of the specimens reached failure or severe cracking or damage. A detailed description of the specimens after the load application is discussed in Chapter 5 of this thesis.

4.3 INSTRUMENTATION

Several sensor types were used to monitor the performance of each specimen subjected to an increasing pseudo-static lateral load. A description of the instruments is presented in this section.

All five full-scale specimens were instrumented using four types of sensors to obtain the required data monitored during the lateral load applications. Strain gauges, string potentiometers, slip meters, and inclinometers were located as described in the following subsections and shown in the corresponding figures.

The sensors transform a physical phenomenon into a measurable electrical property by output voltage, current, electrical resistance, pulses, digital signal, imaging, or wavelength of light.

Every type of sensor has different specifications according to the needs of the project. Range, sensitivity, resolution, accuracy, and precision are examples of specifications that will be considered based on the measurement requirements. Other considerations, such as sensor interfaces and power sources, are essential based on the availability and the testing conditions.

A summary table with all the instrumentation used to monitor each specimen response can be found in Appendix A.

4.3.1 Instrumentation Identification

The system used to identify the instrumentation type, location, and number used in this study is described in Figure 4-8.

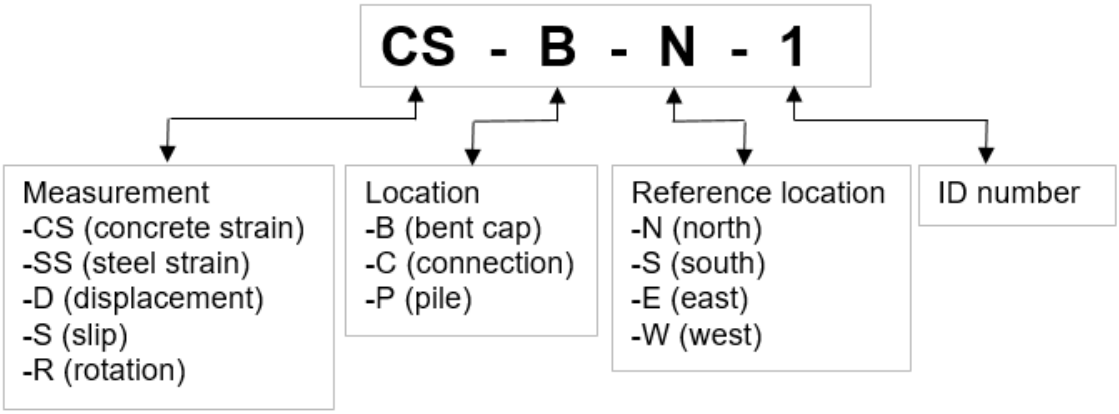

Figure 4-8: Instrumentation identification system

The system presented above is used to identify each of the sensors used to monitor the behavior of each specimen. A total of 144 strain gauges, 6 linear potentiometers, 12 slip meters, and 5 inclinometers were used to monitor all five specimens. Each of the following subsections contains the layout corresponding to each type of sensor.

4.3.2 Strain Gauges

Concrete and steel strains in this study were measured using linear strain gauges made from a thin foil with wires bonded to the surface to be measured.

Strain gauges are a type of sensor that measures the deformation (strain) in a specific area. They operate with the principle that the deformation is proportional to the electrical resistance of the sensor.

Two types of strain gauges were used for these specific tests. Steel (pile or reinforcement) strain was measured with 5 mm, 3-wire strain gauges with a gauge factor of 2.09. Similarly, concrete strain was measured with 120 mm, 3-wire strain gauges with a gauge factor of 2.10. Figure 4-9 shows the two types of strain gauges used in this study.

Since the strain gauges attached to the steel reinforcing bars were embedded in concrete, a special coating was used to avoid damage during concrete placement due to moisture or impact. Good surface preparation, along with a correct installation process, is also very important to prevent gauges from stopping functioning.

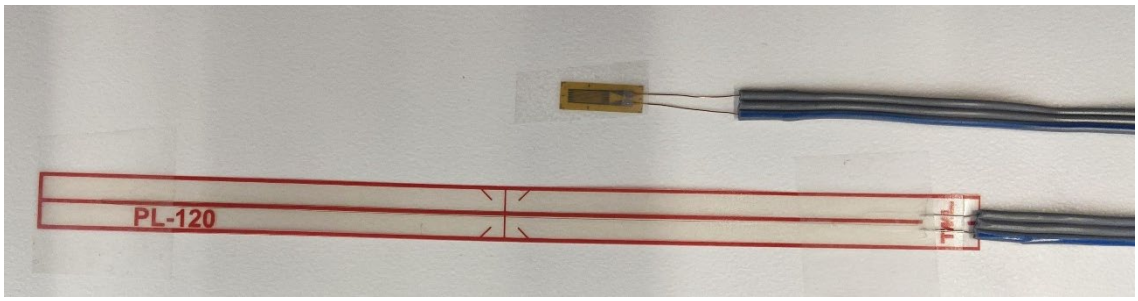

Figure 4-9: Steel (top) and concrete (bottom) strain gauges

4.3.2.1 Strain Gauge Layout

Figures 4-10 through 4-16 describe the strain gauge layout for the concrete bent cap and all five connections for the different specimens.

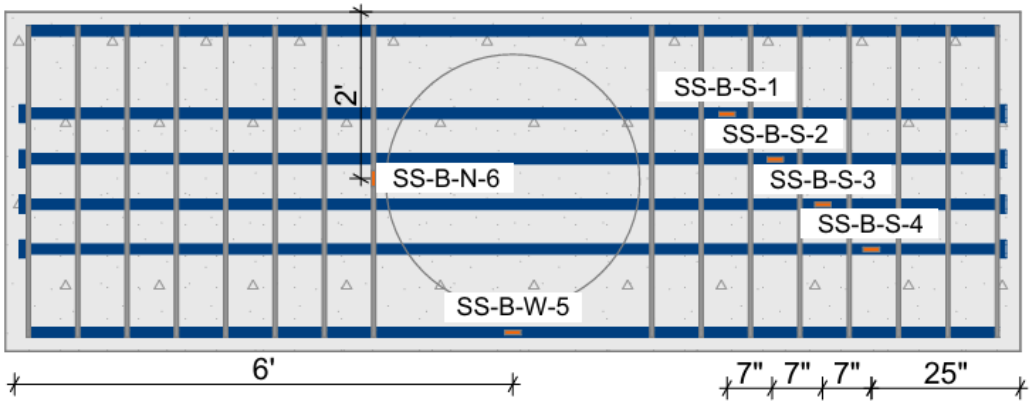

a) Strain gauges on longitudinal reinforcement

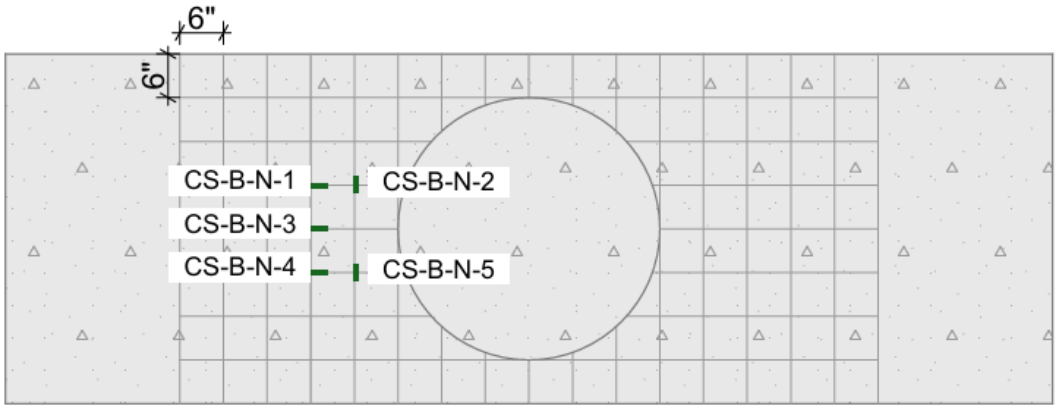

b) Strain gauges on top of concrete

Figure 4-10: Bent cap strain gauge layout

The layout presented in Figure 4-10 a) and b) describes the location of bent cap strain gauges replicated on all five specimens. A 6x6 in. grid was drawn on top of the concrete surface to ensure that all specimens had the same concrete strain gauge locations.

The orientation of the strain gauges is visually described in Figure 4-10. Strain gauges SS-B-N-6, CS-B-N-2, and CS-B-N-5 are oriented east-west. All the other strain gauges are oriented north-south.

Figure 4-11 shows the location of steel strain gauges attached to the 9 ft steel pipe pile replicated for the three reinforcing steel connections. All strain gauges are oriented vertically.

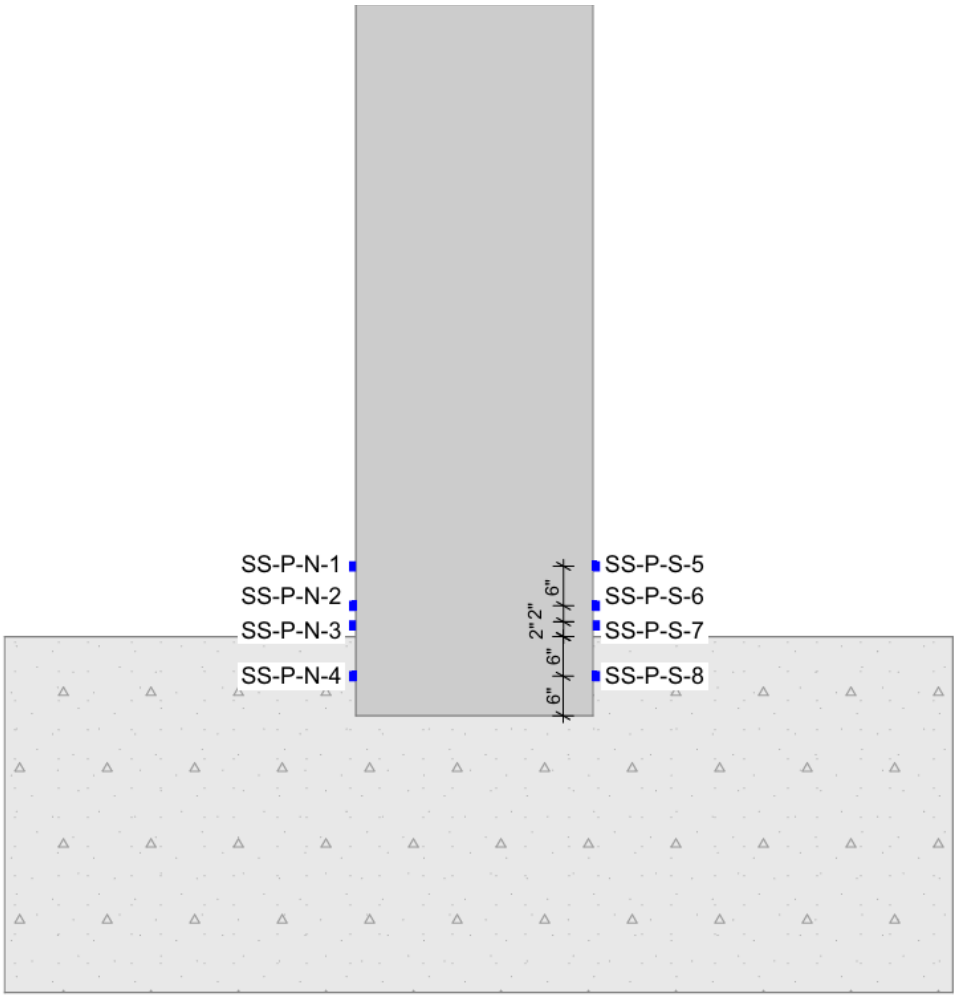

Figure 4-11: Strain gauge layout for 9 ft steel pipe pile in reinforcing steel connections

Figures 4-12 through 4-14 show the strain gauge layout on the reinforcing steel for headed bars, hooked bars, and straight bars.

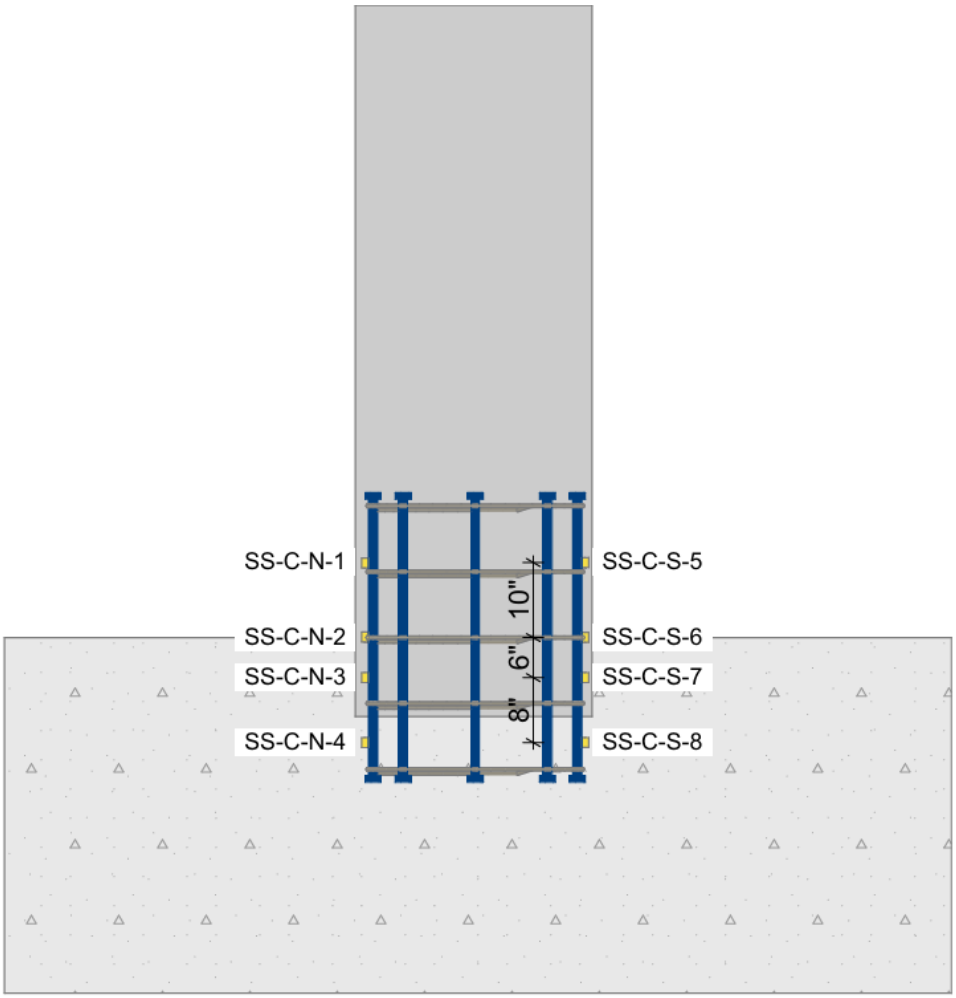

Figure 4-12: Strain gauge layout for Head specimen

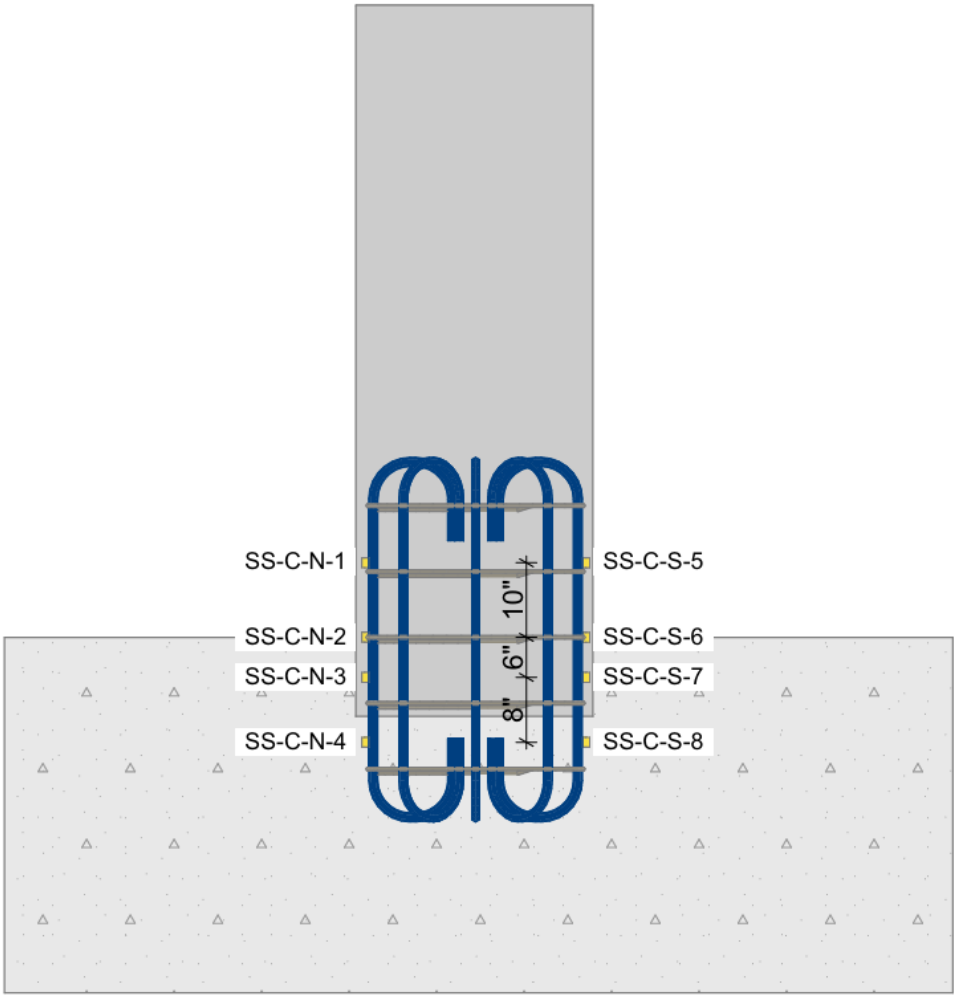

Figure 4-13: Strain gauge layout for Hook specimen

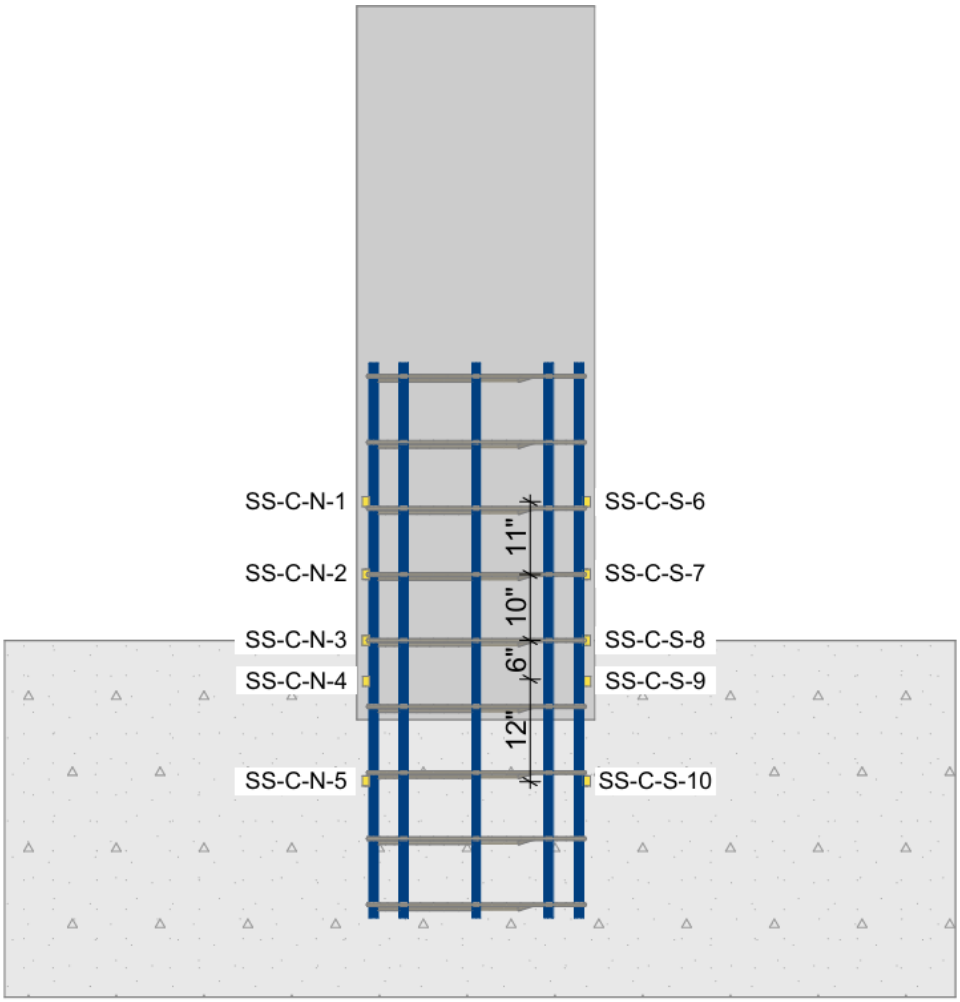

Figure 4-14: Strain gauge layout for Straight specimen

Figures 4-15 and 4-16 describe the strain gauges used to monitor strains of the two specimens with mechanical pile anchorages. These figures correspond to the Stud and Ring specimens, respectively, for 11 ft steel piles.

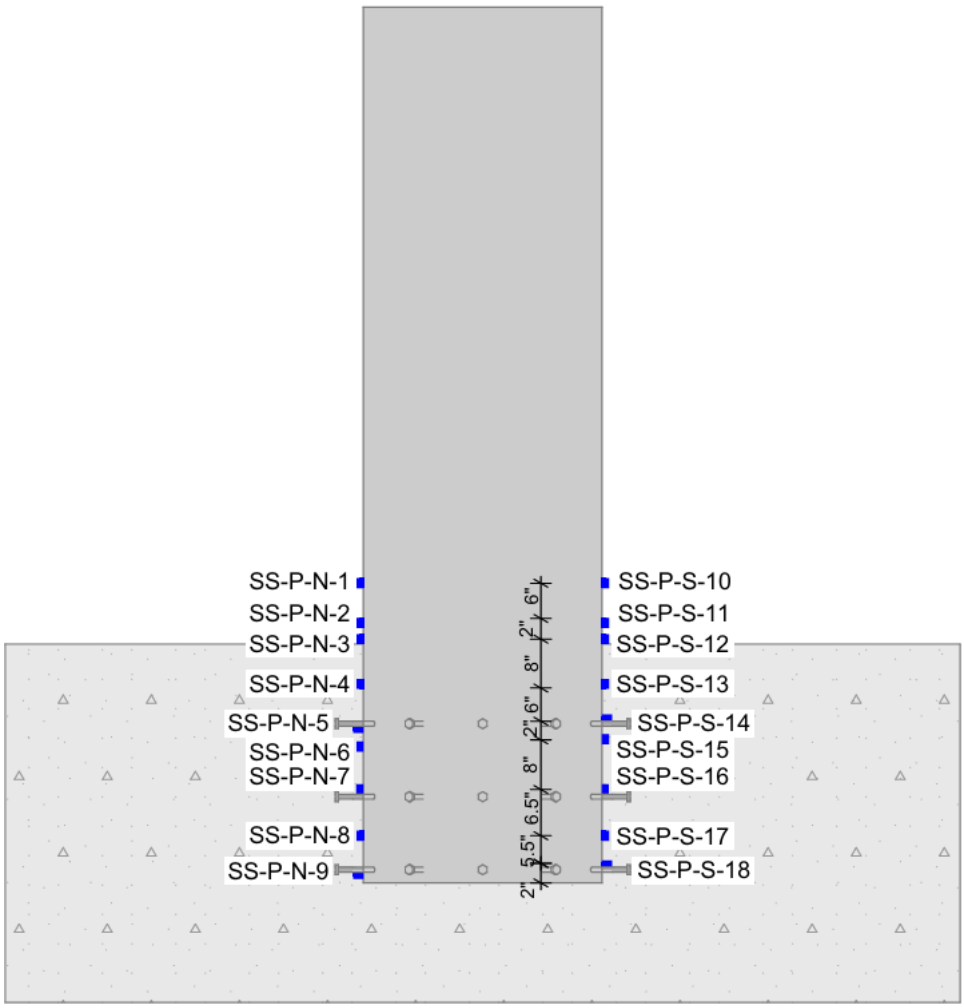

Figure 4-15: Strain gauge layout for Stud specimen

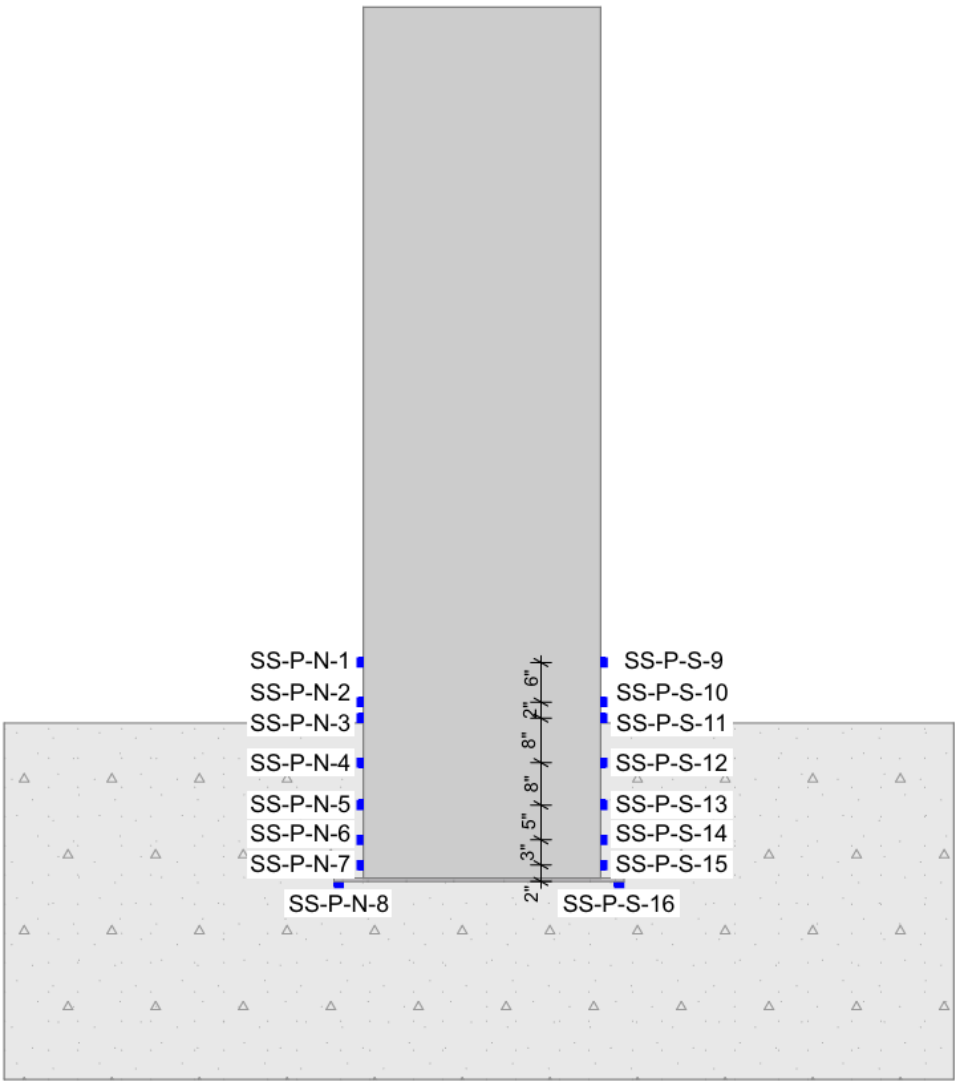

Figure 4-16: Strain gauge layout for Ring specimen

4.3.2.2 Surface Preparation

Steel and concrete need preparation to allow strain gauges to be correctly attached to their surface. The following process was used to prepare steel and concrete surfaces:

1. Grind the surface to remove imperfections and obtain a smooth surface.
2. Use a degreaser product.
3. Use conditioner with fine sandpaper to clean the surface.
4. Wipe down the surface with gauze pads until they come out completely clean.
5. Use neutralizer to clean the surface.

6. Wipe down the surface with gauze pads until they come out completely clean.
7. Let the surface dry.

4.3.2.3 Strain Gauge Installation

The installation step is key to making sure the sensors are reading properly. The following process was used:

1. Remove the protective film.
2. Identify the side with the wires and face it up.
3. Use a few drops of the adequate glue (CN-Y for steel, and CN-E for concrete) on the bottom of the gage.
4. Align in proper orientation.
5. Place the non-adhesive sheet on top and press for 30 seconds.
6. Remove the non-adhesive sheet.
7. Secure the rest of the wire with tape to avoid movement.
8. Test if the strain gauge has readings.

Figures 4-17 and 4-18 depict strain gauges after following the steps and installing a steel and concrete strain gauge, respectively.

Figure 4-17: Steel strain gauge installed on reinforcing bars

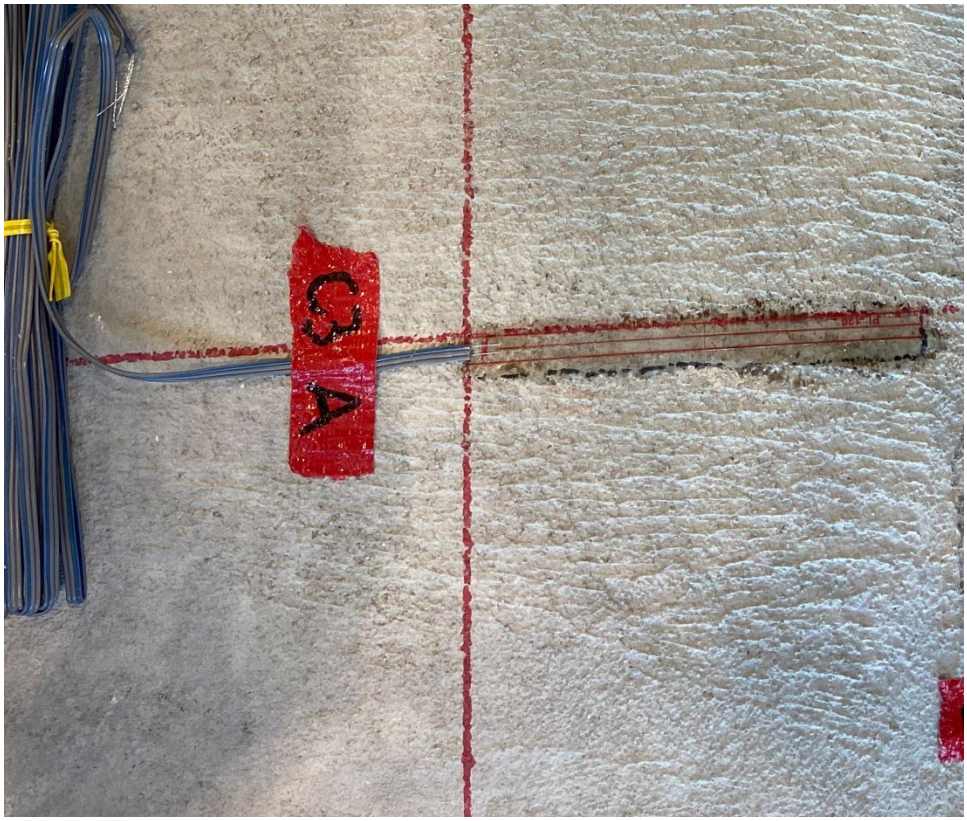

Figure 4-18: Concrete strain gauge

4.3.2.4 Coating Process

There are several ways to protect an installed strain gauge. This process can vary depending on the external conditions that the strain gauges will be subjected to. In this study, this process used three different coating materials to obtain a moisture-proof and impact-resistant finish.

1. Cover the strain gauge with wax previously melted at 120° F.
2. Place a moist and waterproof coat on top of the strain gauge and the exposed wires.
3. Mix equal parts of the epoxy components and cover the moist and waterproof coat.
4. Let the epoxy to dry.

Figure 4-19 depicts the final product after coating a strain gauge following the steps described above.

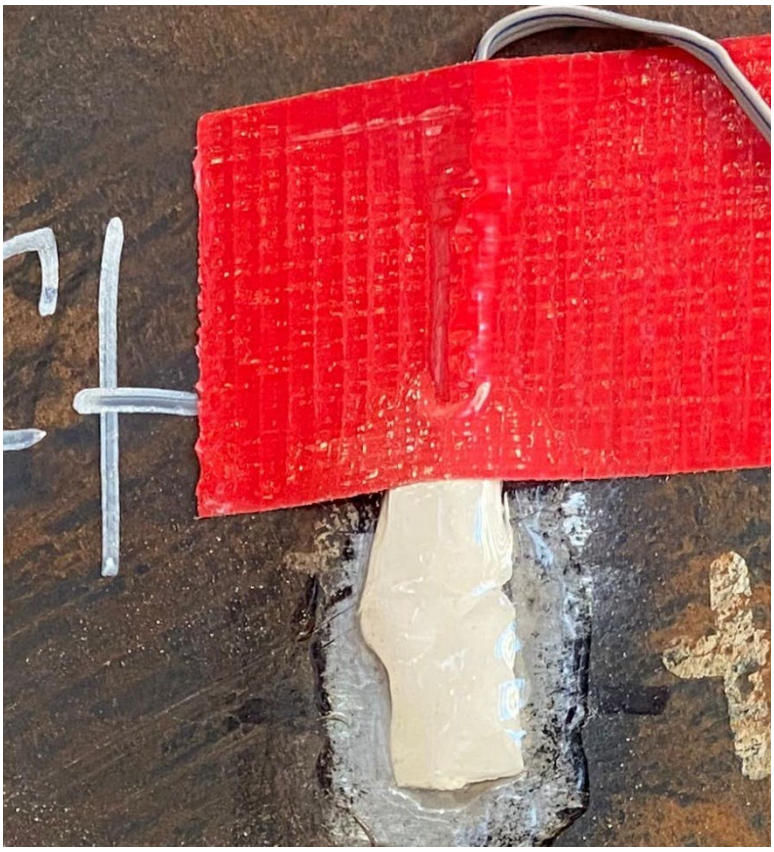

Figure 4-19: Strain gauge after coating

4.3.3 Displacement Potentiometers

A string potentiometer is a type of sensor that measures linear displacement with high sensitivity. It works under the principle of converting the movement into an electrical signal, in this case, voltage change.

String potentiometers were used to measure horizontal displacements of the specimen during testing. Displacements were measured on the concrete bent cap and steel pipe pile relative to the walls on the south and east sides of the specimen. The actual displacement of the specimen relative to the supports was calculated using the data from these sensors. Figure 4-20 shows one of the linear potentiometers used to measure displacement.

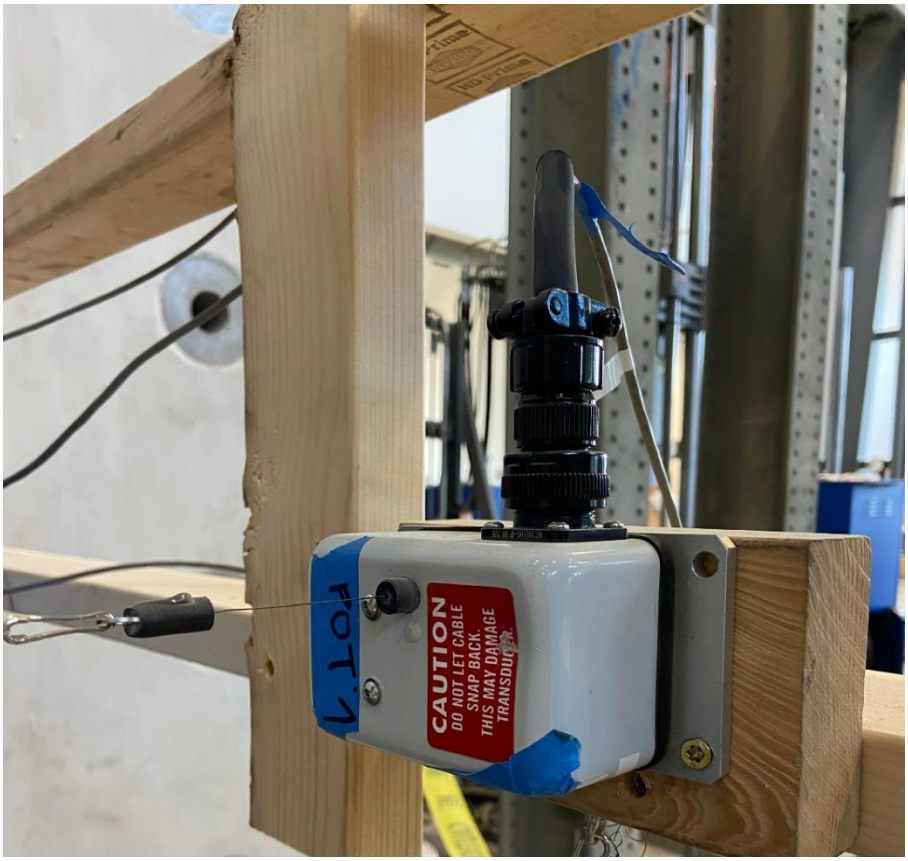

Figure 4-20: String potentiometer

4.3.3.1 Displacement Sensor Positions

Figure 4-21 describes the string potentiometer attached locations on all five specimens.

D-P-E-4 was oriented east-west, and the rest of the displacement sensors were oriented north-south.

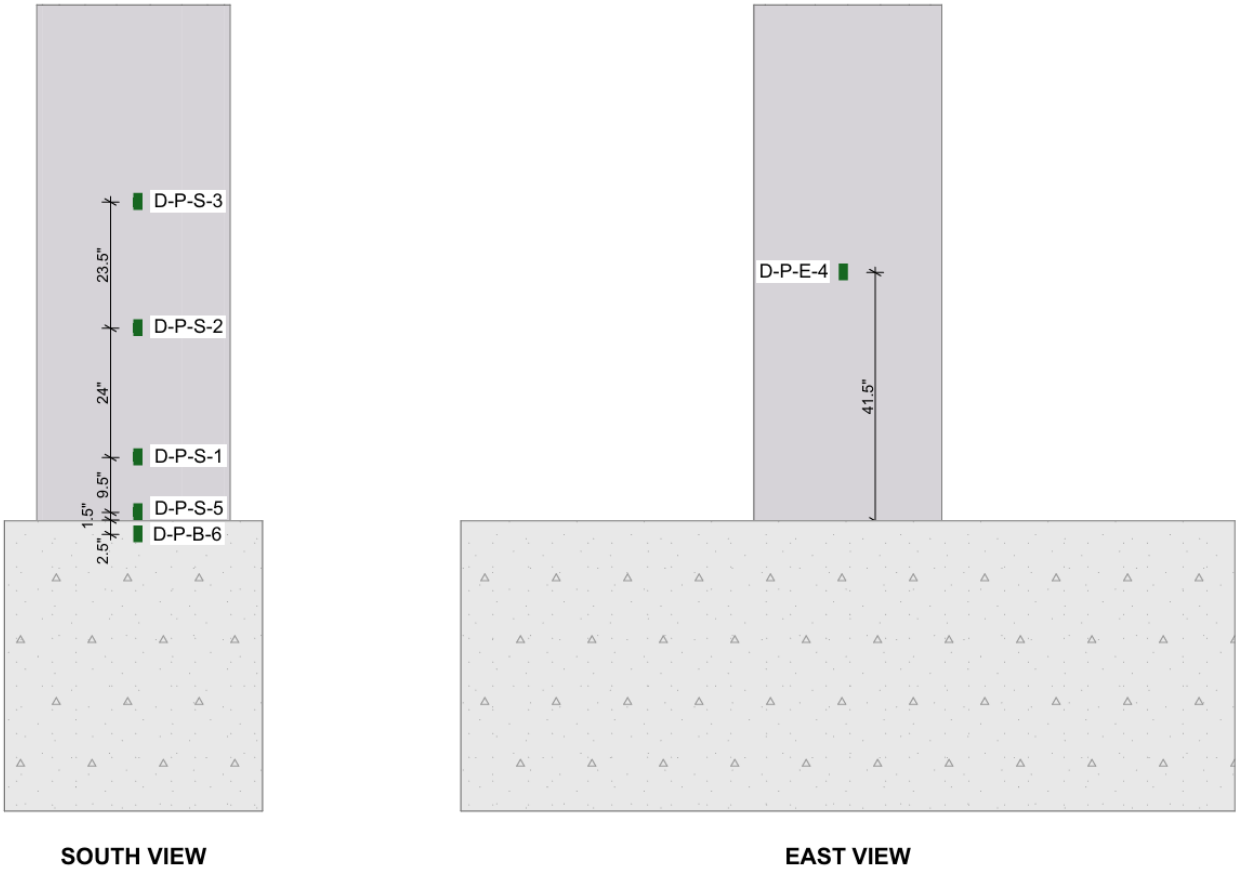

Figure 4-21: String potentiometer layout

4.3.4 Slip Meters

A slip meter is a sensor that uses friction to measure movement or slip. This type of sensor transforms displacement into voltage change, similar to string potentiometers. It is very compact and easy to install.

Slip meters were used to measure the slip of the pile relative to the bent cap surface and the bent cap movement relative to the strong floor. Slip meters were also used to calculate the loading collar displacement relative to the pile. Figure 4-22 shows that they were mounted onto wood blocks and attached to the surfaces with magnets.

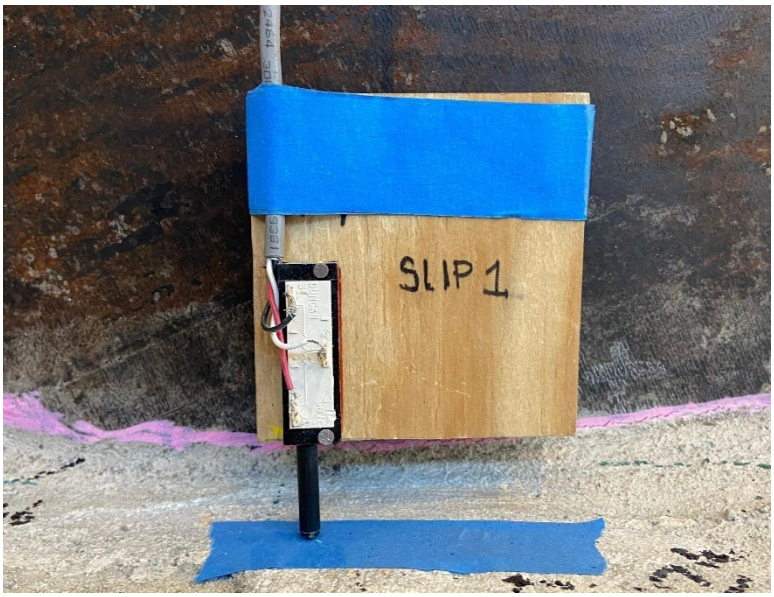

Figure 4-22: Slip meter

4.3.4.1 Slip Meter Positions

Figure 4-23 describes the slip meter positions on all five specimens.

All slip meters, with the exception of S-B-S-9, S-B-S-10, S-B-E-11, and S-B-E-12, were positioned vertically.

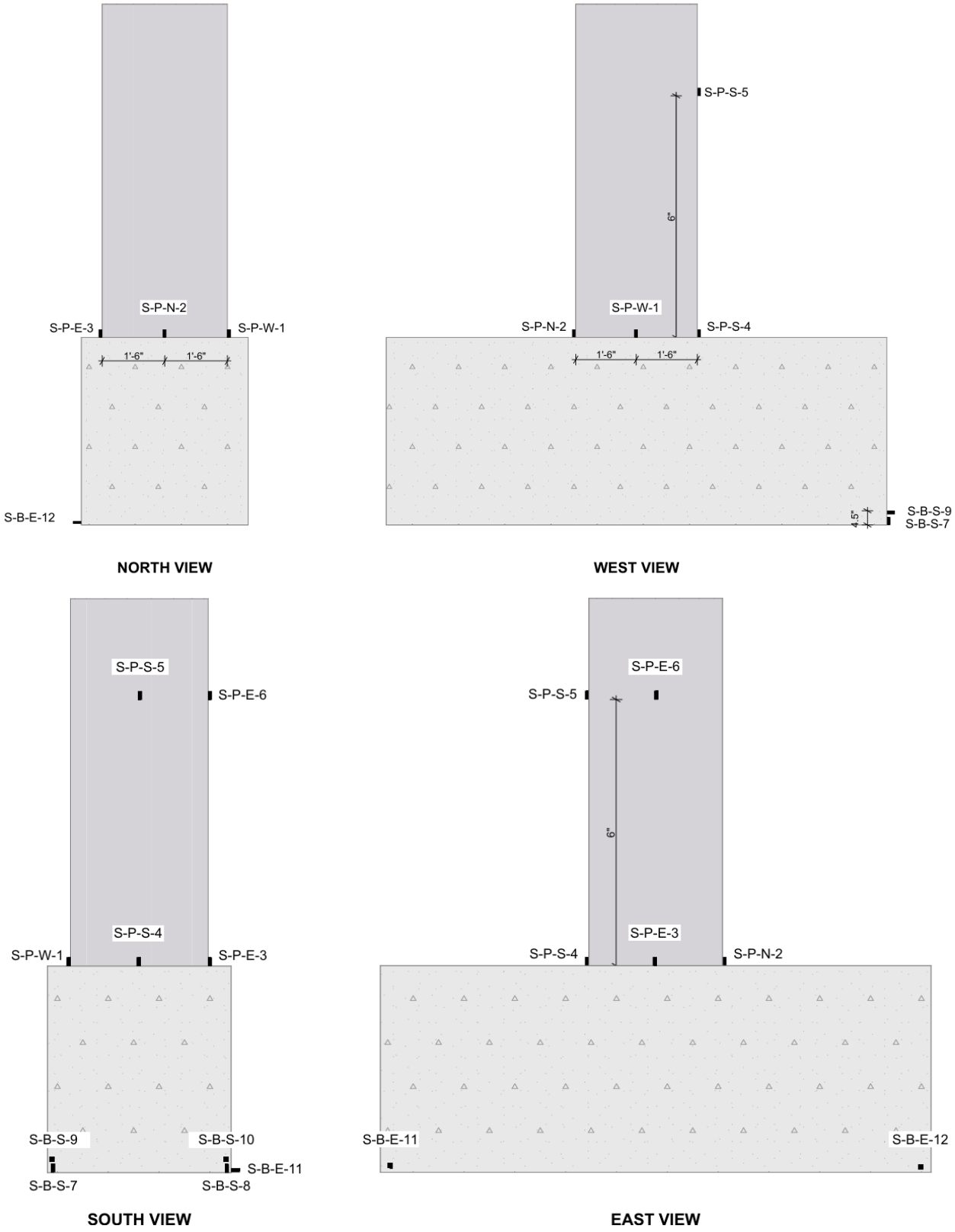

Figure 4-23: Slip meter layout

4.3.5 Inclinometers

Inclinometers, also known as tilt sensors or tilt angles, are devices that measure the rotation of an object relative to the gravitational direction.

In this study, the rotations of the bent cap and the pile were measured on the N-S and E-W directions during the laboratory testing. The devices were mounted onto wood blocks, as shown in Figure 4-24.

Figure 4-24: Inclinometer

4.3.5.1 Inclinometer Positions

Figure 4-25 describes the inclinometer positions on all five specimens.

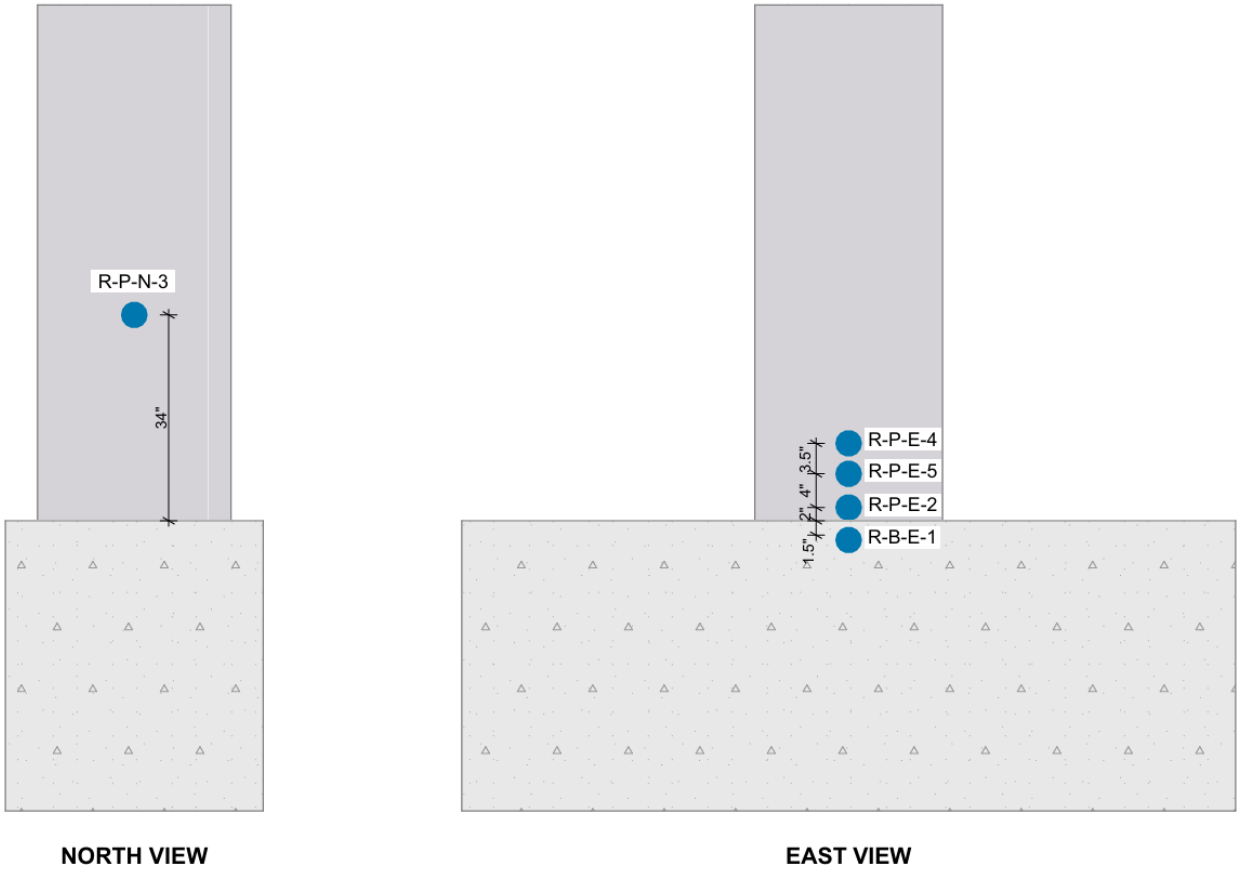

Figure 4-25: Inclinometer layout

4.3.6 Load Cell

The applied load was measured using a load cell between the strong wall and the hydraulic actuator. This built-in force transducer was calibrated and checked prior to beginning each test.

4.3.7 Data Acquisition System

All instrumentation data was recorded using a 5 Hz frequency. The Data Acquisition System (DAQ) used in this study is the Gantner Instruments Unit, which collected and transferred the data to a computer where the information was recorded.

For each test, the corresponding file needed to be adapted to include the different sensors on each specimen. These files are modified to ensure proper readings of all types of sensors plugged into each module of the system. Figure 4-26 shows the modules used to obtain readings from the instrumentation.

Figure 4-26: DAQ modules

Each sensor was calibrated using their corresponding calibration factors or two-point calibration provided by the system. Throughout the test, all strain and displacement readings were monitored with the tools the software provided.

CHAPTER 5 RESULTS AND DISCUSSION

The results of the five full-scale steel pipe pile to concrete bent cap connections tested for this study are presented in this chapter. The individual displacement, drift, concrete, steel reinforcement and pile strains, and rotation plots are presented for each specimen in Appendices B - F of this thesis.

The comparison of all specimens is shown in this section, considering the results of each connection after testing. These results are presented in two groups: 1) steel reinforcing bar connections, including the headed-bar, hooked-bar, and straight-bar connections, and 2) welded mechanical anchorage connections, including the shear stud and annular ring connections. Additionally, the crack evolution of the side and top faces of each bent cap is presented in this chapter.

5.1 LOAD VERSUS DEFORMATION BEHAVIOR

5.1.1 Displacements During Load Cycles

An observation of the displacement at different load levels is done to understand the response of the connection under repeated loads at various levels.

Every specimen was cycled three times to the following loads: 10, 29.4, 58.8, 88.2, and 117.6 kips, as described in Section 4.

The graphs presented in this section include two horizontal dashed lines. One corresponds to the predicted strength of the reinforced concrete connection, which is 147 kips. The second line corresponds to 60% of the predicted, which is the predicted service load level of 88.2 kips.

These curves represent the net displacement of the specimen measured at a height of 58.5 in. from the top of the bent cap after accounting for the slip of the bent cap during the test.

5.1.1.1 Headed-Bar Specimen

Taking a closer look at the cycles for the headed-bar connection in Figure 5-1, it is very hard to identify the different slopes of the lines corresponding to each cycle. This means

there was very little variation in stiffness during the three cycles at each load level and very little residual displacement.

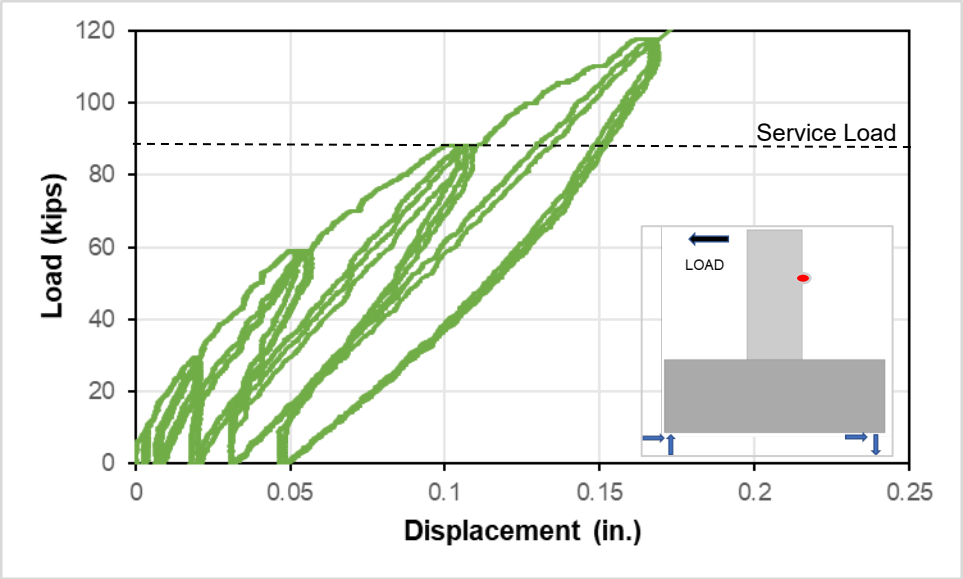

Figure 5-1: Headed-bar specimen cycles

The initial stiffness of the specimen remains constant from the beginning of the test until a load of 58.8 kips. A significant reduction of the slope occurs after this, potentially caused by the flexural cracking of the concrete inside the pipe. A second stiffness slope is visible thereafter until 88.2 kips (predicted service load level). A slightly reduced third slope is observed from 88.2 kips up to 117.6 kips. Another significant reduction of stiffness occurs close to 150 kips, potentially caused by the yielding of the steel reinforcement. Notably, a load of 117.6 kips corresponds to a displacement of 0.17 in. Additionally, at 88.2 kips (predicted service load level), a displacement of 0.11 in. can be observed.

The full test for the headed-bar connection is depicted in Figure 5-2. After 150 kips, the nonlinear behavior of the specimen and a bigger displacement are observed.

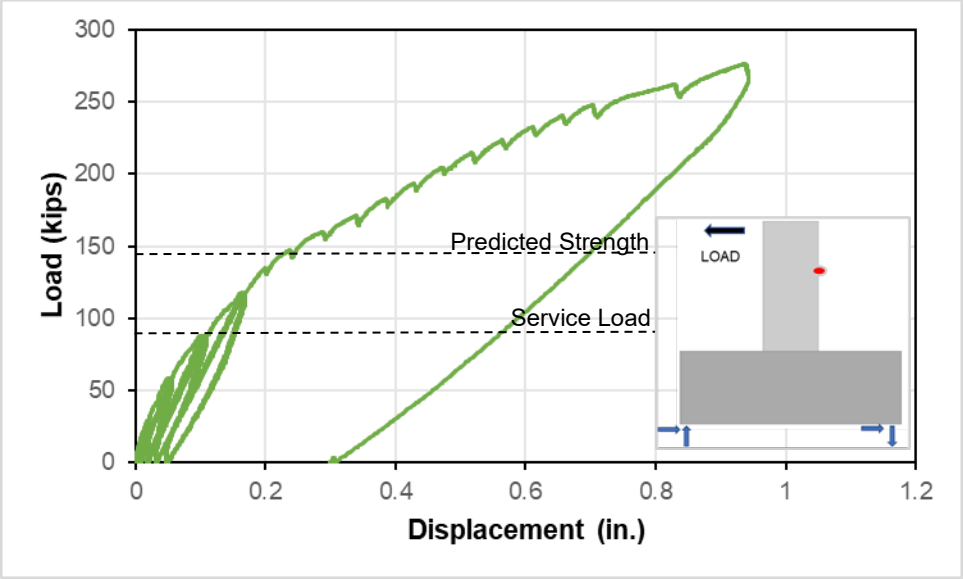

Figure 5-2: Full test headed-bar specimen

A final residual displacement of 0.31 in. was observed after unloading at the end of the test for the headed-bar connection.

5.1.1.2 Hooked-Bar Specimen

Taking a closer look at the cycles for the hooked-bar connection in Figure 5-3, it is very hard to identify the different slopes of the lines corresponding to each cycle until a load of 58.2 kips is reached. This means there was very little variation in stiffness during the three cycles at each load level and very little residual displacement. However, for the cycles at 88.2 kips (predicted service load level) and 117.6 kips, the change in slope and the residual displacement after the cycles are visible.

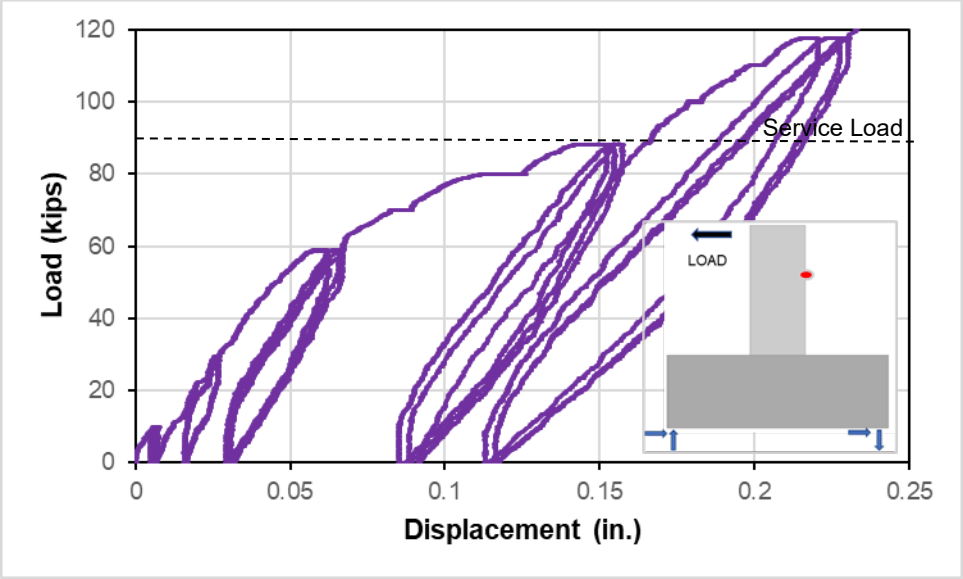

Figure 5-3: Hooked-bar specimen cycles

The initial stiffness of the specimen remains constant from the beginning of the test until a load of 58.8 kips. A significant reduction of the slope occurs after this, potentially caused by the flexural cracking of the concrete inside the pipe. A second slope of the stiffness is visible thereafter until 88.2 kips (predicted service load level). A third slope is observed from 88.2 kips up to 117.6 kips. Another significant reduction of stiffness occurs close to 150 kips, potentially caused by the yielding of the steel reinforcement. Notably, a load of 117.6 kips corresponds to a displacement of 0.23 in. This corresponds to a displacement 35% higher than the headed-bar connection for the same load. Additionally, at 88.2 kips (predicted service load level), a displacement of 0.16 in. can be observed.

The full test for the hooked-bar connection is depicted in Figure 5-4. After 150 kips, the nonlinear behavior of the specimen and a bigger displacement are observed.

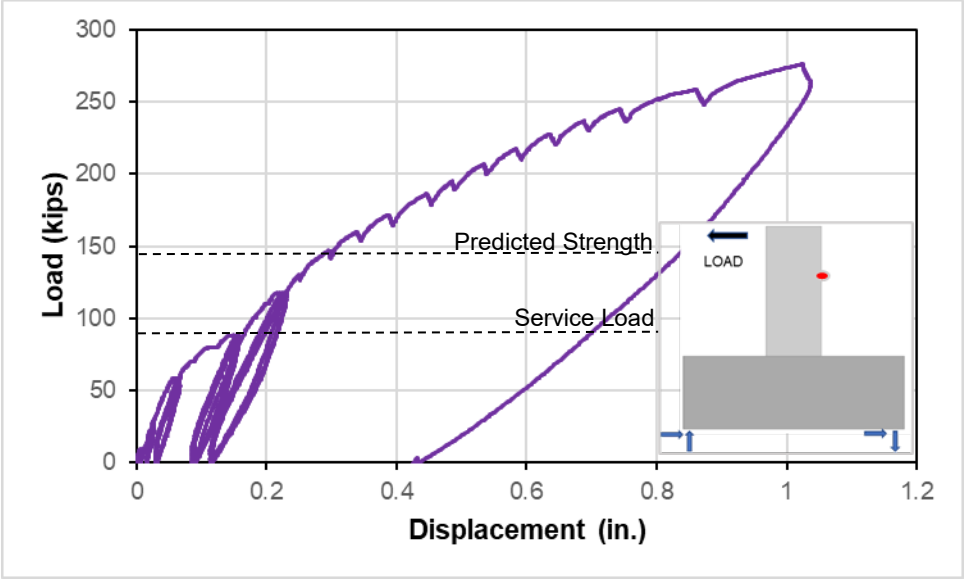

Figure 5-4: Full test hooked-bar specimen

A final residual displacement of 0.43 in. was observed after unloading at the end of the test for the hooked-bar connection.

5.1.1.3 Straight-Bar Specimen

Taking a closer look at the cycles for the straight-bar connection in Figure 5-5, it is very hard to identify the different slopes of the lines corresponding to each cycle for loads up to 88.2 kips (predicted service load level). This means there was very little variation in stiffness during the three cycles at each load level and very little residual displacement.

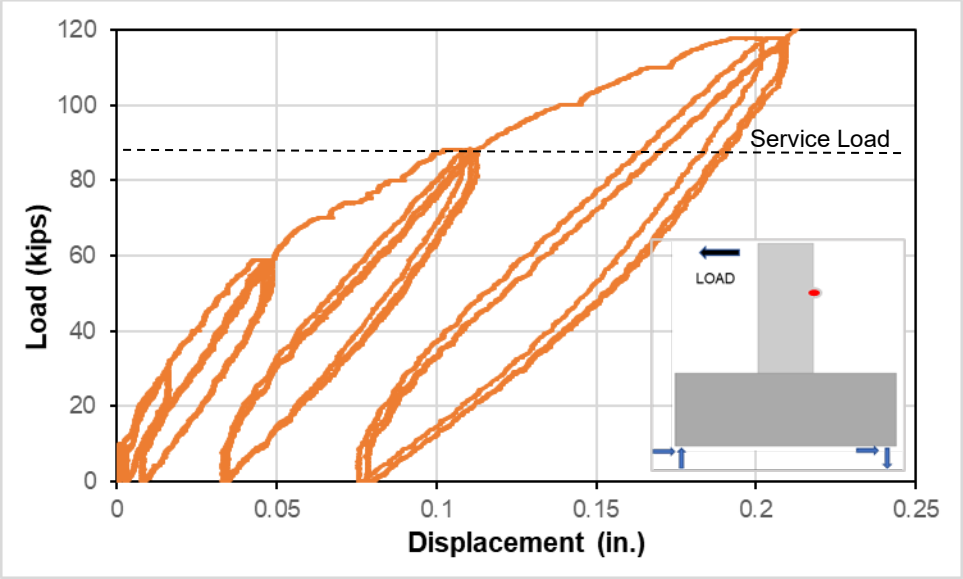

Figure 5-5: Straight-bar specimen cycles

The initial stiffness of the specimen remains constant from the beginning of the test until a load of 58.8 kips. A significant reduction of the slope occurs after this, potentially caused by the flexural cracking of the concrete inside the pipe. A second slope of the stiffness is visible thereafter until 117.6 kips. Another significant reduction of stiffness occurs close to 150 kips, potentially caused by the yielding of the steel reinforcement. Notably, a load of 117.6 kips corresponds to a displacement of 0.21 in. This corresponds to a displacement 23% higher than the headed-bar connection for the same load. Additionally, at 88.2 kips (predicted service load level), a displacement of 0.12 in. can be observed.

The full test for the straight-bar connection is depicted in Figure 5-6. After 150 kips, the nonlinear behavior of the specimen and a bigger displacement are observed.

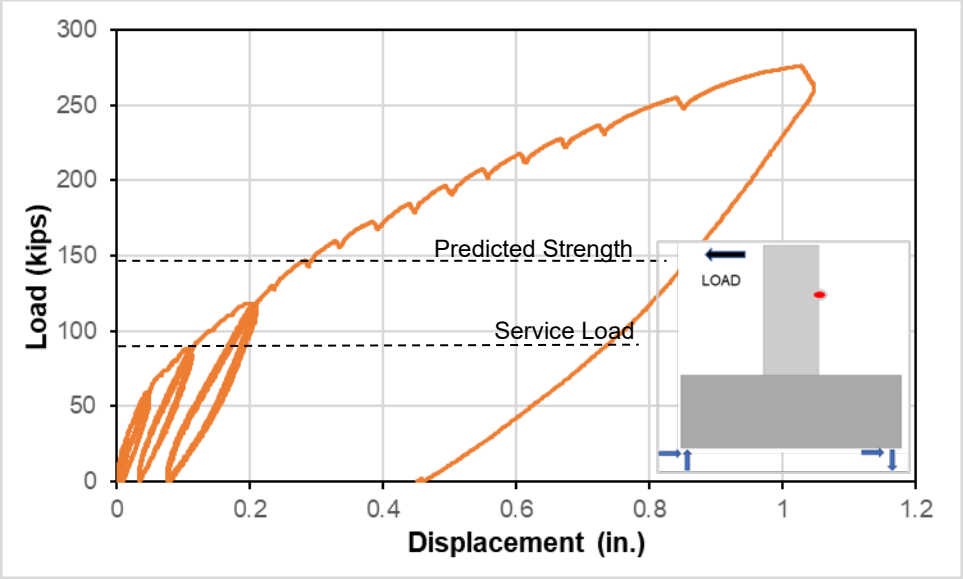

Figure 5-6: Full test straight-bar specimen

A final residual displacement of 0.45 in. was observed after unloading at the end of the test for the straight-bar connection.

5.1.1.4 Shear Stud Specimen

Taking a closer look at the cycles for the shear stud connection in Figure 5-7, it is very hard to identify the different slopes of the lines corresponding to each cycle. This means there was very little variation in stiffness during the three cycles at each load level and very little residual displacement.

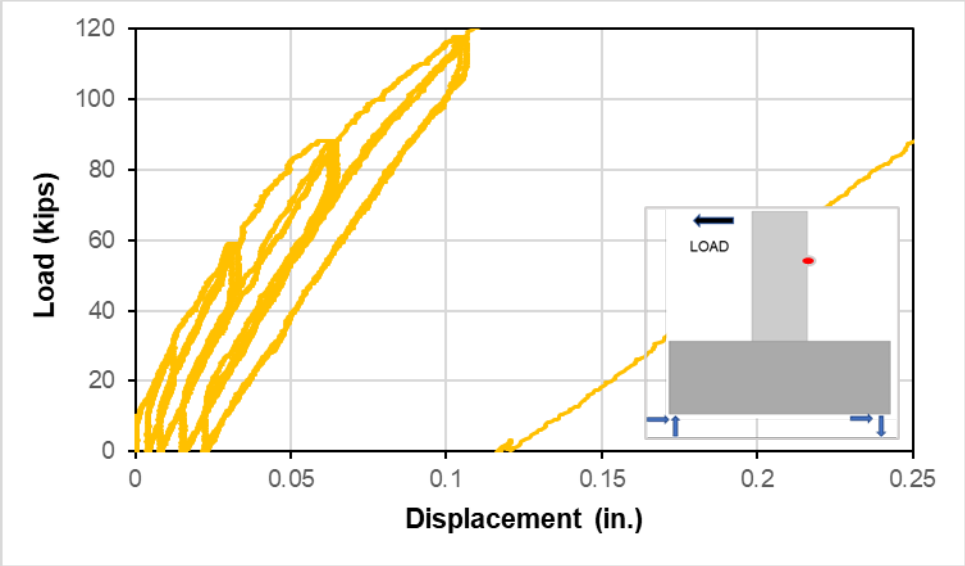

Figure 5-7: Shear stud specimen cycles

The initial stiffness of the specimen remains constant from the beginning of the test until a load of 88.2 kips (predicted service load level). This is caused by the cracking of the concrete. A second reduction in stiffness occurs thereafter until 117.6 kips. Notably, a load of 117.6 kips corresponds to a displacement of 0.11 in. This corresponds to a displacement 35% lower than the headed-bar connection for the same load. This specimen had the least displacement of all five. Additionally, at 88.2 kips (predicted service load level), a displacement of 0.065 in. can be observed.

The full test for the shear stud connection is depicted in Figure 5-8. After 170 kips, the nonlinear behavior of the specimen and a bigger displacement are observed.

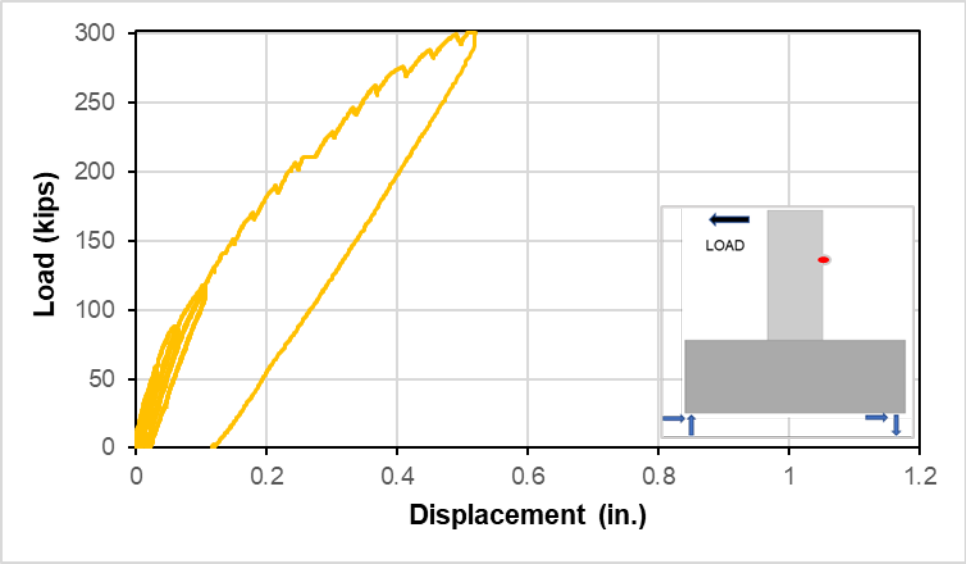

Figure 5-8: Full test shear stud specimen

A final residual displacement of 0.12 in. was observed after unloading at the end of the test for the shear stud connection.

5.1.1.5 Annular Ring Specimen

Taking a closer look at the cycles for the annular ring connection in Figure 5-9, it is very hard to identify the different slopes of the lines corresponding to each cycle. This means there was very little variation in stiffness during the three cycles at each load level and very little residual displacement.

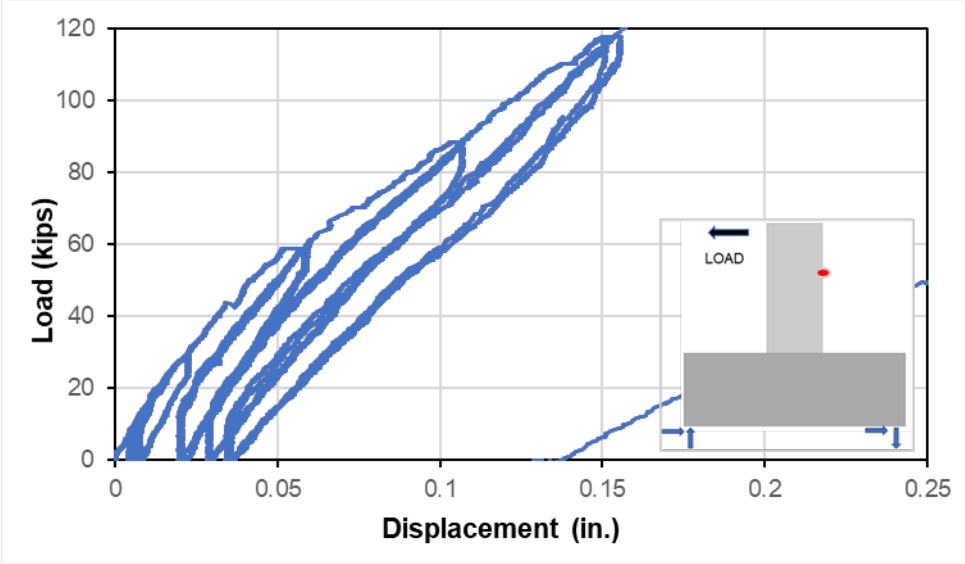

Figure 5-9: Annular ring specimen cycles

The initial stiffness of the specimen remains constant from the beginning of the test until a load of 58.8 kips. This is caused by the cracking of the concrete. A second reduction in stiffness occurs thereafter until 117.6 kips. Notably, a load of 117.6 kips corresponds to a displacement of 0.15 in. This corresponds to a displacement 36% higher than the shear stud connection for the same load.

The full test for the annular ring connection is depicted in Figure 5-10. After 170 kips, the nonlinear behavior of the specimen and a bigger displacement are observed.

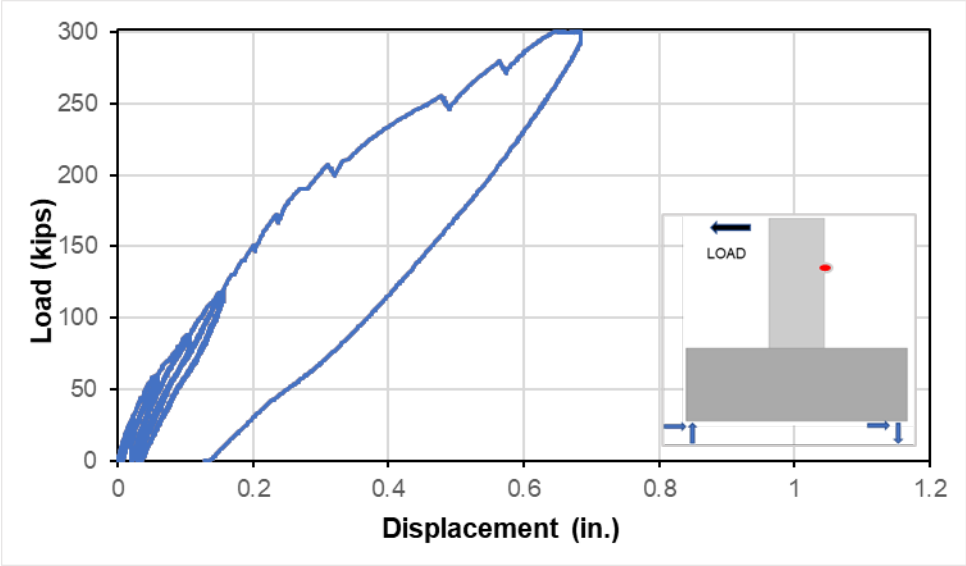

Figure 5-10: Full test annular ring specimen

A final residual displacement of 0.13 in. was observed after unloading at the end of the test for the annular ring connection.

5.1.1.6 Load versus Displacement Stiffness

Table 5-1 summarizes the stiffness slope of the load versus displacement curves at first reload for all five specimens at different load levels.

Table 5-1: Load vs displacement reload stiffness

Reload Range (kips)	Reload Stiffness (kips/in)				
	Head	Hook	Straight	Stud	Ring
0-59	1625	1639	1484	2440	1546
0-89	1176	1230	1119	1781	1142
0-118	980	1028	901	1416	996

Analyzing the cycles for each type of connection, the secant slope of the load versus deflection relationship for the first reload cycle at each load level was calculated. Each of the three reinforcing-bar connections had a similar stiffness between 0 and 59 kips, with the straight-bar connection demonstrating slightly less stiffness than the headed- and hooked-bar connections. There is a decreased stiffness for all three specimens from 0 to 89 kips, as the effects of internal concrete cracking become evident, with the straight bars again exhibiting the least stiffness. For load cycles up to 118 kips, a similar pattern is evident, with continued stiffness degradation in all three connections due to continued cracking.

For the welded mechanical anchorage connections, the shear stud specimen had a greater stiffness than the annular ring connection for the entire range of loadings. These two connection types were expected to exhibit a greater stiffness than the reinforcing-bar connections due to the increased participation of the pile because of its greater embedment depth. However, the annular ring specimen exhibited reloading stiffnesses similar to those of the reinforcing-bar connections.

5.1.1.7 Comparison of Connections at Service Load

Figure 5-11 compares the behavior of all specimens under the predicted service load level for the reinforcing steel connections (88.2 kips). Most of them behaved very

similarly except for the shear stud connection, which had a higher stiffness. All specimens reached a load level of 88.2 kips without any issues and minor cracking.

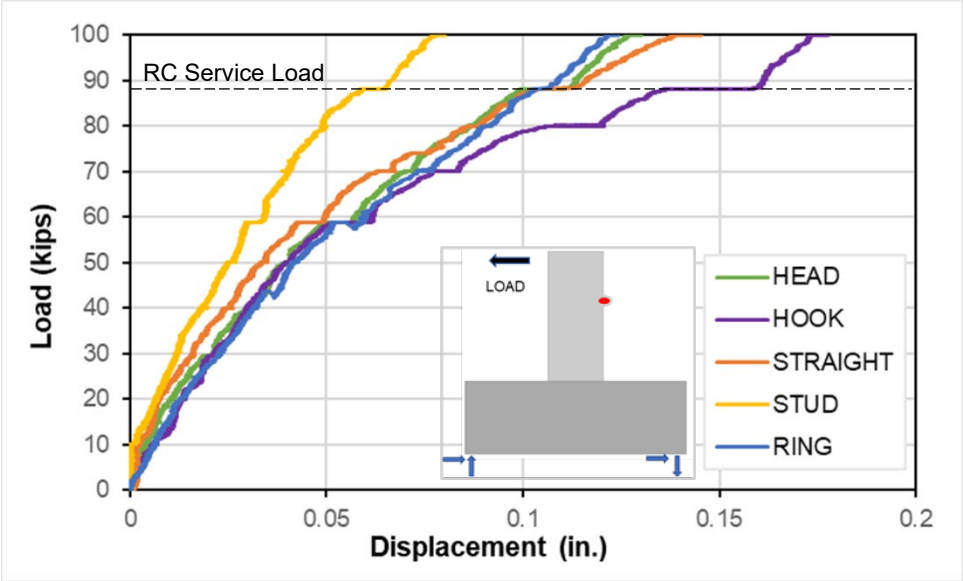

Figure 5-11: Specimen displacement under service load

5.1.2 Load versus Displacement to Maximum Load

The load versus displacement graphs in this section describe the backbone curve for each specimen. The vertical axis represents the force applied by the actuator in kips, and the horizontal axis represents the net displacement of the specimens in inches. These data were obtained by using the readings from the linear potentiometer D-P-S-3 at a height of 58.5 in. after accounting for the slip of the bent cap. The specimens are compared in groups to understand their behavior under the same load protocol.

Figure 5-12 depicts the behavior of the three specimens with reinforcing bar connections. All three specimens performed similar behavior. However, the headed-bar connection showed a slightly higher stiffness throughout the test.

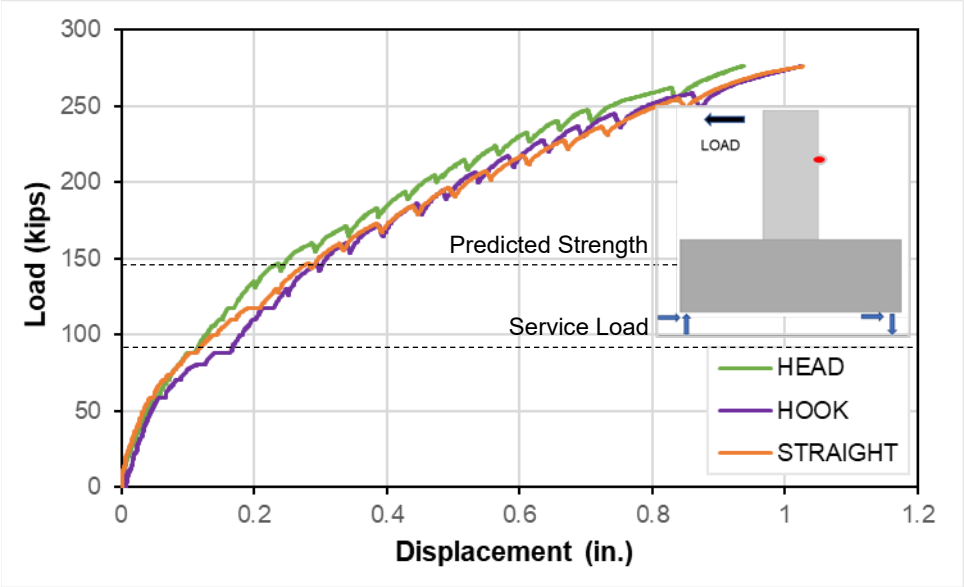

Figure 5-12: Backbone curves of the steel reinforcement connections

Two horizontal dashed lines on the graph represent the 88.2 kips service load level and the calculated reinforced concrete cross-section capacity of 147 kips, not including the potential contribution of the steel pipe pile. All three specimens smoothly reached the service design load level and surpassed the RC cross-section capacity without significant issues. As can be seen, all three reached the final 276 kips load they were subjected to without experiencing failure.

Figure 5-13 depicts the behavior of the two specimens with welded mechanical anchorage connections and deeper embedment. Both specimens performed very well and showed a higher stiffness than those in Figure 5-12. However, the shear stud connection showed a higher stiffness overall throughout the test.

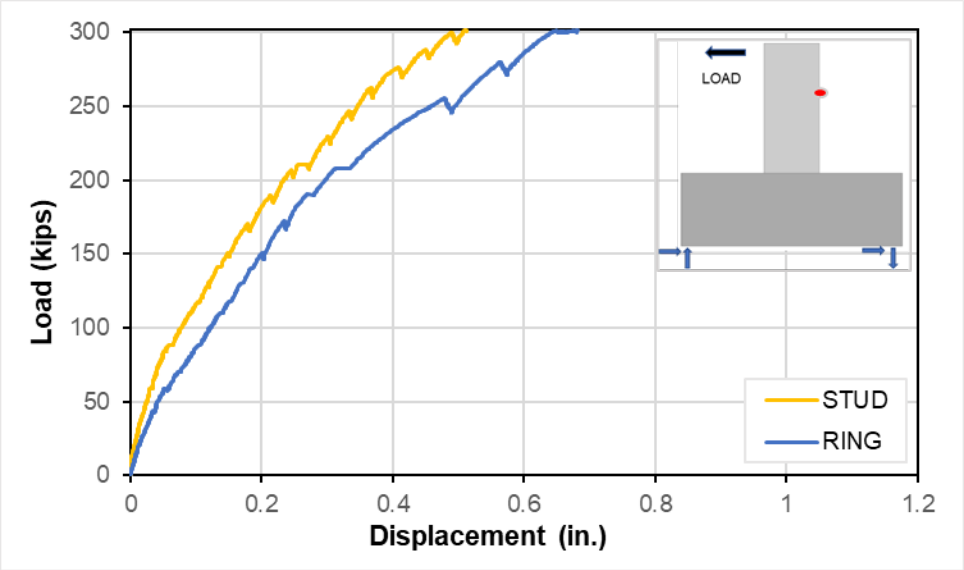

Figure 5-13: Backbone curves of the welded mechanical anchorage connections

5.1.3 Load versus Drift

The load versus drift graphs in this section describe the backbone curves for each specimen. The vertical axis represents the force applied by the actuator in kips at a height of 6 ft 4.5 in., and the horizontal axis represents the drift of the specimens in percentage. These data were obtained using the specimen's net displacement divided by 58.5 in., corresponding to the point where the displacement was measured. The specimens are compared in groups to understand their behavior under the same load protocol.

Figure 5-14 depicts the behavior of the three specimens with reinforcing bar connections. All three specimens performed similar behavior. However, the straight-bar connection showed a higher drift.

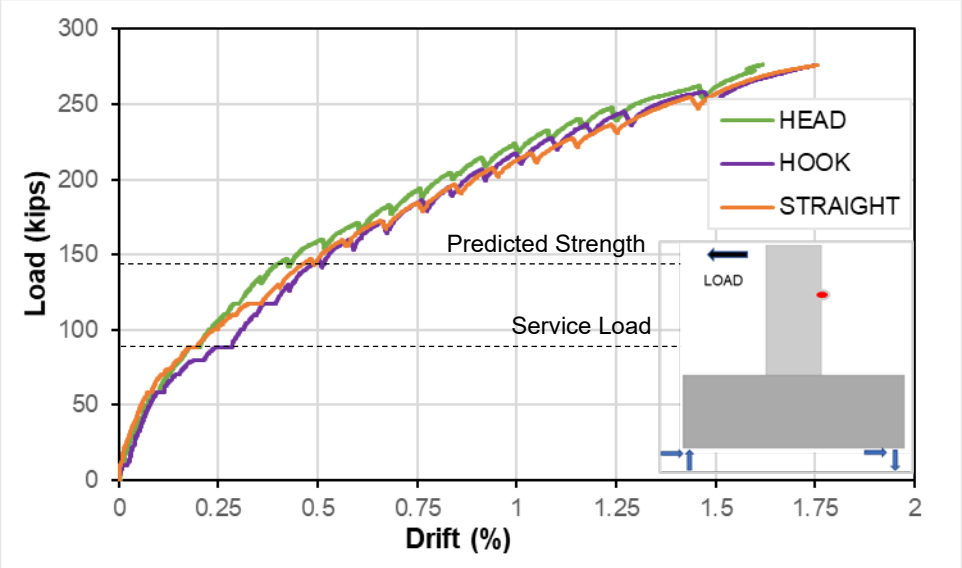

Figure 5-14: Drifts of the reinforcing bar connections

Figure 5-15 depicts the behavior of the two specimens with welded mechanical anchorage connections. Both specimens showed lower drifts than the ones in Figure 5-14. However, the shear stud connection showed the least drift overall throughout the test. Also, the shear stud connection showed the highest stiffness, minor cracking and deformation for the applied 301 kips load. A comparison of the drifts would be more meaningful if the ultimate load was achieved in all cases.

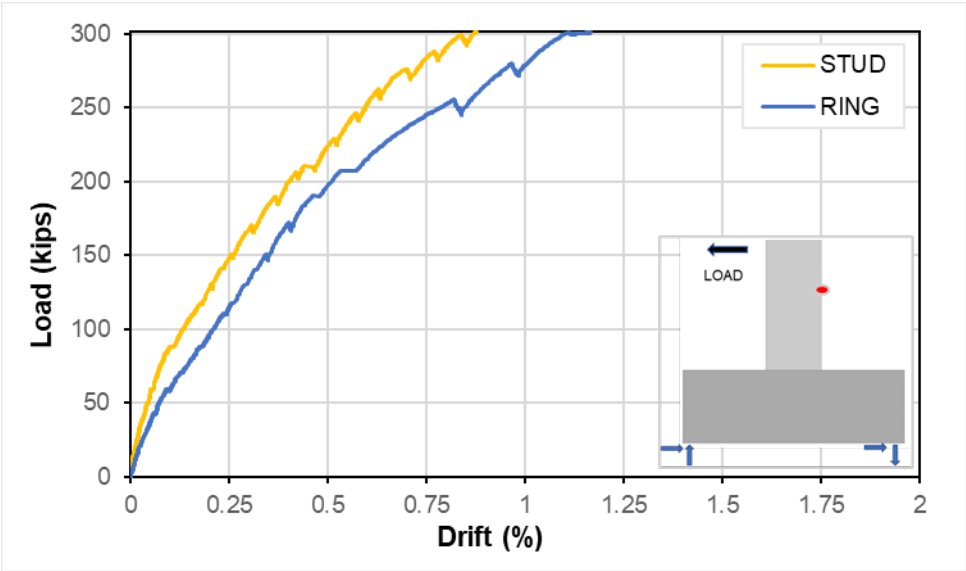

Figure 5-15: Drifts of the welded mechanical anchorage connections

5.1.4 Load versus Pile Rotation

The load versus rotation graphs in this section describe the backbone curves for each specimen. The vertical axis represents the force applied by the actuator in kips at a height of 6 ft 4.5 in. The horizontal axis represents the rotation of the specimens in radians at 11.5 in. on top of the concrete bent cap relative to the rotation of the bent cap. The specimens are compared in groups to understand their behavior under the same load protocol. These plots focus on the flexural deformation of the pile very close to the connection.

Figure 5-16 depicts the behavior of the three specimens with reinforcing bar connections. The headed-bar connection, which showed the least displacement, had a rotation of 0.008 rad at the end of the test, while the straight-bar connection, with the highest displacement, showed a rotation of 0.009 rad.

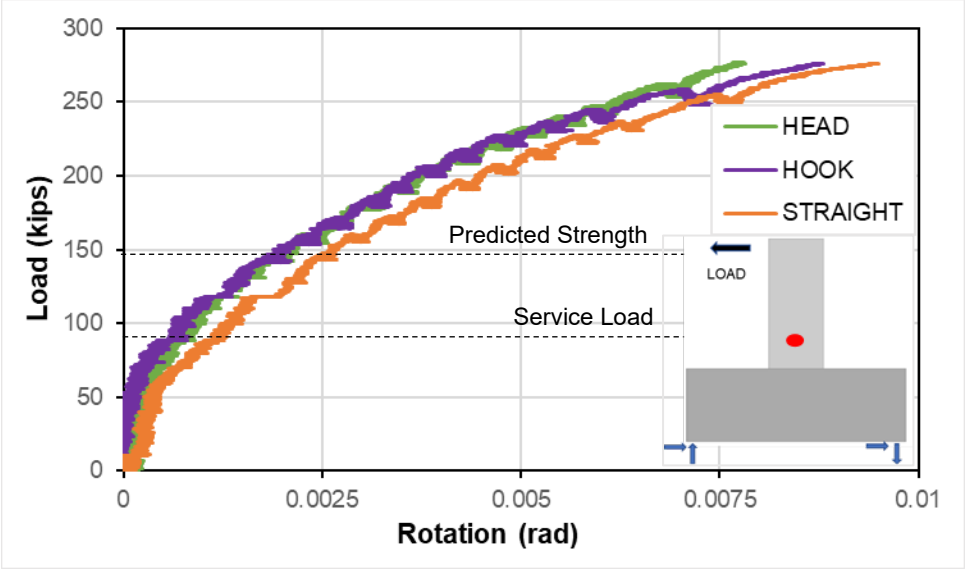

Figure 5-16: Net rotation of the reinforcing bar connections

The curves exhibited behavior similar to those in Figure 5-12, corresponding to the load versus displacement curves. The response shows initial linear elastic behavior followed by the progressive reduction of the stiffness due to concrete cracking and steel reinforcement yielding. The straight-bar connection showed more post-cracking deformation in this local zone. This behavior is similar to the load versus displacement curve presented in Figure 5-12.

Figure 5-17 depicts the behavior of the two specimens with welded mechanical anchorage connections. As previously mentioned, the shear stud connection had the least rotation compared to all specimens, corresponding to 0.0018 rad. The annular ring connection showed a rotation of 0.0033 rad at the end of the test. The annular ring connection showed more post-cracking deformation in this local zone. This behavior is similar to the load versus displacement curve presented in Figure 5-13.

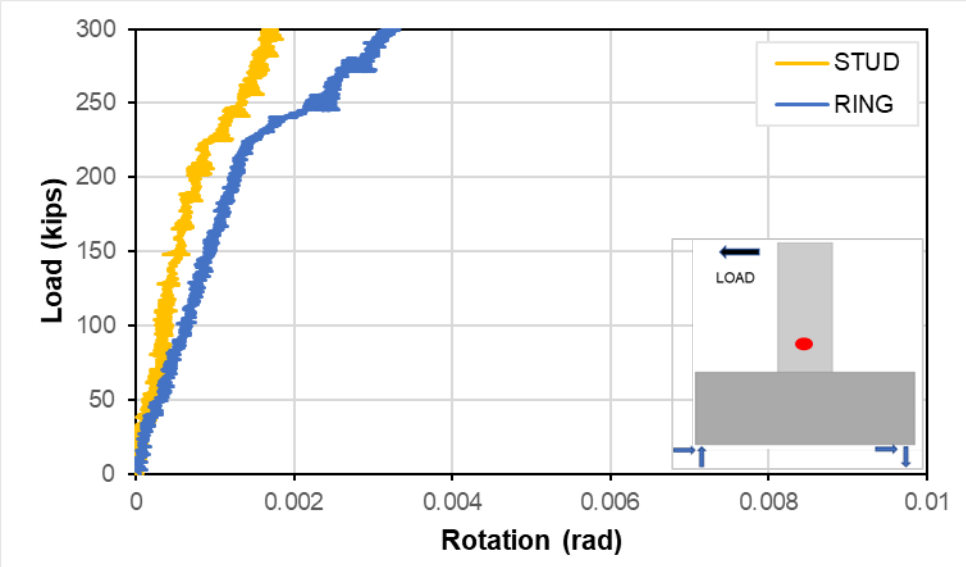

Figure 5-17: Net rotation of the welded mechanical anchorage connections

5.1.5 Steel Reinforcement, Pile, and Concrete Strains

The load versus strain graphs in this section describe the curves of all strain gauges used for each specimen. The vertical axis represents the force applied by the actuator in kips at a height of 6 ft 4.5 in., and the horizontal axis represents the measured strain in microstrain. These data were obtained by using the readings of the concrete and steel strain gauges attached to each specimen. Positive values represent tensile strain, and the negative values represent compressive strain.

Complete data plots for each specimen are presented in the Appendix section.

The uniaxial yielding strain is calculated as $\varepsilon = \frac{fy}{E_s}$. The yielding strain for reinforcing bars corresponds to 2328 με, and the pile yielding strain corresponds to 2269 με. These values are represented by a vertical dashed line, which allows us to understand if the pile or reinforcing bars yielded or approached yielding.

5.1.5.1 Headed-Bar Specimen

Figure 5-18 shows the compressive and tensile strains of the pile during the test for the headed-bar connection. The pile did not show a compressive strain greater than 1100 με and a tensile strain greater than 850 με. The pile did not show any signs of approaching yielding. However, the steady increase of most pile strains with increasing load indicates that the embedded pile contributed significantly to the strength of the connection. This contribution was conservatively neglected in design.

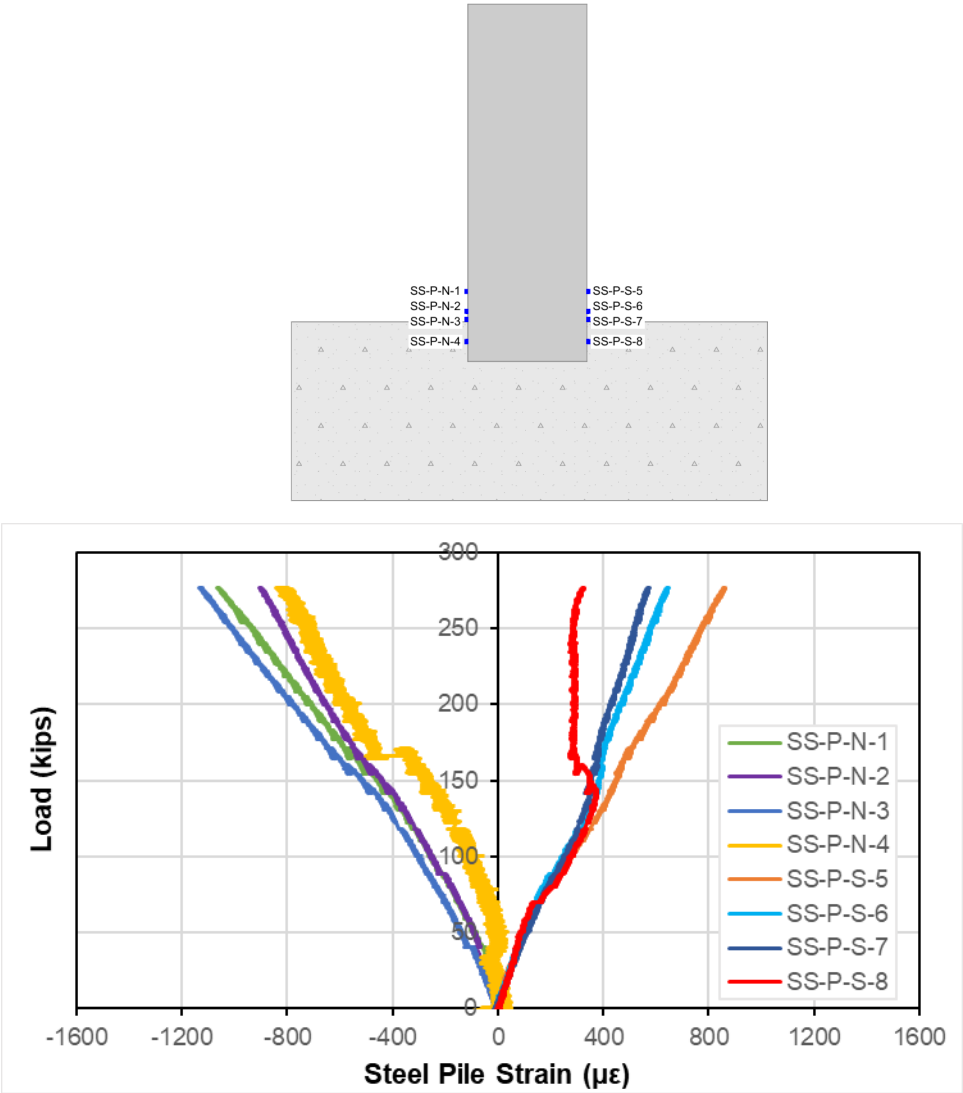

Figure 5-18: Steel pile strains for the headed-bar connection

Figure 5-19 describes the behavior of the headed reinforcing bar connection. As can be seen, the tension rebar yielded, especially in the bottom part of the connection, where the yielding strain was significantly exceeded. The load at which the reinforcing

bars started to yield corresponds to the calculated RC cross-section strength; this confirms that the stiffness reduction observed resulted from reinforcement yielding. This reinforcing steel connection showed the greatest yielding strains.

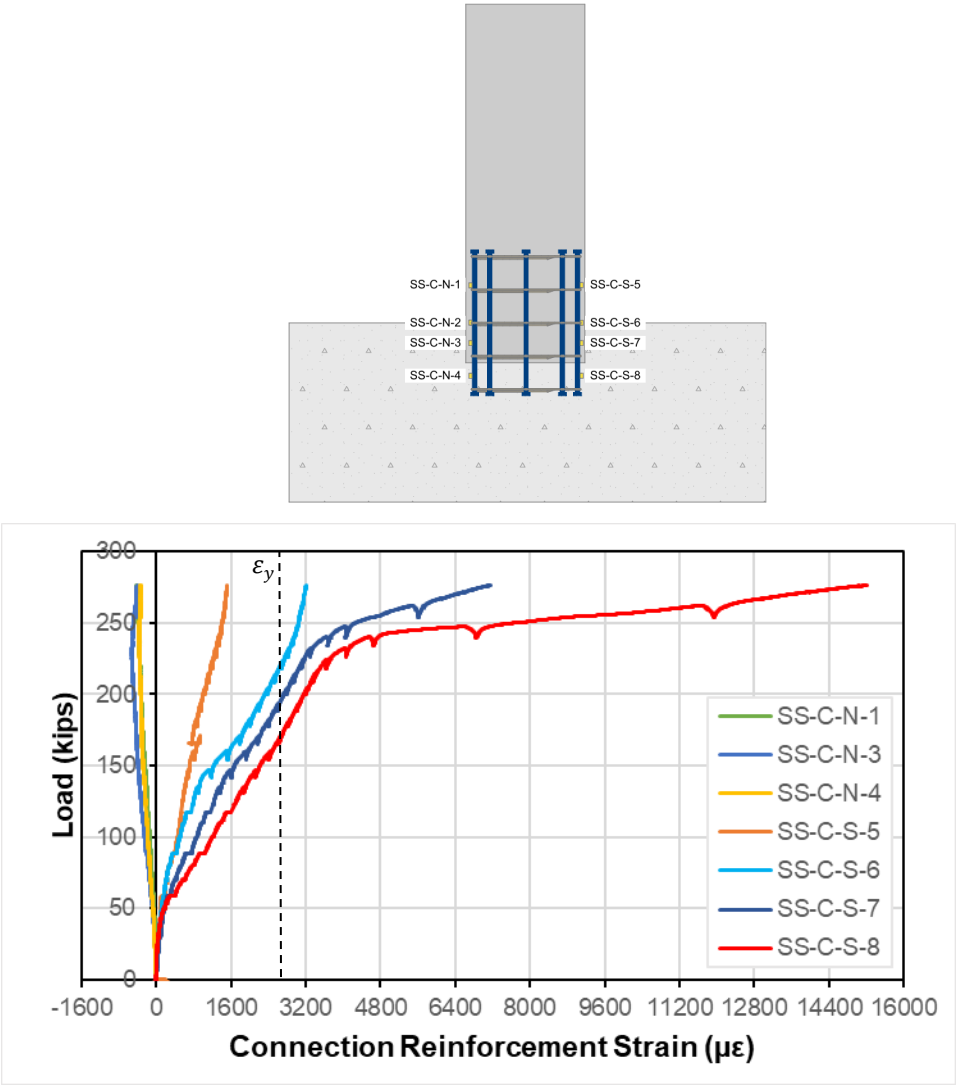

Figure 5-19: Headed reinforcing bars strains

Figure 5-20 shows the load versus concrete strain graph. These were measured on the north top face of the bent cap during testing. All strains were lower than 350 με in compression.

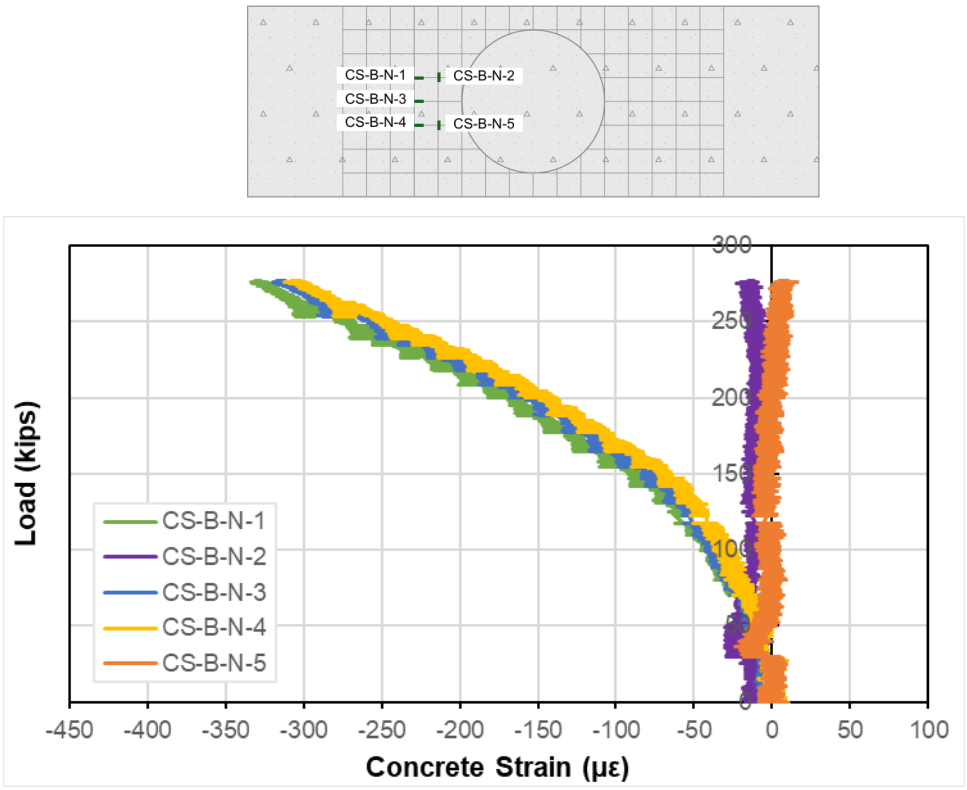

Figure 5-20: Concrete bent cap strains headed-bar specimen

5.1.5.2 Hooked-Bar Specimen

Figure 5-21 shows the compressive and tensile strains of the pile during the test for the hooked-bar connection. The pile did not show a compressive strain greater than 1200 με and a tensile strain greater than 880 με. The pile did not show any signs of approaching yielding. However, the steady increase of most pile strains with increasing load indicates that the embedded pile contributed significantly to the strength of the connection. This contribution was conservatively neglected in design.

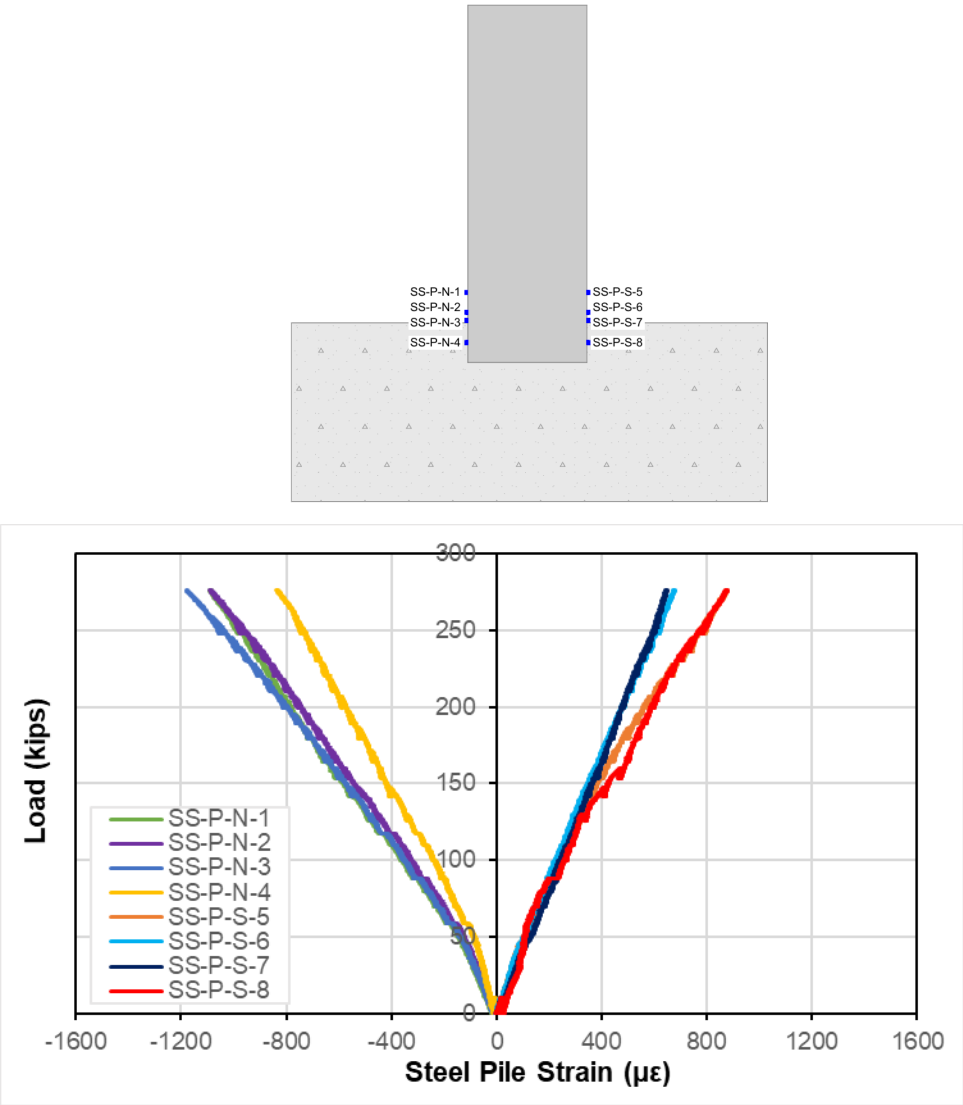

Figure 5-21: Steel pile strains for the hooked-bar connection

Figure 5-22 describes the behavior of the hooked reinforcing bar connection. The tension rebar yielded in the bottom part of the connection, where the yielding strain was exceeded.

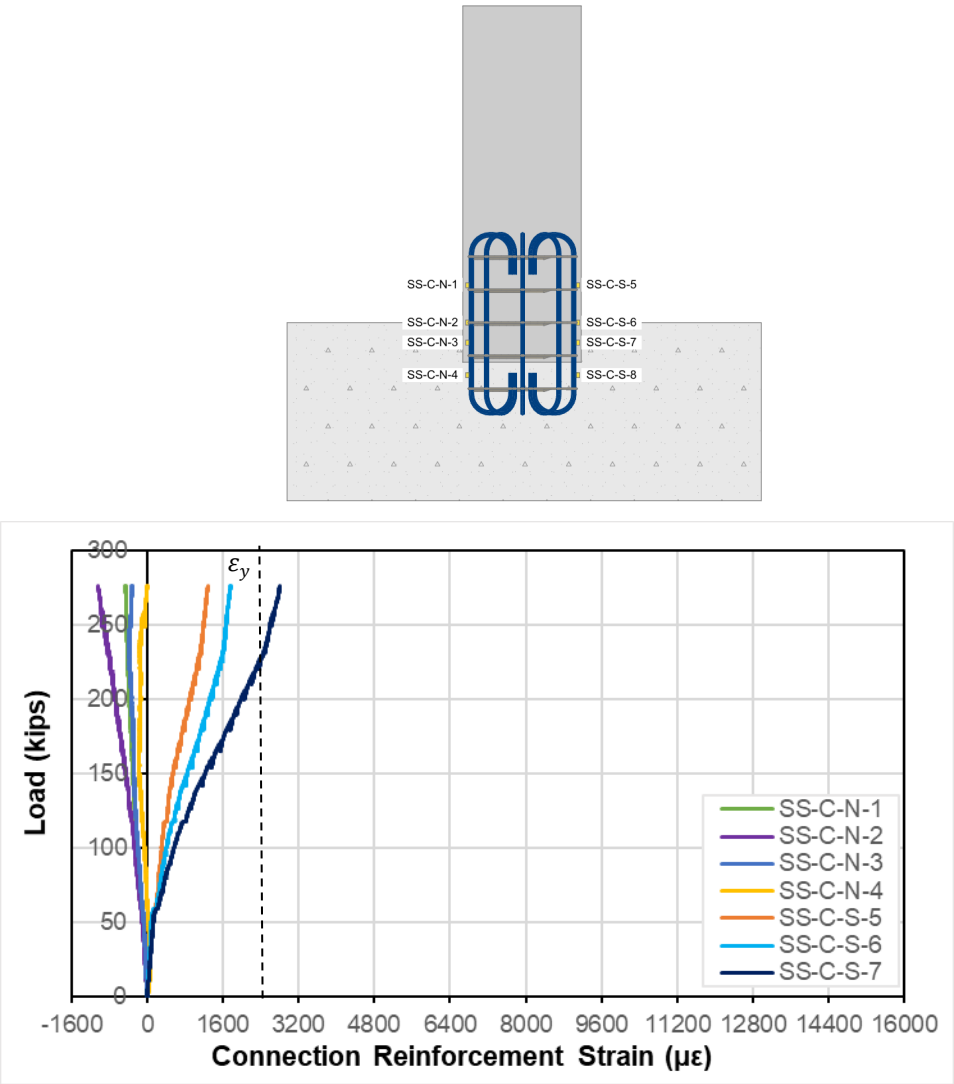

Figure 5-22: Hooked reinforcing bars strains

Figure 5-23 shows the load versus concrete strain graph. These were measured on the north top face of the bent cap during testing. All strains were lower than 450 με in compression.

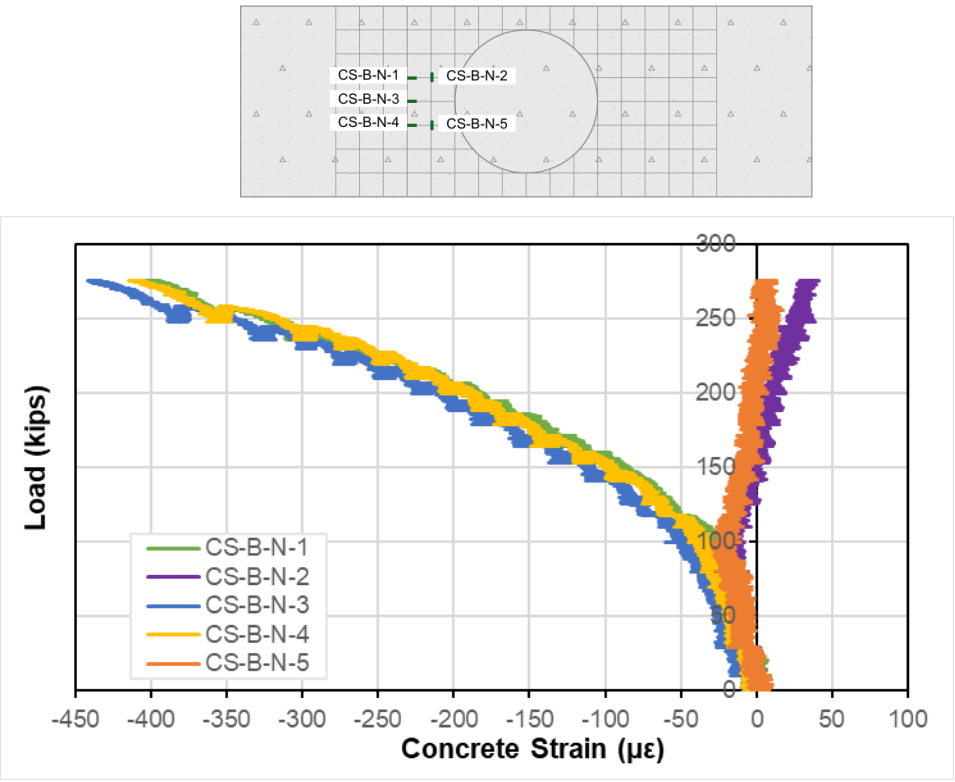

Figure 5-23: Concrete bent cap strains hooked-bar specimen

5.1.5.3 Straight-Bar Specimen

Figure 5-24 shows the compressive and tensile strains of the pile during the test for the straight-bar connection. The pile did not show a compressive strain greater than 1100 με and a tensile strain greater than 650 με. The pile did not show any signs of approaching yielding. However, the steady increase of most pile strains with increasing load indicates that the embedded pile contributed significantly to the strength of the connection. This contribution was conservatively neglected in design.

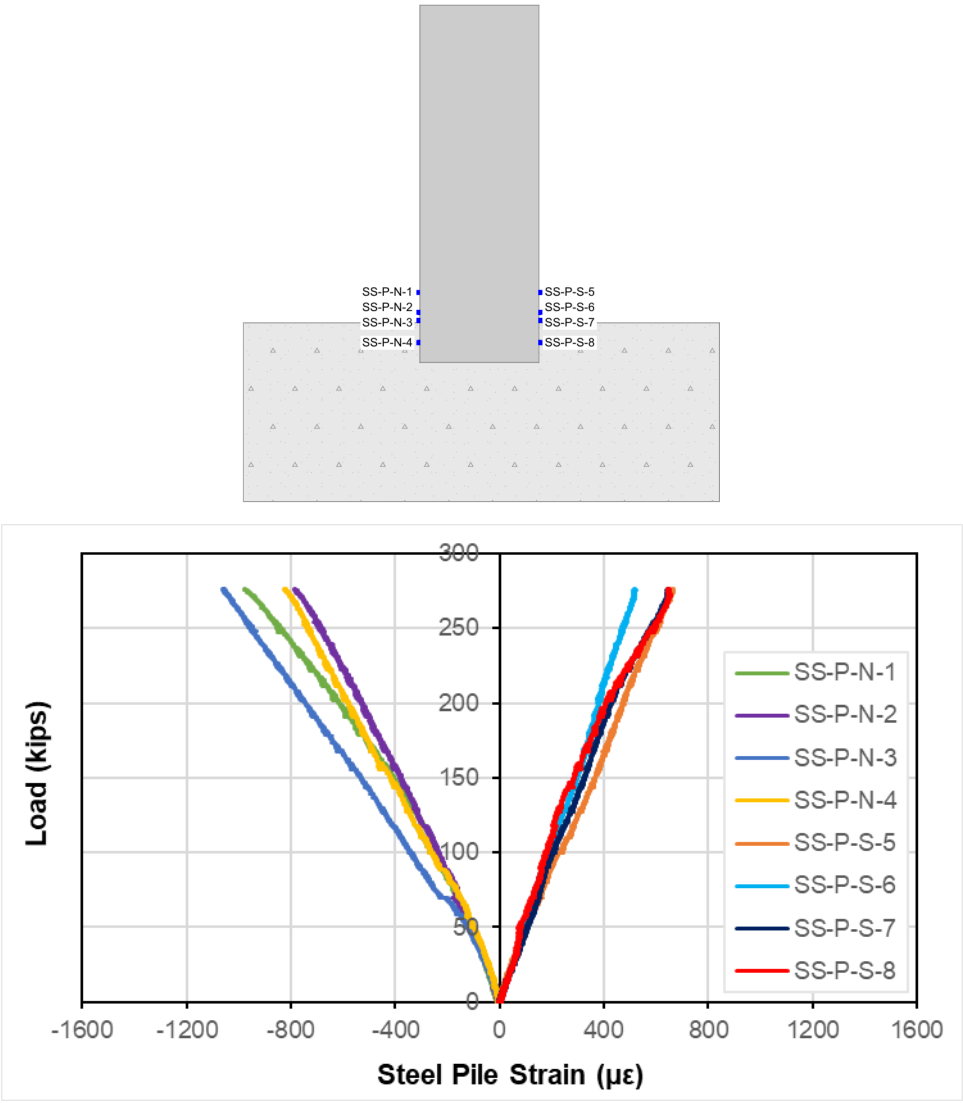

Figure 5-24: Steel pile strains for the straight-bar connection

Figure 5-25 describes the behavior of the straight reinforcing bar connection. As can be seen, the tension rebar yielded, especially in the middle to the bottom part of the connection, where the yielding strain was exceeded.

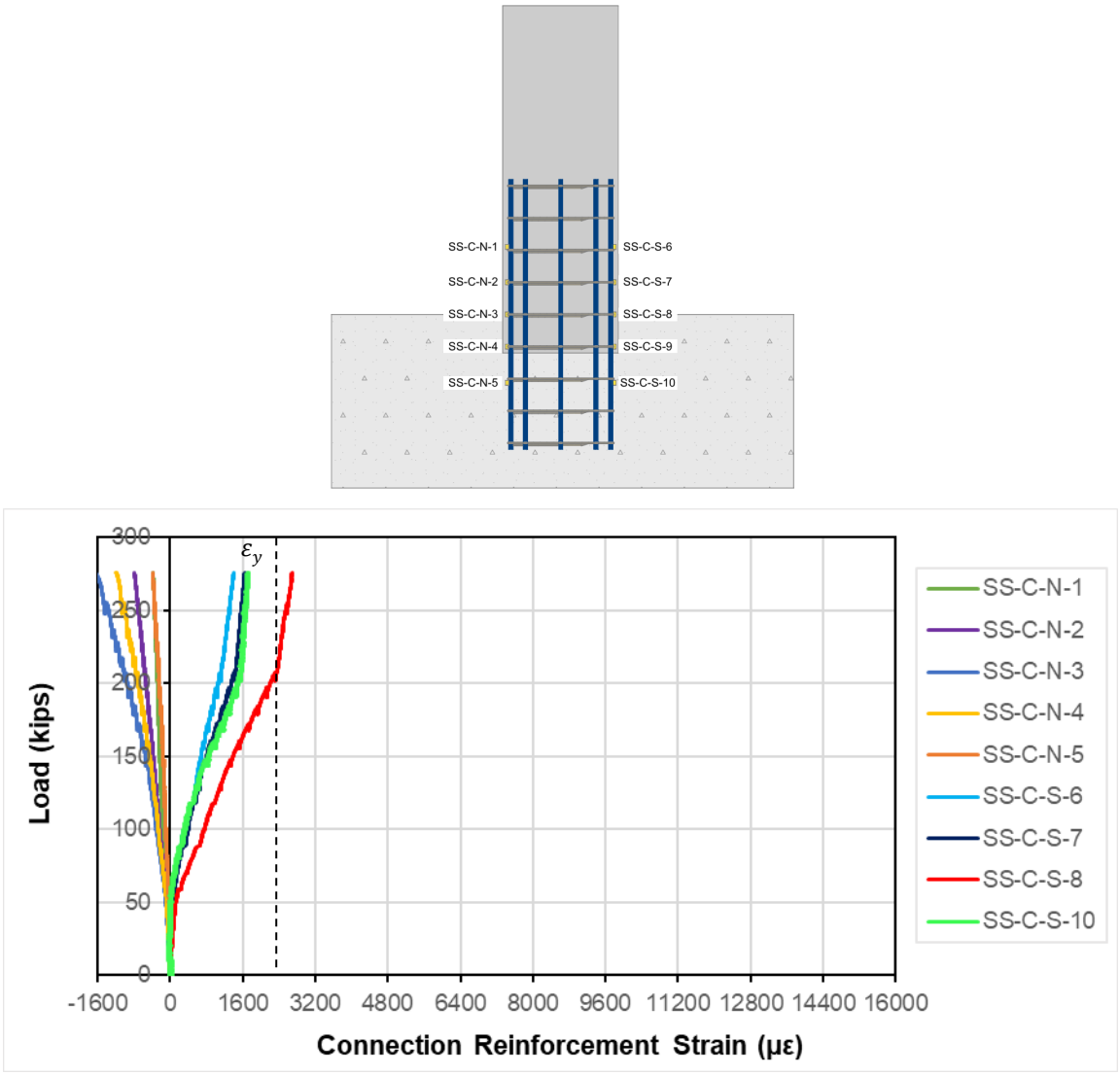

Figure 5-25: Straight reinforcing bars strains

Figure 5-26 shows the load versus concrete strain graph. These were measured on the north top face of the bent cap during testing. All strains were lower than 350 με in compression.

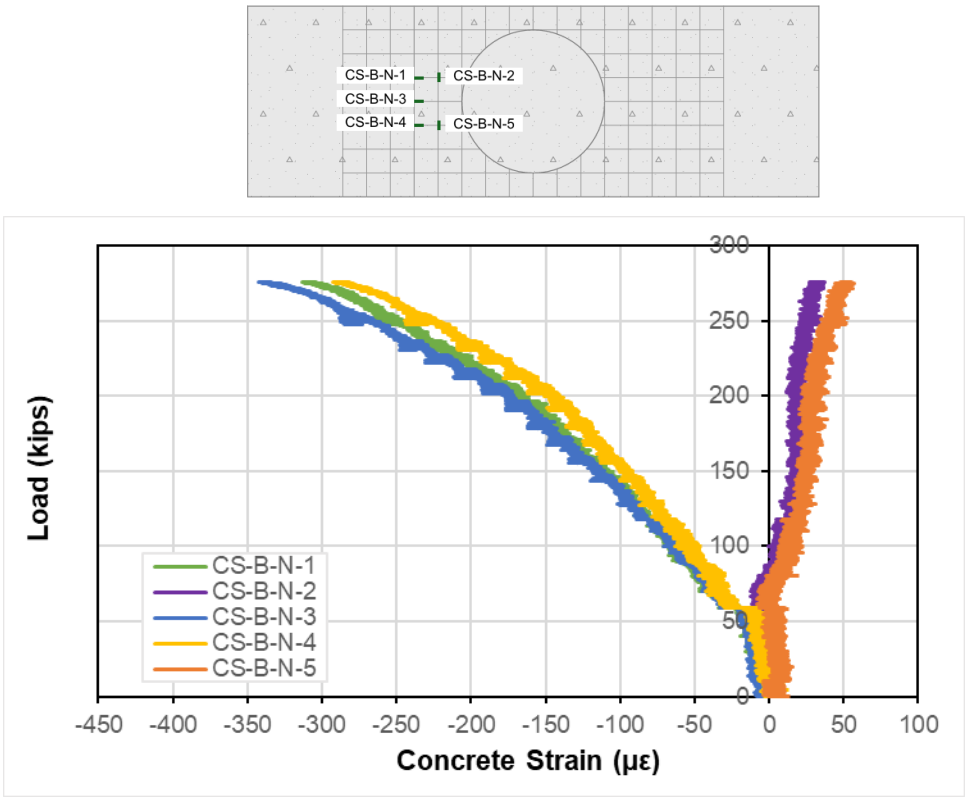

Figure 5-26: Concrete bent cap strains straight-bar specimen

5.1.5.4 Shear Stud Specimen

Figure 5-27 shows the compressive and tensile strains of the pile during the test for the shear stud connection. The pile did not show a compressive strain greater than 1200 με and a tensile strain greater than 1450 με. The pile did not show any signs of approaching yielding. However, the strains indicate the significant contribution of the steel pile.

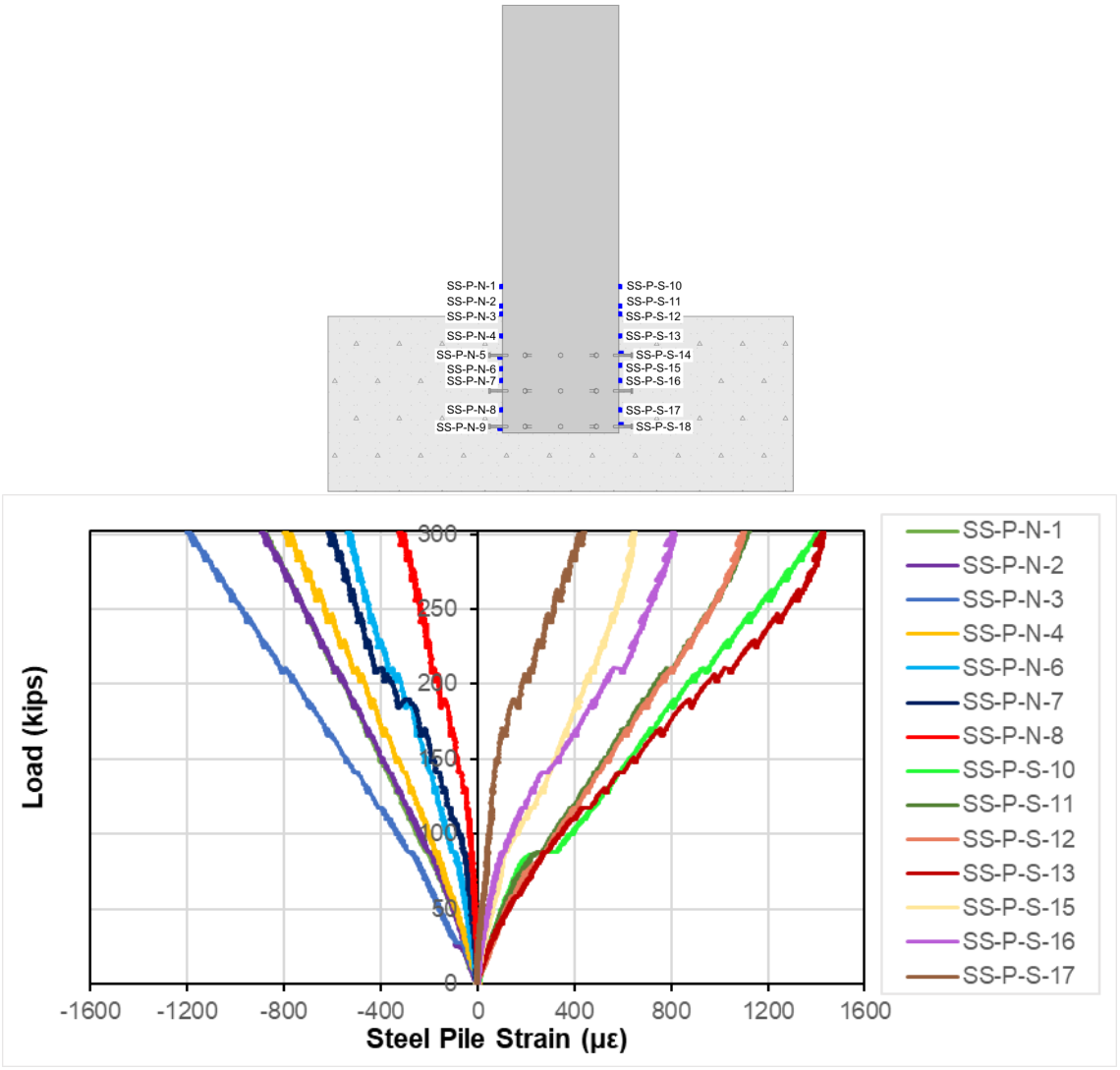

Figure 5-27: Steel pile strains for the shear stud connection

Figure 5-28 describes the behavior of the shear stud connection. As can be seen, none of the shear studs approached yielding on the strain gauge locations. The maximum values are close to the 1200 με for the shear studs in the bottom right layer.

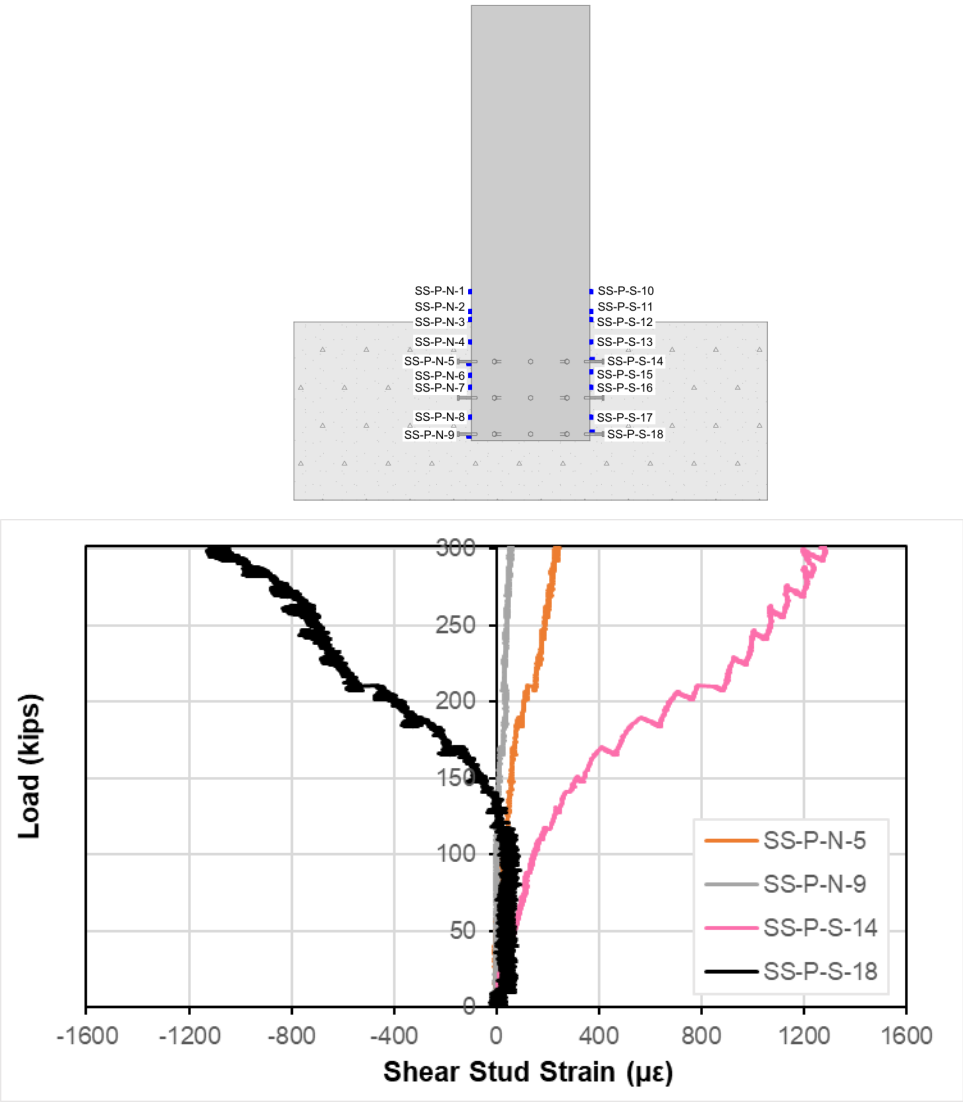

Figure 5-28: Shear studs strains

Figure 5-29 shows the load versus concrete strain graph. These were measured on the north top face of the bent cap during testing. All strains were lower than 200 με in compression.

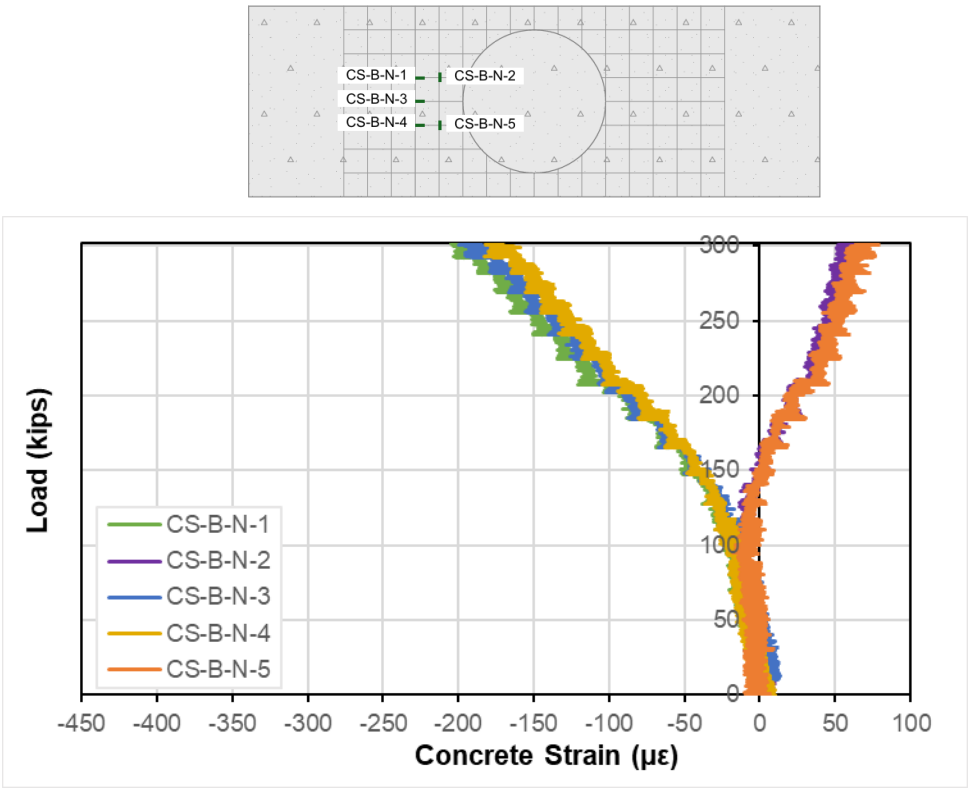

Figure 5-29: Concrete bent cap strains shear stud specimen

5.1.5.5 Annular Ring Specimen

Figure 5-30 shows the compressive and tensile strains of the pile during the test for the annular ring connection. The pile did not show a compressive strain greater than 900 με and a tensile strain greater than 1450 με. The pile did not show any signs of approaching yielding. However, the strains indicate the significant contribution of the steel pile as assumed in the design of this connection.

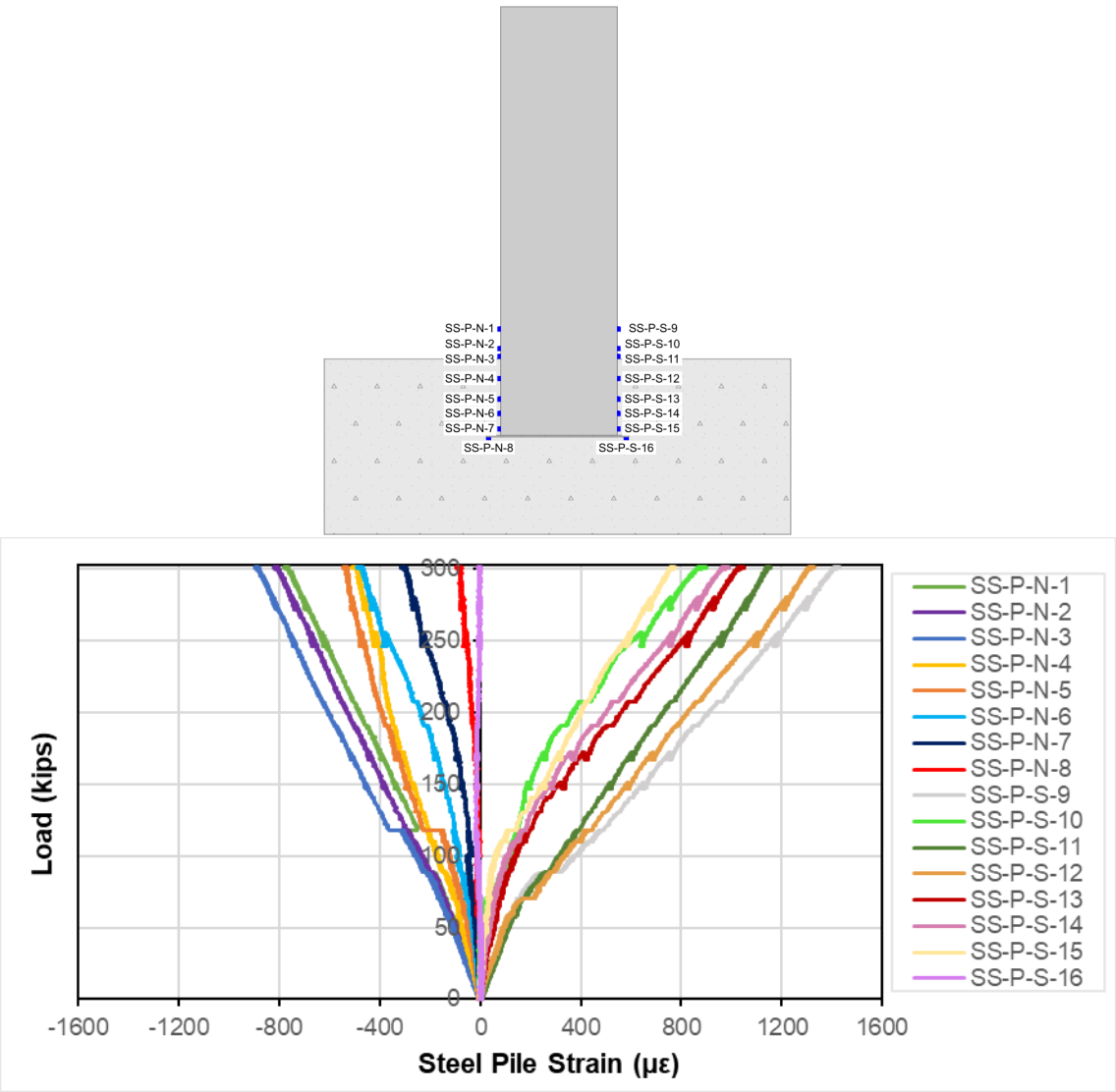

Figure 5-30: Steel pile strains for the annular ring connection

Figure 5-31 shows the load versus concrete strain graph. These were measured on the north top face of the bent cap during testing. All strains were lower than 250 με in compression.

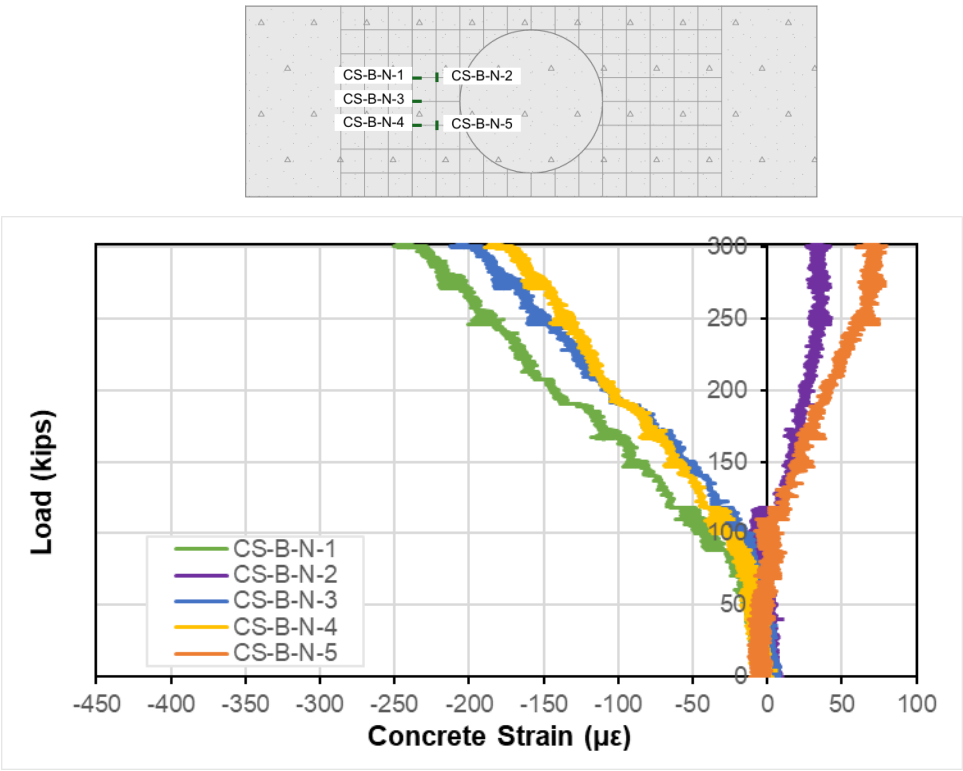

Figure 5-31: Concrete bent cap strains annular ring specimen

5.2 PROGRESSION OF CRACKING

Concrete cracks were marked and measured throughout each loading process. The final crack patterns are depicted in Figures 5-32 to 5-36. Cracks on the top and sides of each specimen are represented with different colors corresponding to different load levels.

The crack pattern was approximately symmetric for the east and west faces of the concrete bent caps.

5.2.1 Headed-Bar Specimen Cracks

Figure 5-32 shows the evolution of the crack pattern of the head specimen. Small vertical cracks started to appear on the east and west faces of the concrete bent cap on the steel pile and concrete bent cap joint between 0 and 60 kips. As shown in Figure 5-32(a), more cracks started appearing on the tension side of the pile and extended while the load increased. Very little cracking is visible at service load levels from 60 and 90 kips. Diagonal cracks emerged between 150 and 220 kips, showing the initiation of a

cone-shaped failure mechanism. This occurred after the predicted strength load was reached. Similarly, on the top of the concrete bent cap, cracks started to show between 60 and 120 kips, as shown in Figure 5-32(b). Cracking can be seen on the top south face of the bent cap following the longitudinal reinforcement.

No crushing or spalling of concrete was observed during the entire test. Between 0 and 120 kips, the opening width of the cracks was about 0.005 in. For loads higher than 120 kips, some cracks reached a width of 0.02 in. by the end of the test. Most cracks are concentrated in the area of the steel reinforcement connection and appeared after 170 kips of lateral load. Once the cracks formed, they were engaged by the longitudinal and transverse reinforcement of the bent cap. This reinforcement is not explicitly considered in the development length equations for these bars. This could be another potential reason for the excess connection capacity exhibited in this test.

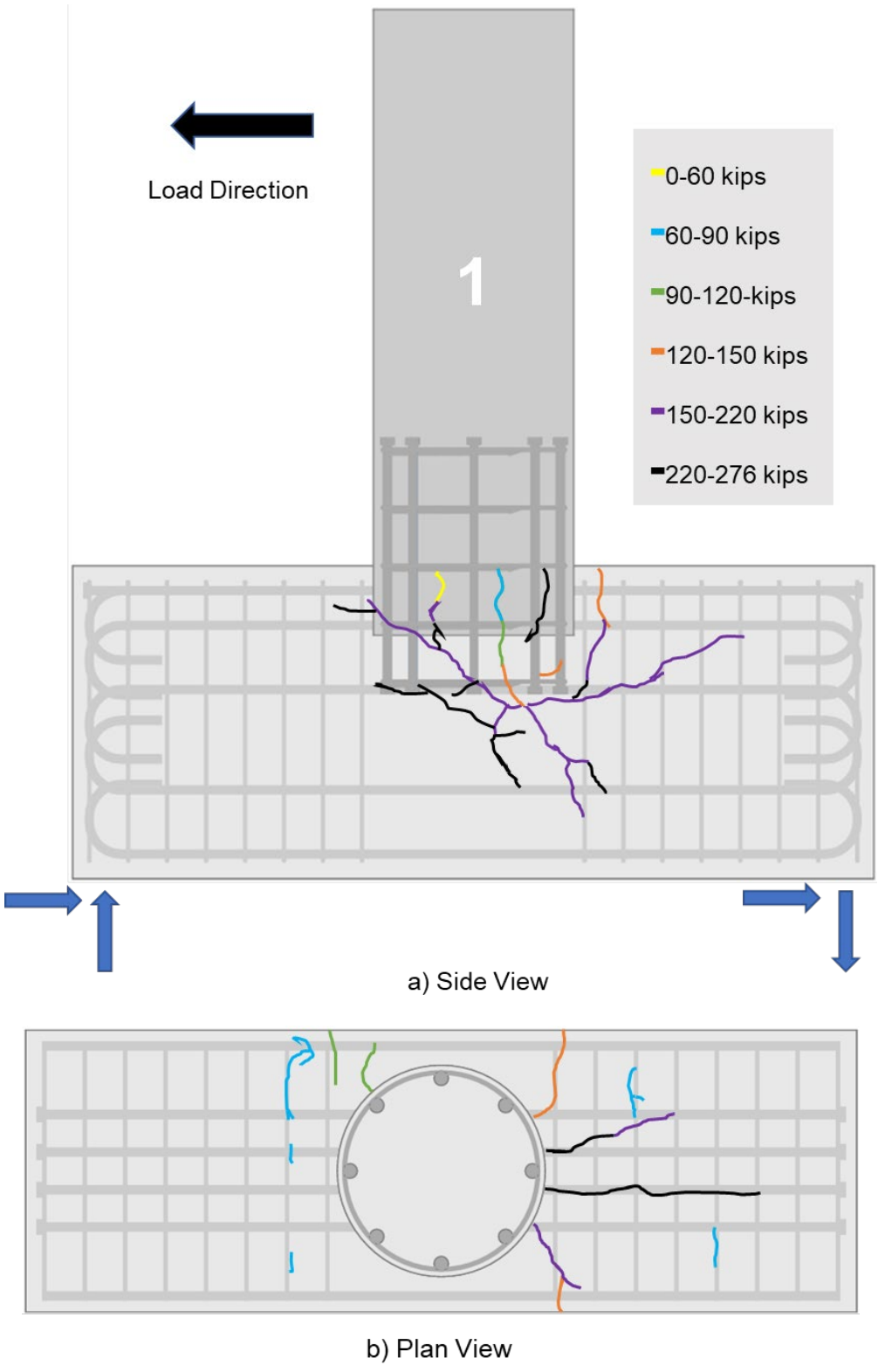

Figure 5-32: Crack pattern for headed-bar specimen

5.2.2 Hook Specimen Cracks

Figure 5-33 shows the crack pattern of the Hook specimen. Small vertical cracks started to appear on the east and west faces of the concrete bent cap on the steel pile and concrete bent cap joint between 0 and 60 kips. As shown in Figure 5-33(a), more cracks started appearing on the tension side of the pile and extended while the load increased. Very little cracking is visible at service load levels from 60 and 90 kips. Diagonal cracks emerged between 150 and 220 kips, showing the initiation of a cone-shaped failure mechanism. This occurred after the predicted strength load was reached.

Similarly, on the top of the concrete bent cap, cracks started to show between 120 and 170 kips, as shown in Figure 5-33(b). Cracking can be seen on the top south face of the bent cap following the longitudinal reinforcement.

No crushing or spalling of concrete was observed during the entire test. For loads higher than 120 kips, some cracks reached an opening width of 0.025 in. by the end of the test. Most cracks are concentrated in the area of the steel reinforcement connection and mainly appeared between 170 and 220 kips of lateral load. Once the cracks formed, they were engaged by the longitudinal and transverse reinforcement of the bent cap. This reinforcement is not explicitly considered in the development length equations for these bars. This could be another potential reason for the excess connection capacity exhibited in this test.

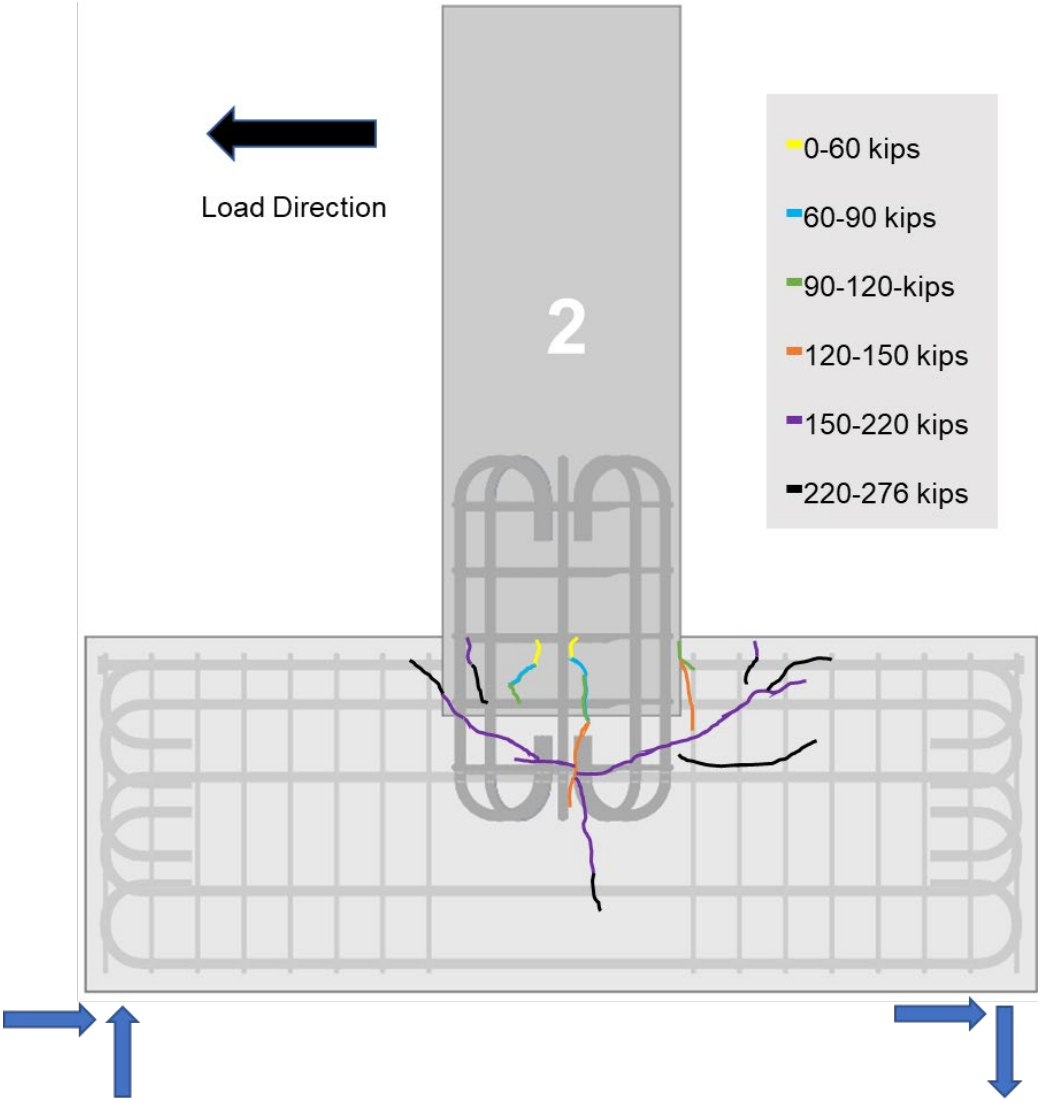

a) Side View

b) Plan View

Figure 5-33: Crack pattern for hooked-bar specimen

5.2.3 Straight Specimen Cracks

Figure 5-34 shows the crack pattern of the Straight specimen. Small vertical cracks started to appear on the east and west faces of the concrete bent cap on the steel pile and concrete bent cap joint between 0 and 60 kips. As shown in Figure 5-34(a), more cracks started appearing on the tension side of the pile and extended while the load increased. Very little cracking is visible at service load levels from 60 and 90 kips. Diagonal cracks emerged between 150 and 220 kips, showing the initiation of a cone-shaped failure mechanism. This occurred after the predicted strength load was reached. Similarly, on the top of the concrete bent cap, cracks started to show between 120 and 170 kips, as shown in Figure 5-34(b). Cracking can be seen on the top south face of the bent cap following the longitudinal reinforcement.

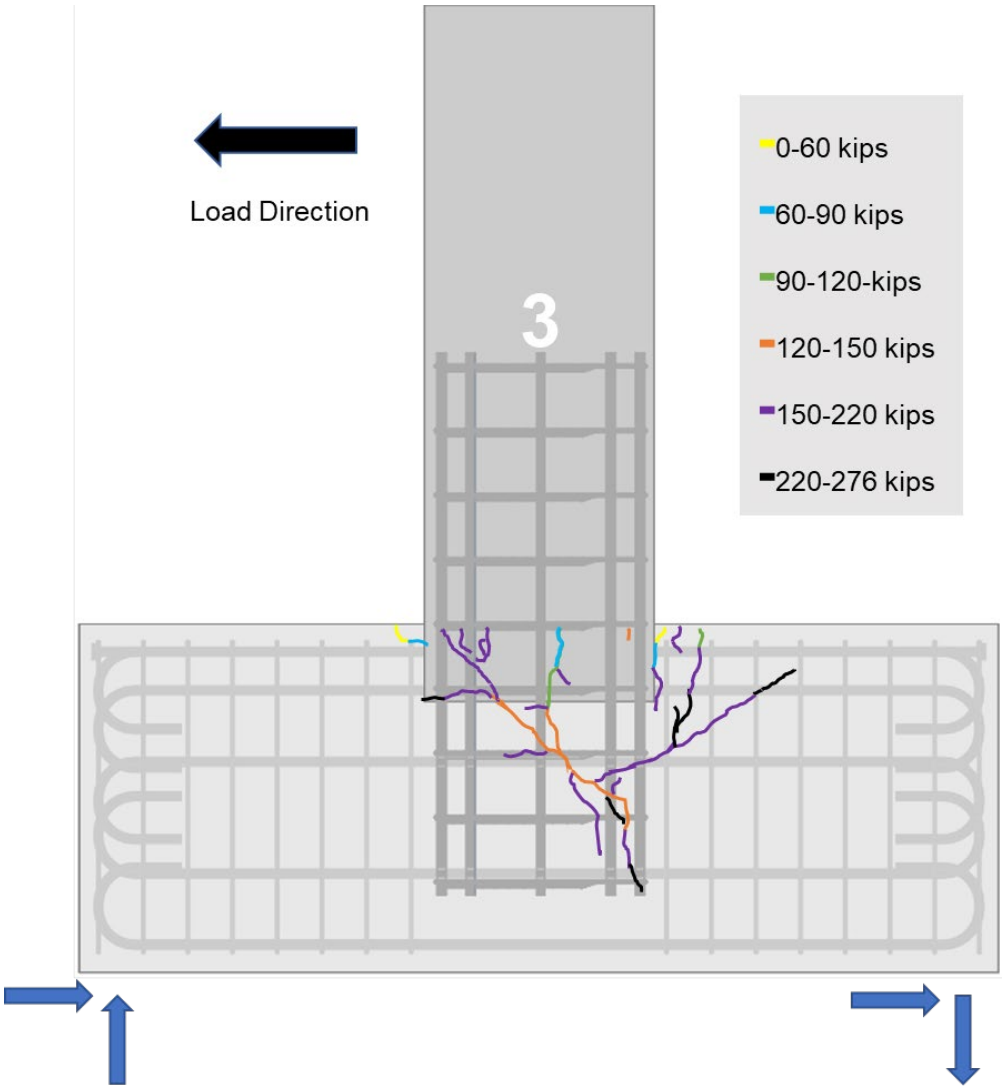

a) Side View

b) Plan View

Figure 5-34: Crack pattern for straight-bar specimen

Concrete spalling was observed during the test next to the southeast and southwest faces of the steel pile, as shown in Figure 5-35. The steel pipe pile showed movement in the vertical direction of around ¼ in, which caused spalling on the adjacent concrete. For loads higher than 120 kips until the end of the test, some cracks reached an opening width of 0.025 in. Most cracks are concentrated in the area of the steel reinforcement connection and appear between 170 and 220 kips of lateral load. Once the cracks formed, they were engaged by the longitudinal and transverse reinforcement of the bent cap. This reinforcement is not explicitly considered in the development length equations for these bars. This could be another potential reason for the excess connection capacity exhibited in this test.

Figure 5-35: Concrete spalling for straight-bar specimen

5.2.4 Stud Specimen Cracks

Figure 5-36 shows the crack pattern of the Stud specimen. Vertical cracks started to appear on the east and west faces of the concrete bent cap on the steel pile and concrete bent cap joint between 60 and 120 kips. Figure 5-36(a) shows that more cracks started appearing on the tension side of the pile and extended while the load increased, reaching the pile embedment. Similarly, on the top of the concrete bent cap, cracks started to develop between 220 and 300 kips on the east and west sides of the pile, as shown in Figure 5-36(b).

No crushing or spalling of concrete was observed during the entire test. For loads higher than 120 kips, some cracks reached an opening width of 0.016 in. by the end of the test. Most cracks are concentrated on the left side of the embedded steel pipe pile and develop mainly between 220 and 300 kips of lateral load.

The Stud specimen presented the least cracks compared to the other four specimens. Similarly, the size of the cracks was not as thick as those developed in the rest of the specimens.

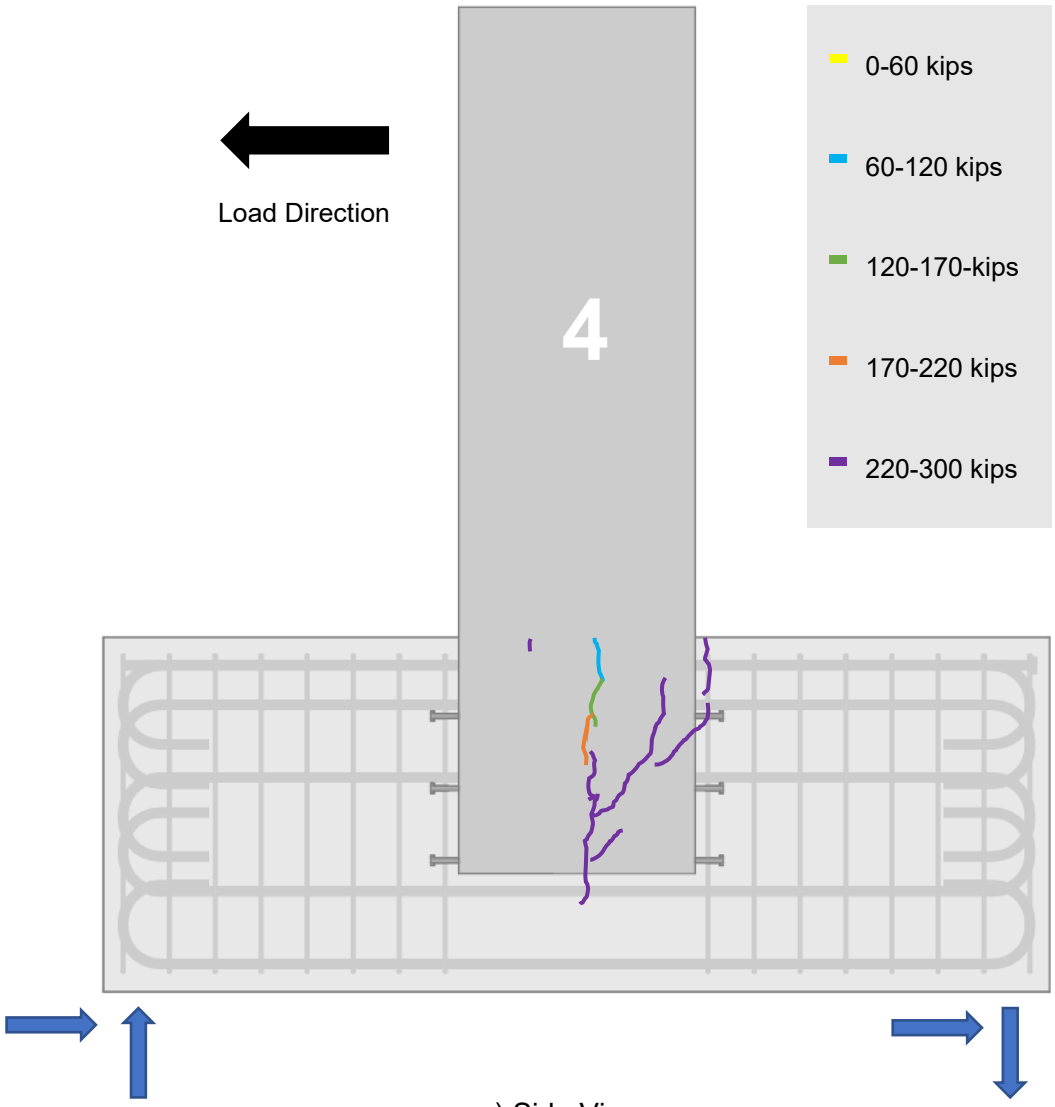

a) Side View

b) Plan View

Figure 5-36: Crack pattern for shear stud specimen

5.2.5 Ring Specimen Cracks

Figure 5-37 shows the crack pattern of the Ring specimen. Small vertical cracks started to appear on the east and west faces of the concrete bent cap on the steel pile and concrete bent cap joint between 0 and 60 kips. Figure 5-37(a) shows that more cracks started appearing on the tension and compression sides of the pile and extended as the load increased. Between 170 and 220 kips, horizontal cracks along the annular ring appeared where the location of stress concentration was. A pull-out crack pattern is visible. Similarly, on the top of the concrete bent cap, cracks started to form between 60 and 120 kips, as shown in Figure 5-37(b).

No crushing or spalling of concrete was observed during the entire test. For loads higher than 120 kips, some cracks reached an opening width of 0.035 in. by the end of the test. Most cracks are concentrated on the embedded steel pipe pile area and developed mainly between 170 and 300 kips of lateral load.

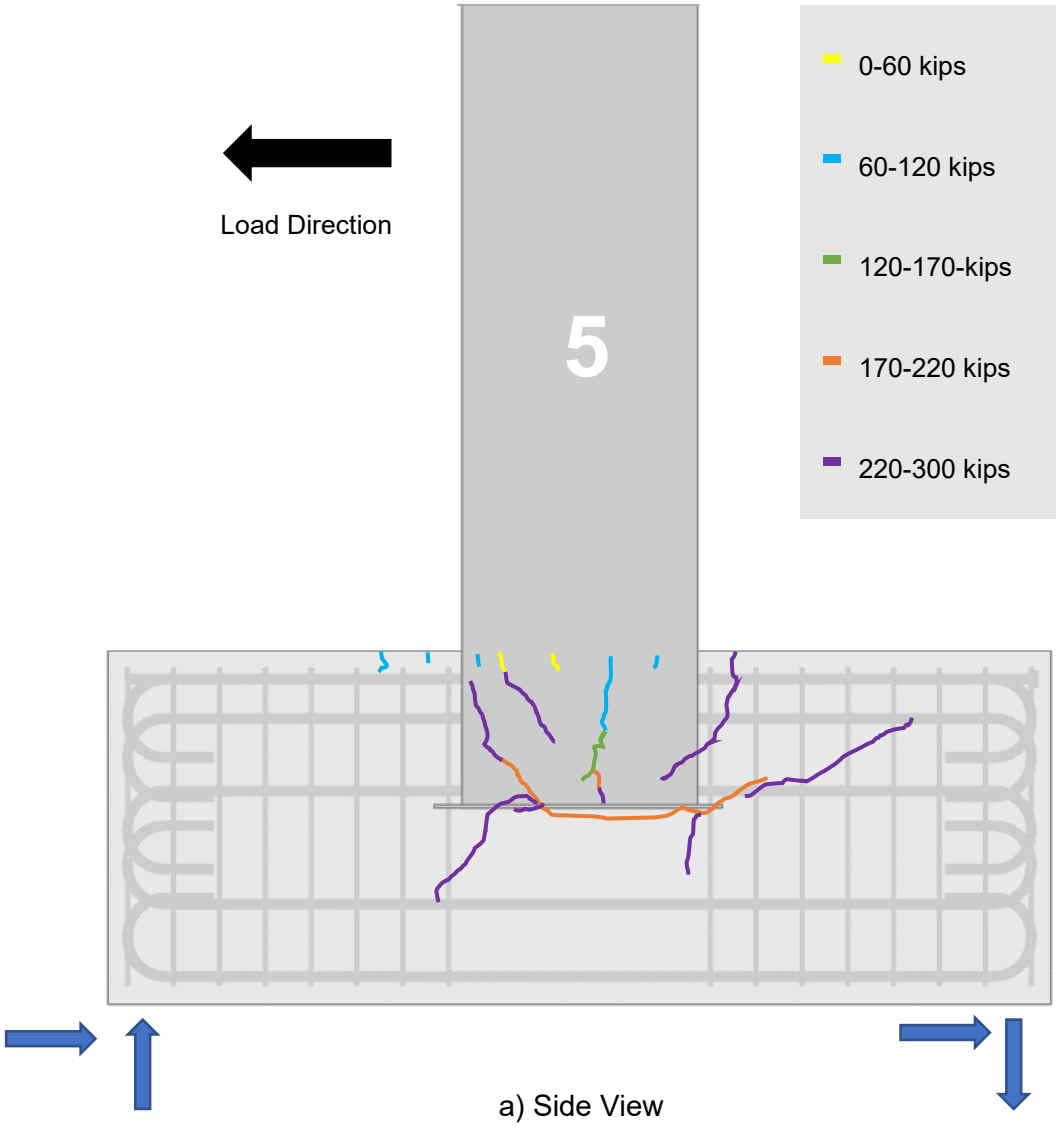

a) Side View

b) Plan View

Figure 5-37: Crack pattern for annular ring specimen

5.3 DISCUSSION

Constructing and testing all five specimens revealed several lessons related to the performance and constructability of the five types of connections.

In terms of constructability, the reinforcing steel connections were significantly harder to build compared to the welded mechanical anchorage connections. Assembling a connection with circular hoops is challenging and time-consuming. The hoops were unevenly bent by the reinforcing bar fabricator, which caused issues in the construction process. Additionally, for the hooked-bar connection, the 180-degree hooks caused congestion in the interior part of the connection. This happened due to the hooks touching each other. Also, it was challenging to keep the reinforcing connection in place between the steel pile and the concrete bent cap. The annular ring and shear stud connections were a much simpler option, as the mechanical anchorages can be shop-welded. However, for these two connections, the large diameter of the pile added to the length of the studs and the ring caused some issues during assemblage. The bent cap reinforcement had to be adjusted in order for them to fit inside the cage.

Regarding the results from the tests, there are several points that need to be discussed. The load versus displacement plots showed that all reinforcing steel connections adequately resisted a load significantly greater than the predicted capacity. The welded mechanical anchorage connections were expected to have a higher capacity due to the contribution of the pile. Cracking and yielding were observed, which reduced the stiffness of the connections. All of the connections exhibited nonlinear behavior for high load levels. However, none of the five connections failed or were severely damaged. Ultimate load was not achieved for any of them, and the predicted service load was reached without any issues. A coned-shaped crack pattern was visible in all connections except for the shear stud connection.

The three reinforcing steel connections reached a load almost 90% greater than the predicted strength load. This significant increase in the capacity of the connections could be due to several reasons. The 1 ft embedment depth of the pile and the corresponding contribution of the pile were conservatively neglected in the design of the reinforcing steel connections. The strains seen in the pile demonstrated its contribution to the flexural resistance. The evolution of the cracks was very similar for the three

reinforcing steel connections. The cracks developed in the bent cap were engaged by the large amount of flexural and shear reinforcement in the bent cap. This is not fully considered in the development length equations for each bar type and could be a potential reason for the excess connection capacity exhibited in these tests. Additionally, the four long bent cap reinforcing bars that pass through the pile may enhance the anchorage of both the pile and the reinforcing connection.

For the headed-bar connection, the AASHTO LRFD Bridge Design Specifications 9th edition did not provide a development length equation for headed bars. ACI 318-19 was followed instead for the design. The new AASHTO 10th edition has the necessary development length equation in section 5.10.8.2.7. A calculation of the development length for headed bars could be updated with the current AASHTO specification.

The two connections with mechanical anchorages welded to the bottom of the pile showed superior lateral stiffness at the end of the test and had the least rotations and strains. The annular ring connection had a similar stiffness to the reinforcing steel connections for loads up to 118 kips. The shear stud connection was stiffer overall and showed the lowest displacements and rotations. The significant stiffness difference can be attributed to the embedment depth of the pile. The shear stud connection showed the highest stiffness, with an embedment depth of 3 ft, followed by the annular ring connection with an embedment depth of 2 ft. These two connections were expected to receive a contribution from the pile as the consideration of the embedment depth was made for the nominal capacity calculations. Similar to the reinforcing steel connections, the four long bent cap reinforcing bars that pass through the pile may enhance the anchorage of the shear stud and annular ring connections. The shear stud specimen demonstrated a more controlled cracking behavior. The annular ring connection showed a cone-shaped cracking pattern. A horizontal crack close to the ring location indicates a concentration of stresses in that zone.

This experimental study included only the application of lateral loads. If axial compression forces were included, a punching failure may be possible through the cap. This is especially for the specimens with piles with deeper embedment, like the shear stud and annular ring connections.

CHAPTER 6 SUMMARY CONCLUSIONS AND RECOMMENDATIONS

6.1 SUMMARY

The scope of the study described in this thesis was limited to the first portion of the research project, “Development of Pipe Pile to Bent Cap Connection for ALDOT Bridges”. This is part of a larger project sponsored by ALDOT to investigate effective methods for connecting steel pipe piles to concrete bent caps. This portion assessed the structural behavior and constructability of five types of connections between steel pipe piles and concrete bent caps.

Five connection types were selected for further study:

1. Headed-bar connection
2. Hooked-bar connection
3. Straight-bar connection
4. Shear stud connection
5. Annular ring connection

To assess these tests, it was necessary to build five full-scale specimens. A 4 ft by 4.5 ft by 12 ft reinforced concrete bent cap was replicated for all specimens. Steel pipe piles with a 3 ft diameter and ½ in. thickness were used.

An ALDOT Class B concrete mixture for bridge substructures was used in all cases. Testing was performed when the specimens reached a concrete compressive strength of 4000 psi or more. An actuator applied the lateral pseudo-static loads at 6.375 ft on top of the bent cap. Cycles were performed at different load levels.

Specimens were monitored throughout the test with different sensor types. Displacement, rotation, and strain were obtained from these measurements.

The behavior of the five connections was compared. Conclusions and recommendations are described in this chapter.

6.2 CONCLUSIONS

Based on the research described in this thesis, the following conclusions may be drawn:

1. All connections performed well with only minor cracking at service load levels.
2. All five specimens demonstrated a high load-carrying capacity. The nominal moment capacity was exceeded for the steel reinforcing connections. These reached a load 90% higher than the predicted strength. The connections with welded mechanical anchorage also reached high loads relative to their design considerations.
3. The design approach used to design the three reinforcing steel connections, in which the contribution of the pile was neglected, proved to be very conservative.
4. All connection specimens withstood a flexural demand well beyond the factored demand in the prototype bridge bent on which the design was based.
5. The embedment depth of the pile demonstrated providing a superior lateral stiffness and significantly contributed to the capacity of the connections. The deeper the embedment of the pile, the stiffer the connection.
6. Large-diameter piles offer several design and construction advantages, such as high load-carrying capacity and stiffness.
7. Mechanical anchorage welded to the pile is easier to build than fabricating reinforcing steel cages on site.
8. Of the reinforcing bar connections, the hooked bars resulted in a level of congestion and complication far greater than the straight- and headed-bar connections.

6.3 RECOMMENDATIONS

Based on the research findings, the following actions are recommended:

1. The headed-bar connection is recommended to be used as it is a simple reinforcing steel connection to build. The heads provide adequate anchorage capacity and reduce steel congestion.
2. The annular ring connection is recommended to be used for its ease of construction and high load-carrying capacity.
3. Similar tests considering different variables, such as pile embedment depth and pile size, are warranted. This will provide a better understanding of the contribution of different pile conditions to the connecting system.

4. It would be beneficial to calibrate and optimize the capacity of the connections. Considering the contribution of the steel pile is crucial for obtaining a more accurate strength capacity of the system. Future work should explore optimized reinforcing steel configurations and welded anchorage connections for more efficient and cost-effective bridge substructures.
5. Further research could encompass cyclic loading performance, fatigue behavior, and tests involving combined axial and lateral loads.
6. Comparing these connections to specimens that include only an embedded steel pile, without any additional exterior or interior anchorage, could enhance the understanding of the connection's contribution to the system's capacity.

REFERENCES

AASHTO. 2020. AASHTO LRFD Bridge Design Specifications. 9 Th Edition. Washington D.C: American Association of State Highway and Transportation Officials.

ACI 318. 2019. Building Code Requirements for Structural Concrete and Commentary. 318-19 Building Code Requirements for Structural Concrete and Commentary. Farmington Hills, MI: American Concrete Institute. https://doi.org/10.14359/51716937.

Alabama Department of Transportation. 2022. “ALDOT Standard Specifications for Highway Construction.”

Arockiasamy, Madasamy, and Prakash Ankitha Arvan. 2022. “Behavior, Performance, and Evaluation of Prestressed Concrete/Steel Pipe/Steel H-Pile to Pile Cap Connections.” Practice Periodical on Structural Design and Construction 27 (2). 1-35. https://doi.org/10.1061/(asce)sc.1943-5576.0000671.

Arvan, Prakash Ankitha, and Madasamy Arockiasamy. 2023. “Analysis Methods for the Design of Pile–to–Pile Cap Connections Concerning Plain Pile Embedment.” Practice Periodical on Structural Design and Construction 28 (3). 1-25. https://doi.org/10.1061/ppscfx.sceng-1202.

Bentz, Evan C. 2000. “Sectional Analysis of Reinforced Concrete Members.” Ph.D. Thesis, University of Toronto. www.ecf.utoronto.ca/-bentdrn2k-htm.

Castilla, Fernando, Phillippe Martin, and John Link. 1984. “Fixity of Members Embedded in Concrete.” Report No. CERL TR M-339. Champaign, IL: U.S. Army Construction Engineering Research Laboratory.

Eastman, Ryan S. 2011. “Experimental Investigation of Steel Pipe Pile to Concrete Cap Connections.” M.S. Thesis, Brigham Young University. https://scholarsarchive.byu.edu/etd/2628.

Fulmer, Steven J, Mervyn J Kowalsky, and James M Nau. 2013. “Seismic Performance of Steel Pipe Pile to Cap Beam Moment Resisting Connections” Report No. DOT FHWA-AK-RD-13-12. Fairbanks, Alaska: Alaska University Transportation Center.

Gonçalves, Vítor Freitas, Rodrigo Gustavo Delalibera, and Márcio Alves de Oliveira Filho. 2022. “Analysis of the Pile-to-Cap Connection of Pile Caps on Two Steel Piles” Engineering Structures 252 (February). 1-13. https://doi.org/10.1016/j.engstruct.2021.113629.

Hannigan, Patrick J., Frank Rausche, Garland E. Likins, Brent R. Robinson, and Matthew L. Becker. 2016. “Design and Construction of Driven Pile Foundations-Volume I.” Report No. FHWA-NHI-16-009. Washington, D.C.: National Highway Institute.

Kappes, Lenci, Michael Berry, Flynn Murray, Jerry Stephens, and Kent Barnes. 2016. “Seismic Performance of Concrete-Filled Steel Tube to Concrete Pile-Cap Connections.” Journal of Bridge Engineering 21 (7). 1-17. https://doi.org/10.1061/(asce)be.1943-5592.0000901.

Kappes, Lenci, Michael Berry, and Jerry Stephens. 2013. “Performance of Steel Pipe Pile-to-Concrete Cap Connections Subject to Seismic or High Transverse Loading: Phase III. Confirmation of Connection Performance.” Report No. FHWA/MT-13-001/8203. Bozeman, Montana: Western Transportation Institute.

Lehman, Dawn E., and Charles W. Roeder. 2012. “Foundation Connections for Circular Concrete-Filled Tubes.” Journal of Constructional Steel Research 78 (November):212–25. https://doi.org/10.1016/j.jcsr.2012.07.001.

Marshall, Justin D, J Brian Anderson, Jonathon Campbell, Zachary Skinner, and Stephen T Hammett. 2017. “Experimental Validation of Analysis Methods and Design Procedures for Steel Pile Bridge Bents.” Report No. ALDOT 930-859. Auburn, Alabama: Auburn University Highway Research Center.

McKittrick, Ladean, Jason Hicks, Jerry Stephens, Dan VanLuchene, and Don Rabern. 1998. “Performance of Steel Pipe Pile-to-Concrete Bent Cap Connections Subjected to Seismic or High Transverse Loading Phase I: Preliminary Investigation” Report No. FHWA/MT-98-005/8117-7. Bozeman, Montana: Montana State University.

Richards, Paul W., Kyle M. Rollins, and Tony E. Stenlund. 2011. “Experimental Testing of Pile-to-Cap Connections for Embedded Pipe Piles.” Journal of Bridge Engineering 16 (2): 286–94. https://doi.org/10.1061/(asce)be.1943-5592.0000144.

Shama, Ayman A., John B. Mander, and Amjad J. Aref. 2002. “Seismic Performance and Retrofit of Steel Pile to Concrete Cap Connections.” ACI Structural Journal V.99. 51-61

Sharma, Rosy. 2023. “Feasibility Studies on the Design and Usage of Steel Pile Piles for ALDOT Bridges.” M.S. Thesis, Auburn University.

Silva, Pedro, Sri Sritharan, Frieder Sciblc, and MJ Nigel Priestley. 1999. “Full-Scale Test of the Alaska Cast-in-Place Steel Shell Three Column Bridge Bent.” Report No. SSRP 98/13. La Joya, California: Charles Lee Powell Structural Research Laboratories.

Singer, Nancy. 2021. “U.S. Department of Transportation Federal Highway Administration.” FHWA Commemorates 50 Years of Bridge Safety. April 30, 2021.

Stephens, Jerry, and Ladean McKittrick. 2005. “Performance of Steel Pipe Pile-to-Concrete Bent Cap Connections Subject to High Transverse Loading: Phase II.” Report No. FHWA/MT-05-001/8144. Helena, Montana: Montana State University.

Stephens, Max Taylor, Dawn E. Lehman, and Charles W. Roeder. 2015. “Concrete-Filled Tube Bridge Pier Connections for Accelerated Bridge Construction.” Report No. CA15-2417. Seattle, Washington: University of Washington.

Steunenberg, M, R G Sexsmith, and S F Stiemer. 1998. “Seismic Behavior of Steel Pile to Precast Concrete Cap Beam Connections.” Journal of Bridge Engineering 3(4): 177-185.

Tan, Shasha, Chen Jia, Lanhui Guo, Fusheng Ou, and Yan Xu. 2022. “Experimental Investigation on Punching Shear Behavior of the Embedded Column Base for CFSTs.” Engineering Structures 263: 1-11. https://doi.org/10.1016/j.engstruct.2022.114371.

Washington State Department of Transportation. 2024. “Design Manual.” https://wsdot.wa.gov/engineering-standards/all-manuals-and-standards/manuals/.

Xiao, Y, H Wu, T Yaprak, G Martin, and J Mander. 2006. “Experimental Studies on Seismic Behavior of Steel Pile-to-Pile-Cap Connections.” Journal of Bridge Engineering 11(2): 151-59. https://doi.org/10.1061/ASCE1084-0702200611:2151.

APPENDIX A: Sensor List

Table A- 1: Instrumentation list

Instrument	Type	Location	Name	Quantity	Notes
Strain Gauge	Concrete	Bent cap 1, 2, 3, 4, 5	CS-B-N-1	5	North top surface
			CS-B-N-2	5	North top surface
			CS-B-N-3	5	North top surface
			CS-B-N-4	5	North top surface
			CS-B-N-5	5	North top surface
	Steel	Bent cap 1, 2, 3, 4, 5	SS-B-S-1	5	Headed Rebar
			SS-B-S-2	5	Headed Rebar
			SS-B-S-3	5	Headed Rebar
			SS-B-S-4	5	Headed Rebar
			SS-B-W-5	5	Hooked Rebar
			SS-B-N-6	5	Stirrup
		Pile 1, 2, 3	SS-P-N-1	3	North face
			SS-P-N-2	3	North face
			SS-P-N-3	3	North face
			SS-P-N-4	3	North face
			SS-P-S-5	3	South face
			SS-P-S-6	3	South face
			SS-P-S-7	3	South face
			SS-P-S-8	3	South face
			SS-P-S-9	3	West face
		Headed Bars, Hooked Bars	SS-C-N-1	2	North face
			SS-C-N-2	2	North face
			SS-C-N-3	2	North face
			SS-C-N-4	2	North face
			SS-C-S-5	2	South face
			SS-C-S-6	2	South face
			SS-C-S-7	2	South face
			SS-C-S-8	2	South face
		Straight Bars	SS-C-N-1	1	North face
			SS-C-N-2	1	North face
			SS-C-N-3	1	North face
			SS-C-N-4	1	North face
			SS-C-N-5	1	North face
			SS-C-S-6	1	South face
			SS-C-S-7	1	South face
			SS-C-S-8	1	South face
			SS-C-S-9	1	South face

		SS-C-S-10	1	South face
	Pile 4	SS-P-N-1	1	North face
		SS-P-N-2	1	North face
		SS-P-N-3	1	North face
		SS-P-N-4	1	North face
		SS-P-N-5	1	Placed on shear stud
		SS-P-N-6	1	North face
		SS-P-N-7	1	North face
		SS-P-N-8	1	North face
		SS-P-N-9	1	Placed on shear stud
		SS-P-S-10	1	South face
		SS-P-S-11	1	South face
		SS-P-S-12	1	South face
		SS-P-S-13	1	South face
		SS-P-S-14	1	Placed on shear stud
		SS-P-S-15	1	South face
		SS-P-S-16	1	South face
		SS-P-S-17	1	South face
		SS-P-S-18	1	Placed on shear stud
		SS-P-W-19	1	West face
	Pile 5	SS-P-N-1	1	North face
		SS-P-N-2	1	North face
		SS-P-N-3	1	North face
		SS-P-N-4	1	North face
		SS-P-N-5	1	North face
		SS-P-N-6	1	North face
		SS-P-N-7	1	North face
		SS-P-N-8	1	Placed on annular ring
		SS-P-S-9	1	South face
		SS-P-S-10	1	South face
		SS-P-S-11	1	South face
		SS-P-S-12	1	South face
		SS-P-S-13	1	South face
		SS-P-S-14	1	South face
		SS-P-S-15	1	South face
		SS-P-S-16	1	Placed on annular ring
		SS-P-W-17	1	West face
		Total	144	
String Potentiometers	Pile 1, 2, 3, 4, 5	D-P-S-1	1	South face
		D-P-S-2	1	South face
		D-P-S-3	1	South face
		D-P-E-4	1	East face
		D-P-S-5	1	South face

	Bent cap 1, 2, 3, 4, 5	D-P-B-6	1	South face
		Total	6	
Slip Meters	Pile 1, 2, 3, 4, 5	S-P-W-1	1	West face
		S-P-N-2	1	North face
		S-P-E-3	1	East face
		S-P-S-4	1	South face
		S-P-S-5	1	South face
		S-P-E-6	1	East face
	Bent cap 1, 2, 3, 4, 5	S-B-S-7	1	South face
		S-B-S-8	1	South face
		S-B-S-9	1	South face
		S-B-S-10	1	South face
		S-B-E-11	1	East face
		S-B-E-12	1	East face
		Total	12	
Inclinometers	Bent cap 1, 2, 3, 4, 5	R-B-E-1	1	East face
	Pile 1, 2, 3, 4, 5	R-P-E-2	1	East face
		R-P-N-3	1	North face
		R-P-E-4	1	East face
		R-P-E-5	1	East face
		Total	5	

APPENDIX B: Head Specimen

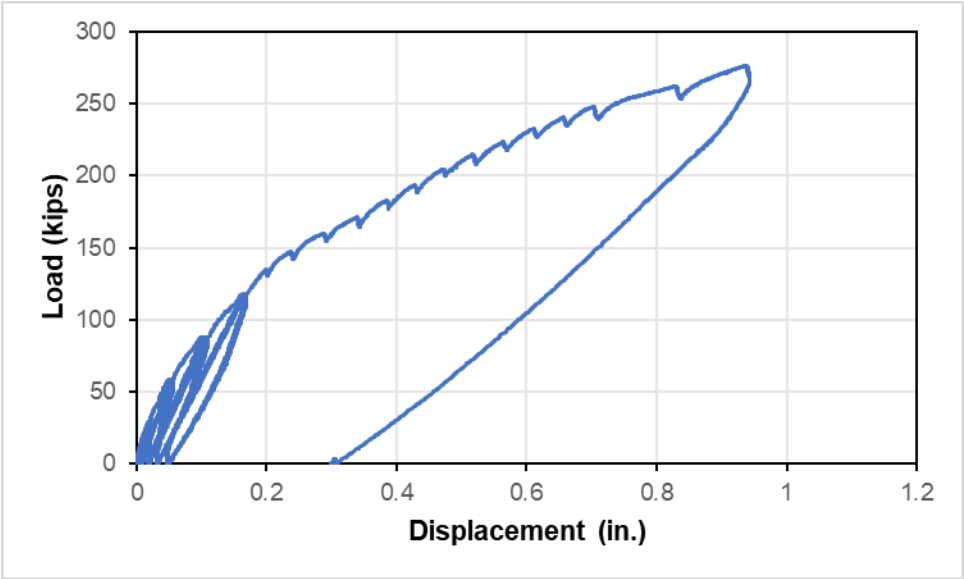

Figure B- 1: Full test data

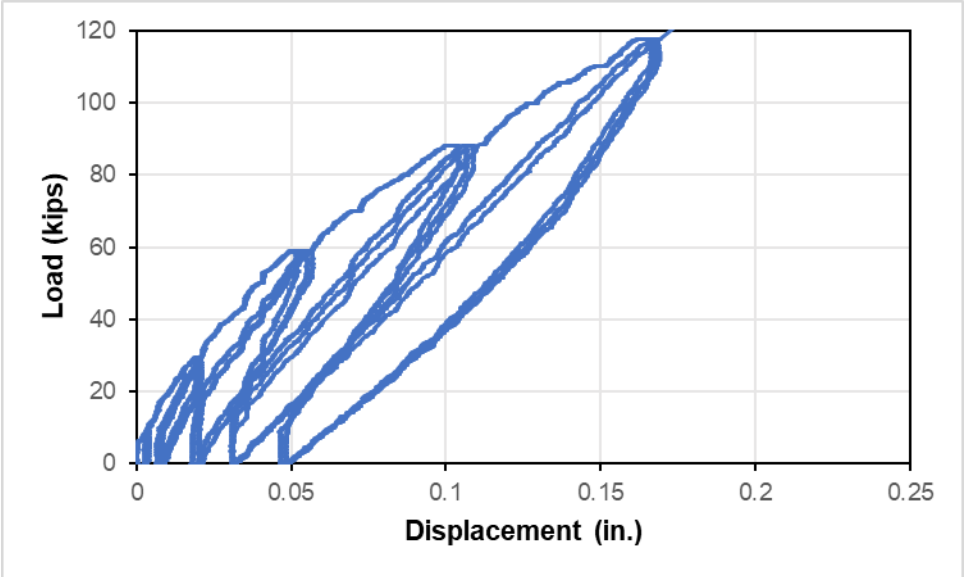

Figure B- 2: Cycles

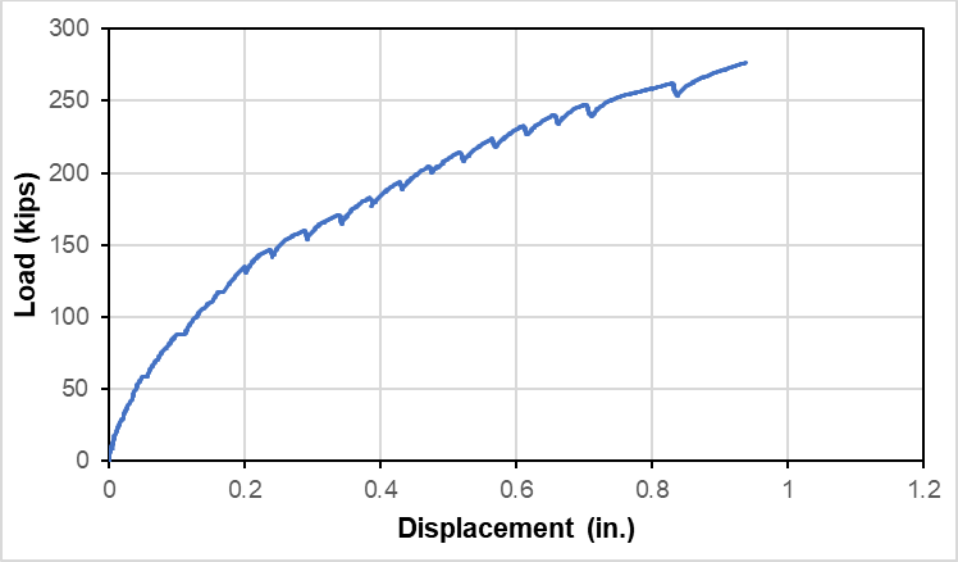

Figure B- 3: Net displacement backbone curve

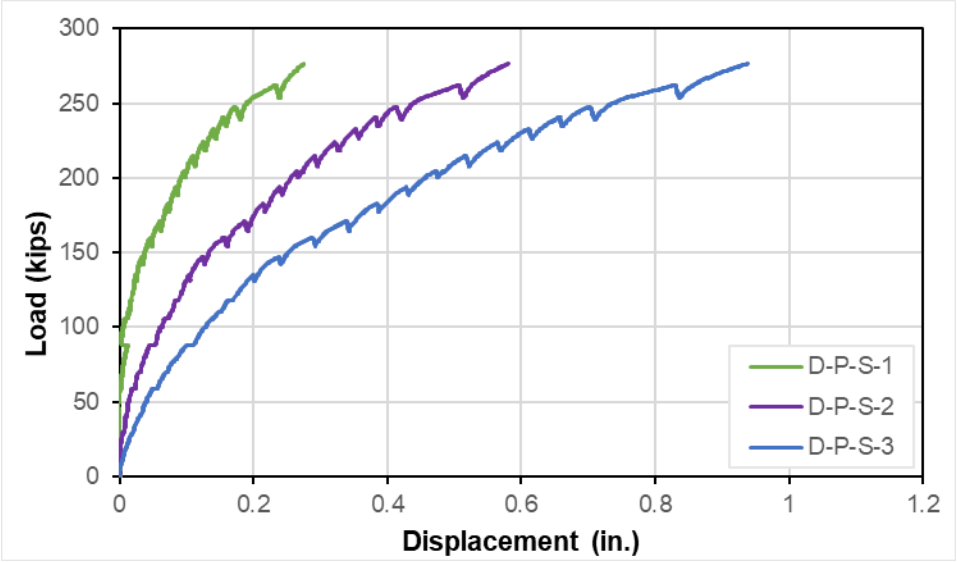

Figure B- 4: Net displacement measured at different points

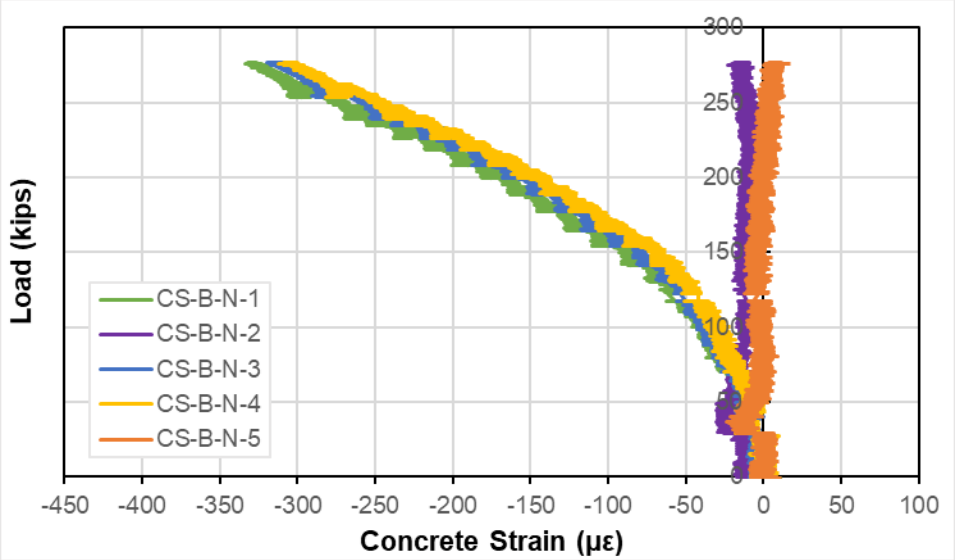

Figure B- 5: Concrete bent cap surface strains

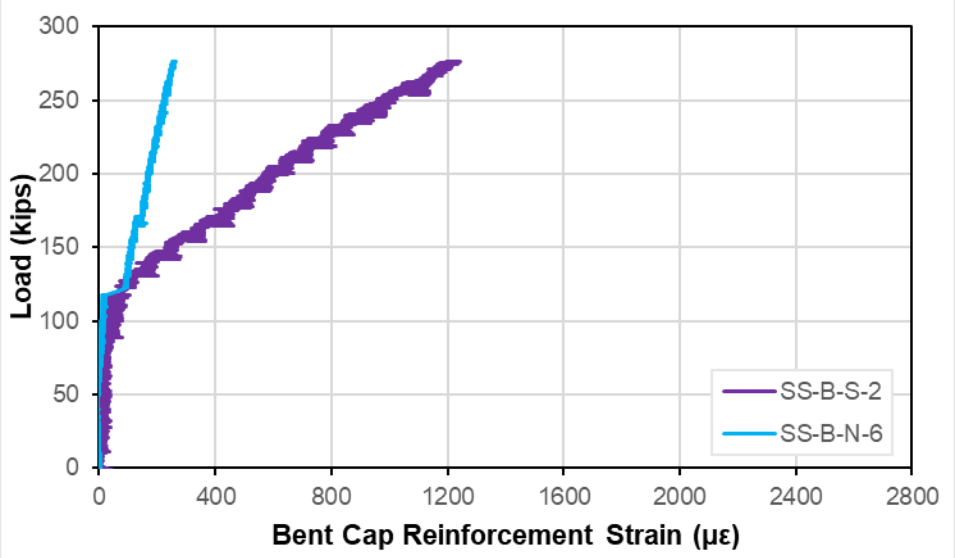

Figure B- 6: Bent cap steel reinforcement strains

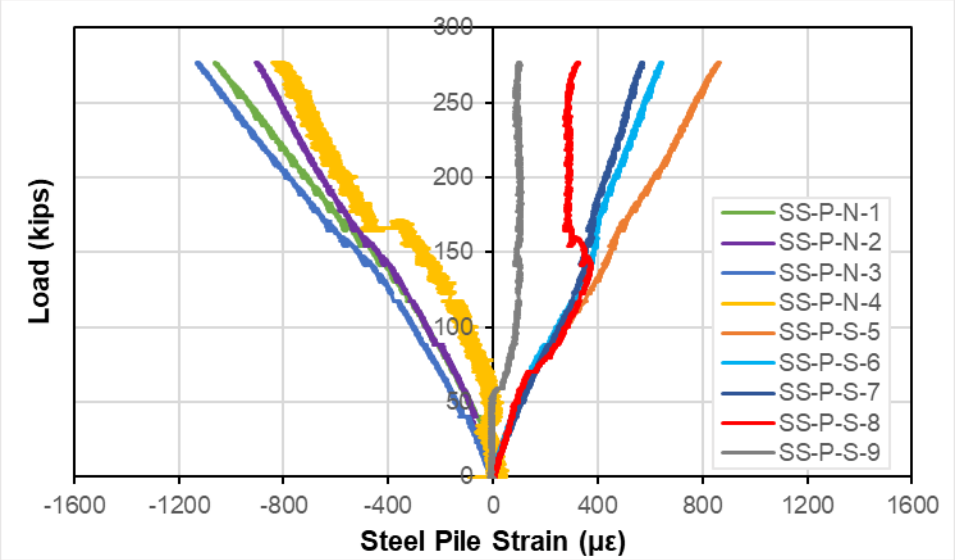

Figure B- 7: Steel pipe pile strains

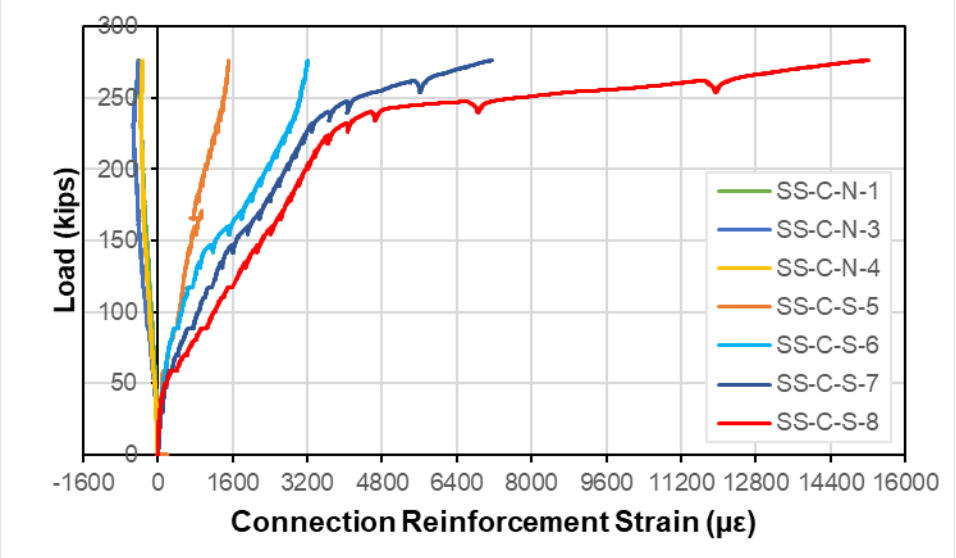

Figure B- 8: Headed reinforcing bars strains

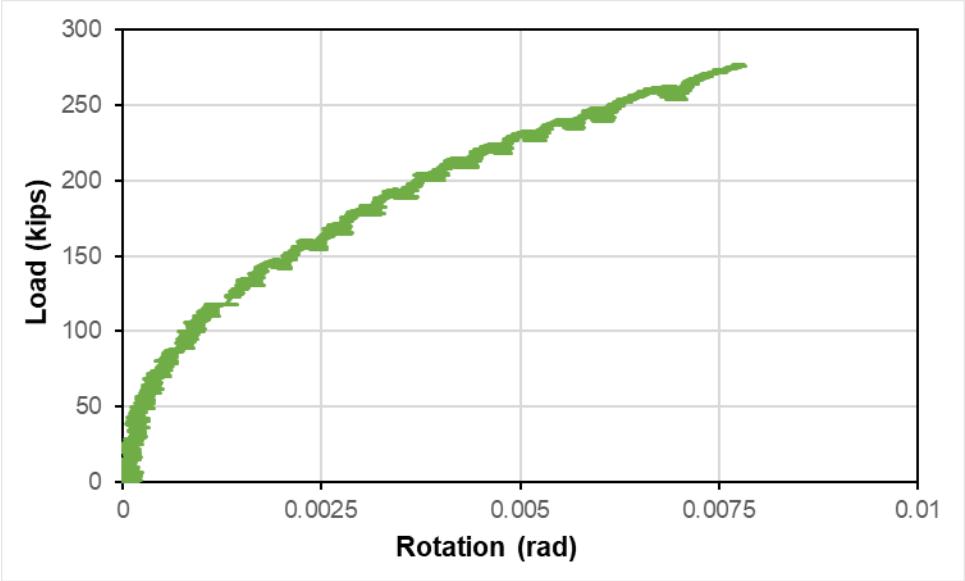

Figure B- 9: Net rotation

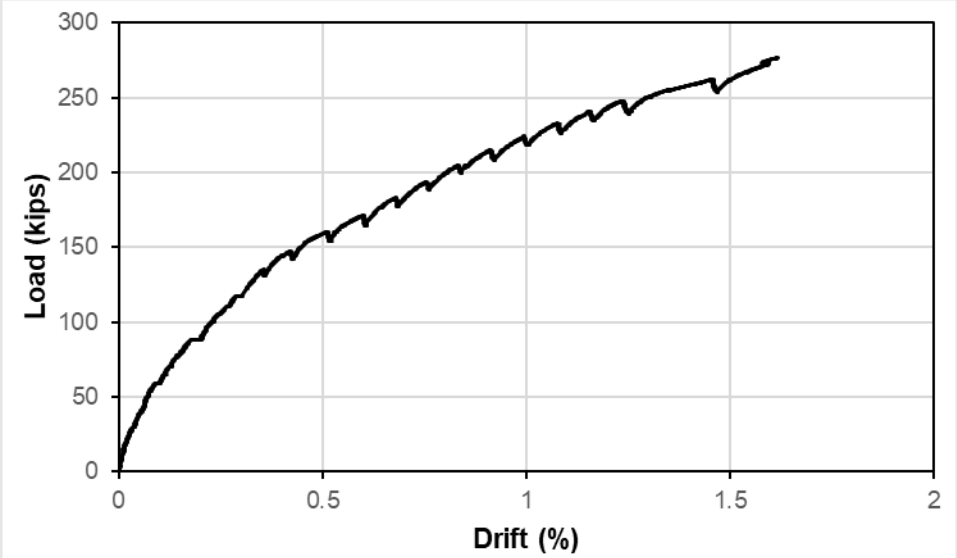

Figure B- 10: Head specimen drift

APPENDIX C: Hook Specimen

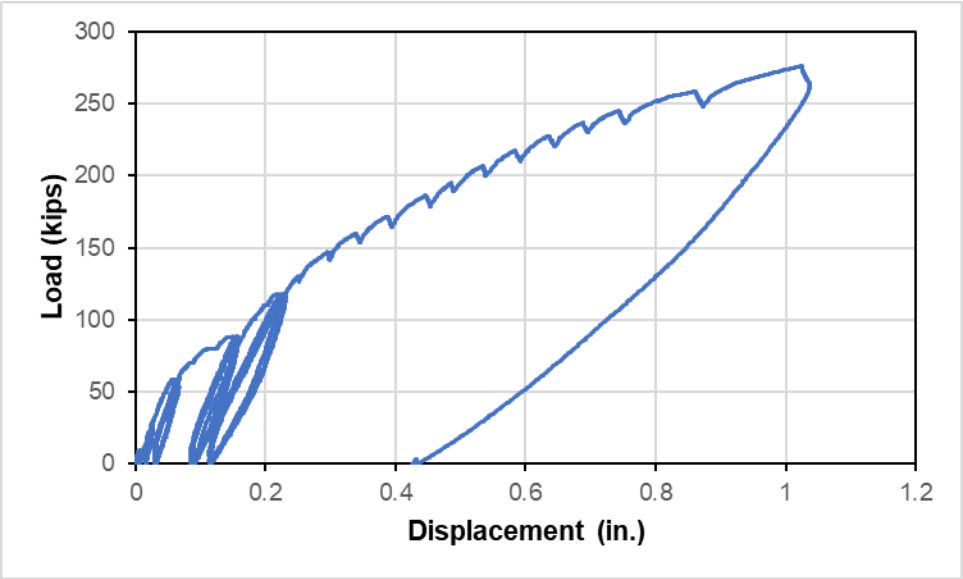

Figure C- 1: Full test data

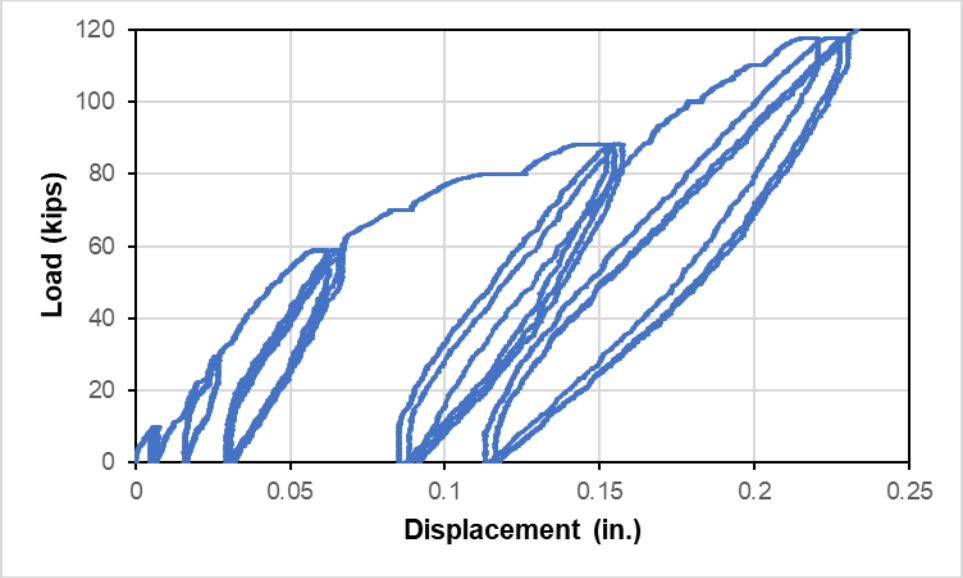

Figure C- 2: Cycles

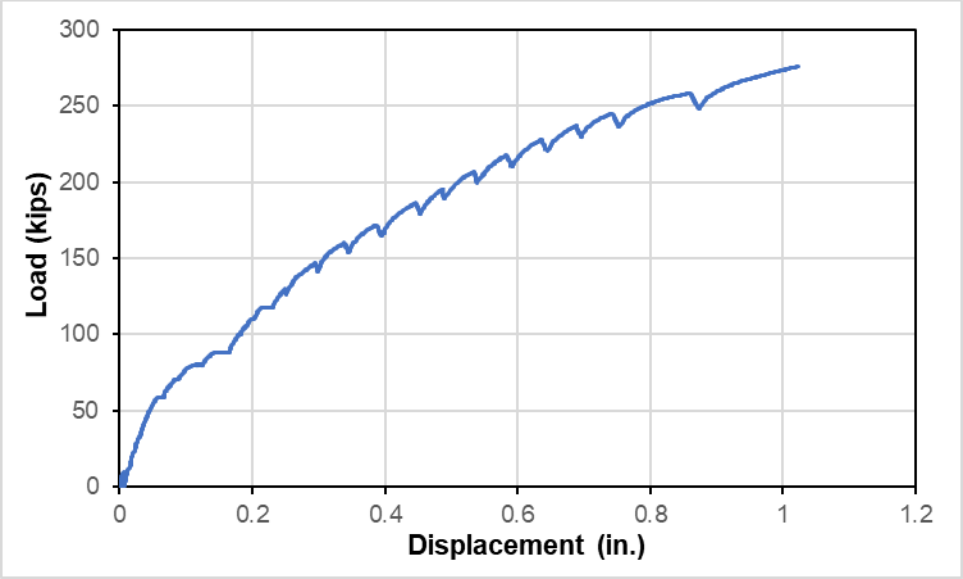

Figure C- 3: Net displacement backbone curve

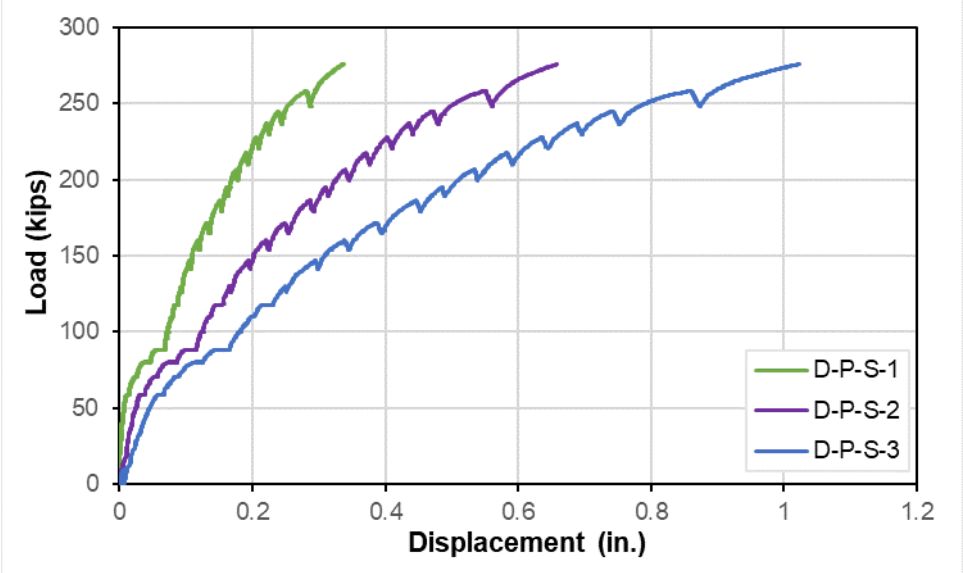

Figure C- 4: Net displacement measured at different points

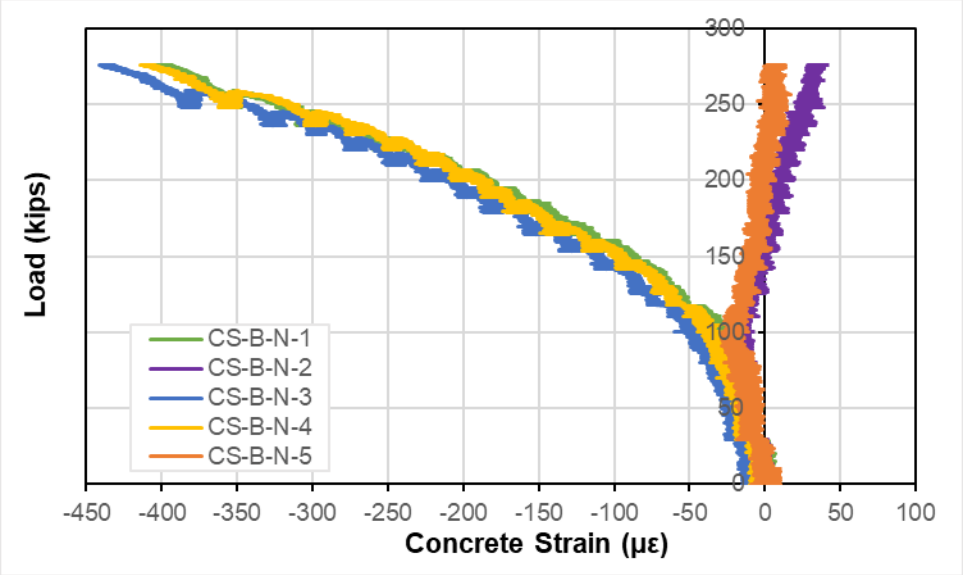

Figure C- 5: Concrete bent cap concrete strains

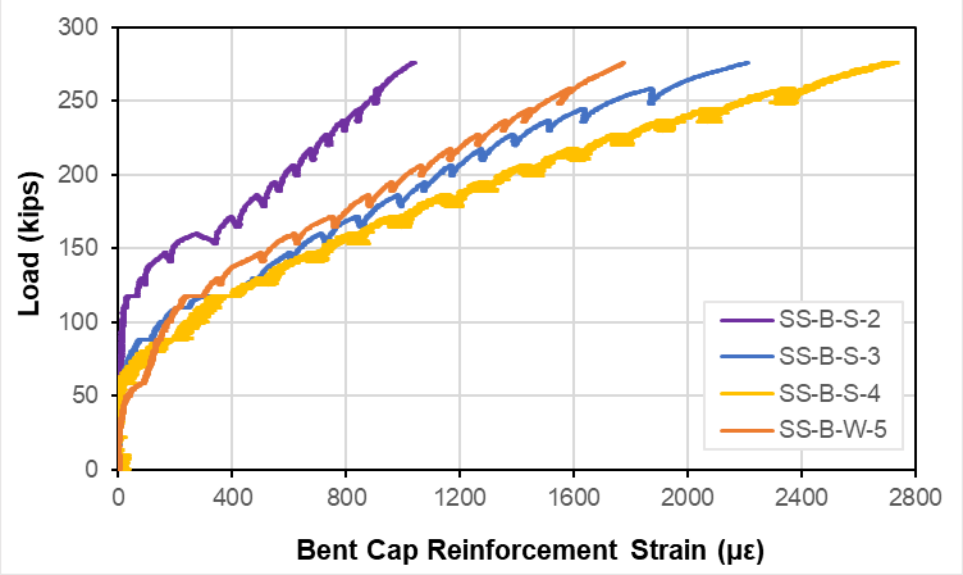

Figure C- 6: Bent cap steel reinforcement strains

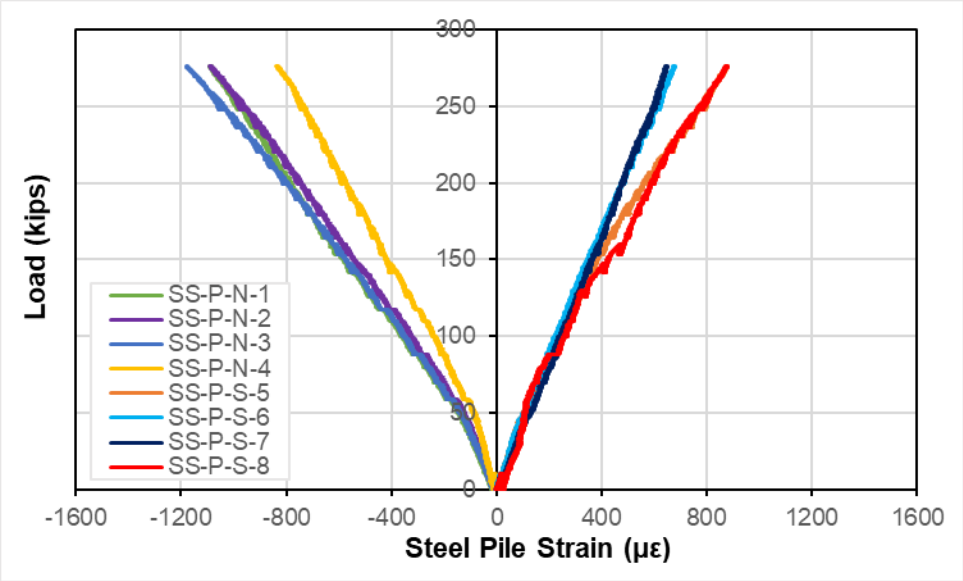

Figure C- 7: Steel pipe pile strains

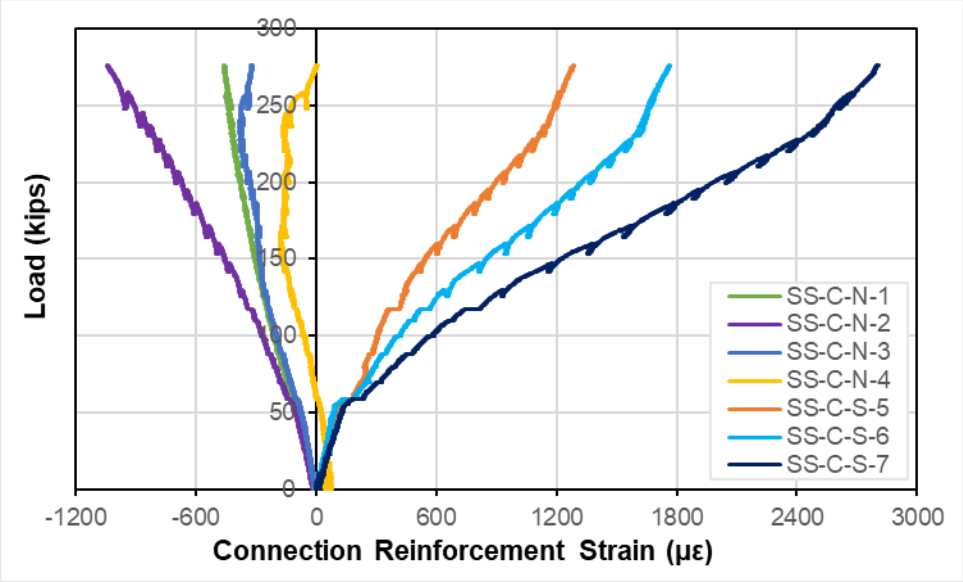

Figure C- 8: Hooked reinforcing bars strains

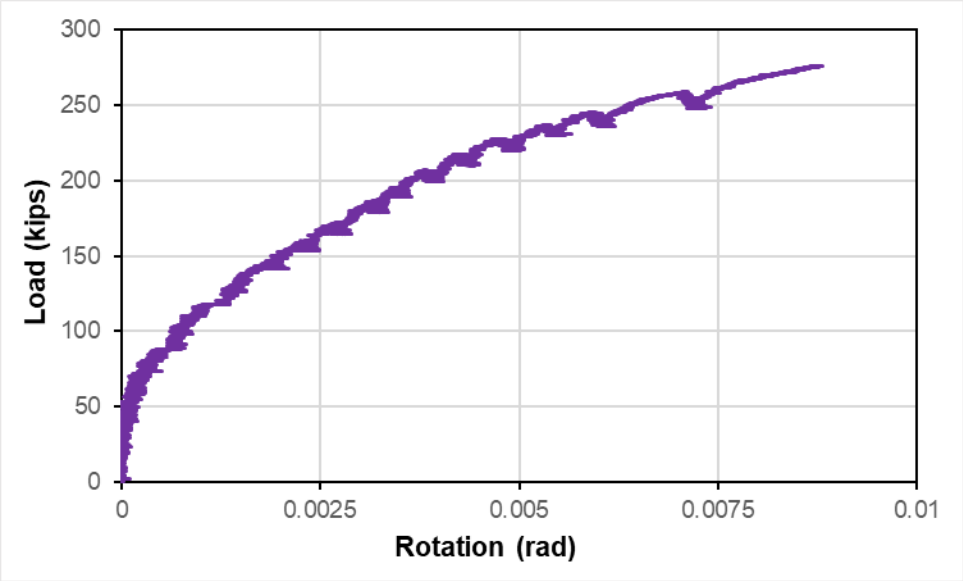

Figure C- 9: Net rotation

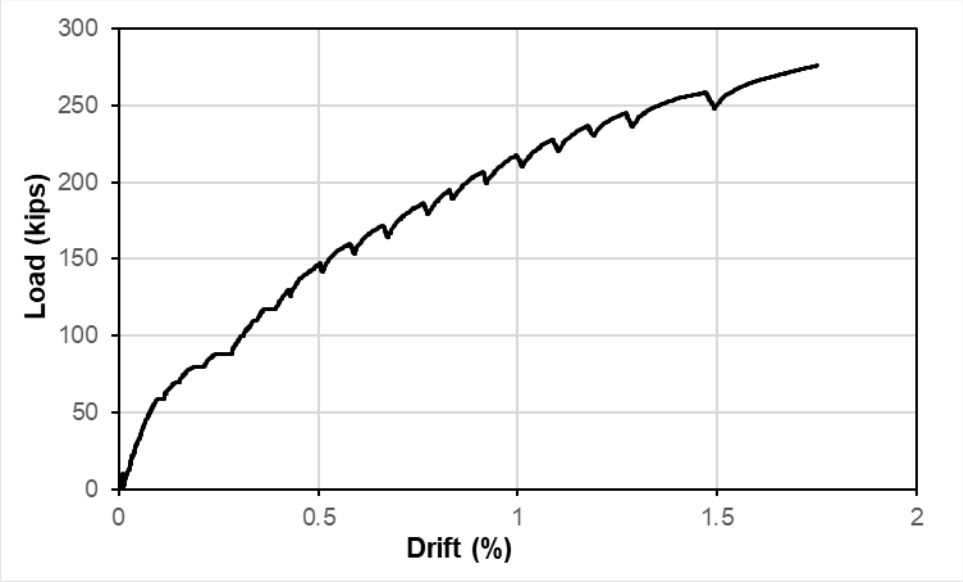

Figure C- 10: Hook specimen drift

APPENDIX D: Straight Specimen

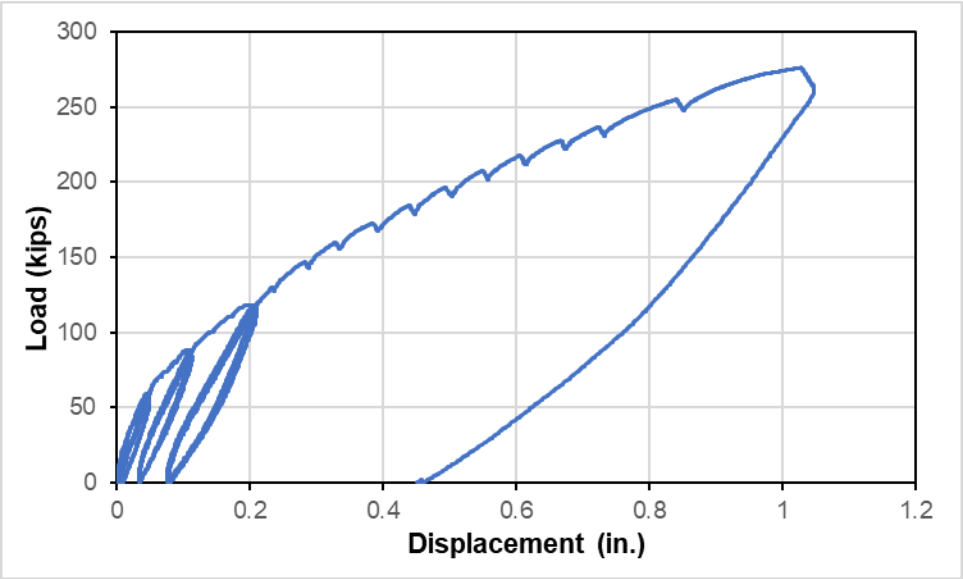

Figure D- 1: Full test data

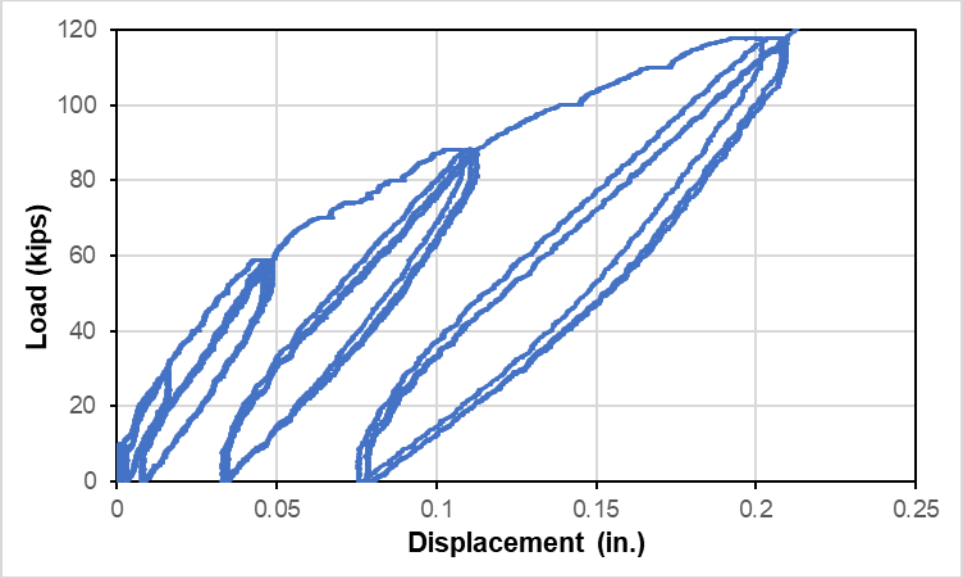

Figure D- 2: Cycles

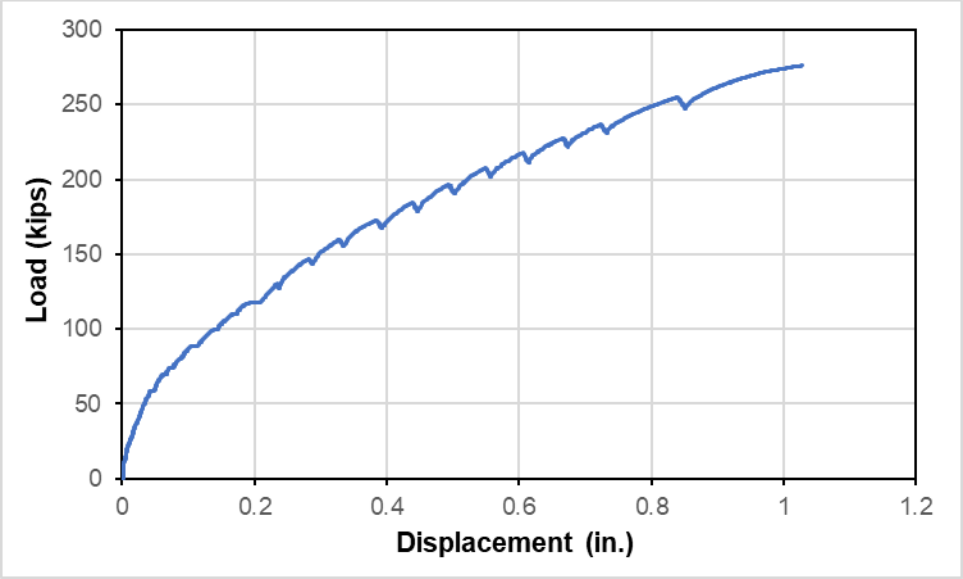

Figure D- 3: Net displacement backbone curve

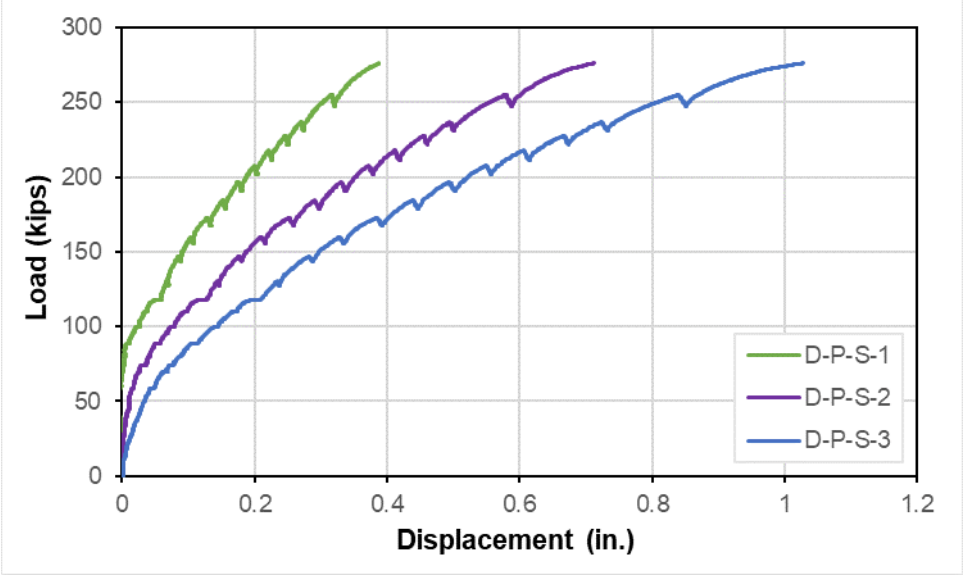

Figure D- 4: Net displacement measured at different points

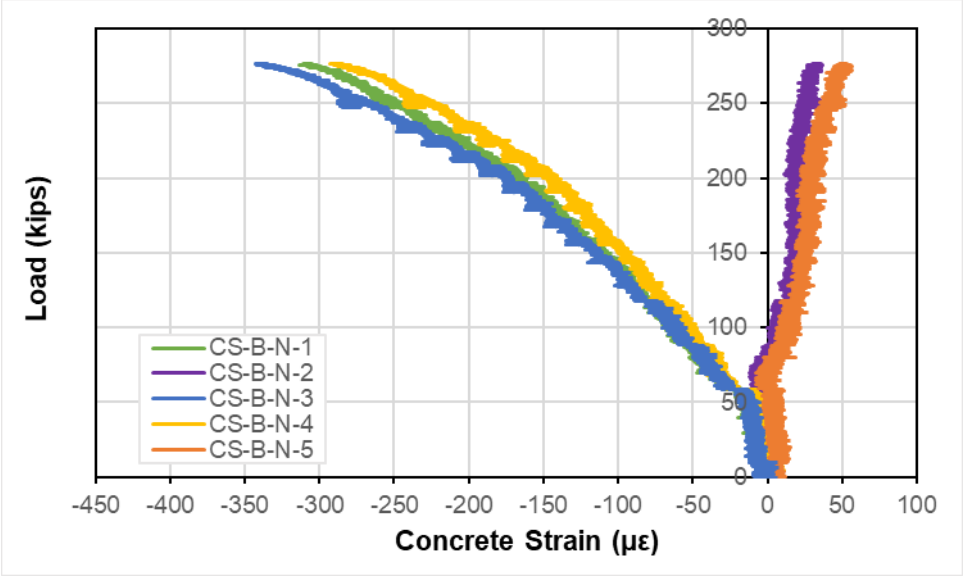

Figure D- 5: Concrete bent cap surface strains

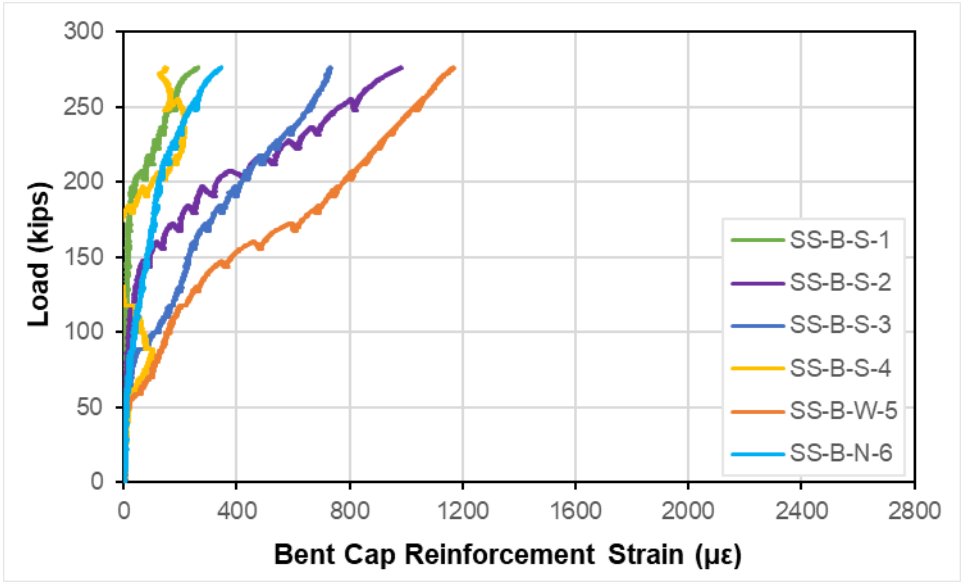

Figure D- 6: Bent cap steel reinforcement strains

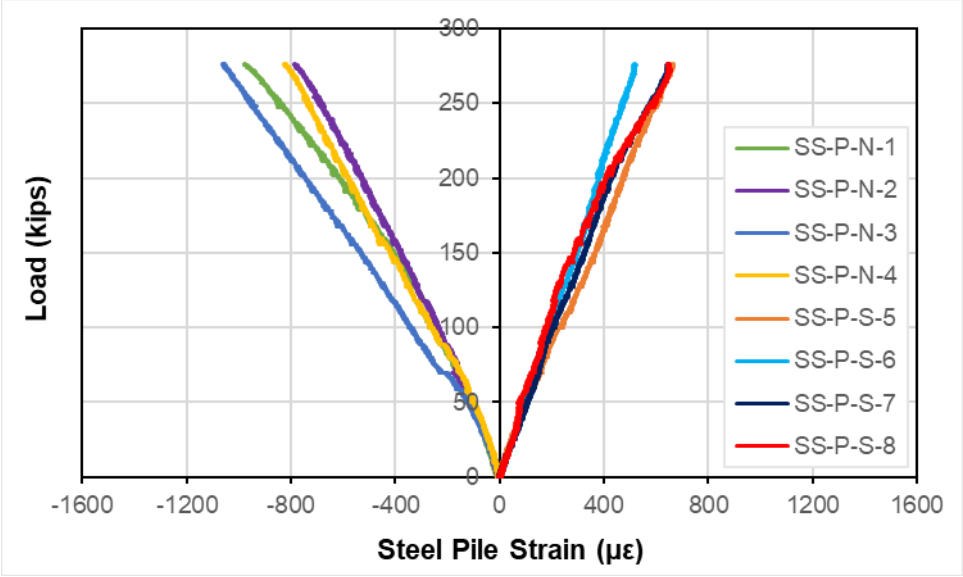

Figure D- 7: Steel pipe pile strains

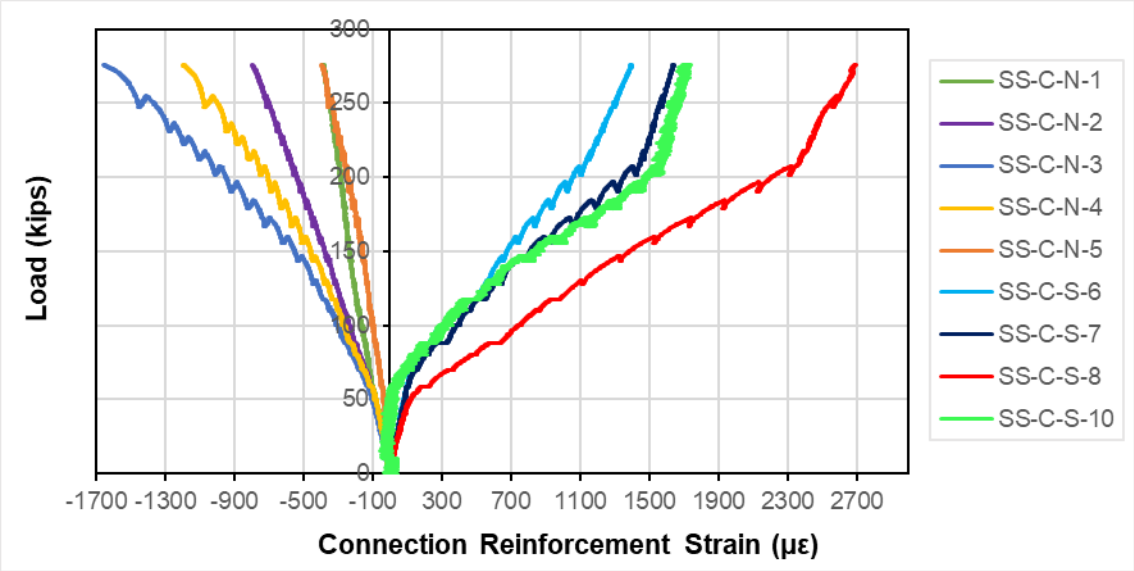

Figure D- 8: Straight reinforcing bars strains

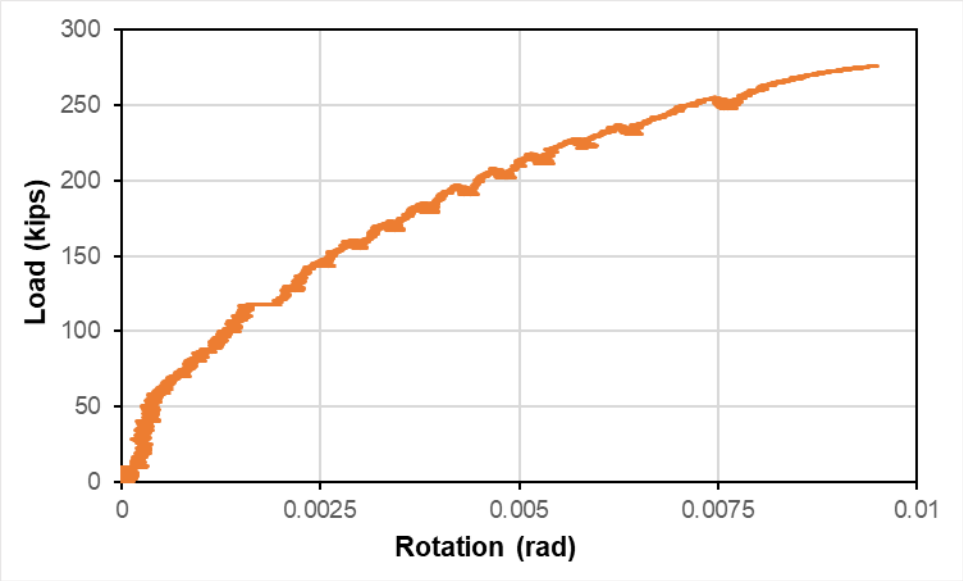

Figure D- 9: Net rotation

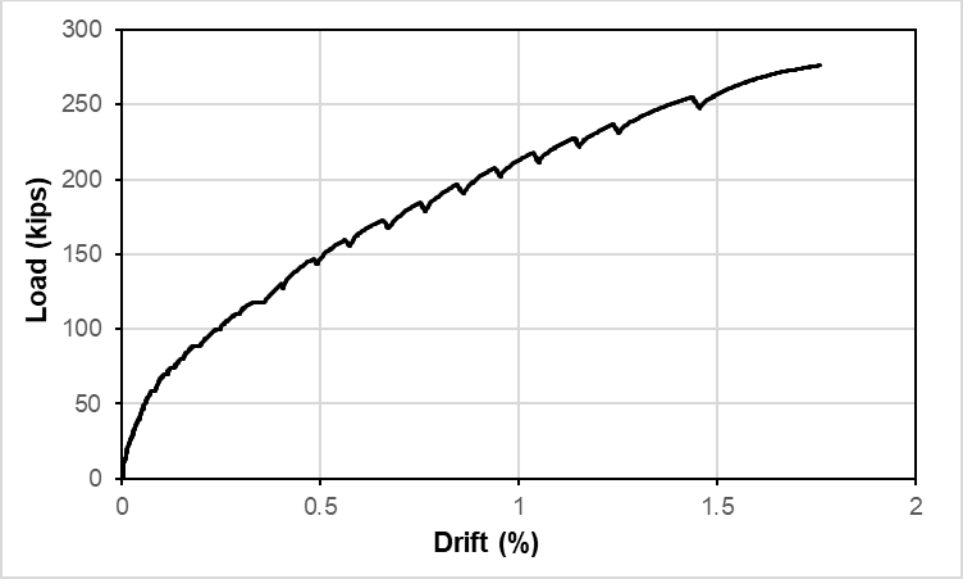

Figure D- 10: Straight specimen drift

APPENDIX E: Stud Specimen

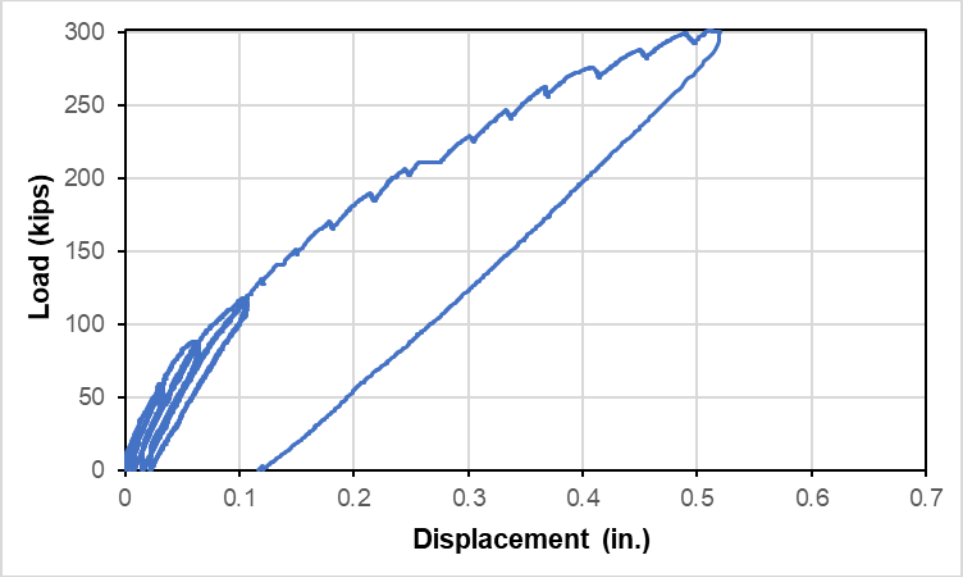

Figure E- 1: Full test data

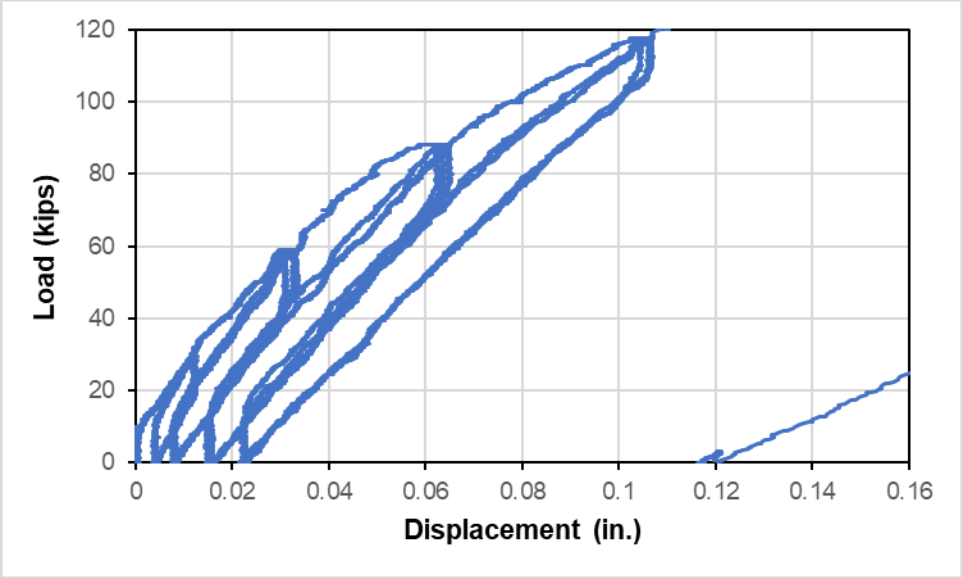

Figure E- 2: Cycles

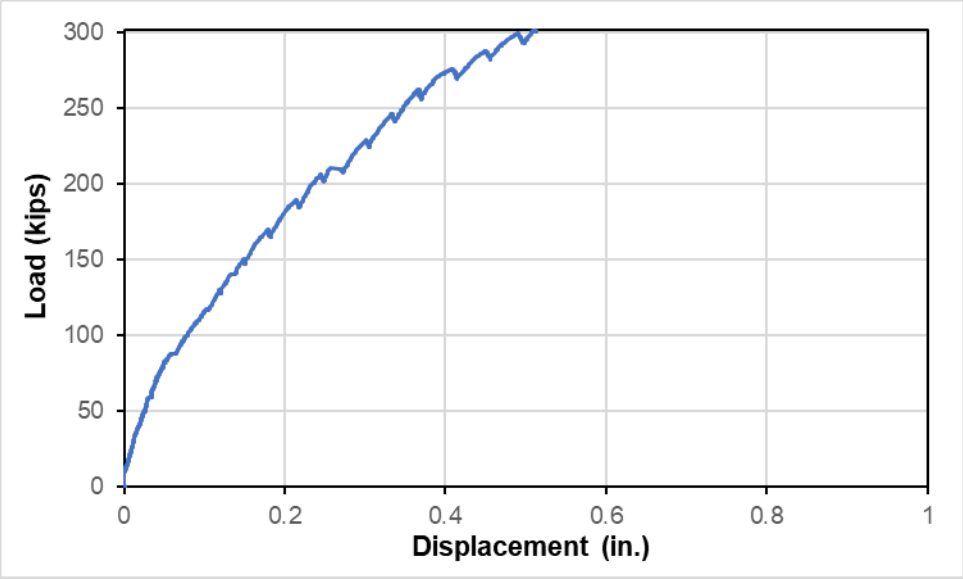

Figure E- 3: Net displacement backbone curve

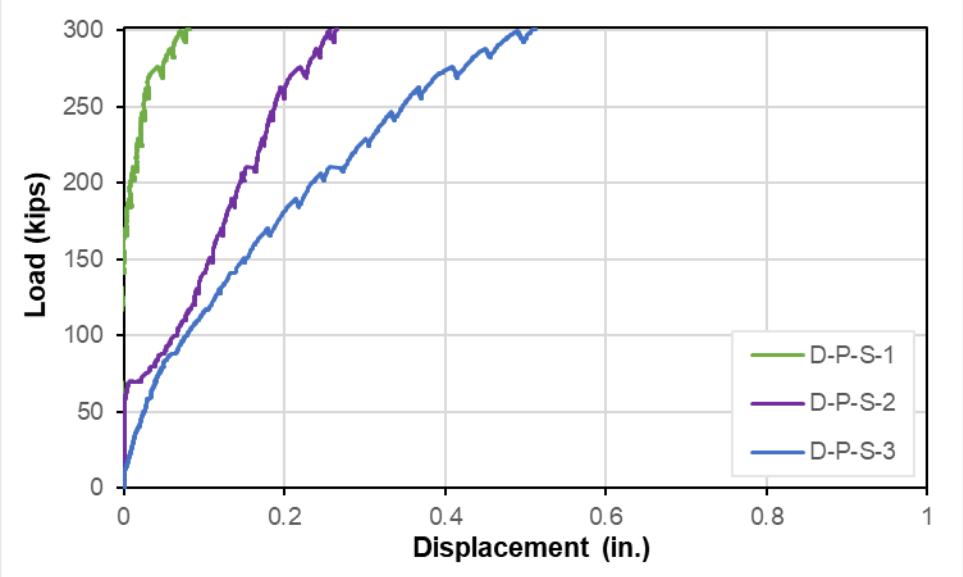

Figure E- 4: Net displacement measured at different points

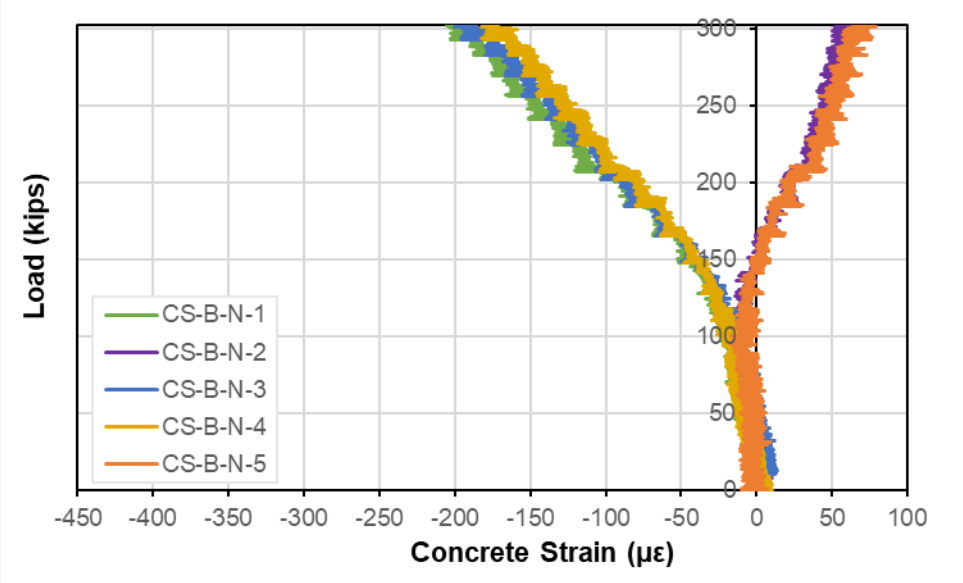

Figure E- 5: Concrete bent cap surface strains

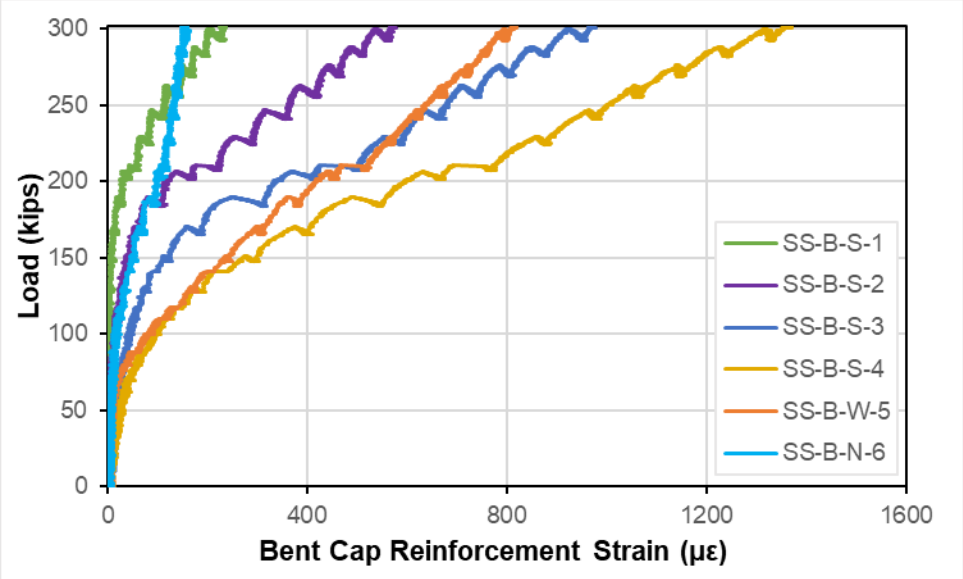

Figure E- 6: Bent cap steel reinforcement strains

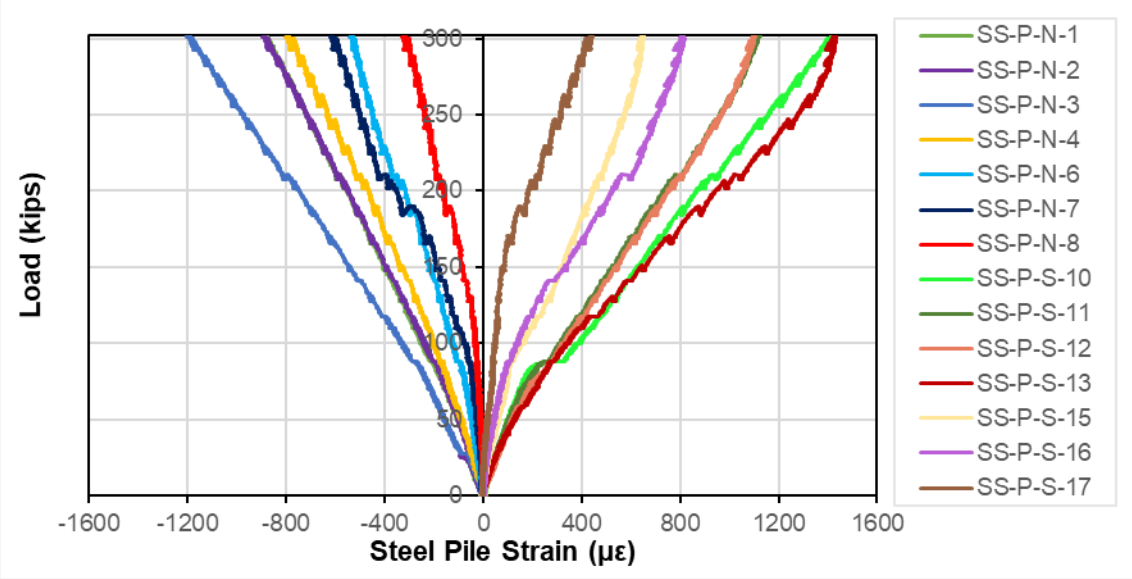

Figure E- 7: Steel pipe pile strains

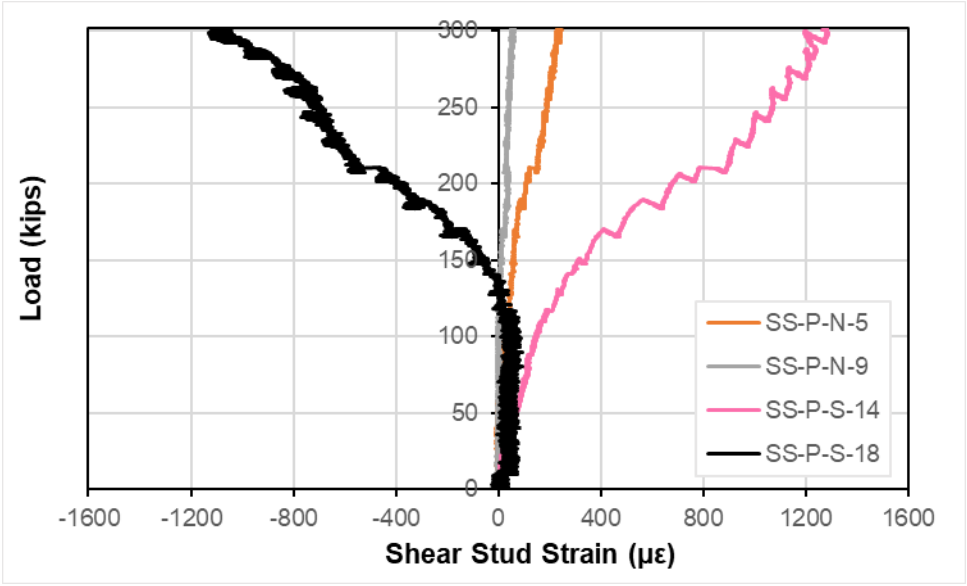

Figure E- 8: Shear stud strains

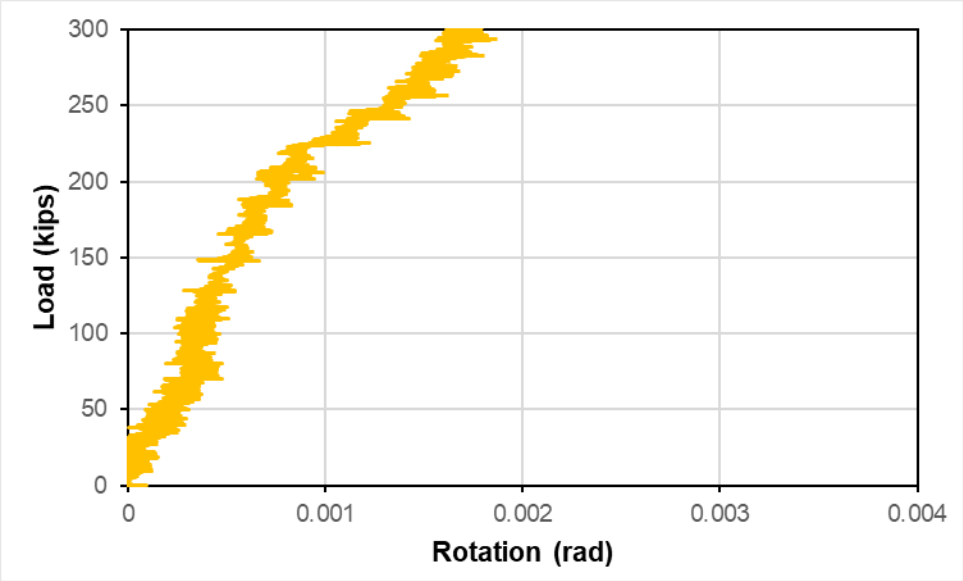

Figure E- 9: Net rotation

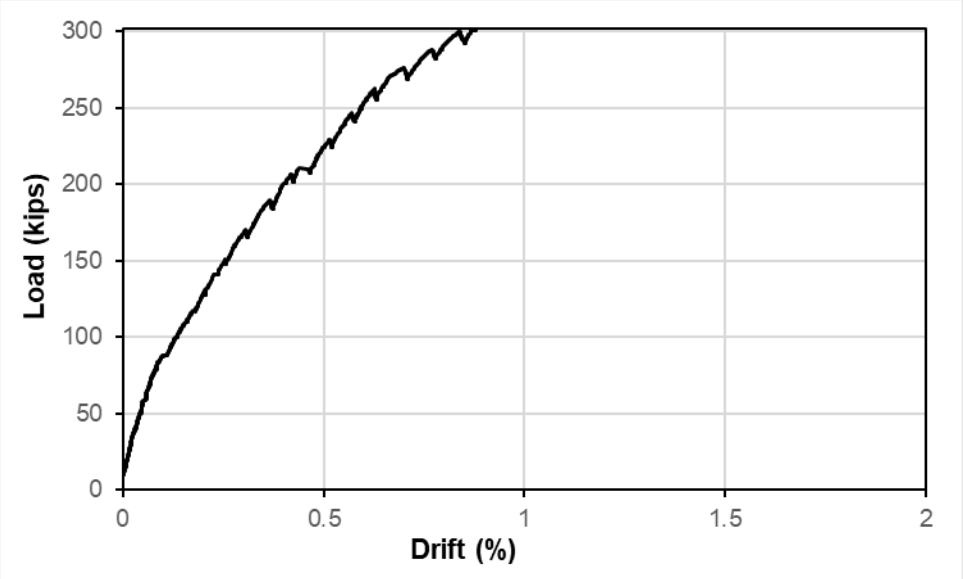

Figure E- 10: Stud specimen drift

APPENDIX F: Ring Specimen

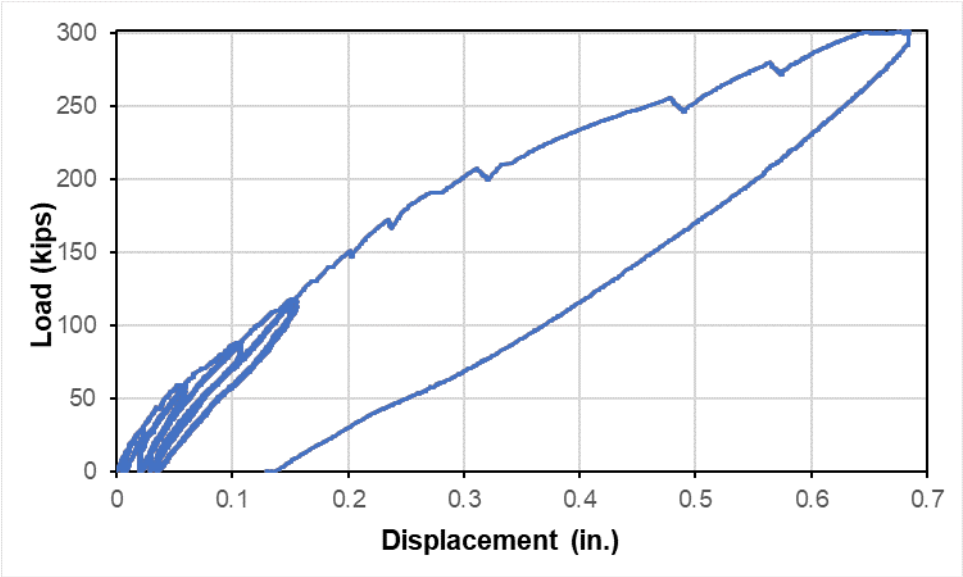

Figure F- 1: Full test data

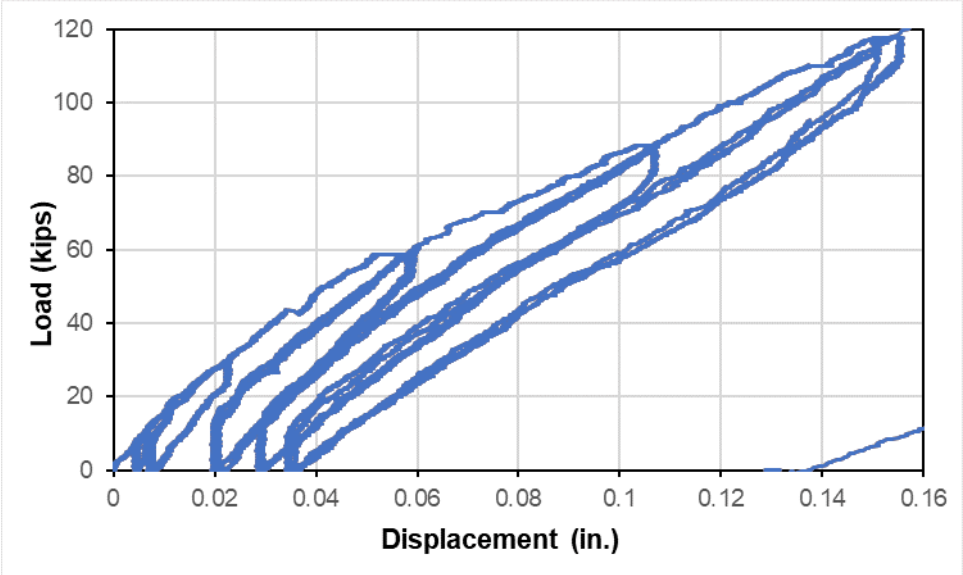

Figure F- 2: Cycles

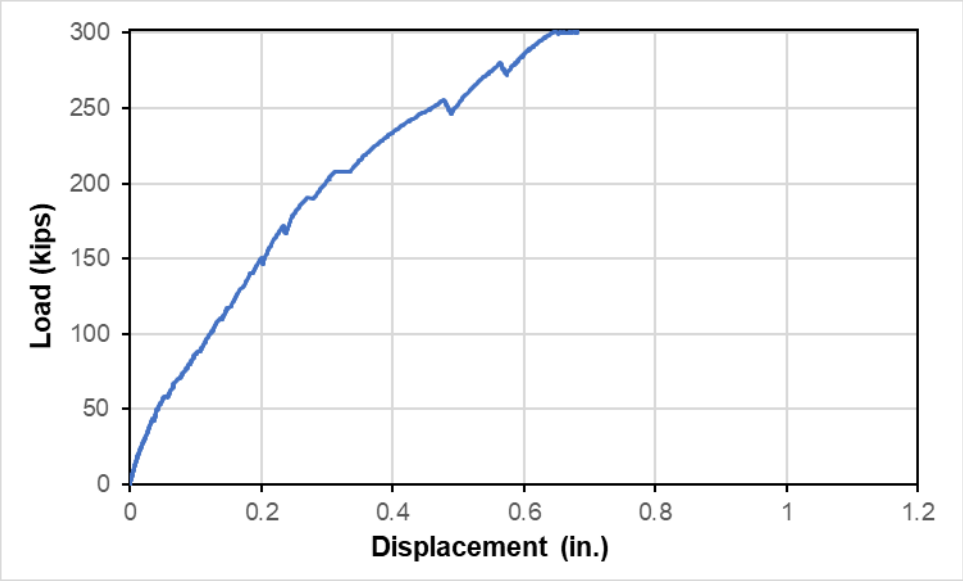

Figure F- 3: Net displacement backbone curve

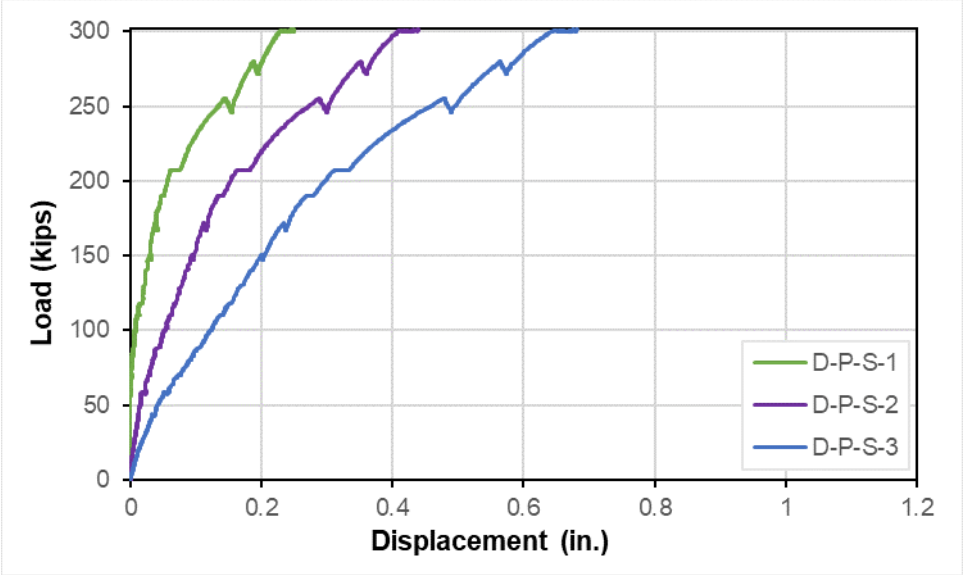

Figure F- 4: Net displacement measured at different points

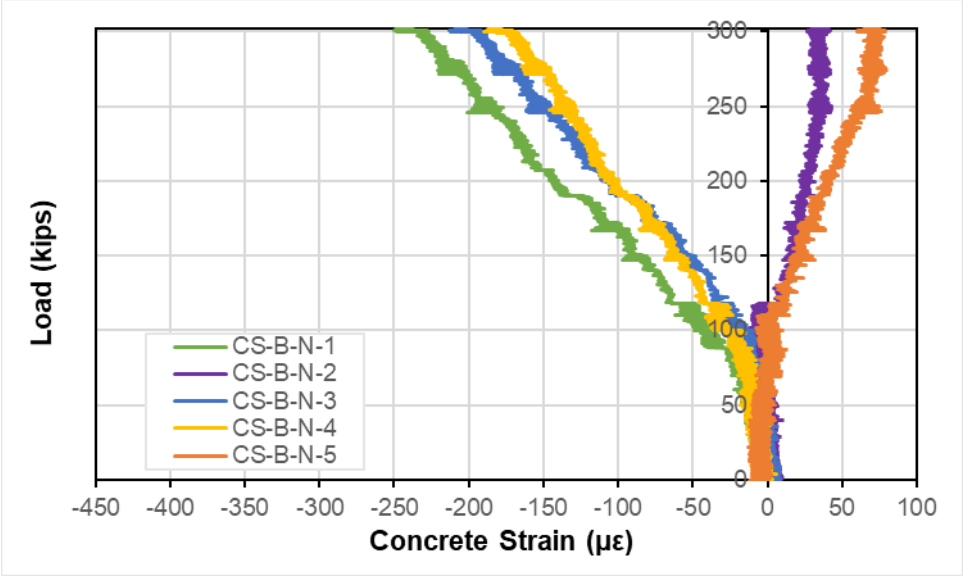

Figure F- 5: Concrete bent cap surface strains

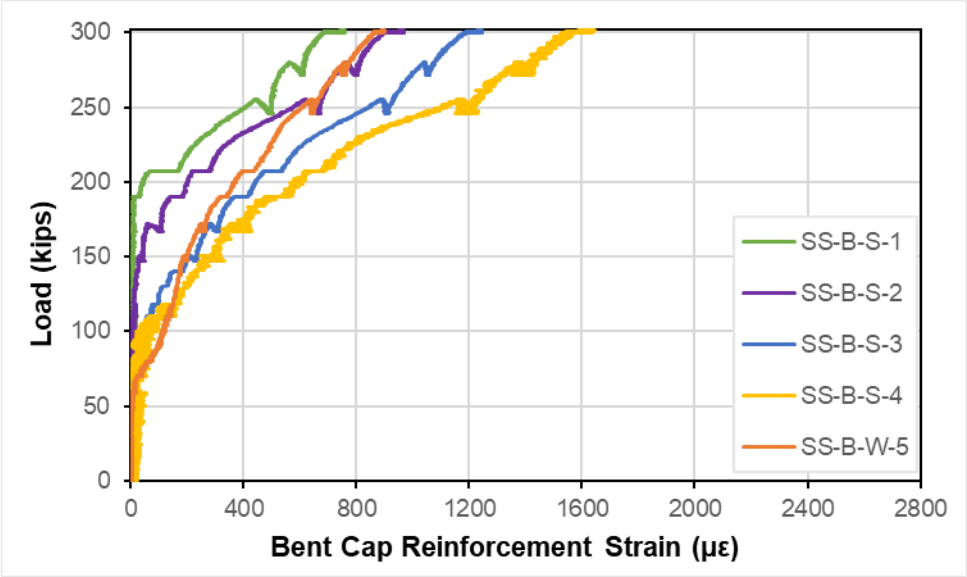

Figure F- 6: Bent cap steel reinforcement strains

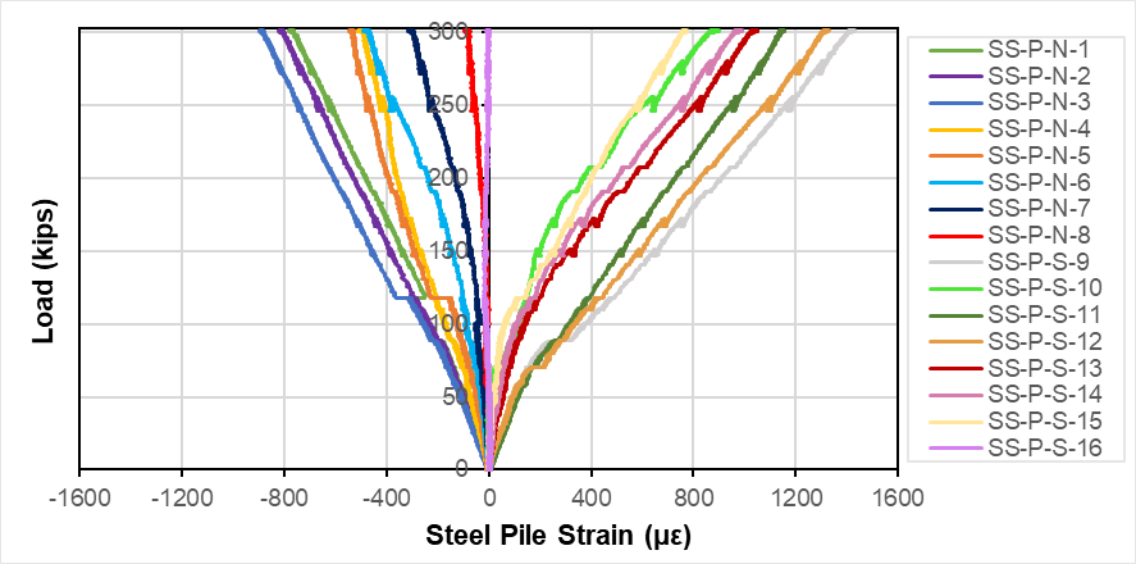

Figure F- 7: Steel pipe pile strains

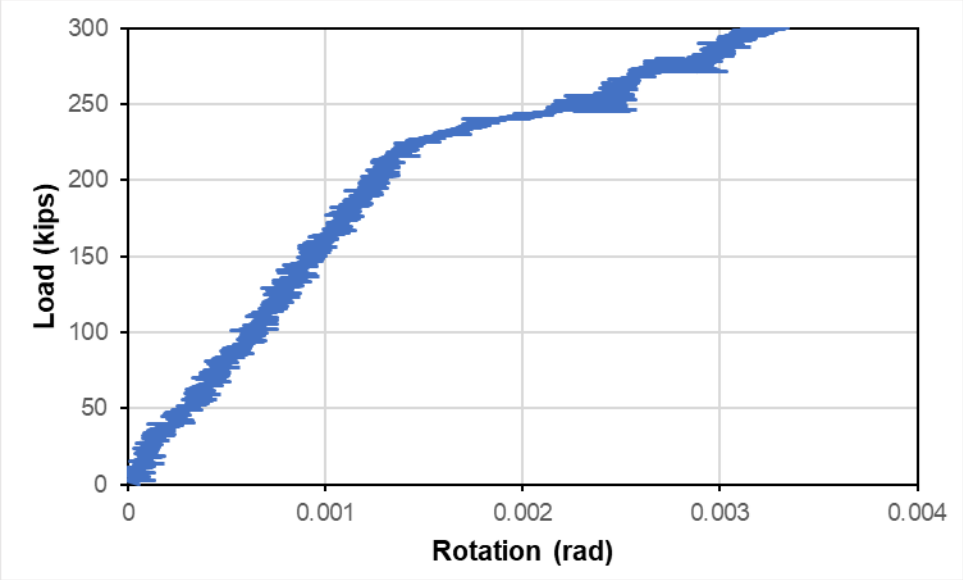

Figure F- 8: Net rotation

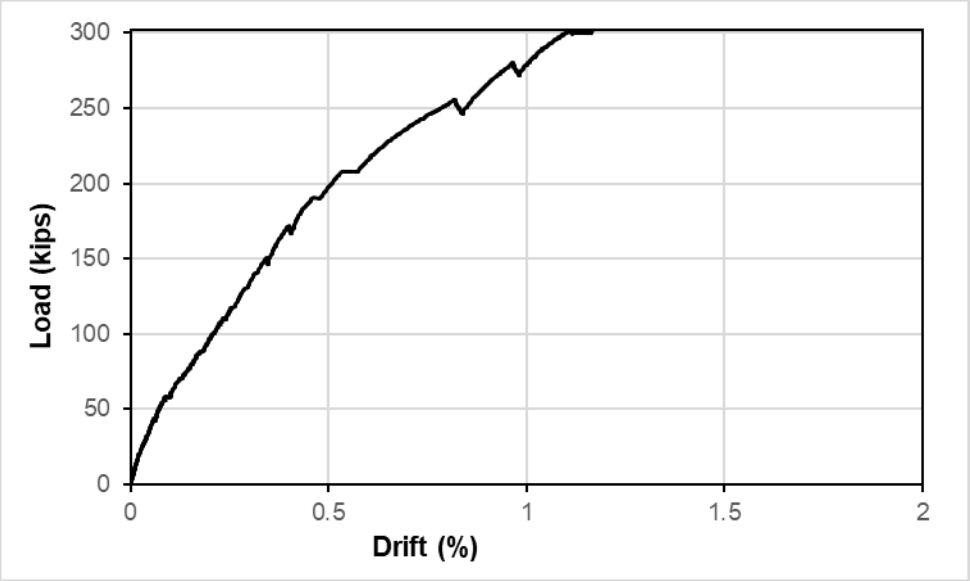

Figure F- 9: Ring specimen drift

APPENDIX G: Material Certificates

Shear Studs

1/24/24 Certificate of Compliance NELSON STUD WELDING® 83

NELSON STUD WELDING, INC.
9324 BAYTHORNE DR
HOUSTON, TX 77041

AUBURN UNIVERSITY
CIVIL ENGINEERING CENTER
238 HARBERT ENGINEERING CENTER
AUBURN UNIVERSITY AL
36849

Material Description/Part Numbers	Quantity	Heat Number	Lab Number
S3L 3/4 X 6 3/16 MS	60	10864960	
101098015			27978

Nelson Order Number: 1396370 Customer P.O.: LEVENT ISBILIROGLU

The product supplied under the contract or purchase order number shown is certified to comply with the latest revision of one or more of the applicable product specifications therein; AWS D1.1, AWS D1.5, AWS D1.6, ISO 13918, BS 5950, ASTM A108, ASTM A29, ASTM A276, ASTM A493, ASTM A1064, ASTM A496, ASTM A479, ASTM A1022.

The chemical analysis reported below was extracted from the certified mill test report. This report will be supplied when specified in the customer order or upon request. The physical properties reported were determined to be in conformance using ASTM A370 testing procedure.

Nelson Stud Welding is an IATF 16949:2016 certified supplier. This material is free from mercury contamination and is RoHS compliant. This product is melted and manufactured in the USA. No weld repair was performed on the raw material or the studs. Parts are manufactured from cold drawn bar.

Grade	C-1015
Heat Number	10864960
Ultimate PSI	73,600
Yield PSI	59,400
% Reduction of Area	62.0
% Elong. (in 2"or4D)	20.0
% Elong. (in 5D)	15.000
Carbon	.160
Manganese	.560
Phosphorous	.005
Sulphur	.014

I hereby certify that the data listed in this Certificate of Compliance is true and correct as as contained in the company test records and that it complies with the specifications shown.

Authorized by: _____

CHARTER STEEL
A Division of
Charter Manufacturing Company, Inc.

1658 Cold Springs Road
Saukville, Wisconsin 53080
(262) 268-2400
1-800-437-8789
Fax (262) 268-2570

CHARTER STEEL TEST REPORT

Melted in USA Manufactured in USA

Nelson Stud Welding - A Nelson Fastener Systems Company
7900 West Ridge Road
QC Department
Elyria,OH-44035

Cust P.O.	429539
Customer Part #	103004320
Charter Sales Order	10370082
Heat #	10864960
Ship Lot #	1386042
Grade	1015 R SK FG RHQ 49/64 RNDCOIL
Process	HR
Finish Size	49/64
Ship date	09-NOV-23

I hereby certify that the material described herein has been manufactured in accordance with the specifications and standards listed below and that it satisfies these requirements. The recording of false, fictitious and fraudulent statements or entries on this document may be punishable as a felony under federal statute.

Test results of Heat Lot # 10864960

Lab Code: 7388

CHEM	C	MN	P	S	SI	NI	CR	MO	CU	SN	V
%Wt	.16	.56	.005	.014	.160	.05	.05	.02	.09	.005	.001

AL	N	B	TI	CA	NB	SB	AS
.025	.0060	.0001	.001	.0001	.001	.001	.003

PB
.001

JOMINY(HRC)

J1	J3
42	20

JOMINY SAMPLE TYPE ENGLISH=C

QUALITY CONTROL 180 11.20.23 SERNELSON STUD WELDING

Test results of Rolling Lot # 1386042

	# of Tests	Min Value	Max Value	Mean Value	
TENSILE (KSI)	4	64.2	64.6	64.4	TENSILE LAB = 0358-02
REDUCTION OF AREA (%)	4	32	41	35	RA LAB = 0358-02

REDUCTION RATIO=66:1

Specifications: Manufactured per Charter Steel Quality Manual Rev Date 05/12/17
Charter Steel certifies this product is indistinguishable from background radiation levels by having process radiation detectors in place to measure for the presence of radiation within our process & products.
Meets customer specifications with any applicable Charter Steel exceptions for the following customer documents:
Customer Document = MPS-102C Revision = H Dated = 03-JUL-18

Additional Comments: This material meets the chemistry requirements of ASTM-A108 (latest version), ASTM A29 (latest version), and EN 10025-2 S-235-J2G3

Cust 27978

Melt Source:

Charter Steel

Saukville, WI, USA

Trip: R5282821

This MTR supersedes all previously dated MTRs for this order

Douglas Jones Division Mgr. of Quality Assurance

jonesdo@chartersteel.com

Printed Date : 11/09/2023

The following statements are applicable to the material described on the front of this Test Report:
1. The laboratory that generated the analytical or test results can be identified by the following key:

Certificate Number	Lab Code	Laboratory		Address
0358-01	7388	CSSM	Charter Steel Melting Division	1658 Cold Springs Road, Saukville, WI 53080
0358-02	8171	CSSR	Charter Steel Rolling	1658 Cold Springs Road, Saukville, WI 53080
0358-07	8171	CSSP	Charter Steel Processing Division	1658 Cold Springs Road, Saukville, WI 53080
0358-03	123633	CSFP	Charter Steel Ohio Processing Division	6255 US Highway 23, Rising Sun, OH 43457
0358-04	125544	CSCM/ CSCR	Charter Steel Cleveland	4300 E. 49th St., Cuyahoga Heights, OH 44125-1004
*	*	--	Subcontracted test performed by laboratory not in Charter Steel System	

2. When run by a Charter Steel laboratory, the following tests were performed according to the latest revisions of the specifications listed below, as noted in the Charter Steel Laboratory Quality Manual:

Test	Specifications	CSSM	CSSR	CSSP	CSFP	CSCM/ CSCR
Chemistry Analysis	ASTM E415; ASTM E1019	X				X
Macroetch	ASTM E381	X				X
Hardenability (Jominy)	ASTM A255; SAE J406; JIS G0561	X				X
Grain Size	ASTM E112	X	X	X	X	X
Tensile Test	ASTM E8; ASTM A370		X	X	X	X
Rockwelll Hardness	ASTM E18; ASTM A370	X	X	X	X	X
Microstructure (spheroidization)	ASTM A892		X	X	X	
Inclusion Content (Methods A, E)	ASTM E45		X			X
Decarburization	ASTM E1077		X	X	X	X

Charter Steel has been accredited to perform all of the above tests by the American Association for Laboratory Accreditation (A2LA). These accreditations expire 01/31/25. All other test results associated with a Charter Steel laboratory that appear on the front of this report, if any, were performed according to documented procedures developed by Charter Steel and are not accredited by A2LA.

3. The test results on the front of this report are the true values measured on the samples taken from the production lot. They do not apply to any other sample. Any statement of conformity is based on simple acceptance, whether the test result is within or outside the specification/acceptance limits. Measurement uncertainty is not taken into account in the statement of conformity.
4. This test report cannot be reproduced or distributed except in full without the written permission of Charter Steel. The primary customer whose name and address appear on the front of this form may reproduce this test report subject to the following restrictions:
   - It may be distributed only to their customers
   - All pages must be reproduced in full
5. This certification is given subject to the terms and conditions of sale provided in Charter Steel's acknowledgement (designated by our Sales Order number) to the customer's purchase order. Both order numbers appear on the front page of this Report.
6. Where the customer has provided a specification, the results on the front of this test report conform to that specification unless otherwise noted on this test report.
7. Certificate type 3.1 per EN 10204 rev. 2005-01
8. Charter Steel melting is a continuous cast electric arc furnace

ACCREDITED
Testing Laboratory

Steel Pipe Piles

NUCOR®
SKYLINE

Certificate of Conformance

Cert Number 54152 2/28/2024
Test Reference 268353

Skyline - Iuka
77 Country Road 351
Iuka, MS 38852

Issued from
Skyline Steel - Iuka
77 County Road 351
Iuka, MS 38852

Sold To: Skyline - Iuka, 77 Country Road 351, Iuka, MS 38852
Ship To: Iuka, 77 Country Road 351, Iuka, MS 38852

Product Information

Spiralweld Pipe ASTM A252 Gr. 3
Bare
36" OD x .500 x 11'
Square x Square

Heat NM4918

Tag 202363FAA

Chemical Composition

C	Mn	P	S	Si	Al	Cu	Ni
0.04	1.42	0.008	0.003	0.173	0.024	0.12	0.04
Cr	**Mo**	**V**	**Ti**	**B**	**Sn**	**Ca**	**Zn**
0.05	0.01	0.063	0.013	0.0001	0.001	0.0031	0.0061

Physical Tests

Elong 2% Offset (L)	Yield KSI (L)	Tensile (ksi) (L)
31.1 %	73.6 KSI	84.8 KSI

The undersigned hereby certifies that the above materials have been manufactured, inspected and tested in accordance with the methods prescribed in the applicable specifications and results of such test shown above. In determining properties or characteristics for which no methods of inspection and testing are prescribed by said specifications, the standard mill inspection and testing practices of this Corporation have been applied. Unless specified otherwise in the results of such inspection and tests shown above, the undersigned believes that said materials conform to said specifications.
*** Melted and Manufactured in the U.S.A.***

Name & Title

Subscribed and Sworn to before me
This 29 day of FEB 2024

STATE OF MISSISSIPPI
NOTARY PUBLIC
ID # [illegible]
KAREN S. STRICKLAND
Commission Expires
Jan. 9, 2026
TISHOMINGO COUNTY

Annular Ring

NUCOR®

NUCOR STEEL TUSCALOOSA, INC.

MILL TEST CERTIFICATE

Nucor Steel Tuscaloosa, Inc.
1700 HOLT RD N.E.
Tuscaloosa, AL 35404-1000 USA
800 800-8204
customerservice@nucortusk.com

Load Number	Tally	Mill Order Number	PO NO | Line NO	Part Number	Certificate Number	Prepared
T330725	00000001136346	N-204296-002	BRM-6462 2		S13634602-1	08/04/2023 10:34

Grade

Order Description:
Hot Roll Plate From Coil
A572 50, 0.5000 IN x 96.000 IN x 480.000 IN
Quality Plan Description:
A57250 IMP 70MAX: ASTM A572-50-21/A709-50-21 H Freq charpys 70 max

Customer:

Sold TO:
CHAPEL STEEL Birmingham AL
Ship TO:
CHAPEL STEEL COMPANY Birmingham AL
Sent TO:

Shipped Item	Heat/Slab Number	Certified By	C	Mn	P	S	Si	Cu	Ni	Cr	Mo	Cb	V	Al	Ti	N2	B	Ca	Sn	CEV	ACI
3G2277C	23A4602-03 ***	23A4602	0.07	1.14	0.012	0.004	0.18	0.17	0.06	0.07	0.019	0.031	0.004	0.033	0.013	0.009	0.0002	0.0020		0.29	
3G2277D	23A4602-03 ***	23A4602	0.07	1.14	0.012	0.004	0.18	0.17	0.06	0.07	0.019	0.031	0.004	0.033	0.013	0.009	0.0002	0.0020		0.29	
3G2277E	23A4602-03 ***	23A4602	0.07	1.14	0.012	0.004	0.18	0.17	0.06	0.07	0.019	0.031	0.004	0.033	0.013	0.009	0.0002	0.0020		0.29	
3G2277F	23A4602-03 ***	23A4602	0.07	1.14	0.012	0.004	0.18	0.17	0.06	0.07	0.019	0.031	0.004	0.033	0.013	0.009	0.0002	0.0020		0.29	

Mercury has not come in contact with this product during the manufacturing process nor has any mercury been used by the manufacturing process. Certified in accordance with EN 10204 3.1. No weld repair has been performed on this material. Yield strength is determined by the 0.2% offset method unless otherwise noted. Manufactured to a fully killed fine grain practice.
NUTEMPER TEMPER PASSED plate from coil
ISO 9001:2015 Registered, PED Certified

"***" indicates Heats melted and Manufactured in the U.S.A.

We hereby certify that the product described above passed all of the tests required by the specifications.

Jon Walton - Metallurgist

NUCOR®

NUCOR STEEL TUSCALOOSA, INC.

MILL TEST CERTIFICATE

Nucor Steel Tuscaloosa, Inc.
1700 HOLT RD N.E.
Tuscaloosa, AL 35404-1000 USA
800 800-8204
customerservice@nucortusk.com

Load Number	Tally	Mill Order Number	PO NO | Line NO	Part Number	Certificate Number	Prepared
T330725	00000001136346	N-204296-002	BRM-6462 2		S13634602-1	08/04/2023 10:34

Grade

Order Description:
Hot Roll Plate From Coil
A572 50, 0.5000 IN x 96.000 IN x 480.000 IN
Quality Plan Description:
A57250 IMP 70MAX: ASTM A572-50-21/A709-50-21 H Freq charpys 70 max

Customer:

Sold TO:
CHAPEL STEEL Birmingham AL
Ship TO:
CHAPEL STEEL COMPANY Birmingham AL
Sent TO:

Shipped Item	Certified By	Heat/Slab Number	Yield ksi	Tensile ksi	Y/T %	ELONGATION % 2"	ELONGATION % 8"	Bend OK?	Hard HB	Charpy Impacts (ft-lbs) Size	mm	1	2	3	Avg	Shear % 1	2	3	Avg	Test Temp
3G2277C	S3G2277FTT	23A4602-03 ***	58.2	69.7	83.5	38.8														
3G2277C	S3G2277BLI	23A4602-03 ***								7.5	196	190	199	195.0						-22 F
3G2277C	S3G2277FLI	23A4602-03 ***								7.5	199	197	208	201.3						-22 F
3G2277C	S3G2277MLI	23A4602-03 ***								7.5	198	191	203	197.3						-22 F
3G2277C	S3G2277MTT	23A4602-03 ***	59.7	69.7	85.7	37.2														
3G2277D	S3G2277FTT	23A4602-03 ***	58.2	69.7	83.5	38.8														
3G2277D	S3G2277BLI	23A4602-03 ***								7.5	196	190	199	195.0						-22 F
3G2277D	S3G2277FLI	23A4602-03 ***								7.5	199	197	208	201.3						-22 F
3G2277D	S3G2277MLI	23A4602-03 ***								7.5	198	191	203	197.3						-22 F
3G2277D	S3G2277MTT	23A4602-03 ***	59.7	69.7	85.7	37.2														
3G2277E	S3G2277FTT	23A4602-03 ***	58.2	69.7	83.5	38.8														
3G2277E	S3G2277BLI	23A4602-03 ***								7.5	196	190	199	195.0						-22 F
3G2277E	S3G2277FLI	23A4602-03 ***								7.5	199	197	208	201.3						-22 F
3G2277E	S3G2277MLI	23A4602-03 ***								7.5	198	191	203	197.3						-22 F
3G2277E	S3G2277MTT	23A4602-03 ***	59.7	69.7	85.7	37.2														
3G2277F	S3G2277FTT	23A4602-03 ***	58.2	69.7	83.5	38.8														
3G2277F	S3G2277BLI	23A4602-03 ***								7.5	196	190	199	195.0						-22 F
3G2277F	S3G2277FLI	23A4602-03 ***								7.5	199	197	208	201.3						-22 F

Mercury has not come in contact with this product during the manufacturing process nor has any mercury been used by the manufacturing process. Certified in accordance with EN 10204 3.1. No weld repair has been performed on this material. Yield strength is determined by the 0.2% offset method unless otherwise noted. Manufactured to a fully killed fine grain practice.
NUTEMPER TEMPER PASSED plate from coil
ISO 9001:2015 Registered, PED Certified

We hereby certify that the product described above passed all of the tests required by the specifications.

Jon Walton - Metallurgist

"***" indicates Heats melted and Manufactured in the U.S.A.

NUCOR®

NUCOR STEEL TUSCALOOSA, INC.

MILL TEST CERTIFICATE

Nucor Steel Tuscaloosa, Inc.
1700 HOLT RD N.E.
Tuscaloosa, AL 35404-1000 USA
800 800-8204
customerservice@nucortusk.com

Load Number	Tally	Mill Order Number	PO NO | Line NO	Part Number	Certificate Number	Prepared
T330725	00000001136346	N-204296-002	BRM-6462 2		S13634602-1	08/04/2023 10:34

Grade

Order Description:
Hot Roll Plate From Coil
A572 50, 0.5000 IN x 96.000 IN x 480.000 IN
Quality Plan Description:
A57250 IMP 70MAX: ASTM A572-50-21/A709-50-21 H Freq charpys 70 max

Customer:

Sold TO:
CHAPEL STEEL Birmingham AL
Ship TO:
CHAPEL STEEL COMPANY Birmingham AL
Sent TO:

Shipped Item	Certified By	Heat/Slab Number	Yield ksi	Tensile ksi	Y/T %	ELONGATION % 2"	ELONGATION % 8"	Bend OK?	Hard HB	Charpy Impacts (ft-lbs) Size	mm	1	2	3	Avg	Shear % 1	2	3	Avg	Test Temp
3G2277F	S3G2277MLI	23A4602-03 ***								7.5	198	191	203	197.3						-22 F
3G2277F	S3G2277MTT	23A4602-03 ***	59.7	69.7	85.7	37.2														

Items: 4 **PCS:** 7 **Weight:** 45739 **LBS**

Mercury has not come in contact with this product during the manufacturing process nor has any mercury been used by the manufacturing process. Certified in accordance with EN 10204 3.1. No weld repair has been performed on this material. Yield strength is determined by the 0.2% offset method unless otherwise noted. Manufactured to a fully killed fine grain practice.
NUTEMPER TEMPER PASSED plate from coil
ISO 9001:2015 Registered, PED Certified

We hereby certify that the product described above passed all of the tests required by the specifications.

Jon Walton - Metallurgist

"***" indicates Heats melted and Manufactured in the U.S.A.

Headed Rebar

BarSplice PRODUCTS INC.
A SUBSIDIARY OF FC INDUSTRIES INC.
4900 Webster Street
Dayton, OH 45414-4831
Phone: 937-275-8700 Fax:937-275-9566

Packing List

Ship Date	Packing List No.	Page
12/26/2023	0117486	1 of 1

Date Printed: 12/27/2023
Time Printed: 4:56:13PM

Sold To:
SABEL STEEL
P O BOX 4747
MONTGOMERY, AL 36103-4747
USA

Ship To:
SABEL STEEL
704 LAFAYETTE STREET
MONTGOMERY, AL 36104
USA

Job Site Contact: MIKE ROOKER **Phone:** 334-265-6771

Sales Order No	Order Date	Customer P. O.	Ship Via
0250339	12/18/2023	06-2023-219	LTL - R&L

Line/WT #	Item Number	Description	Ordered Qty	Shipped Qty	Backordered Qty
001	BS	BARSPLICER BS-Y #11 UNCOATED A615 GRADE 60 W/XP THRD C = 140.00 " W/TERMINATION	20	20	0
002	BS	BARSPLICER BS-Y #11 UNCOATED A615 GRADE 60 W/XP THRD C = 54.00 " W/TERMINATION	8	8	0

Comments: FOB: DAYTON, OH USA
TRACEY
MICHAEL ROOKER
COMMERCIAL
1 - Type 1, Grade 60
MILL CERTS

BarSplice PRODUCTS INC.

CERTIFICATE OF COMPLIANCE

FOR **BPI® TYPE 1** MECHANICAL SPLICES & ASTM A970 HEADED DEVICES (GRADE 60)

DATE	CUSTOMER	PURCHASE ORDER	ITEM	PROJECT NAME
12/27/2023	SABEL STEEL	06-2023-219	--	COMMERCIAL

QTY	PRODUCT	IDENTIFICATION	HEAT LOT No.	ASTM Spec or Rebar Mill
269.033 FT	#11 REBAR, UNCOATED A615 GRADE	11RB_11Y	7033300	ASTM A615-22
40 EA	#11 THREADED HEAD 5Ab	11TERM_7W2	A191470	ASTM A576-17
41.508 FT	#11 REBAR, UNCOATED A615 GRADE	11RB_11Y	7033300	ASTM A615-22
16 EA	#11 THREADED HEAD 5Ab	11TERM_7W2	A191470	ASTM A576-17

This certifies the following:

1. Barsplice Products, Inc. (BPI) designs, manufactures, and supplies available mechanical splices and headed devices for reinforcing bars under an approved quality system in accordance with ISO 9001:2015.
2. This Certificate of Compliance was issued upon the date shown above to the customer noted with reference to the customer purchase order and project name if provided. This certifies that the coupler systems and headed devices shipped from BPI comply with general descriptions, dimensions and representations made in published BPI literature and data sheet(s) in effect at the time of issue.
3. Supplied products shown above are broken down by heat lot number for each quantity of product(s) listed. The BPI identification codes uniquely identify the products provided and are marked upon the finished parts where applicable. These codes match the raw material Certified Material Test Reports (CMTR) and the heat lot number. When required by material specifications, chemical analyses, tests, examinations, and heat treatments have been performed by the supplier(s) and the results have been verified by BPI to be included on the CMTR. Any required test not performed (if applicable) is noted on the CMTR, and any operation not performed per specification (if applicable) is reported.
4. Raw materials used in the products listed were obtained from, and processed through, BPI qualified sources/suppliers in accordance with ISO 9001:2015. All ferrous raw materials (iron and steel) used, and their coatings if applicable, have been domestically sourced, processed and manufactured in the United States of America in full compliance with the following: Federal Highway Administration (FHWA) 23 USC § 313 – Buy America; 23 CFR § 635.410, American Recovery and Reinvestment Act of 2009 Section 1605 – Buy American, 41 USC § 8302 – Buy America; American Iron and Steel (AIS) requirements in the EPA State Revolving Fund Programs, and; the Build America, Buy America (BABA) Act.
5. Product and/or material specifications are verified to be met, and products are mechanically tested when appropriate, prior to shipment to ensure the mechanical splices and headed devices provided meet applicable compression and tensile strength requirements. Type 1 mechanical splices provided conform to Section 25.5.7 of ACI 318-19 and develop 125% x specified yield (f_y) strength of the reinforcing bar when installed on Grade 60 (metric Grade 420) reinforcing bar manufactured to the latest requirements of ASTM A615/A615M or A706/A706M. Headed devices provided meet the full tensile strength requirements of ASTM A970 (confirmed with in-air testing) and conform to Class A/HA. Performance claims are only applicable when BPI supplies all components of the mechanical splice system. When components are supplied by others, performance is not included in the scope of this certificate.
6. The above referenced iron and steel product(s) additionally meet all requirements of the following:
   - Arizona Department of Transportation Specification Section 106.05(B), with legal authority to bind BPI
   - Illinois Department of Transportation Specification Section 106.01
   - Michigan Department of Transportation Specification Section 105.10
   - West Virginia Department of Transportation Approval Code #1456220A.

When coated splices and headed devices are installed on galvanized or epoxy coated bars, some touch-up and/or repair of the coating may be required after installation.

NOTICE

The products described herein must be installed in accordance with the latest edition of the appropriate BPI SPLICING MANUAL and/or INSTALLATION INSTRUCTIONS (and any special supplements) supplied with the product or to the project. These documents must be read and fully understood by the operator before use. In accordance with project specifications, tensile tests may be required before and during production splicing to verify correct usage, rebar grade, and operator proficiency. Other terms and conditions are applicable as may have been previously supplied on quotations and order acknowledgments, either directly or to the dealer, distributor or representative.

SIGNED: _____ **DATE:** 12/27/2023 **SHOP ORDER #** 0250339

Amber Hare, Shipping Clerk
BARSPLICE PRODUCTS, INC.

4900 Webster Street, Dayton OH 45414, USA • Tel: (937) 275-8700 • email: bar@barsplice.com

CMC STEEL TENNESSEE
1919 Tennessee Avenue
Knoxville TN 37921-2686

CERTIFIED MILL TEST REPORT
For additional copies call
865-202-5972/888-870-0766

We hereby certify that the test results presented here are accurate and conform to the reported grade specification

Jim Hall
Quality Assurance Manager

HEAT NO.:7033300 SECTION: REBAR 36MM (#11) 40'0" 420/60 CLD CQ GRADE: ASTM A615-22 Gr 420/60 CLD ROLL DATE: 04/09/2023 MELT DATE: 04/07/2023 Cert. No.: 85386425 / 033300L202	SOLD TO	Barsplice Products Inc 4900 WEBSTER ST DAYTON OH US 45414-4831 9372758700	SHIP TO	Barsplice Products Inc 4900 WEBSTER ST DAYTON OH US 45414-4831 9372758700	Delivery#: 85386425 BOL#: 75303893 CUST PO#: 54137 CUST P/N: DLVRY LBS / HEAT: 48456.000 LB DLVRY PCS / HEAT: 228 EA

Characteristic	Value
C	0.41%
Mn	0.73%
P	0.016%
S	0.054%
Si	0.19%
Cu	0.33%
Cr	0.16%
Ni	0.12%
Mo	0.046%
V	0.003%
Sn	0.006%
Yield Strength test 1	83.3ksi
Yield Strength test 1 (metri	574MPa
Tensile Strength test 1	110.5ksi
Tensile Strength 1 (metric)	762MPa
Elongation test 1	12%
Elongation Gage Lgth test 1	8IN
Tensile to Yield ratio test1	1.33
Elongation Gage Lgth 1(metri	200mm

Characteristic	Value
Bend Test 1	Passed
Rebar Deformation Avg. Spaci	0.797IN
Rebar Deformation Avg. Heigh	0.087IN
Rebar Deformation Max. Gap	0.224IN

BarSplice PRODUCTS INC. REVIEWED BY
ENG. & APPROVED FOR MANUFACTURE
DATE 4/26/2023 HT# 7033300
SIG [signature] CODE 11RB 11Y

The Following is true of the material represented by this MTR:

*Material is fully killed and is Hot Rolled Steel
*100% melted, rolled, and manufactured in the USA
*EN10204:2004 3.1 compliant
*Contains no weld repair
*Contains no Mercury contamination
*Manufactured in accordance with the latest version of the plant quality manual
*Meets the "Buy America" requirements of 23 CFR635.410, 49 CFR 661
*Warning: This product can expose you to chemicals which are known to the State of California to cause cancer, birth defects or other reproductive harm. For more information go to www.P65Warnings.ca.gov

REMARKS :

TT14M 7W	TT14F 7W	14PF 7W	TT14SC 7W
TT14FWFL 7W	TT14/11F 7W	TT14/10F 7W	TT14/09F 7W
TT14/08F 7W	XT11SC 7W	07TDX 7W	09BNH 7W
07BNX 7W	10TERM 7W	10ETERM 7W*30M-BNH-7W	

BarSplice PRODUCTS INC. REVIEWED BY ENG. & APPROVED FOR MANUFACTURE
DATE 04/29/2019 HT# A191470
SIG CODE LISTED

Steel Dynamics, Inc.
Long Products Group
Engineered Bar Division

8000 N. County Road 225 East
Pittsboro, IN 46167
Phone: (317) 892-7000
Fax: (317) 892-7285

Certified Material Test Report

Cert #: 313588 **Mill Order:** 1907788 **Heat #:** A191470 **Issued:** 4/29/2019 09:04:24
Work Order: **Sales Order:** 214414-1 **Customer:** Barsplice Products, Inc **PO #:** N-3543-1
Load #: **Reference #:** N14TGTP_7W **Reference Desc:** Bar End = WHITE **End Use:**
Size: 2-7/8" **Shape:** Round **Grade:** 1018 **Length:** 24'
Grain Practice: Al Fine Grain (5-8) per ASTM A29 **Reduction Ratio:** 21.4 to 1 **Disposition:** Rolled Prime

Ladle Chemistry Analysis (ASTM A29)

C	Mn	P	S	Si	Al	Cu	Ni	Cr	Mo	Sn	N	V	Cb	B	Ca	W	Ti	Dl
0.19	0.74	0.010	0.017	0.12	0.024	0.21	0.07	0.12	0.02	0.008	0.0081	0.002	0.000	0.0000	0.0014	0.002	0.003	0.56

Pb	Co	As	Sb	Zr	Bi	H (ppm)	O (ppm)	Ceq	J-Factor
0.001	0.006	0.003	0.000	0.001	0.000	0.7		0.36	155

Product Check Analysis (ASTM A29)

	C	Mn	P	S	Si	Al	Cu	Ni	Cr	Mo	Sn	N	V	Cb	Ti	B	Ca	O
Front																		
Back																		

Jominy (ASTM A255)

	J1	J2	J3	J4	J5	J6	J7	J8	J9	J10	J12	J14	J16	J18	J20	J24	J28	J32
Calc'd Standard																		
	1.5	3	5	7	9	11	13	15	20	25	30	35	40	45	50			
Calc'd Metric																		
	J1	J2	J3	J4	J5	J6	J7	J8	J9	J10	J12	J14	J16	J18	J20	J24	J28	J32
Front																		
Back																		

Microcleanliness (ASTM E45)

Method A								Method C (SAE J422)		Method E	
AT	AH	BT	BH	CT	CH	DT	DH	S	O	SAM "B"	SAM "D"

Microcleanliness (DIN 50602)

K		M
S	O	Tot	Tot

Decarb		Grainsize		Macrostructure (ASTM E381)			Magnetic Particle Inspection	
Depth	% of Diameter	Austenitic	Ferritic	S	R	C	Frequency	Severity

Mechanical Properties (ASTM A370)

Tensile Properties						Hardness	
Tensile Strength		0.2% Yield Strength		% Elong (2")	% ROA	0.35% EUL Yield Strength	(MR)	(Surf)
70,000	psi	42,300	psi	33.0	59.0			

Steel Dynamics - Engineered Bar Products has a quality system in place which has been certified ISO 9001:2015 compliant, including PED certification.

Comments/Specs

Electric Arc Furnace Melted - Vacuum Tank Degassed --- Turn, Polish, Rotary Eddy Current Test --- Turn, Polish, Rotary Eddy Current Test --- Bar Splice Spec. BPI 4.6-38 Rev Level 0 --- Produced to ASME Sec III, NCA 3800, 2017 edition --- , inc. 10 CFR Part 21 --- Audited to QSM-9001 R9 dtd 3-22-18 --- ASTM A576-17

Condition: Turned & Polished, Eddy Current Inspected

I hereby certify that the content of this report is correct and accurate, and that all tests and operations performed on this material were in compliance with applicable material specifications and purchaser designated requirements.

Jason Sawa - Rolling Mill Metallurgist (ES)

BarSplice PRODUCTS INC.
A SUBSIDIARY OF FC INDUSTRIES INC.
4900 Webster Street • Dayton, OH 45414 • Ph: (937) 275-8700

Prior to following the installation instructions below, verify this document is the latest version in use. The latest version can be found at www.barsplice.com.

INSTALLATION INSTRUCTIONS FOR FIELD ASSEMBLY OF BPI® BARSPLICER COUPLERS ON THREADED REINFORCEMENT BAR

Internal coupler threads are protected by plastic plugs and external rebar threads are protected by plastic caps, both of which should be kept in place until the time of assembly. If missing, ***obtain the correct plugs/caps*** *from the manufacturer or supplier. If you see minor external* ***thread damage****, try using a thread file to correct the problem. For other thread damage, it may be necessary to use a thread die tool. DO NOT TRY TO ASSEMBLE DAMAGED THREADS. You may cause premature binding. DO NOT USE THIS COUPLER IN CONJUNCTION WITH A REBAR WHICH IS LARGER OR SMALLER THAN THE INTENDED BAR SIZE. DO NOT USE WITH ANYTHING OTHER THAN UNIFIED NATIONAL COURSE (UNC) THREADS. STORE COUPLERS IN A CLEAN, DRY PLACE UNTIL READY TO INSTALL. When the bar cannot be turned, use a BPI® Barsplicer Position coupler or an alternate splice system such as the ZAP Screwlok®.*

1 If the Barsplicer coupler is placed first, make sure the internal coupler thread is protected from the concrete before pouring concrete around or near the coupler. If present, make sure the coupler flange is properly secured to the form. Make sure the bar is properly supported and tied off. If the threaded rebar is placed first, make sure the rebar thread is protected from the concrete before pouring concrete around or near the thread. DO NOT PLACE REINFORCING BAR OR COUPLER IF THE THREADS ARE DAMAGED AND CANNOT BE REPAIRED.

2 When joining the threaded rebar and Barsplicer coupler, remove the protective caps and plugs and then line up both sides as straight as possible as shown in the pre-assembled condition below.

PRE-ASSEMBLED CONNECTION

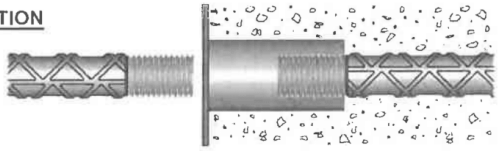

Just before assembly, check both internal and external threads for cleanliness. Clean off any foreign matter. DO NOT USE CORROSIVE ACIDS. Any thread damage must be corrected as noted above before installation.

3 After the initial thread location, rotate the free rebar clockwise making sure that the threaded ends remain aligned. NOTE: If the threaded end of the rebar is bent, **DO NOT ALIGN THE REBARS. ALIGN THE THREADS SO THAT THE THREADS SCREW TOGETHER**. Continue to rotate the free rebar by hand. If you feel the threads starting to prematurely bind, DO NOT FORCE THEM. **Shake the free end of the rebar while turning**. Allow the free end of the rebar to rotate in its own natural circle. **ASSEMBLE UNTIL THREADS ARE FULLY ENGAGED.**

ASSEMBLED CONNECTION

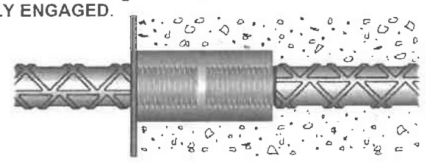

If the threaded rebar end does not properly engage into the Barsplicer coupler during assembly, stop immediately. Disassemble the connection to determine the problem. Possible causes of mis-assembly may be: mis-matched thread sizes; bars rubbing against each other; contaminated threads (i.e. concrete, dirt, etc.); or threads that have been damaged. Reassemble only after the problem has been identified and corrected.

4 To ensure the threads are fully engaged, use a pipe wrench or chain wrench to snug and tighten the assembly. Long lengths of rebar, especially large diameter bars, are heavy. To overcome this bar weight, it may be necessary to use an extension bar. As necessary, use the following wrench lengths as a guide: Bar sizes #4-#6 (13-19 mm) = 8-12" (20-30 cm) length; Sizes #7-#8 (22-25 mm) = 12-18" (30-45 cm) length; and Sizes #9-#11 (29-36 mm) = 18-24" (45-60 cm) length. DO NOT WIRE TIE BARS UNTIL AFTER FULL ASSEMBLY per step 5. In all cases, consider your own **personal safety** during installation. Make sure you are securely positioned and that you will not slip or fall during installation. Use only good quality wrenches that will not round-out.

5 Insert the threaded rebar end into the Barsplicer coupler, and turn clockwise until the connection is snug. Once threads are fully engaged, turn the threaded bar one half additional turn into the coupler using a pipe or chain wrench as described above. If a setting bar was supplied with the coupler already attached, no additional installation is required on that bar. If both sides of the coupler require rebar to be installed into it, tighten the first side as described before tightening the second side as described.

6 Inspect the splice for proper thread engagement. For Barsplicer threads, some variation in the number of exposed threads is natural due to thread tolerance build-up and thread run-out. In general, it is usual to see 0 to 1 threads after full assembly. Fully assembled threads can be double-checked by the application of a pipe wrench, which overcomes the weight of the bar as described above. **IT IS NOT NECESSARY TO USE A TORQUE WRENCH OR APPLY A HIGH TORQUE VALUE.**

7 When installing epoxy coated couplers and rebar, apply wrench to the rebar, not the Barsplicer coupler. Once installed, touch-up damaged areas with epoxy repair kit. Seal off the rebar at the point of entry of the rebar into the coupler using epoxy repair material.

Please direct all assembly questions to BarSplice Products, Inc.

BARSPLICER-INSTALL-INS REV 2: 06/12/2018

Reinforcing Steel Bars

NUCOR

Mill Certification

10/02/2023

MTR#:1480057-2
Lot #:370004058020
2301 F.L. Shuttlesworth Drive
Birmingham, AL 35234 US
205 250-7400
Fax: 205 250-7465

Sold To: SABEL STEEL SERVICE INC
PO BOX 4747
MONTGOMERY, AL 36103 US

Ship To: SABEL STEEL SERVICES INC
704 LAFAYETTE ST
MONTGOMERY, AL 36104 US

Customer PO	06-2023-178	Sales Order #	37027546 - 2.1
Product Group	Rebar	Product #	3020959
Grade	A615 Gr 60/AASHTO M31	Lot #	370004058020
Size	#11	Heat #	3700040580
BOL #	BOL-1540953	Load #	1480057
Description	Rebar #11/36mm A615 Gr 60/AASHTO M31 60' 0" [720"] 6001-10000 lbs	Customer Part #	
Production Date	06/21/2023	Qty Shipped LBS	15302
Product Country Of Origin	United States	Qty Shipped EA	48
Original Item Description		Original Item Number	

I hereby certify that the material described herein has been manufactured in accordance with the specifications and standards listed above and that it satisfies those requirements.

Melt Country of Origin : United States — Melting Date: 06/16/2023

C (%)	Mn (%)	P (%)	S (%)	Si (%)	Ni (%)	Cr (%)	Mo (%)	Cu (%)	V (%)	Nb (%)
0.45	0.80	0.016	0.038	0.184	0.12	0.15	0.03	0.35	0.041	0.001

ASTM A706 6.4 CE & ASTM F1554 CE (%) : 0.61

Tensile testing

	Yield (PSI)	Tensile (PSI)	Elongation in 8" (%)
(1)	67400	104600	15.0

Mechanical

	Average Deformation Height (IN)	Bend Test
(1)	0.083	Pass

Other Test Results

Weight Percent Variance (%) : -4.95

Comments:

Nucor-Birmingham is ISO 9001-2015 and ISO 14001 certified. All manufacturing processes of the steel materials in this product, including melting, have occurred within the United States. Mercury, in any form, has not been used in the production or testing of this material. Meets (FTA) Buy America Requirements (49 C.F.R. part 661). Radium, or Alpha source materials in any form have not been used in the production of this material. All Products are manufactured in the United States and comply with Title 23 CFR 635.410 of the "Buy America Requirements". No weld repair was performed. Parts meet the requirements of the purchase order and have been produced under the Nucor Steel Birmingham quality manual rev 9 dated 9/2/2021.

George P. Miljus

George Miljus, Division Metallurgist

Page 1 of 1

NUCOR

Mill Certification

10/02/2023

MTR#:1480057-2
Lot #:370004058120
2301 F.L. Shuttlesworth Drive
Birmingham, AL 35234 US
205 250-7400
Fax: 205 250-7465

Sold To: SABEL STEEL SERVICE INC
PO BOX 4747
MONTGOMERY, AL 36103 US

Ship To: SABEL STEEL SERVICES INC
704 LAFAYETTE ST
MONTGOMERY, AL 36104 US

Customer PO	06-2023-178	Sales Order #	37027546 - 2.1
Product Group	Rebar	Product #	3020959
Grade	A615 Gr 60/AASHTO M31	Lot #	370004058120
Size	#11	Heat #	3700040581
BOL #	BOL-1540953	Load #	1480057
Description	Rebar #11/36mm A615 Gr 60/AASHTO M31 60' 0" [720"] 6001-10000 lbs	Customer Part #	
Production Date	06/21/2023	Qty Shipped LBS	30604
Product Country Of Origin	United States	Qty Shipped EA	96
Original Item Description		Original Item Number	

I hereby certify that the material described herein has been manufactured in accordance with the specifications and standards listed above and that it satisfies those requirements.

Melt Country of Origin : United States

Melting Date: 06/16/2023

C (%)	Mn (%)	P (%)	S (%)	Si (%)	Ni (%)	Cr (%)	Mo (%)	Cu (%)	V (%)	Nb (%)
0.44	0.81	0.014	0.031	0.187	0.14	0.14	0.03	0.29	0.032	0.001

ASTM A706 6.4 CE & ASTM F1554 CE (%) : 0.60

Tensile testing

	Yield (PSI)	Tensile (PSI)	Elongation in 8" (%)
(1)	67600	99900	9.0

Mechanical

	Average Deformation Height (IN)	Bend Test
(1)	0.082	Pass

Other Test Results

Weight Percent Variance (%) : -5.51

Comments:

Nucor-Birmingham is ISO 9001-2015 and ISO 14001 certified. All manufacturing processes of the steel materials in this product, including melting, have occurred within the United States. Mercury, in any form, has not been used in the production or testing of this material. Meets (FTA) Buy America Requirements (49 C.F.R. part 661). Radium, or Alpha source materials in any form have not been used in the production of this material. All Products are manufactured in the United States and comply with Title 23 CFR 635.410 of the "Buy America Requirements". No weld repair was performed. Parts meet the requirements of the purchase order and have been produced under the Nucor Steel Birmingham quality manual rev 9 dated 9/2/2021.

George Miljus, Division Metallurgist

NUCOR®

Mill Certification

12/04/2023

MTR#:1541516-3
Lot #:370004456020
2301 F.L. Shuttlesworth Drive
Birmingham, AL 35234 US
205 250-7400
Fax: 205 250-7465

Sold To: SABEL STEEL SERVICE INC
PO BOX 4747
MONTGOMERY, AL 36103 US

Ship To: SABEL STEEL SERVICES INC
704 LAFAYETTE ST
MONTGOMERY, AL 36104 US

Customer PO	06-2023-15	Sales Order #	37028743 - 1.5
Product Group	Rebar	Product #	3019447
Grade	A615 Gr 60/AASHTO M31	Lot #	370004456020
Size	#5	Heat #	3700044560
BOL #	BOL-1590026	Load #	1541516
Description	Rebar #5/16mm A615 Gr 60/AASHTO M31 60' 0" [720"] 6001-10000 lbs	Customer Part #	
Production Date	11/17/2023	Qty Shipped LBS	7885
Product Country Of Origin	United States	Qty Shipped EA	126
Original Item Description		Original Item Number	

I hereby certify that the material described herein has been manufactured in accordance with the specifications and standards listed above and that it satisfies those requirements.

Melt Country of Origin : United States — Melting Date: 11/12/2023

C (%)	Mn (%)	P (%)	S (%)	Si (%)	Ni (%)	Cr (%)	Mo (%)	Cu (%)	V (%)	Nb (%)
0.47	0.71	0.011	0.029	0.190	0.12	0.13	0.04	0.24	0.022	0.002

Tensile testing

	Yield (PSI)	Tensile (PSI)	Elongation in 8" (%)
(1)	74400	111200	9.0

Mechanical

	Average Deformation Height (IN)	Bend Test
(1)	0.042	Pass

Other Test Results

Weight Percent Variance (%) : -5.47

Comments:

Nucor-Birmingham is ISO 9001-2015 and ISO 14001 certified. All manufacturing processes of the steel materials in this product, including melting, have occurred within the United States. Mercury, in any form, has not been used in the production or testing of this material. Meets (FTA) Buy America Requirements (49 C.F.R. part 661). Radium, or Alpha source materials in any form have not been used in the production of this material. All Products are manufactured in the United States and comply with Title 23 CFR 635.410 of the "Buy America Requirements". No weld repair was performed. Parts meet the requirements of the purchase order and have been produced under the Nucor Steel Birmingham quality manual rev 9 dated 9/2/2021.

George P. Miljus

George Miljus, Division Metallurgist

NUCOR

Mill Certification

01/20/2023

MTR#:1233252-4
Lot #:370003617920
2301 F.L. Shuttlesworth Drive
Birmingham, AL 35234 US
205 250-7400
Fax: 205 250-7465

Sold To: SABEL STEEL SERVICE INC
PO BOX 4747
MONTGOMERY, AL 36103 US

Ship To: SABEL STEEL SERVICES INC
704 LAFAYETTE ST
MONTGOMERY, AL 36104 US

Customer PO	06-2023-106	Sales Order #	37023797 - 1.1
Product Group	Rebar	Product #	2110320
Grade	A615 Gr 60/AASHTO M31	Lot #	370003617920
Size	#8	Heat #	3700036179
BOL #	BOL-1330197	Load #	1233252
Description	Rebar #8/25mm A615 Gr 60/AASHTO M31 40' 0" [480"] 2001-6000 lbs	Customer Part #	
Production Date	01/05/2023	Qty Shipped LBS	5126
Product Country Of Origin	United States	Qty Shipped EA	48
Original Item Description		Original Item Number	

I hereby certify that the material described herein has been manufactured in accordance with the specifications and standards listed above and that it satisfies those requirements.

Melt Country of Origin : United States

Melting Date: 01/04/2023

C (%)	Mn (%)	P (%)	S (%)	Si (%)	Ni (%)	Cr (%)	Mo (%)	Cu (%)	V (%)	Nb (%)
0.40	0.71	0.009	0.029	0.220	0.11	0.09	0.03	0.30	0.025	0.001

Tensile testing

	Yield (PSI)	Tensile (PSI)	Elongation in 8" (%)
(1)	68700	100700	15.0

Mechanical

	Average Deformation Height (IN)	Bend Test
(1)	0.060	Pass

Other Test Results

Weight Percent Variance (%) : -4.79

Comments:

Nucor-Birmingham is ISO 9001-2015 and ISO 14001 certified. All manufacturing processes of the steel materials in this product, including melting, have occurred within the United States. Mercury, in any form, has not been used in the production or testing of this material. Meets (FTA) Buy America Requirements (49 C.F.R. part 661). Radium, or Alpha source materials in any form have not been used in the production of this material. All Products are manufactured in the United States and comply with Title 23 CFR 635.410 of the "Buy America Requirements". No weld repair was performed. Parts meet the requirements of the purchase order and have been produced under the Nucor Steel Birmingham quality manual rev 9 dated 9/2/2021.

George P. Miljus

George Miljus, Division Metallurgist